Analysis of the Effects of Anti-Icing Agents on the Mechanical Properties of Concrete

by
Mark Cremasco

A thesis
presented to the University of Waterloo
in fulfillment of the
thesis requirement for the degree of
Master of Applied Science
in
Mechanical Engineering

Waterloo, Ontario, Canada, 2012

I hereby declare that I am the sole author of this thesis. This is a true copy of the thesis including any required final revisions, as accepted by my examiners.

I understand that my thesis may be made electronically available to the public.

ABSTRACT

Anti-icing agents are applied to road surfaces to prevent ice formation and to melt any hail or snow as it falls. The specific agent is selected to provide optimum anti-icing properties for the particular local climate in different municipalities taking into account cost, availability and properties. These anti-icing agents are generally applied in liquid form, and due to their low freezing temperatures, are able to remain liquid at the low ambient temperatures. Unfortunately, the negative aspect of the use of liquid agents is that they are able to penetrate concrete structures to a greater extent than can the solid de-icers, such as rock salt. Once the chloride solutions penetrate the concrete, they can have serious deleterious effects on both the reinforcing steel as well as the concrete [**1**]. It has been shown in previous studies that the cations of the solutions will tend to react with the cementitious materials to form precipitates of expansive nature. More specifically, the reaction of $CaCl_2$ with $Ca(OH)_2$ results in the formation of expansive calcium hydroxy-chloride [**2**]. The reaction of $MgCl_2$ with $Ca(OH)_2$ forms $Mg(OH)_2$ in the capillary pores with $CaCl_2$ as a by-product after which the $MgCl_2$ can react with the calcium-silicate-hydrate to form magnesium-silicate-hydrate – a gel-like material with no inherent binding properties or strength. The calcium hydroxy-chloride and $Mg(OH)_2$ precipitates can have a positive effect at early onset, but will eventually cause deterioration of concrete due to the internal forces applied by the precipitates as their volume increases. This can affect the strength and create notable interior strain in the concrete.

There are a number of mechanical properties that can be analyzed using short-term testing that will help to determine any changes occurring due to salt solution exposure. To gain a general

understanding of the effects of the salt solution exposure in this project, compressive strength, tensile strength, elastic modulus, and strain were measured using a number of exposure conditions.

While the results of testing confirm that there are initial benefits beyond minimizing ice formation and bonding, there ultimately exist a number of concerns with respect to the reactions that occur between the salts and hardened cement paste. Although the formation of calcium hydroxy-chloride is known to be expansive [**3**], evidence of this compound was only seen indirectly through elevated strain and micro-cracking. There was no deterioration of compressive strength, tensile strength, or elastic modulus over the short-term testing. Similarly, and again due to the short testing period, the formation of magnesium-silicate-hydrate (M-S-H) is unlikely to have occurred, though its formation during long-term exposure can result in complete loss of binding strength [**2**]. However, the precipitation of $Mg(OH)_2$ is believed to be responsible for the lower chloride diffusion rate as well as the increase in strength of the concrete exposed to $MgCl_2$. The only agent which did not yield changes of concern with respect to concrete is the NaCl solution while $CaCl_2$ produced the most deleterious effects.

ACKNOWLEDGEMENTS

- Ministry of Transportation of Ontario, Funding and support
- Holcim Canada, Provision of materials
- Dr. C.M. Hansson, Project supervisor and second mother
- Douglas Hirst and Richard Morrisson, Civil engineering laboratory technicians
- Matt Hunt, Brad Bergsma, and James Cameron; University of Waterloo Team Corrosion
- Dr. S. Walbridge and Dr. A. Gerlich, Thesis reviewers
- Dr. G. Cascante, Ultrasonic testing advisor
- Centre for Pavement and Transportation Technology (CPATT), Provision of equipment
- Cartoon Fish, Moral support

Table of Contents

List of Figures x

List of Tables xvi

List of Equations xix

1 Introduction 1

2 Literature Review 4

2.1 Chemical Composition of Cement and Concrete 4

2.1.1 Portland Cement 4

2.1.2 Hardened Cement Paste 5

2.1.3 Concrete Admixtures 7

2.1.4 Effects of Supplementary Cementitious Materials (SCMs) 9

2.2 Anti-Icing Solutions 10

2.2.1 Magnesium Chloride ($MgCl_2$) 11

2.2.2 Calcium Chloride ($CaCl_2$) 14

2.2.3 Sodium Chloride (NaCl) 17

2.2.4 Multi-Chloride 18

2.2.5 Salt Scaling 19

3 Experimental Procedure: 20

3.1 Materials 20

3.1.1 Concrete Mixture Design 20

3.1.2 Anti-Icing Solutions 21

3.2 Test Procedures 26

3.2.1 Freezing and Thawing 26

3.2.2 Internal strain 32
3.2.3 Compressive Strength 35
3.2.4 Tensile Strength 37
3.2.5 Chloride Penetration 38
3.2.6 pH and Chloride Penetration by Spray Methods 40
3.2.7 Energy Dispersive X-Ray Spectroscopy (EDS) 41
3.2.8 Air Void and Crack Analysis 43
4 Results: 45
4.1 Freezing and thawing 45
4.2 Internal strain 56
4.3 Compressive Strength 66
4.4 Tensile Strength 72
4.5 Chloride Penetration 84
4.6 pH and Chloride Penetration by Spray Methods 88
4.7 Energy Dispersive X-Ray Spectroscopy (EDS) 95
4.8 Air Void Analysis 102
5 Discussion: 105
5.1 Freezing and Thawing 105
5.2 Internal Strain 118
5.3 Compressive Strength 124
5.3.1 Cylinders Set 1 - Continuous Soaking 124
5.3.2 Cylinders Set 2 – Wet and Dry Cycles 125
5.4 Tensile Strength 126
5.5 Chloride Penetration 129

5.6 pH and Chloride Penetration by Spray Methods 132
5.7 Energy Dispersive X-Ray Spectroscopy (EDS) 135
5.8 General Observations and Discussion 141
6 Conclusions: 146
7 Recommendations 152
7.1 Testing Methods 152
7.1.1 Freezing and Thawing Testing 152
7.1.2 Compressive Testing 154
7.1.3 pH Analysis 154
7.1.4 Chemical Composition Analysis 154
7.1.5 Chloride Penetration 155
7.2 Salt-Based Anti-Icing Application 155
7.2.1 $MgCl_2$ 156
7.2.2 $CaCl_2$ 156
7.2.3 Multi-Cl^- 157
7.2.4 NaCl 157
References 158
Appendix A Background 164
Appendix A.1 Casting Information 164
Appendix B Results 173
Appendix B.1 28-Day Strengths 173
Appendix B.2 Freeze and Thaw Results 175
Appendix B.2.1 Freezing and Thawing Temperature Data 175
Appendix B.2.2 Freezing and Thawing Set 1 Data 176

Appendix B.2.3 Freezing and Thawing Set 2 Data 180
Appendix B.3 Compressive Strength Testing Results 184
Appendix B.3.1 Set 1 Raw Compressive Testing Results 184
Appendix B.3.2 Set 1 Normalized Compressive Testing Results 189
Appendix B.3.3 Set 2 Compressive Testing Results 194
Appendix B.3.4 Set 2 Normalized Compressive Testing Results 199
Appendix B.4 Chloride Penetration 204
Appendix B.4.1 Chloride Penetration Curves by Exposure Solution 204
Appendix B.4.2 Chloride Penetration Diffusion Coefficients with Respect to Depth 208
Appendix B.4.3 Diffusion Coefficient Analysis by Visual Approximation 213
Appendix B.5 Environmental Scanning Electron Microscopy Raw Data 221
Appendix B.6 Air Void Analysis 226
Appendix B.6.1 Raw Data 226
Appendix B.6.2 Microscopy Images 228

List of Figures

Figure 2.1-1 - Hydration of ordinary portland cement [14] 9
Figure 2.1-2 - Hydration of ordinary portland cement with blast furnace slag as an SCM [14] ... 10
Figure 2.2-1 - $MgCl_2$-H_2O phase diagram (the solid line represents as-received solution concentration and the dashed line the diluted solution concentration for the current study) [16] 12
Figure 2.2-2 - Fracture of mortar specimen caused by $CaCl_2$ [1] 15
Figure 2.2-3 - $CaCl_2$-H_2O phase diagram (the solid line represents as-received solution concentration and the dashed line the diluted solution concentration for the current study) [16] 16
Figure 2.2-4 - NaCl-H_2O phase diagram (the solid line represents as-received solution concentration and the dashed line the diluted solution concentration for the current study) [16] 18
Figure 3.1-1 - Liquidus lines for NaCl, $CaCl_2$, and $MgCl_2$ adapted from United States Department of Transportation [28] 25
Figure 3.2-1 - Freezing and thawing chamber with lid open, prisms submerged in solution or water 28
Figure 3.2-2 - Ultrasonic frequency analysis setup 29
Figure 3.2-3 - Solution concentrations and liquidus lines for as-received solutions 30
Figure 3.2-4 - Solution concentrations and liquidus lines for diluted solutions 31
Figure 3.2-5 - Slab design schematic 34
Figure 3.2-6 - Outdoor slab construction. Side view (left), top view (right) 34
Figure 3.2-7 - (A) Fully constructed mould with gauges, rebar, and ponding well and (B) outdoor slab testing setup 35
Figure 3.2-8 - Compressive strength testing apparatus 36
Figure 3.2-9 - Tensile testing apparatus and setup 38
Figure 3.2-10 - Profile grinding equipment and setup 39
Figure 3.2-11 - Post-grinding chloride penetration samples 40

Figure 3.2-12 - pH (top) and $AgNO_3$ (bottom) spray indicators on concrete specimens 41
Figure 3.2-13 - Environmental scanning electron microscope with energy dispersive x-ray spectroscopy setup 42
Figure 3.2-14 - Sample polishing equipment 44
Figure 3.2-15 - Air void analyzer 44
Figure 4.1-1 - $MgCl_2$ prism 3, Set 2 data set from freeze and thaw testing 46
Figure 4.1-2 – Average elastic modulus of prisms in as-received solutions as a function of freezing and thawing cycles 47
Figure 4.1-3 – Average elastic modulus of prisms in solutions diluted to 1/3-as-received as a function of freezing and thawing cycles 48
Figure 4.1-4 - Freeze and thaw average elastic modulus per solution, comparison 50
Figure 4.1-5 - Cumulative average mass change of freeze and thaw prisms, Set 1, exposed to as-received solutions 51
Figure 4.1-6 – Cumulative average mass change of freeze and thaw prisms, Set 2, exposed to diluted solutions 52
Figure 4.1-7 – Cumulative average mass change of freeze thaw specimens, comparison 53
Figure 4.1-8 - Freeze and thaw Set 1, as-received solutions, prism debris for each of the three individual prisms in those solutions where scaling occurred 54
Figure 4.1-9 - Freeze and thaw Set 2, diluted solutions, prism debris for each of the three individual prisms in those solutions where scaling occurred 55
Figure 4.1-10 - Freeze and thaw Set 1 and Set 2 average debris mass 56
Figure 4.2-1 - Adjusted strain from all gauges such that the first value from each data set has been subtracted from all subsequent raw values 58
Figure 4.2-2 – Water corrected strain in $MgCl_2$ at three levels on the primary ordinate and temperature on the secondary ordinate 59
Figure 4.2-3 - Water corrected strain from the top-most gauge in each of the four solution samples 60
Figure 4.2-4 - Water corrected strain from the $MgCl_2$ slab 61
Figure 4.2-5 - Water corrected strain from the $CaCl_2$ slab 62

Figure 4.2-6 - Water and corrected strain from the Multi-Cl^- slab 63
Figure 4.2-7 - Water corrected strain from the NaCl slab 64
Figure 4.2-8 – Temperature profiles from the $MgCl_2$ slab 65
Figure 4.3-1 – Average compressive strength for continuously soaked samples starting at 28 day strength and measured every 2 weeks 68
Figure 4.3-2 - Average compressive strength for alternating wet and dry samples starting at 28 day strength and measured every 2 weeks 70
Figure 4.3-3 – Average compressive strength results from Set 1 including statistically insufficient measurements at 37 weeks with associated error bars 71
Figure 4.4-1 - Load versus displacement curves obtained from 3-point bend tensile testing 73
Figure 4.4-2 - Median curves for load versus displacement from tensile testing 74
Figure 4.4-3 – True (adjusted) load versus displacement curves obtained from 3-point bend tensile testing 75
Figure 4.4-4 – True (adjusted) median curves for load versus displacement from tensile testing 76
Figure 4.4-5 - Calculated elastic modulii in tension from three-point bend tensile testing 80
Figure 4.4-6 - Modulii of rupture calculated from results of three-point bend tensile testing ... 81
Figure 4.4-7 - Peak strength of prisms tested in tension by three-point bending 82
Figure 4.4-8 - Maximum displacement adjusted to remove effects of equipment settling for tension testing by three-point bend 83
Figure 4.5-1 - Chloride penetration into concrete from one direction measured after 2, 19, and 59 weeks soaking by weight of cementitious materials 85
Figure 4.5-2 - Fick's second law for diffusion [35] 87
Figure 4.6-1 - $MgCl_2$ pH results by spray method 90
Figure 4.6-2 - $CaCl_2$ pH results by spray method 90
Figure 4.6-3 - Multi-Cl^- pH results by spray method 91
Figure 4.6-4 - NaCl pH results by spray method 91
Figure 4.6-5 - H_2O pH results by spray method 92
Figure 4.6-6 - Chloride penetration by $AgNO_3$ sample chord measurement layout 93

Figure 4.7-1 - Energy dispersive x-ray spectroscopy composition profile for the first $MgCl_2$ sample 96
Figure 4.7-2 - Energy dispersive x-ray spectroscopy composition profile for the second $MgCl_2$ sample 97
Figure 4.7-3 - Energy dispersive x-ray spectroscopy composition profile for the $CaCl_2$ sample .. 98
Figure 4.7-4 - Energy dispersive x-ray spectroscopy composition profile for the multi-Cl^- sample 99
Figure 4.7-5 - Energy dispersive x-ray spectroscopy composition profile for the NaCl sample . 100
Figure 4.7-6 – Energy dispersive x-ray spectroscopy chloride profile for each of the four samples 101
Figure 4.7-7 - Comparison of chloride selective electrode testing and energy dispersive x-ray spectroscopy results from the same samples after 59 weeks soaking in salt solutions 102
Figure 5.1-1 - Stress versus strain profiles for concrete of increasing compressive strength [38] 109
Figure 5.1-2 - H_2O freeze and thaw prism number one front after 385 freeze and thaw cycles 113
Figure 5.1-3 - $MgCl_2$ freeze and thaw prism number one front after 385 freeze and thaw cycles 113
Figure 5.1-4 - freezing and thawing set 2, diluted solutions, NaCl prism one prior to exposure 115
Figure 5.1-5 - freezing and thawing set 2, diluted solutions, NaCl prism one after 355 freezing and thawing cycles 115
Figure 5.1-6 - Severe crack in freezing and thawing Set 1 temperature control prism 117
Figure 5.2-1 - Surface images of slabs after 19 months outdoor exposure (A), and surface damage to $MgCl_2$ slab after 19 months outdoor exposure (B) 122
Figure 5.7-1 - Cracks found after 59 weeks exposure to $CaCl_2$ using environmental scanning electron microscopy 138
Figure 5.7-2 - Cracks found after 59 weeks exposure to $MgCl_2$ using environmental scanning electron microscopy 139

Figure 5.7-3 - Cracks found after 59 weeks exposure to multi-Cl^- using environmental scanning electron microscopy 140
Figure 5.7-4 – Absence of cracks after 59 weeks exposure to NaCl using environmental scanning electron microscopy 141
Figure B.2-1 - Freeze and thaw Set 1, full strength solutions, temperature profile..... 175
Figure B.2-2 - Freeze and thaw Set 2, diluted solutions, temperature profile 176
Figure B.4-1 - Chloride penetration curves from $MgCl_2$ samples at 2, 19, and 59 weeks soaking 205
Figure B.4-2 - Chloride penetration curves from $CaCl_2$ samples at 2, 19, and 59 weeks soaking 206
Figure B.4-3 - Chloride penetration curves from multi-Cl^- samples at 2, 19, and 59 weeks soaking 207
Figure B.4-4 - Chloride penetration curves from NaCl samples at 2, 19, and 59 weeks soaking208
Figure B.4-5 - Diffusion Coefficients (m^2/s) for all four solutions at each depth at 2, 19, and 59 weeks soaking 209
Figure B.4-6 - Diffusion coefficients versus time at each measurement depth from chloride penetration for $MgCl_2$ 210
Figure B.4-7 - Diffusion coefficients versus time at each measurement depth from chloride penetration for $CaCl_2$ 211
Figure B.4-8 - Diffusion coefficients versus time at each measurement depth from chloride penetration for multi-Cl^- 212
Figure B.4-9 - Diffusion coefficients versus time at each measurement depth from chloride penetration for NaCl 213
Figure B.4-10 - $MgCl_2$ penetration curves, measured and calculated, for effective diffusion coefficient determination by chloride selective electrode..... 214
Figure B.4-11 - $CaCl_2$ penetration curves, measured and calculated, for effective diffusion coefficient determination by chloride selective electrode..... 215
Figure B.4-12 - Multi-Cl^- penetration curves, measured and calculated, for effective diffusion coefficient determination by chloride selective electrode..... 216

Figure B.4-13 - NaCl penetration curves, measured and calculated, for effective diffusion coefficient determination by chloride selective electrode 217
Figure B.4-14 - $MgCl_2$ penetration curves, measured and calculated, for effective diffusion coefficient determination by EDS 218
Figure B.4-15 - $CaCl_2$ penetration curves, measured and calculated, for effective diffusion coefficient determination by EDS 219
Figure B.4-16 - Multi-Cl^- penetration curves, measured and calculated, for effective diffusion coefficient determination by EDS 220
Figure B.4-17 - NaCl penetration curves, measured and calculated, for effective diffusion coefficient determination by EDS 221
Figure B.6-1 - Microscopy image of H_2O sample from air void analysis 229
Figure B.6-2 - Microscopy image of $MgCl_2$ sample from air void analysis 229
Figure B.6-3 - Microscopy image of $CaCl_2$ sample from air void analysis 230
Figure B.6-4 - Microscopy image of multi-Cl^- sample from air void analysis 230
Figure B.6-5 - Microscopy image of NaCl sample from air void analysis 231

List of Tables

Table 3.1-1 - Concrete mixture design 20
Table 3.1-2 - Anti-icing solution major elements 21
Table 3.1-3 - Overall anti-icing solution composition and eutectic points 26
Table 4.4-1 - Results and material properties calculations from three-point bend tensile testing 77
Table 4.4-2 - Average material properties calculated from three-point bend tensile testing 78
Table 4.5-1 - Effective diffusion coefficients by curve approximation 88
Table 4.6-1 - Chloride penetration by $AgNO_3$ spray method results 94
Table 4.6-2 - Data averages for chloride penetration by $AgNO_3$ spray method 95
Table 4.8-1 - Air void analysis results 103
Table 5.6-1 - Ionic mobility relative to potassium (K) for Na^+, Ca^{2+}, Mg^{2+}, and Cl^- [40] 134
Table A.1-1 - Freeze and thaw testing Set 1 prisms casting information 164
Table A.1-2 - Freeze and thaw testing Set 2 prisms casting information 165
Table A.1-3 - Internal strain slabs casting information 166
Table A.1-4 - Compressive strength testing Set 1, batch "X" cylinder casting information 167
Table A.1-5 - Compressive strength testing Set 1, batch "O" cylinder casting information 168
Table A.1-6 - Compressive strength testing Set 2, batch "X" cylinder casting information 169
Table A.1-7 - Compressive strength testing Set 2, batch "O" cylinder casting information 170
Table A.1-8 - Tensile strength testing prisms casting information 171
Table A.1-9 - Chloride penetration block casting information 172
Table B.1-1 - 28-day strength data for all concrete batches cast for testing purposes 174
Table B.2-1 - Freeze and thaw data from Set 1, full strength solutions, for $MgCl_2$, $CaCl_2$, and H_2O for the first 35 days 177
Table B.2-2 - Freeze and thaw data from Set 1, full strength solutions, for $MgCl_2$, $CaCl_2$, and H_2O for days 36 to 56 178
Table B.2-3 - Freeze and thaw data from Set 1, full strength solutions, for Multi-Cl^- and NaCl for the first 35 days 179

Table B.2-4 - Freeze and thaw data from Set 1, full strength solutions, for Multi-Cl- and NaCl for days 36 to 56 180
Table B.2-5 - Freeze and thaw data from Set 2, diluted solutions, for $MgCl_2$, $CaCl_2$, and H_2O for the first 35 days 181
Table B.2-6 - Freeze and thaw data from Set 2, diluted solutions, for $MgCl_2$, $CaCl_2$, and H_2O for days 36 through 56 182
Table B.2-7 - Freeze and thaw data from Set 2, diluted solutions, for Multi-Cl- and NaCl for the first 35 days 183
Table B.2-8 - Freeze and thaw data from Set 2, diluted solutions, for Multi-Cl- and NaCl for days 36 to 56 184
Table B.3-1 - Compressive strength testing results for Set 1, continuous soaking, weeks 0-2 .. 185
Table B.3-2 - Compressive strength testing results for Set 1, continuous soaking, weeks 4-6 .. 186
Table B.3-3 - Compressive strength testing results for Set 1, continuous soaking, weeks 8-10 187
Table B.3-4 - Compressive strength testing results for Set 1, continuous soaking, weeks 12-14 188
Table B.3-5 - Compressive strength testing results for Set 1, continuous soaking, weeks 16-37 189
Table B.3-6 – Normalized compressive strength testing results for Set 1, continuous soaking, weeks 0-2 190
Table B.3-7 – Normalized compressive strength testing results for Set 1, continuous soaking, weeks 4-6 191
Table B.3-8 – Normalized compressive strength testing results for Set 1, continuous soaking, weeks 8-10 192
Table B.3-9 – Normalized compressive strength testing results for Set 1, continuous soaking, weeks 12-14 193
Table B.3-10 – Normalized compressive strength testing results for Set 1, continuous soaking, weeks 16-37 194
Table B.3-11 - Compressive strength testing results for Set 2, wet and dry cycling, weeks 0-4 195
Table B.3-12 - Compressive strength testing results for Set 2, wet and dry cycling, weeks 6-8 196

Table B.3-13 - Compressive strength testing results for Set 2, wet and dry cycling, weeks 10-12 197
Table B.3-14 - Compressive strength testing results for Set 2, wet and dry cycling, weeks 14-16 198
Table B.3-15 - Compressive strength testing results for Set 2, wet and dry cycling, weeks 18-20 199
Table B.3-16 – Normalized compressive strength testing results for Set 2, wet and dry cycling, weeks 0-4 200
Table B.3-17 – Normalized compressive strength testing results for Set 2, wet and dry cycling, weeks 6-8 201
Table B.3-18 – Normalized compressive strength testing results for Set 2, wet and dry cycling, weeks 10-12 202
Table B.3-19 – Normalized compressive strength testing results for Set 2, wet and dry cycling, weeks 14-16 203
Table B.3-20 – Normalized compressive strength testing results for Set 2, wet and dry cycling, weeks 18-20 204
Table B.5-1 - Environmental scanning electron microscopy results in percent for the first $MgCl_2$ sample 222
Table B.5-2 - Environmental scanning electron microscopy results in percent for the second $MgCl_2$ sample 223
Table B.5-3 - Environmental scanning electron microscopy results in percent for the $CaCl_2$ sample 224
Table B.5-4 - Environmental scanning electron microscopy results in percent for the multi-Cl^- sample 225
Table B.5-5 - Environmental scanning electron microscopy results in percent for the NaCl sample 226
Table B.6-1 - Air Void Analysis Raw Data Part 1 227
Table B.6-2 - Air Void Analysis Raw Data Part 2 228

List of Equations

Equation 2.1-1 adapted from [11] 6
Equation 2.1-2 adapted from [11] 6
Equation 2.1-3 adapted from [11] 6
Equation 2.1-4 adapted from [11] 6
Equation 2.1-5 adapted from [11] 6
Equation 2.1-6 adapted from [11] 6
Equation 2.2-1 [3] 13
Equation 2.2-2 [3] 14
Equation 2.2-3 [2] 15
Equation 3.2-1 [30] 28
Equation 4.1-1 45
Equation 4.2-1 57
Equation 4.2-2 60
Equation 4.3-1 67
Equation 4.4-1 [34] 78
Equation 4.4-2 [32] 79
Equation 5.1-1 106
Equation 5.1-2 [34] 108
Equation 5.1-3 [39] 109

1 Introduction

The state of highway infrastructure is a challenge not only to the driver frustrated by potholes, but also to government officials at all levels. With a Canadian civil infrastructure deficit estimated in 2003 as $125 billion and growing since then [**4**], there are major challenges not only to install, replace, and repair, but to further tackle the issues at a more fundamental level and work towards reducing this deficit and develop preventative measures to avoid recreating it. This has been very clearly highlighted by the current concerns and actions relating to the Champlain Bridge in Montreal, Quebec, Canada, where $370 million are required to maintain the current bridge long enough for construction of a $5 billion bridge to take place over a ten year period [**5**]. A major contributor to the infrastructure deterioration is the application of anti-icing and de-icing agents, which are used to prevent ice formation or melt that already formed in sub-freezing temperatures. The most common agents employed are chloride based solids and solutions. It is well known that the presence of chlorides can have serious deleterious effects on the reinforcing steel in concrete, but they can also have significant deleterious effects on the concrete with sufficient exposure time, the level of which can vary depending on the cation(s) associated with the salt [**1**], [**3**], [**6**], [**7**]. While the damage to concrete is concerning, it is an area that has not been as thoroughly explored as the damage to the reinforcing steel. This knowledge gap is even greater when considering high solution concentrations - up to 23.3% chlorides - as used in some parts of Ontario, Canada, since most research considers solutions up to only 5% chlorides.

Anti-icing agents are becoming more common as a pre-precipitation method to minimize ice formation and adhesion of ice to the pavement. This process makes the removal of ice and snow much easier. Due to the sub-freezing temperatures, it is important that these anti-icing agents, generally applied in liquid form or as a wetting agent on rock salt or sand, stay liquid when applied. This requires high concentrations of salt in solution in order to lower the freezing point to an effective level. These solutions present great concern as they have not only a high concentration of chlorides, but also a corresponding high concentration of cations – typically Na^{+}, Ca^{2+}, Mg^{2+} - some of which have been shown to have deleterious effects on the concrete [**1**], [**3**], [**7**], [**8**]. The majority of research analyzing these interactions considers only 3-5% chlorides, while Ontario roads experience three to seven times that amount. Although it is the chlorides that are responsible for the corrosion of the metallic reinforcement, it is generally the reaction of the concrete constituents with the cations that causes deterioration of the concrete [**3**], [**7**], [**8**]. In order to tackle the infrastructure deficit, it is imperative to understand the effects these interactions have on long-term durability and, in-turn, on concrete structure life expectancy.

The goal of this project is to characterize the effects of salt solutions on the general mechanical properties of concrete in order to develop a basis for recommendations with respect to salt solution usage. Recommendations are made based upon the benefits and detriments on a solution-by-solution basis, with each being analyzed equally throughout the course of testing. While there are numerous combinations of concrete mixture designs and salt solutions that can be analyzed, the scope of the current analysis is much more refined. To develop analytical

results, a single concrete mixture design based upon the standard bridge deck mixture was used, and the effects of the four most commonly applied salt solutions – $CaCl_2$, $MgCl_2$, NaCl, and a multi-chloride brine – were analyzed and compared to each other and to concrete not exposed to salt solutions.

2 Literature Review

2.1 Chemical Composition of Cement and Concrete

Concrete is the most commonly used material in the world, and has been used for over 9000 years as a building and infrastructure material [**9**]. The terms cement and concrete, though often used interchangeably, actually refer to two very different materials. Cement refers to the dry powder composed of alumina, silica, iron oxide, lime, and magnesium oxide burned together and finely pulverized that, when mixed with water, provides a strong, durable solid [**9**]. Concrete, by contrast, is the combination of both hydrated cement and aggregate (which is usually in the form of rock, stone, and sand). Hydrated cement on its own is known as cement paste, which is the binding agent holding the aggregate together in concrete. If the cement is mixed with sand prior to hydration, the resultant product is known as mortar or grout – a product often used to join masonry. Portland cement, the most common cement used, is a type of hydraulic cement made by heating a limestone and clay mixture in a kiln and then pulverizing it into a fine material [**9**].

2.1.1 Portland Cement

Portland cement clinker – the pulverized form of portland cement – has four primary components: alite (C_3S), belite (C_2S), aluminate (C_3A), and alumino-ferrite (C_4AF), with calcium sulphate ($C\bar{S}$) added during grinding to control the setting rate. C, A, S, F, and $\bar{S}$ correspond to the oxides of calcium, aluminum, silicon, ferrite (iron), and sulphur, respectively [**9**], [**10**]. H is also often used to represent H_2O.

In a portland cement mixture, the C_2S and C_3S are the primary phases for strength development. The C_3A and C_4AF acting as a catalyst to the formation of the calcium silicates. The typical composition of portland cement is about 50-60% C_3S, 10-20% C_2S, 1-10% C_4AF, 1-12% C_3A, and 4% $C\bar{S}$ [**9**], [**10**].

There is a wide number of cement types which can be used depending on the particular application and service demands. These include hydraulic cements, portland cements, and blended cements. Each of these has six sub-types including: general use (GU), high early strength (HE), moderate sulphate resistance (MS), high sulphate resistance (HS), moderate heat of hydration (MH), and low heat of hydration (LH). There is a fourth cement type, blended hydraulic cement, which has its own six sub-types which include: portland blast-furnace slag cement (type IS), portland-pozzolan cement (type IP), portland-pozzolan cement (type P), pozzolan-modified portland cement (type I(PM)), slag cement (type S), and slag-modified portland cement (type I(SM)), each with its own applications and properties [**9**].

2.1.2 Hardened Cement Paste

The hardened cement paste refers to the hydrated and cured portland cement powders. When mixed with water, the portland cement reacts to form a number of products which provides the binding in concrete. There are six main portland cement hydration reactions, which are listed in [**11**].

$$2C_3S + 11H_2O \rightarrow CSH + 3Ca(OH)_2$$

Equation 2.1-1 adapted from [11]

$$2C_2S + 9H_2O \rightarrow CSH + Ca(OH)_2$$

Equation 2.1-2 adapted from [11]

$$C_3A + 3(CaO \cdot SO_3 \cdot H_2O) + 26H_2O \rightarrow 6CaO \cdot Al_2O_3 \cdot 3SO_3 \cdot 32H_2O$$

Equation 2.1-3 adapted from [11]

Where $6CaO \cdot Al_2O_3 \cdot 3SO_3 \cdot 32H_2O$ is known as ettringite.

$$2(C_3A) + ettringite + 4H_2O \rightarrow 3(4CaO \cdot Al_2O_3 \cdot SO_3 \cdot 12H_2O)$$

Equation 2.1-4 adapted from [11]

Where $4CaO \cdot Al_2O_3 \cdot SO_3 \cdot 12H_2O$ is known as monosulphate.

$$C_3A + Ca(OH)_2 + 12H_2O \rightarrow 4CaO \cdot Al_2O_3 \cdot 13H_2O$$

Equation 2.1-5 adapted from [11]

$$C_4AF + 10H_2O + 2(Ca(OH)_2) \rightarrow 6CaO \cdot Al_2O_3 \cdot Fe_2O_3 \cdot 12H_2O$$

Equation 2.1-6 adapted from [11]

The majority of the reactants are the portland cement powder constituents or water with the exception of $CaO \cdot SO_3 \cdot H_2O$ which is gypsum; $CaO \cdot H_2O$ which is calcium hydroxide produced

in the reactions of C_2S and C_3S with water; and $CaO \cdot Al_2O_3 \cdot 3SO_3 \cdot 32H_2O$ which is ettringite, a product of the reaction of C_3A with gypsum and water.

The C-S-H phase makes up about 50-60% of the volume of solids in completely hydrated portland cement paste, and thus is the key determinant of the properties [**12**]. Van der Waals forces within the material and a 100 to 700m^2/g surface area make the C-S-H a high strength material, responsible for much of the strength and binding properties of concrete. The $Ca(OH)_2$ constitutes about 20-25% of the volume of solids in large crystals. Due to the large crystal size, the $Ca(OH)_2$ has a relatively low surface area to volume ratio, thus providing very little strength itself, although its contribution to ettringite plays a major role in setting prior to C-S-H formation [**12**]. The calcium sulfo-aluminates occupy 15-20% of the solids volume and thus do not have a significant effect on the structure-property relationships [**12**].

2.1.3 Concrete Admixtures

There are a number of chemical additives that, when combined with water in the mixing phase, allow for various properties to be improved. The most commonly used additives include accelerators, retarders, water reducing agents, air entraining agents, and super-plasticizers. Admixtures are used primarily to reduce cost of construction, achieve certain properties, maintain quality until the concrete has cured, and overcome emergencies during concreting operations [**9**].

Air entraining admixtures are used to create small (micrometric-dimensioned) air bubbles in concrete [**9**]. The presence of air bubbles throughout the concrete allows for space for moisture to collect and allows room for expansion during freezing. This significantly improves the concrete's durability when exposed to freezing and thawing cycles. The presence of entrained air can also help to improve resistance to surface scaling from de-icing agents, improve workability, and reduce segregation and bleeding of the concrete [**9**].

Low-range water-reducing admixtures reduce the amount of water need to produce concrete of a certain flowability, to increase the flowability, and to reduce the water-cement ratio and, thus, the porosity [**9**]. Typical water reducers will decrease the water content by 5-10% or alternatively produce a concrete with a higher flowability. When the water content is reduced with the use of the admixture, increases in 28-day strength of 10-25% as compared to the same concrete without the admixture can be achieved [**9**].

High-range water-reducing admixtures have similar properties to low-range water-reducing admixtures, but in a much more efficient manner [**9**]. They can reduce water requirements by 12-30%, or conversely provide significant improvement to flowability. Concrete produced using high-range water-reducing admixtures can also cause larger entrained air voids and greater space between air voids than normal concrete, thus improving freezing and thawing resistance [**9**].

2.1.4 Effects of Supplementary Cementitious Materials (SCMs)

The addition of supplementary cementitious materials to a concrete mixture can be done for numerous reasons and have various effects depending on the supplementary material used. Commonly used SCMs include fly ash, silica fume, and blast furnace slag, the latter of which is often used in Ontario [**13**]. Blast furnace slag, a by-product of iron manufacturing, is pozzolanic in nature – a term used to describe reactive alumino-silicate materials that, when finely ground and hydrated, form compounds with cementitious properties [**12**], [**13**]. The addition of blast furnace slag as an SCM not only displaces the volume of cement needed, but also provides an improved resistance to diffusion of chlorides and other substances. The presence of slag causes the formation of a precipitate of calcium silicate hydrate and calcium aluminate hydrates that acts similar to a mesh to resist diffusion [**14**]. The hydrated phases of ordinary portland cement and ordinary portland cement with slag are shown in Figure 2.1-1 and Figure 2.1-2 respectively.

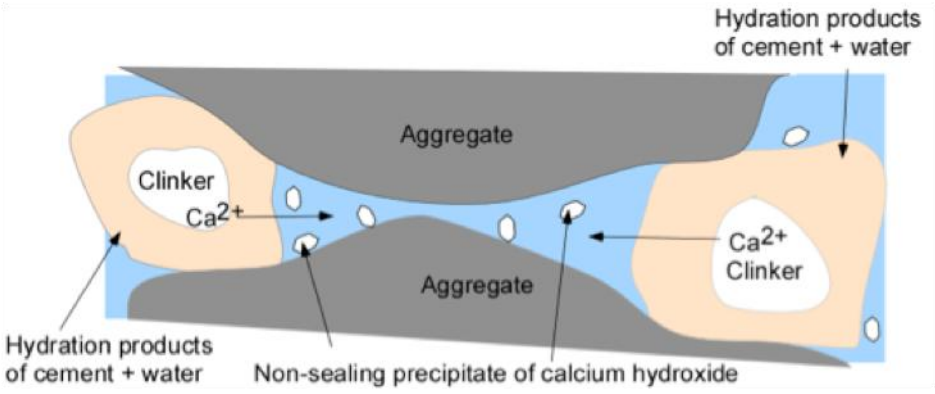

Figure 2.1-1 - Hydration of ordinary portland cement [14**]**

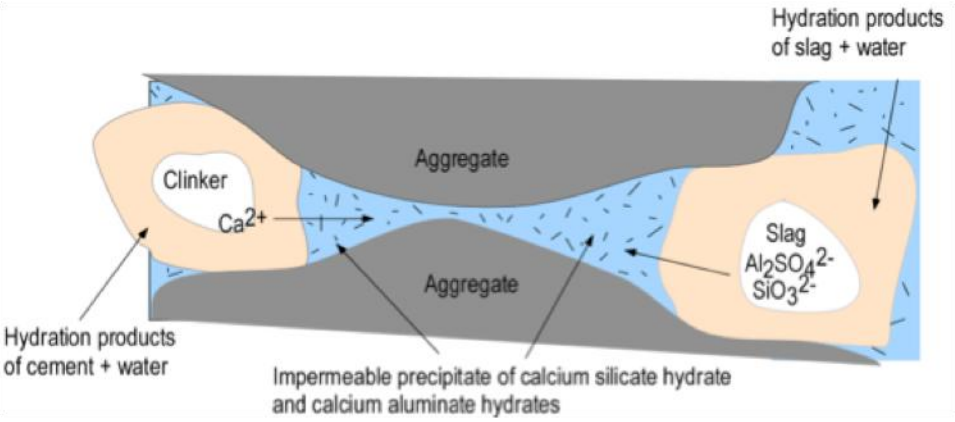

Figure 2.1-2 - Hydration of ordinary portland cement with blast furnace slag as an SCM [14**]**

2.2 Anti-Icing Solutions

The effects of de-icing and anti-icing solutions on the composition and properties of concrete are often overlooked due to the severely deleterious effects of chlorides on embedded reinforcing steel. The presence of chlorides at the surface of steel reinforcement causes corrosion and the resultant products are known to be expansive in nature, causing further detriment to the structure [**1**], [**15**]. This phenomenon can be regularly observed in areas where chloride-based anti-icing and de-icing solutions are used. For example, as on bridge structures, barrier walls, and parking garages which will show rust stains, cracks, and sometimes loss of concrete cover at severely corroded areas. While this is the common result associated with application of chloride solutions as anti-icing and de-icing agents, there are also detrimental effects on the concrete which must be considered. Each solution has different effects on the concrete based upon the composition of the solution and the concrete components. The majority of the research below describes testing using more dilute solutions -

in the 3-5% chlorides range – which is indicative of the expected reactions and results, but will not necessarily directly correlate to the results at higher concentrations.

2.2.1 Magnesium Chloride ($MgCl_2$)

Magnesium chloride, $MgCl_2$, is one of the three primary anti-icing solutions used in Ontario, Canada. While it is commonly used in brine form for anti-icing treatment, there are relatively few data available about the solution as compared to NaCl and $CaCl_2$ solutions. This may be due, in part, to the complexity of the $MgCl_2$-H_2O system, as seen in Figure 2.2-1 [**16**].

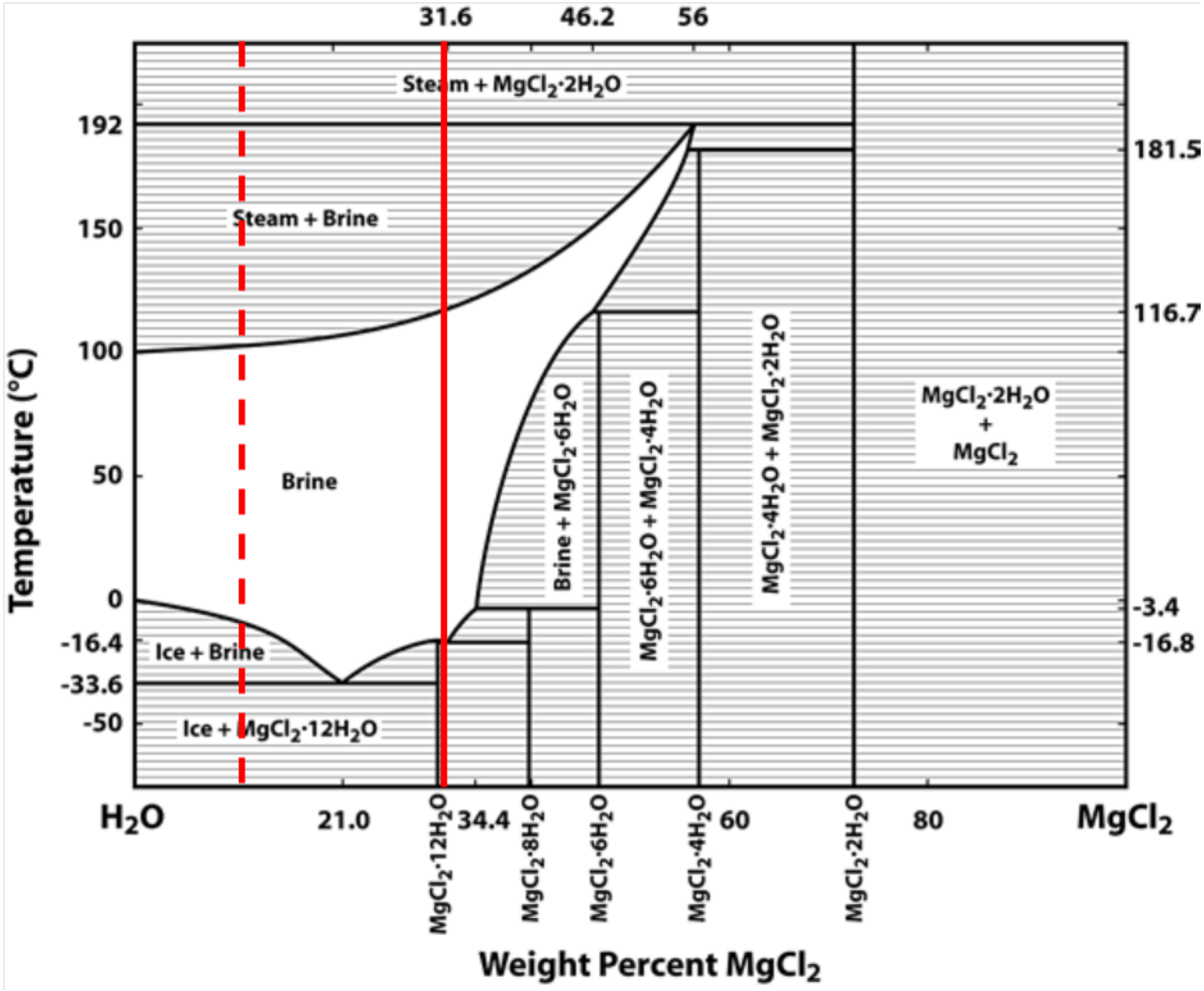

Figure 2.2-1 - $MgCl_2$-H_2O phase diagram (the solid line represents as-received solution concentration and the dashed line the diluted solution concentration for the current study) [16]

There are numerous solid phases that exist between about 30% $MgCl_2$ in H_2O and 80% $MgCl_2$ in H_2O, seen in Figure 2.2-1. Due to this complexity, there is a wide variety of possible phases existing during application based on the actual concentration of the solution and the temperature. While most solutions would be expected to be below 35% $MgCl_2$, it is possible that there may be some evaporation which can cause higher concentrations. Even at concentrations below 35% $MgCl_2$, there are three solids including ice, as well as two eutectic

reactions, leaving a variety of possible combinations depending on actual concentration and temperature.

The reaction of magnesium chloride with the paste in concrete has been thoroughly investigated due to the significant detrimental effects it causes. The work of Frigione and Sersale [**8**] as well as work of Kurdowski [**7**] shows the reaction of $MgCl_2$ with $Ca(OH)_2$ (also known as portlandite), a component of the cement paste phase of concrete:

$$MgCl_2 + Ca(OH)_2 \rightarrow Mg(OH)_2 + CaCl_2$$

Equation 2.2-1 [3**]**

The products of this reaction are calcium chloride and magnesium hydroxide, (also known as brucite) [**3**]. Frigione and Sersale found that the brucite had no binding properties, consistent with the lack of binding properties of portlandite [**8**]. Initially, the brucite layer protects the concrete by precipitating in the pores, effectively blocking them and minimizing further penetration of the salt; however, this protective nature is eventually overcome, and the reaction continues [**7**].

The reaction between $MgCl_2$ and $Ca(OH)_2$ is the primary reaction of the brine with concrete. However, if the $Ca(OH)_2$ is consumed, the $MgCl_2$ will begin to react with the calcium-silicate-hydrate (C-S-H) to form magnesium-silicate-hydrate (M-S-H) by the following reaction:

$$MgCl_2 + C\text{-}S\text{-}H \rightarrow M\text{-}S\text{-}H + CaCl_2$$

Equation 2.2-2 [3]

The M-S-H phase has no inherent binding properties or strength due to its gel-like structure which causes significant deterioration of the concrete and subsequent reduction in strength [**8**]. It is a non-cementitious phase [**17**]. Both brucite and M-S-H are expansive and the latter causes softening of the concrete because of its gel-like texture [**3**], [**7**]. While these two products are known to cause significant deterioration of the surface as well as replacing the cementitious phases with non-cementitious phases, the reaction also produces calcium chloride, which is known to have further damaging effects. These effects are described in the following section.

2.2.2 Calcium Chloride ($CaCl_2$)

Although the chloride aspect of $CaCl_2$ is known to have detrimental effects on reinforcing steel, it is used not only in anti-icing and de-icing but also as a set and hardening accelerator [**18**], [**19**]. The $CaCl_2$, usually in amounts of 2% to 5% by weight of cement, helps increase set time in cold weather which reduces the time the concrete must be protected as well as minimizing the time to use of the structure. It has been found to have a set retarding effect not only in ordinary portland cement but also in high alumina cement, calcium-alumino-fluorite cement, and slag cements [**19**]. While these may be beneficial, the $CaCl_2$ is known to react with the $Ca(OH)_2$ phase by the following reaction:

$$CaCl_2 + 3Ca(OH)_2 + 9H_2O \rightarrow 3CaO{\cdot}CaCl_2{\cdot}12H_2O$$

Equation 2.2-3 [2]

The resultant product, $3CaO{\cdot}CaCl_2{\cdot}12H_2O$, is known as calcium hydroxy-chloride which is an expansive, complex salt [**2**]. Through the work of Poursaee, Laurent, and Hansson it was found that the application of a combination of 3% followed by 35% $CaCl_2$ solution to mortar created sufficient expansive pressure to cause the sample to fracture in numerous locations, leaving the appearance as though the sample had exploded [**1**]. The image of one of the samples is shown in Figure 2.2-2.

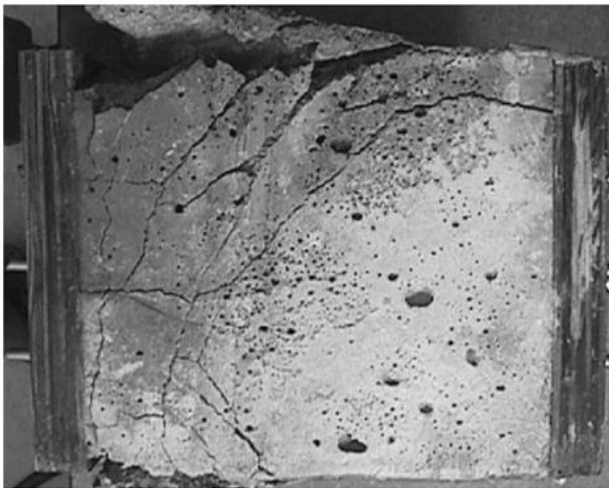

Figure 2.2-2 - Fracture of mortar specimen caused by $CaCl_2$ [1]

The samples were constructed with mortar as opposed to concrete, with a 0.5:1.0:3.0 water:cement:sand ratio [**1**].

The $CaCl_2$-H_2O system is one of the most favourable systems for anti-icing and de-icing applications due to its low-temperature eutectic point and mid-range liquidus slope sharpness as compared to other solutions, as seen in Figure 2.2-3 from Brady [**16**].

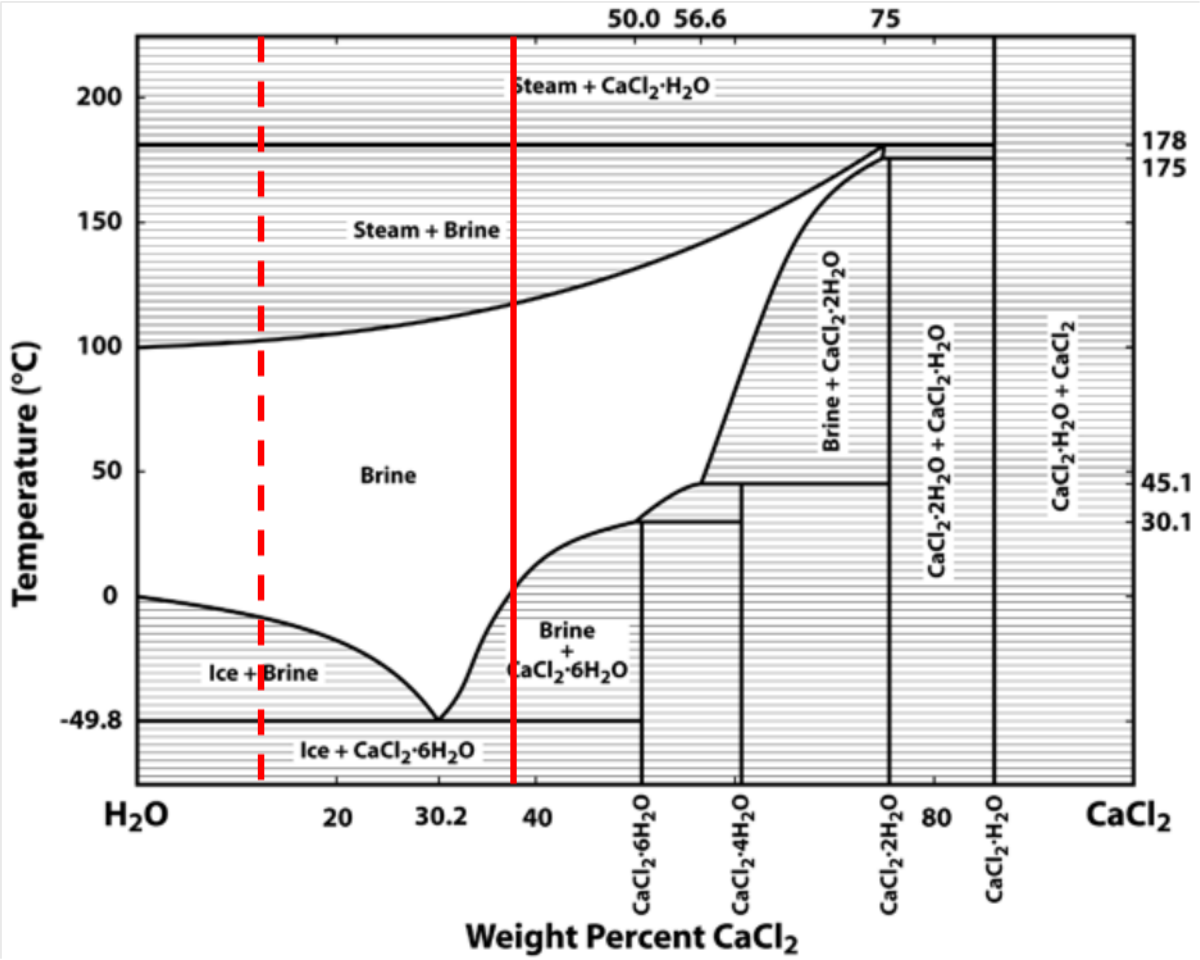

Figure 2.2-3 - $CaCl_2$-H_2O phase diagram (the solid line represents as-received solution concentration and the dashed line the diluted solution concentration for the current study) [16**]**

As seen in Figure 2.2-3, the eutectic temperature of the system is around -50°C (it is listed in this figure as -49.8°C, though -51.1°C is a more commonly accepted value for this point), which makes it the lowest of the three commonly used anti-icing salts – $MgCl_2$, $CaCl_2$, and NaCl.

2.2.3 Sodium Chloride (NaCl)

Unlike magnesium and calcium chloride solutions, sodium chloride has been found to be much less detrimental to the properties of concrete [**6**], [**17**]. Due to its lower hygroscopic nature, the reactions with NaCl will form higher density (and thus lower volume) crystals, than those of $MgCl_2$ and $CaCl_2$ [**6**]. The ingress of NaCl into concrete can result in an increase of pH of the pore to greater than 13.5, which is beneficial to embedded steel reinforcement [**20**]. This elevation of pH is due to the formation of Na(OH), which is known to have a pH above 13.5 [**21**].

As pertaining to the phase diagram, seen in Figure 2.2-4, the NaCl-H_2O system is notably different than the $MgCl_2$-H_2O and $CaCl_2$-H_2O systems [**16**]. The NaCl system has a much smaller brine region than the other two solutions, minimizing the concentrations at which it is effective. NaCl also shows the highest eutectic temperature, making it the least effective with regards to temperature variance as well.

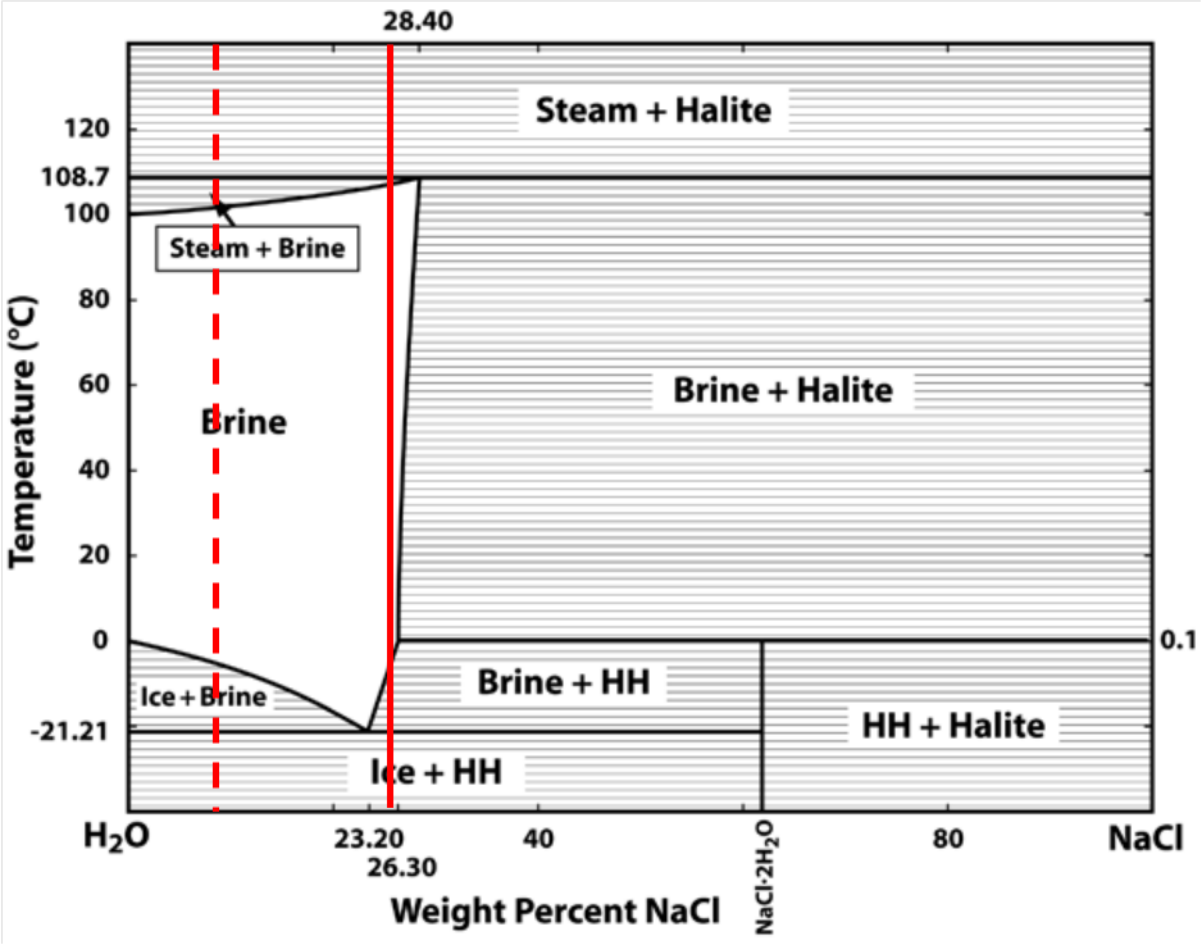

Figure 2.2-4 - NaCl-H_2O phase diagram (the solid line represents as-received solution concentration and the dashed line the diluted solution concentration for the current study) [16**]**

2.2.4 Multi-Chloride

The multi-chloride brine used in Ontario is predominantly a mixture of NaCl and $CaCl_2$, with some $MgCl_2$ and potassium chloride (KCl) also present. A literature search has not uncovered any research on this mixture as an anti-icing agent.

2.2.5 Salt Scaling

Salt scaling, the removal of flakes of surface material from concrete structures due to freezing and thawing in the presence of salt solutions, is a common mechanism by which salt solutions are known to cause damage to concrete [**22**], [**23**],[**24**]. The layer of damage is generally about one millimeter in depth caused by the freezing of salt solution with greater than one percent salt in the liquid solution [**22**]. Valenza and Scherer postulate that the cause of the damage is based on the difference in coefficient of thermal expansion between the concrete and the ice, where the greater expansion of the ice causes tensile stresses in the surface of the concrete. The presence of brine pockets in the ice makes it more susceptible to cracking and, if that crack were to reach the surface of the concrete, it may cause damage to the surface layer of the concrete [**22**]. The crystallization of salt in pores within the concrete, known to cause potentially harmful internal damage, may also play a contributing role in the damage due to salt scaling [**24**], [**25**]. While a salt concentration above one percent in solution can lead to salt scaling, high solute concentration will decrease or eliminate the volume fraction of ice and can make the frozen layer too weak to apply a consistent stress, thus avoiding damage [**22**]. The result of salt scaling is the removal of surface material, eventually exposing the course aggregate. Scaling may continue between the aggregate though will appear to slow due to the decreased surface area of hydrated cement paste. It has been shown by Valenza and Scherer that sufficient scaling can lead to sufficient loss of mechanical properties to cause failure of the entire component, not just the surface [**23**].

3 Experimental Procedure:

3.1 Materials

3.1.1 Concrete Mixture Design

The concrete used in this study is the equivalent to the standard concrete mixture design specified for highway bridge construction in Ontario. The mix is adjusted to allow for 12.7 mm (1/2 in) aggregate as opposed to the more commonly used 19.06 mm (3/4 in) aggregate. The mixture design is given in Table 3.1-1:

Table 3.1-1 - Concrete mixture design

Constituent	Amt/m^3
Gravel (12.7mm, 0.5in)	1045 kg
Sand	705 kg
Cement (GU (US Type 1))	297 kg
Slag	98 kg
Air Entraining Agent	237 mL
Low-Range Water Reducer	800 mL
Water	155 L

All concrete was mixed, cast, compacted and cured according to ASTM C192 [**26**] and OPSS 1350 [**27**]. The different specimens are described in the sections below. The specific details of each cast – including mass of each material, air volume, slump, and curing conditions – are shown in Appendix A in Table A.1-1 through Table A.1-9. Note that the chloride penetration blocks were cut from the leftover prisms from the first set of freeze and thaw prisms. The 28-day strength measurements from each batch of concrete are shown in Appendix B in Table B.1-1.

3.1.2 Anti-Icing Solutions

The influence of the four solutions on the integrity of concrete has been investigated using a variety of mechanical, chemical, and microscopy techniques. The solutions considered representative of the most commonly used solutions in Ontario, Canada, include: sodium chloride (listed as 22% salt solution), calcium chloride (listed as 29% salt solution), magnesium chloride (listed as 22% chloride), and a multi-chloride brine mainly composed of sodium and calcium chloride. The solutions used are Ministry of Transportation of Ontario specified and were provided by individual municipalities from the in-use product batches. The concentrations of major ions in each solution were analyzed by Activation Laboratories Inc. using inductively coupled plasma (ICP) and ion chromatography (IC), and are listed in Table 3.1-2:

Table 3.1-2 - Anti-icing solution major elements

Analyte Symbol	K	Mg	Ca	Fe	Na	S	Sr	Cl	Br	SO_4
Unit Symbol	mg/L	mg/L	mg/L	mg/L	mg/L	mg/L	mg/L	mg/L	mg/L	mg/L
$CaCl_2$	7500	< 10	134000	1.14	4490	< 100	2450	245000	3140	83.4
$MgCl_2$	1640	82100	98.6	4.34	1650	539	4.22	233000	3730	1470
Multi-Chloride	5990	9940	58500	3.57	46100	< 100	1110	211000	2640	125
NaCl	172	157	1840	< 1	98000	1030	26.6	157000	< 50	2970

From the results shown in Table 3.1-2, the elements can be divided into two groups: cations, which include potassium (K), magnesium (Mg), calcium (Ca), iron (Fe), Sodium (Na), sulphur (S), and strontium (Sr); and anions, which include chlorine (Cl), bromine (Br), and sulphate (SO_4). The results shown in Table 3.1-2 represent the elements and compounds with significant concentrations. Other elements analyzed include: Barium, aluminum, manganese, silicon,

silver, Arsenic, beryllium, bismuth, cadmium, Cesium, cobalt, copper, lithium, molybdenum, nickel, phosphorus, lead, antimony, selenium, tin, tellurium, titanium, thallium, uranium, vanadium, tungsten, yttrium, zinc; and anions: fluorine, nitrite, nitrate, and phosphate.

Considering the elements present in Table 3.1-2, it is interesting to note that the $CaCl_2$, $MgCl_2$, and multi-chloride each have relatively high concentrations (1640-7500 mg/L) of potassium probably as KCl, while there is a very small amount (172 mg/L) present in the NaCl solution. Considering magnesium, there is a negligible amount in the $CaCl_2$ and a relatively low amount (157 mg/L) in NaCl, with an intermediate amount (9940 mg/L) in the multi-chloride solution. The third cation present in bulk, calcium, is the highest concentration cation in the multi-chloride solution (58,500 mg/L), but shows low amounts in the $MgCl_2$ and NaCl (98.6 mg/L and 1840 mg/L respectively). The fourth common element, iron, showed small amounts (1.14-4.34 mg/L) in the $CaCl_2$, $MgCl_2$, and multi-chloride solutions, but similar to potassium, showed a very low level (<1 mg/L) in the NaCl solution. The fifth element returning high results is sodium, which was in intermediate concentration (46,100 mg/L) in the multi-chloride, and low concentration – 4,490 mg/L and 1,650 mg/L – in the $CaCl_2$ and $MgCl_2$, respectively. The sulphur levels were generally low (529-1030 mg/L), with the calcium and multi-chloride solutions showing <100 mg/L. An interesting result was the presence of strontium in the solutions. While the $MgCl_2$ and NaCl showed low levels (4.22-26.6 mg/L), both solutions containing higher levels of $CaCl_2$ showed elevated levels of strontium (1,110-2,450 mg/L). It is thus hypothesized that the strontium is present with calcium salts.

Considering the anions, there is a higher concentration of chloride than the nominal amount in all four solutions. The $MgCl_2$ and $CaCl_2$ solutions contain almost double the volume as NaCl (245,000mg/L and 233,000mg/L versus 157,000 mg/L respectively), while the multi-chloride showed an intermediate amount of chlorine (211,000mg/L). These results are expected as $CaCl_2$ and $MgCl_2$ contain two chlorine atoms for each cation, where the NaCl as has a one-to-one ratio. These results are extended to the multi-chloride, where a mixture of salts is seen, but is predominantly composed of $CaCl_2$ and NaCl, thus resulting in a concentration between the two for chlorine ions. Small amounts of bromide (2,640-3,730mg/L) are found in the $CaCl_2$, $MgCl_2$, and multi-chloride, but once again negligible amounts in the NaCl solution (<50mg/L). Finally, the sulphate ions were found in low levels in the $MgCl_2$ and NaCl solutions (1,470mg/L and 2,970mg/L respectively), and very low levels in the $CaCl_2$ and multi-chloride solutions (83.4mg/L and 125mg/L respectively) suggesting a trend between calcium and a low probability for sulphates being present in solution.

In general, it seems that there are two trends present with overlapping implications. First, the sodium chloride solution contains lower levels of other elements than do the calcium, magnesium, and multi-chloride solutions. The second general trend is that the additional species in the multi-chloride solution tends to be more similar to the calcium chloride solution than to those in the sodium chloride, even though there are similar amounts of calcium and sodium present in the solution.

The specific solutions used in different regions of the province vary depending on batch and manufacturer, but will remain relatively consistent with those presented above in terms of chloride content due to the eutectic points of the solutions. The ideal concentrations will be close to the eutectic point of the solution, which is the lowest temperature at which the solution remains liquid. This maximizes the anti-icing effectiveness of the solution. The liquidus line, representing the boundary between the pure liquid and liquid-plus-solid regions of the phase diagrams, for each of the salts is shown in Figure 3.1-1, adapted from the reference 28 [**28**].

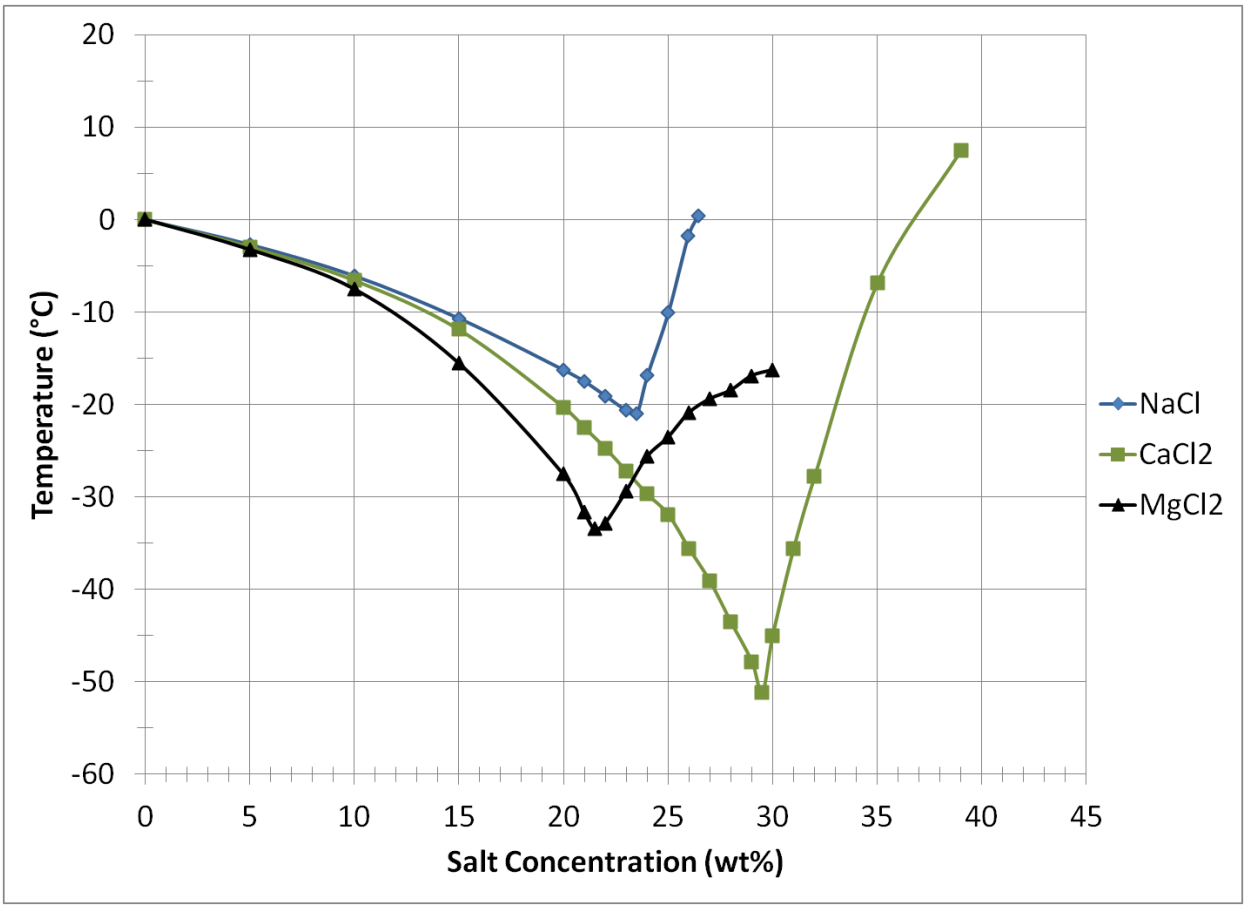

Figure 3.1-1 - Liquidus lines for NaCl, $CaCl_2$, and $MgCl_2$ adapted from United States Department of Transportation [28]

Solutions for a given region are chosen based upon local climate history. As seen in Figure 3.1-1, each solution has its own characteristics with varying slopes and freezing points. In a milder climate, the sodium chloride solution may be most appropriate due to its higher eutectic temperature. In severe climates, the calcium chloride solution may be more appropriate for use as it is able to remain liquid to a much lower temperature than the other solutions. The solution compositions and eutectic point references are provided in Table 3.1-3:

Table 3.1-3 - Overall anti-icing solution composition and eutectic points

	Eutectic Point	Salt % in Solution	Chloride % in Solution
$CaCl_2$	-51°C (-59.8°F) @ 29.8% salt	37.9	**24.5**
$MgCl_2$	-33.9°C (-29°F) @ 21.7% salt	31.51	**23.3**
Multi-Cl^-	N/A	31.56	**21.1**
NaCl (type 1)	-21.1°C (-5.98°F) @ 23.3% salt	25.5	**15.7**

3.2 Test Procedures

To develop an understanding of the effects of the anti-icing agents on the mechanical properties of concrete, eight groups of testing were conducted:

(i) freezing and thawing testing of prisms in anti-icing solutions;

(ii) internal strain and temperature measurement of concrete slabs exposed to anti-icing solution outdoors;

(iii) soaking of cylinders in anti-icing solution followed by compressive strength testing;

(iv) flexural strength testing to provide a modulus of rupture value;

(v) soaking of prisms in anti-icing solution followed by chloride profile analysis;

(vi) pH and chloride penetration analysis of freeze/thaw samples by spray methods;

(vii) environmental scanning electron microscopy (ESEM) for chemical profile; and

(viii) air void and crack analysis of freeze/thaw samples.

3.2.1 Freezing and Thawing

Sixteen concrete prisms, 101.6 mm (4 in) x 76.2 mm (3 in) by 406.4 mm (16 in) in length, were cast, compacted and demoulded after 24 hours. They were cured for a total of 4 weeks under

wet burlap and plastic. Thereafter, they were left in the laboratory atmosphere for 9 weeks until testing.

For freezing and thawing testing, a sealed chamber cycles the temperature between +4°C (+39°F) and -18°C (0°F) approximately every 3.5 hours, according to ASTM C666 [**29**]. The chamber contains 15 sample prisms with a 16^{th} prism used as a temperature control with two probes inside the prism: one monitored by the controller to switch between heating and cooling cycles, and one monitored by a data logger to record temperature variation versus time. The experimental setup can be seen in Figure 3.2-1**Error! Reference source not found.** and Figure 3.2-2. The lid of the freezing and thawing chamber, which is open in Figure 3.2-1, is environmentally sealed when closed. The white spots on the top of the specimens are caused by the grease used to provide contact during measurement of the resonant frequency. The length between supports in Figure 3.2-2 is 230 mm. Three prisms were immersed in each of the four anti-icing solutions, and three prisms immersed in potable tap water. At the end of each week, after approximately 45 to 50 cycles, the prisms were allowed to reach room temperature overnight, rinsed with potable tap water, and then surface dried. The mass of the prism, mass of the collectible debris, and the resonant frequency for elastic modulus determination were then measured. These data were used to calculate the elastic modulus of the prism according to Equation 3.2-1 [**30**].

$$E = \left[\frac{2\pi L^2 f_r}{\beta^2 \frac{t}{\sqrt{12}}}\right]^2 \rho$$

Equation 3.2-1 [30**]**

where:

E = modulus of elasticity

L = length

f_r = resonant frequency

β = constant (4.730 for a rectangular cross-section)

t = thickness

ρ = density

Figure 3.2-1 - Freezing and thawing chamber with lid open, prisms submerged in solution or water

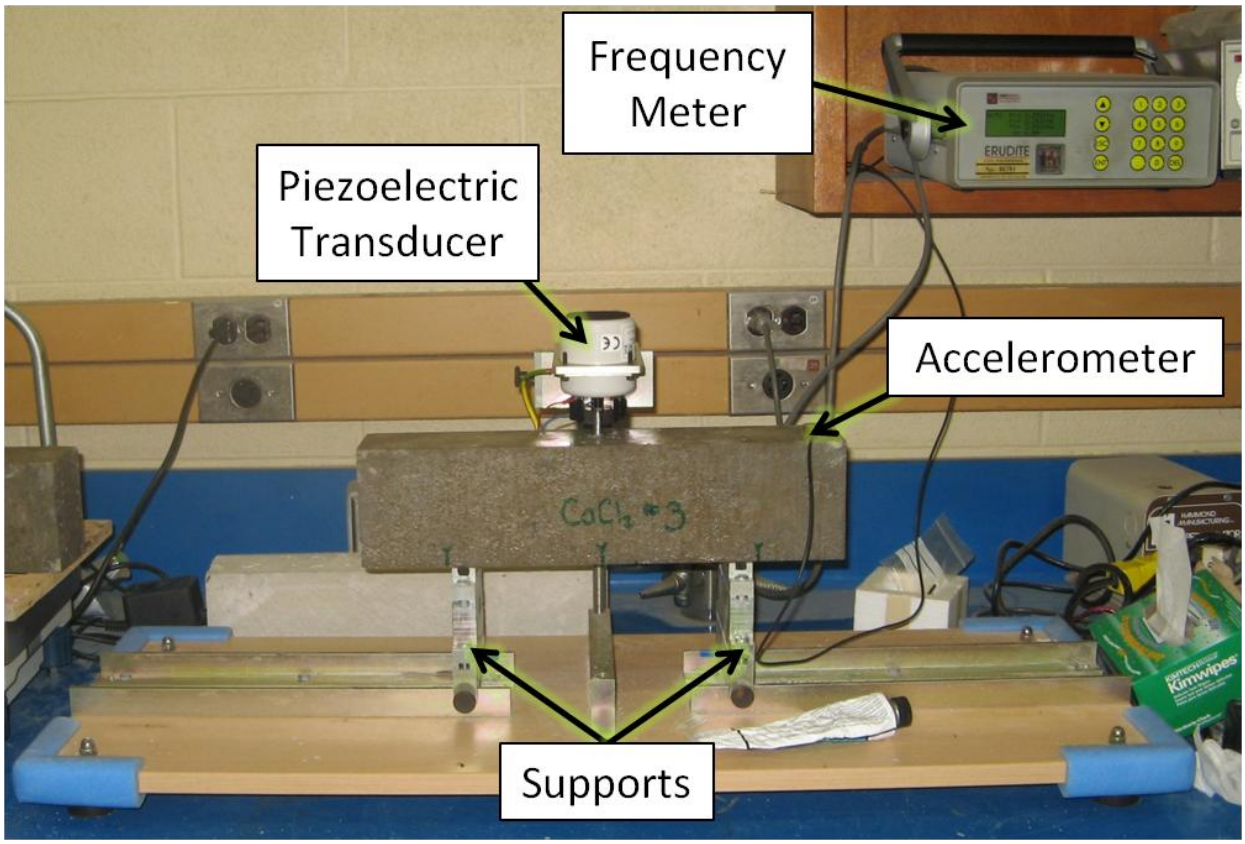

Figure 3.2-2 - Ultrasonic frequency analysis setup

Two sets of freezing and thawing testing were completed; the first with as-received solution as seen in Figure 3.2-3, and the second diluted to one part solution with two parts water as seen in Figure 3.2-4.

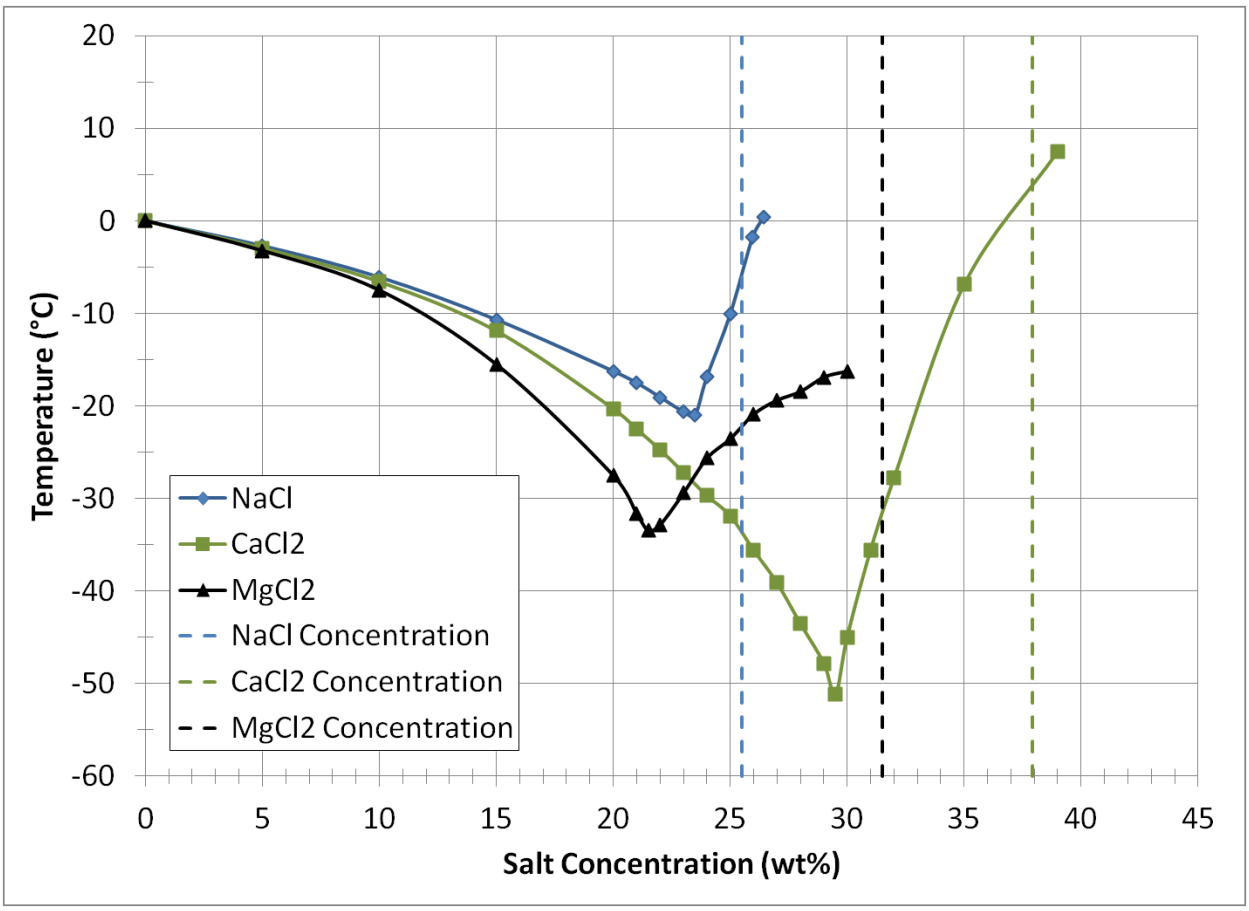

Figure 3.2-3 - Solution concentrations and liquidus lines for as-received solutions

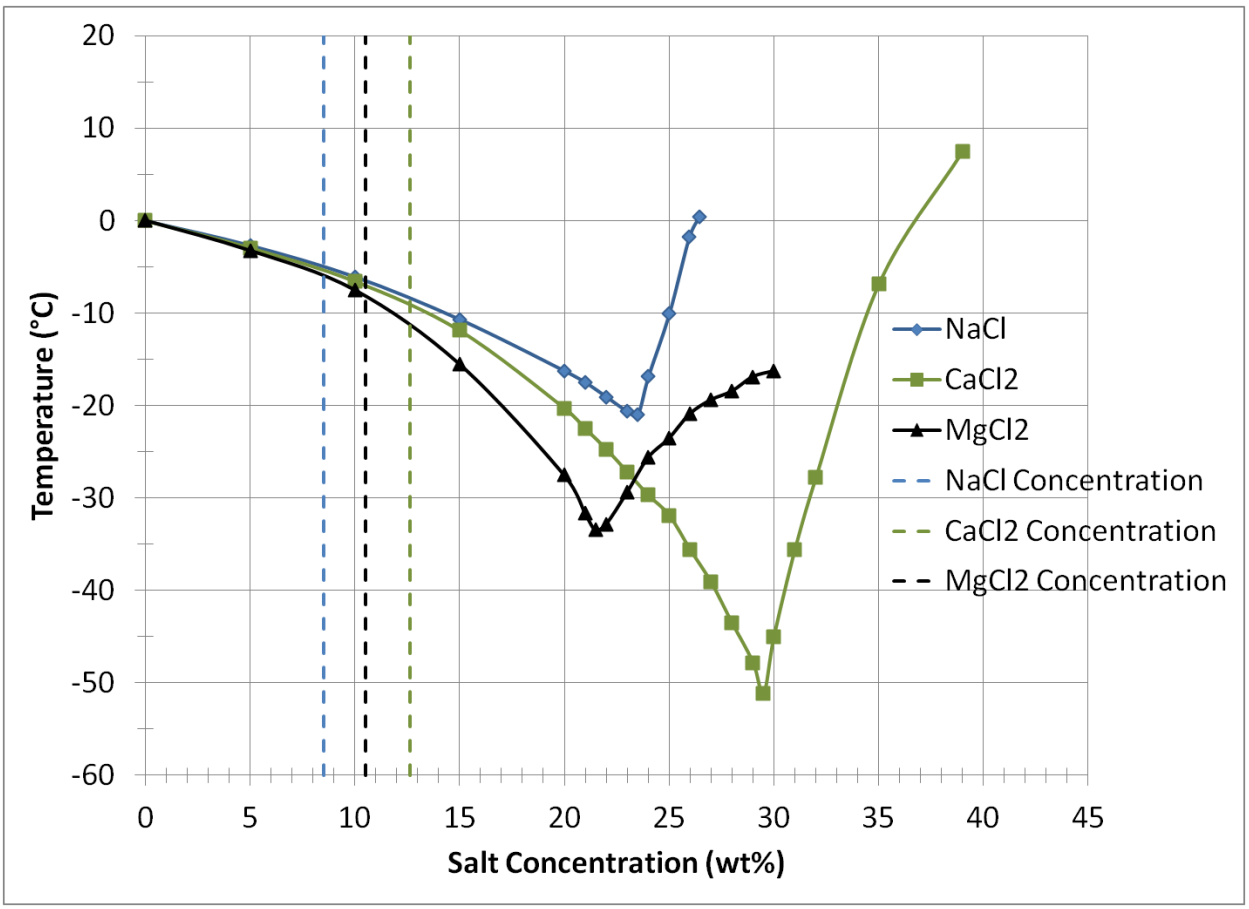

Figure 3.2-4 - Solution concentrations and liquidus lines for diluted solutions

In the initial testing using the as-received solutions, the lowest temperature achieved, -18°C, is in the brine plus salt or eutectic regions for the solutions. In review of Figure 2.2-1, Figure 2.2-3, and Figure 2.2-4, it can be seen that in hypereutectic compositions, the solutions are expected to separate into brine with a precipitated hydro-halite phase. These phases include $CaCl_2 \cdot 6H_2O$ for the calcium chloride solution, $MgCl_2 \cdot 2H_2O$ and/or $MgCl_2 \cdot 8H_2O$ for the magnesium chloride solution, and $NaCl \cdot 2H_2O$ for the sodium chloride solution. It is expected that a combination of these three hydrated salts plus sylvite (KCl) would form in the multi-chloride solution, with $CaCl_2 \cdot 6H_2O$ and $NaCl \cdot 2H_2O$ being the most dominant phases formed.

Due to these phases, ice formation is not expected for these concentrations of solution in the specified test temperature. Only the samples exposed to potable tap water and NaCl solutions exhibited any ice formation during this set of testing. Due to this, the results do not reflect any effects of the solution freezing for the samples exposed to $CaCl_2$, $MgCl_2$, or multi-Cl^- solutions and, thus, the second set used reduced concentrations to achieve ice formation.

At a dilution of one part brine and two parts water, the liquidus temperature of all solutions is higher than -10°C and the concentrations are all hypoeutectic, thus the solutions should partially freeze during each cycle. This is reflected through a consideration of Figure 3.2-4, Figure 2.2-1, Figure 2.2-3, and Figure 2.2-4 on which the diluted concentrations are indicated by the vertical dashed lines. In each case, the solutions will form ice and brine when the temperature falls below the liquidus and this is reflected by the freezing observed at low temperatures during cycling. This dilution of the solutions is intended to reflect precipitation of ice, snow, or rain where the solution would become diluted by the precipitation. The reduction in solution concentrations will affect the diffusion properties, effects of the solutions, and the phase transformations of the solutions.

3.2.2 Internal strain

In order to determine the effects of anti-icing agents on the strain in the concrete and how this relationship is influenced by the ambient temperature, the procedure described below was followed. The specimens were slabs of width 330.2 mm (13 in), length 457.2 mm (18 in), and height 254 mm (10 in) with a cast-in ponding well at the top measuring 228.6 mm (9 in) wide by

355.6 mm (14 in) long by 50.4 mm (2 in) height. Vibrating wire strain gauges with thermistors were cast-in to each slab at three different depths: 50.4 mm (2 in), 76.2 mm (3 in), and 101.6 mm (4 in) below the bottom of the ponding well. The gauges are centred in the width direction, and the gauge at 76.2 mm below the pond is centred in the length direction, with the others four inches towards the ends. During the casting process, the strain gauges were supported by steel wires running through the moulds, a manufacturer-approved support method that will not affect strain measurement. The slabs are illustrated in Figure 3.2-6 and Figure 3.2-7(a). The slabs were wet cured under burlap and plastic for 14 days, after which they were placed outdoors completely exposed to the elements, as shown in Figure 3.2-7(b). The ponding wells were filled seven weeks after casting (5 weeks after outdoor exposure began) and were emptied and re-filled every two weeks. There are five samples, one for each of the four solutions and one with water in the pond as a control reference. After 11 weeks exposure, the ponding wells were left empty for ten weeks and then the ponding wells were filled and refilled as before. The intention of leaving the ponding wells empty was to closer mimic actual application conditions. However, it was elected to restart prior to winter to conditions to maximize effects of salt ingress. Measurements of the internal temperature and strain have been made once per hour for nineteen months via automatic data logger.

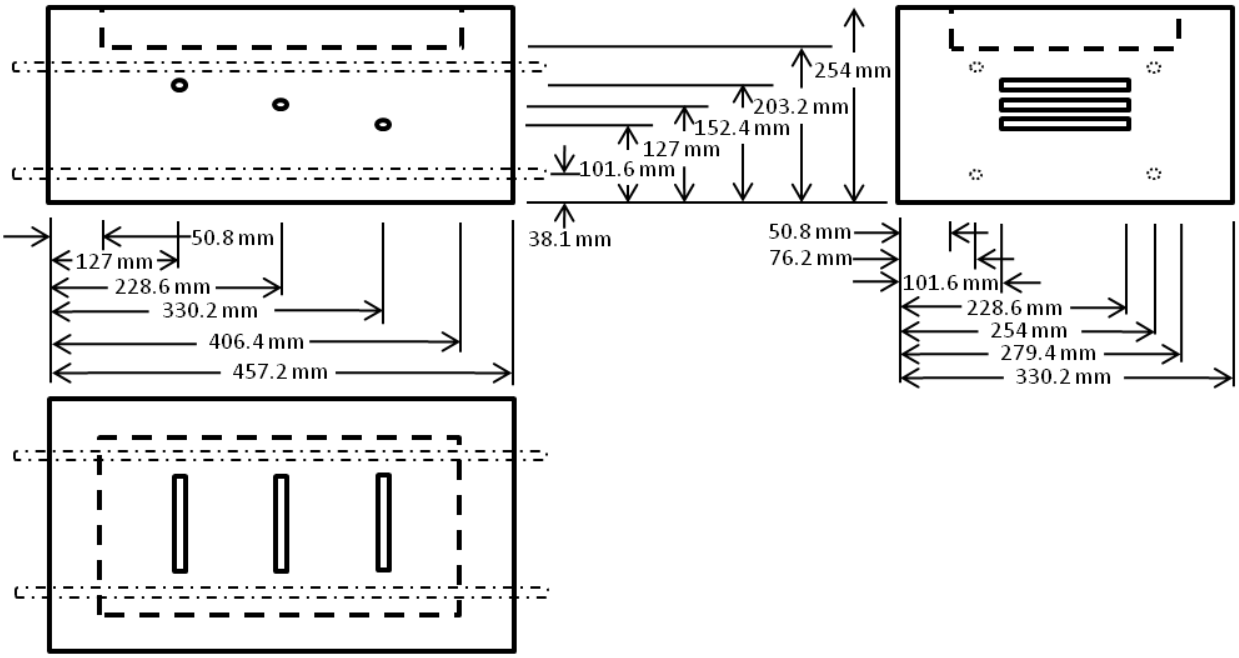

Figure 3.2-5 - Slab design schematic

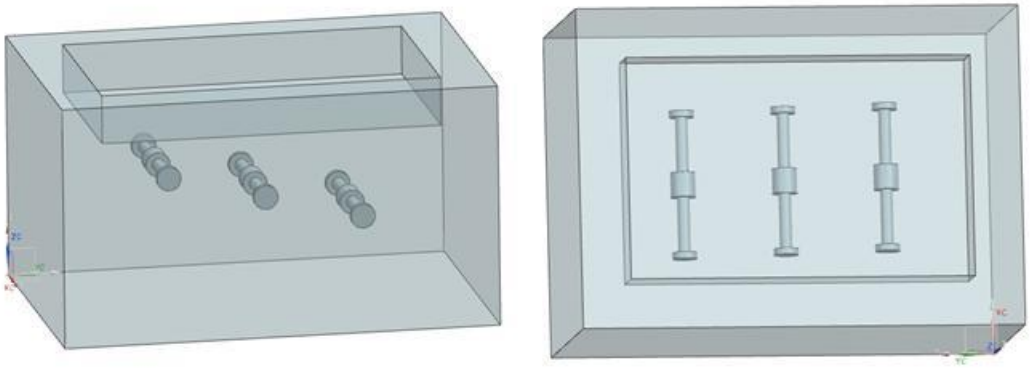

Figure 3.2-6 - Outdoor slab construction. Side view (left), top view (right)

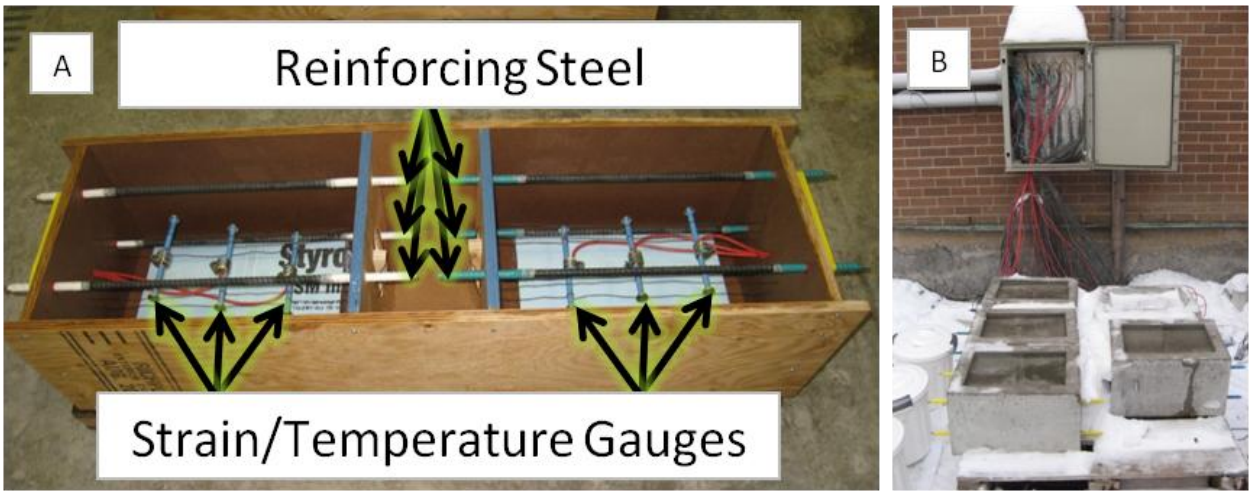

Figure 3.2-7 - (A) Fully constructed mould with gauges, rebar, and ponding well and (B) outdoor slab testing setup

With this setup, the intention is to measure the effects of both the solutions and the environment on the internal strain. By including a control sample with water in the ponding well, the results can be adjusted such that they reflect the summative effects, or the effects of only the salts. By subtracting the equivalent values of the control sample, the remainder can be considered the effects of the salt, above and beyond any natural effects the concrete experienced from curing, temperature and precipitation. The presence of embedded thermistors allows for measurement of temperature at the location of the gauges. This can show the seasonal variations in temperature which may cause additional effects on the strain in the concrete.

3.2.3 Compressive Strength

Two batches of compressive strength testing have been completed with variations to the exposure conditions to understand the effects of the solution on the strength of the exposed concrete. In the first batch, twenty five cylinders, which were 101mm in diameter (4in) and

203mm (8in) in height, were completely submerged in each of the salt solutions after 28 days of curing in a humidity chamber. Twenty five additional cylinders were maintained in the humidity chamber as a reference set for the solution-exposed cylinders. Three samples from each solution and three from the control set were tested in compression according to ASTM C39 [**31**] every two weeks for a total of 16 weeks. The testing apparatus is shown in Figure 3.2-8. The remaining cylinders from each of the solutions and the control set were measured after 37 weeks exposure to determine if trends could be observed.

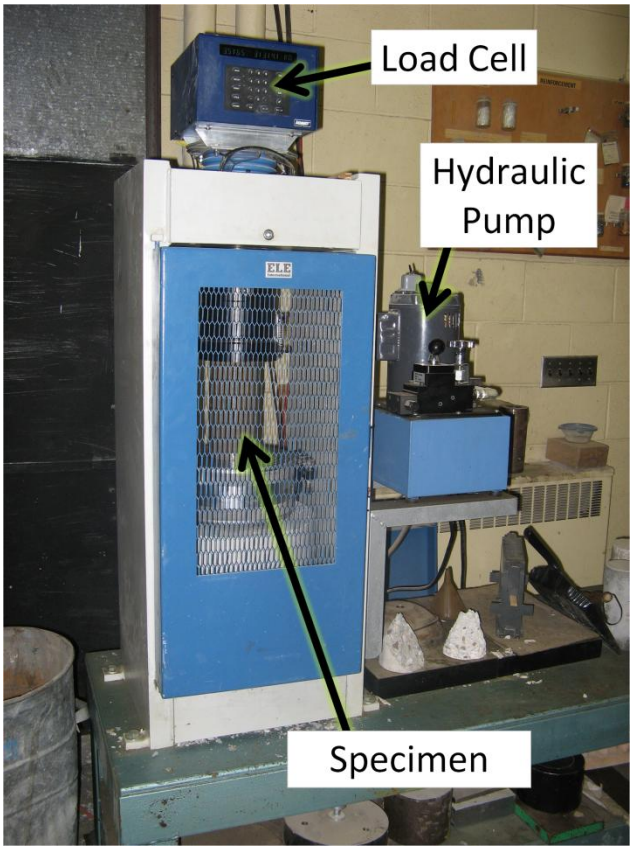

Figure 3.2-8 - Compressive strength testing apparatus

In the second batch of compressive strength testing, the same concentration solutions were used. However, the samples were exposed to alternating wet and dry cycles over two week periods. Samples were allowed to dry for ten days, followed by four days of soaking. Testing for compressive strength was conducted at the end of the wet cycles. In order to extend the period of time over which samples could be tested, 24 samples were exposed to water as control samples while 30 samples were exposed to each of the four solutions. This allowed extension of the test period to 20 weeks for the salt-exposed samples, and maintained the 16 week test period for the control samples. The purpose of switching from continuous soaking to wet/dry cycles is to promote drying of the samples in hopes of increasing the salt ingress into the samples by absorption to maximize the effects.

3.2.4 Tensile Strength

Prisms cast in the same moulds as used for the freezing and thawing test prisms (76.2 mm by 101.4 mm by 406.4 mm) were tested in 3-point bending to determine their tensile strength and modulus of rupture. The preparation of the samples was similar to that for freeze and thaw testing, including a long period of drying prior to baseline testing. A set of three samples were tested for baseline reference data, henceforth referred to as pre-soak samples, which were dry at the time of testing. Following this baseline testing three samples were placed in each anti-icing solution, as well as three in potable tap water. These samples alternated between four days of soaking and three days drying in order to improve chloride penetration. After five months of wet/dry cycling, each of the 15 samples were tested in tension using the same testing procedure as the baseline samples. This procedure involves a load-controlled approach

with a loading rate of 983N/min following ASTM C293 [**32**]. The testing setup is shown in Figure 3.2-9. The gauge length is 304.8 mm (12 in) and the ram is centred on the prism.

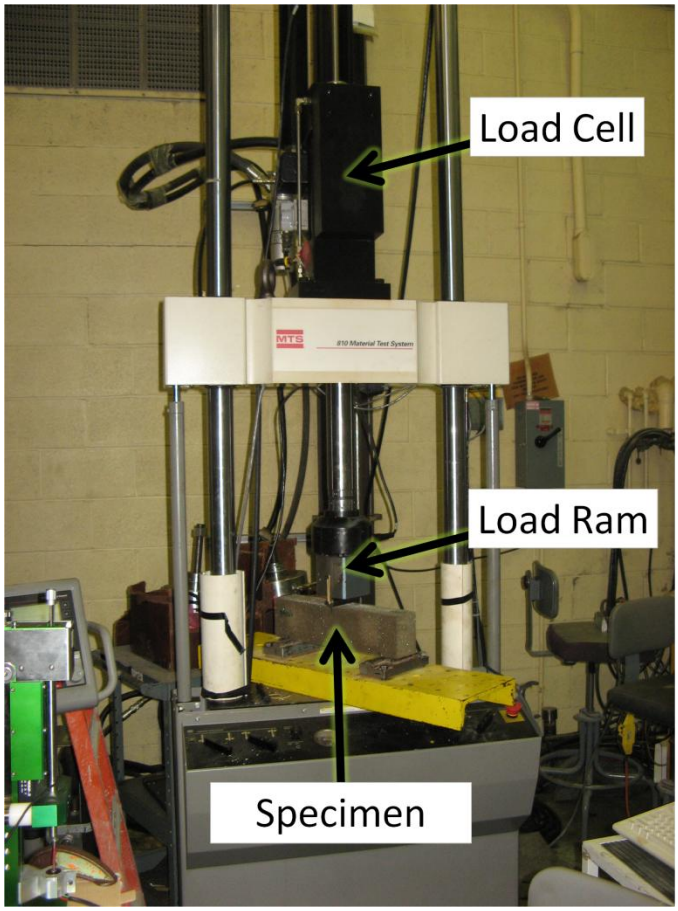

Figure 3.2-9 - Tensile testing apparatus and setup

3.2.5 Chloride Penetration

Simultaneously with the cylinder soaking, 101 mm (4 in) square blocks with a 25 mm (1 in) depth coated with epoxy on five sides to ensure penetration occurred in one direction. They were immersed in the solution and, after two weeks, one specimen was removed from the solution for analysis. The surface was ground incrementally with a profile grinder and the

powdered sample collected for each grinding increment. The profile grinding setup is shown in Figure 3.2-10.

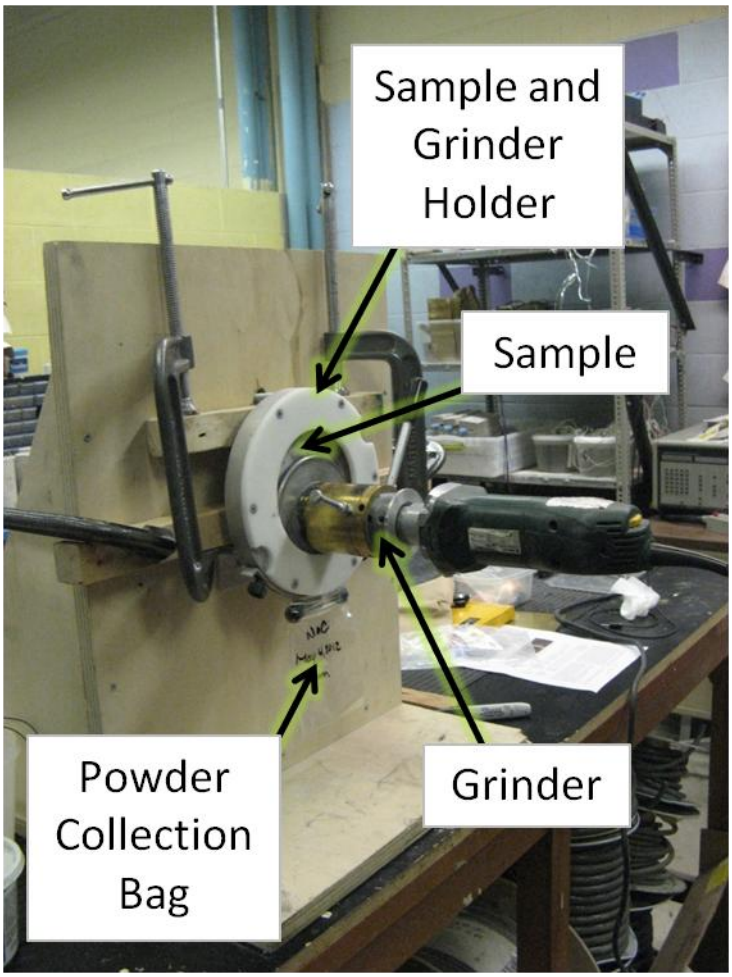

Figure 3.2-10 - Profile grinding equipment and setup

Samples were taken over a 77 mm (3 in) diameter from: 0-1 mm (0-0.04 in), 1-2 mm (0.04-0.08 in), 2-4 mm (0.08-0.16 in), 4-6 mm (0.16-0.24 in), 6-8 mm (0.24-0.32 in), 8-10 mm (0.32-0.39 in) depth from the exposed surface. This procedure was repeated after a further 17 week soaking period (19 weeks exposure), as well as another 40 weeks (59 weeks exposure). The powders

were analyzed using a chloride selective electrode to establish the chloride content of each powder. An image of the blocks following grinding is shown in Figure 3.2-11.

Figure 3.2-11 - Post-grinding chloride penetration samples

3.2.6 pH and Chloride Penetration by Spray Methods

As prescribed by Otsuki et al. [**33**], the application of a 0.1M silver nitrate ($AgNO_3$) solution to a fracture surface of concrete exposed to chlorides can provide a visual indication of the depth of penetration of the chlorides. Following the completion of the second batch of freeze and thaw testing, the prisms tested through the process were split in half using a sledge hammer and the fracture surfaces sprayed – one with $AgNO_3$ to measure chloride penetration, and the other with pH indicator spray.

Figure 3.2-12 - pH (top) and $AgNO_3$ (bottom) spray indicators on concrete specimens

3.2.7 Energy Dispersive X-Ray Spectroscopy (EDS)

Usually a standard scanning electron microscope (SEM) with energy dispersive x-ray spectroscopy (EDS) is used for analyzing the surface microstructure of a sample. With a standard SEM and EDS setup, the surface of the material must be conductive in order to prevent charging by the electron beam. In the case of concrete, where the surface is non-conductive and application of a conductive paint would reduce the viability of EDS, an environmental scanning electron microscope (ESEM) can be used. The ESEM uses a humidified chamber to produce a similar effect to the conductive coating on the material which allows for EDS to be applied to the sample to create a profile of the constituents as well as high-resolution

imaging of the sample. Through the use of ESEM, a slice from the chloride penetration samples was analyzed to determine the composition profile for eight key elements: calcium, silicon, magnesium, aluminium, iron, sodium, potassium, and chlorine. Through this analysis, a further chloride penetration profile can be measured, while element mapping can show where the varying elements are in higher and lower concentrations. This variation is most apparent at paste-aggregate boundaries where there will be notable differences in composition on either side of the interface. The ESEM setup can be seen in Figure 3.2-13.

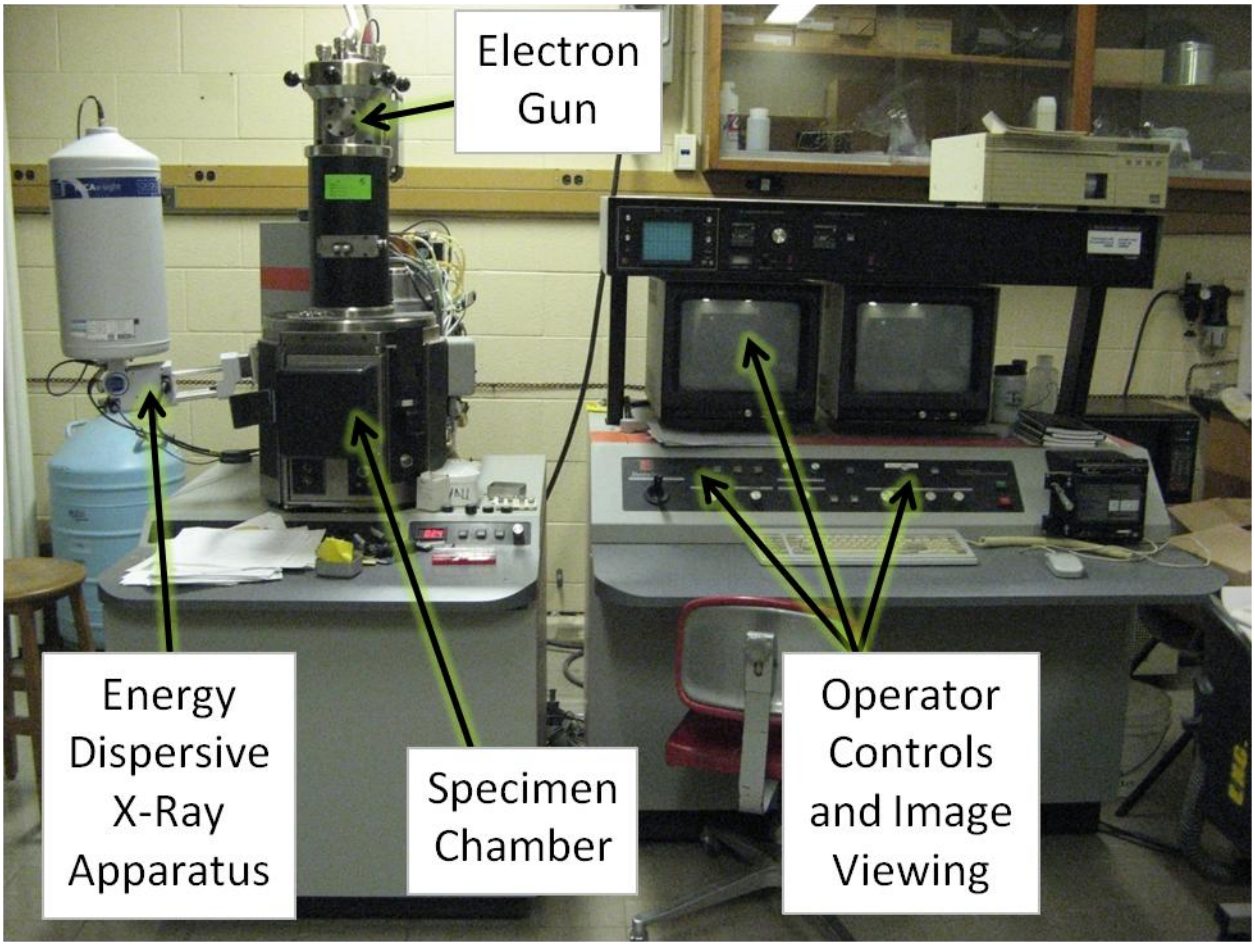

Figure 3.2-13 - Environmental scanning electron microscope with energy dispersive x-ray spectroscopy setup

3.2.8 Air Void and Crack Analysis

There are two important microstructural factors that should be analyzed when dealing with concrete exposed to chloride solutions: the state of pores and air voids in the concrete, and whether there is significant crack formation. With respect to air voids and pores, the presence of these voids in concrete allows for concrete to freeze and thaw without the expansive freezing process causing immediate failure of the concrete structure. The pore fluid is able to expand within the pores when it freezes, preventing the expansive pressures it would cause if there was a lack of pores and air voids. This requires that the pores and voids be free of other materials, such as crystallized salts, which would consume the space otherwise necessary for freezing expansion. By analyzing a cross section, it can be seen whether these pores have been filled with crystallized salts or whether they remain free. The presence of cracks can be due to a number of factors but most importantly due to two factors as pertaining to chloride solutions: filling of the pores with crystallized salt eliminating space for expansion, or the expansive reaction of the salts with the concrete constituents. With respect to the air void and crack analysis testing, the samples were cut from freeze and thaw prisms, which may have potentially undergone both freezing expansion pressures as well as reaction pressure.

The equipment used is an air void analyzer which can also create a magnified image of a polished concrete surface, which will allow for the air voids and cracks to be clearly seen. The polishing equipment and air void analyzer can be seen in Figure 3.2-14 and Figure 3.2-15, respectively.

Figure 3.2-14 - Sample polishing equipment

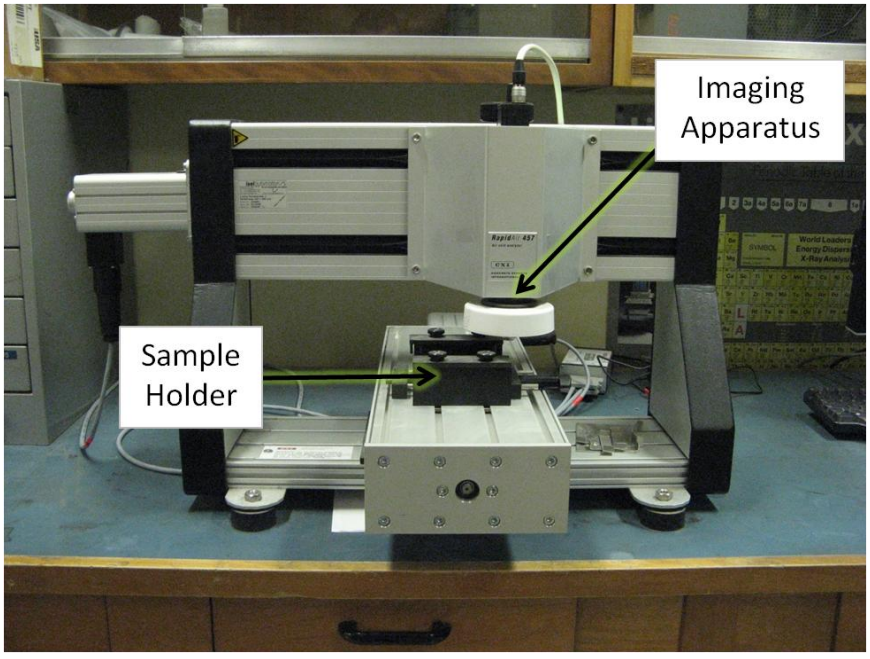

Figure 3.2-15 - Air void analyzer

4 Results:

4.1 Freezing and thawing

The freezing and thawing testing provided a number of data sets representing various aspects of the material properties. The most important of these are the resonant frequency, F_r, of the prisms and the mass after each period of freeze thaw cycling. The ultrasonic equipment also measures the frequency points F_l and F_h, which represent the locations greater and less than the resonant frequency where the frequency of the concrete has fallen to 0.707 of the resonant frequency. Finally, a damping coefficient, Q, is provided which is defined by the following equation:

$$Q = \frac{F_r}{F_h - F_l}$$

Equation 4.1-1

An example of these data, taken from the $MgCl_2$ prism #3 from the second set of prisms measured, can be seen in Figure 4.1-1. The data for all prisms are given in Table B.2-1 through Table B.2-8 in the appendices. The recorded temperature profiles from inside the chamber for Set 1 and Set 2 are shown in Appendix B in Figure B.2-1 and Figure B.2-2, respectively.

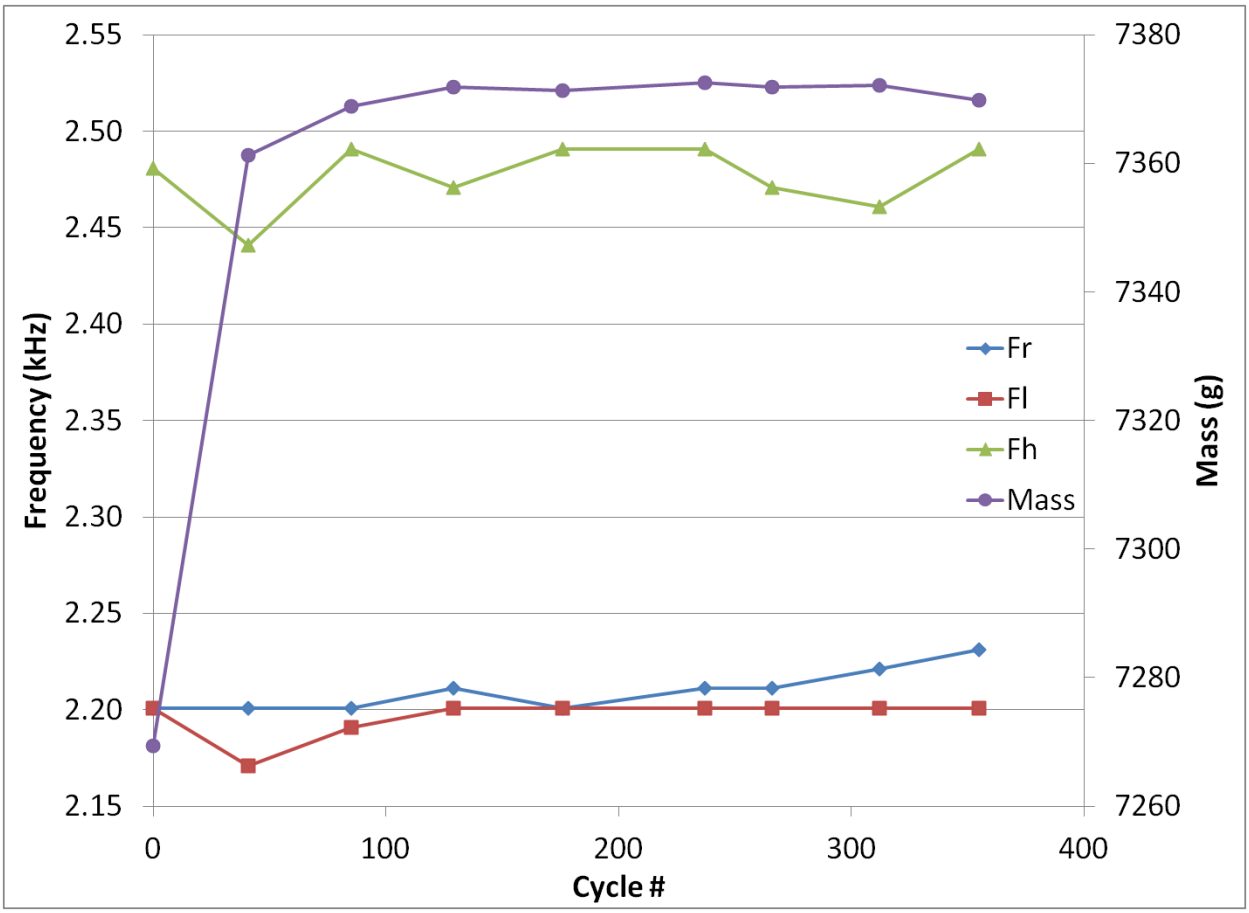

Figure 4.1-1 - $MgCl_2$ prism 3, Set 2 data set from freeze and thaw testing

The average elastic modulus results for each of the four solution types at full concentration and the water set can be seen in Figure 4.1-2. It is clear that there is a general increasing trend initially, followed by a plateau for the prisms exposed to $CaCl_2$, $MgCl_2$, and the multi-chloride. Conversely, the elastic modulus of the prisms exposed to water decreased from the initial value. Those prisms exposed to the sodium chloride solution decreased initially, similar to the water samples, and then increased in a similar manner to the other samples exposed to salt solution.

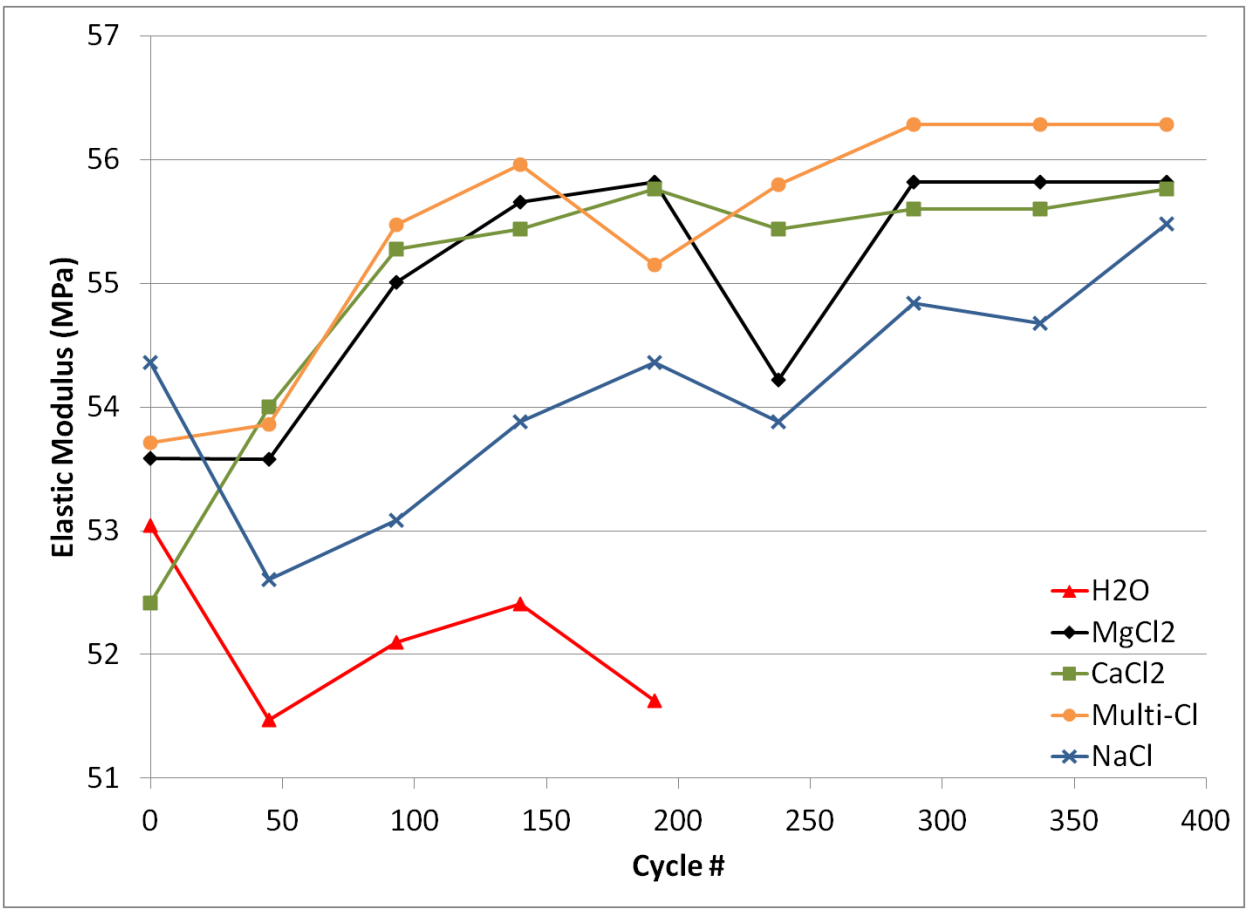

Figure 4.1-2 – Average elastic modulus of prisms in as-received solutions as a function of freezing and thawing cycles

The measurements on the prisms exposed to water had to be terminated around 200 cycles due to the severity of damage to the surface of the samples. The surface degradation was so significant due to the effects of freezing and thawing that a measurement could not be obtained using the ultrasonic equipment. With respect to the uncharacteristic dip at 238 cycles, this is the effect of completing the measurements while the samples were in their cold state as opposed to at room temperature. This is the result a failure of the freeze and thaw chamber thereby keeping the prisms in their coldest state. This problem was solved for subsequent cycles.

The test procedure was repeated a second time with the solution concentration diluted to one-third the as–received solution. The purpose of this repetition was to understand the effects of the solutions when the samples freeze (which was not the case with full strength solution exposure). This was intended to reflect a case where the solution has been diluted by precipitation, which is expected to be common in practice. The elastic modulus results from this testing are shown in Figure 4.1-3.

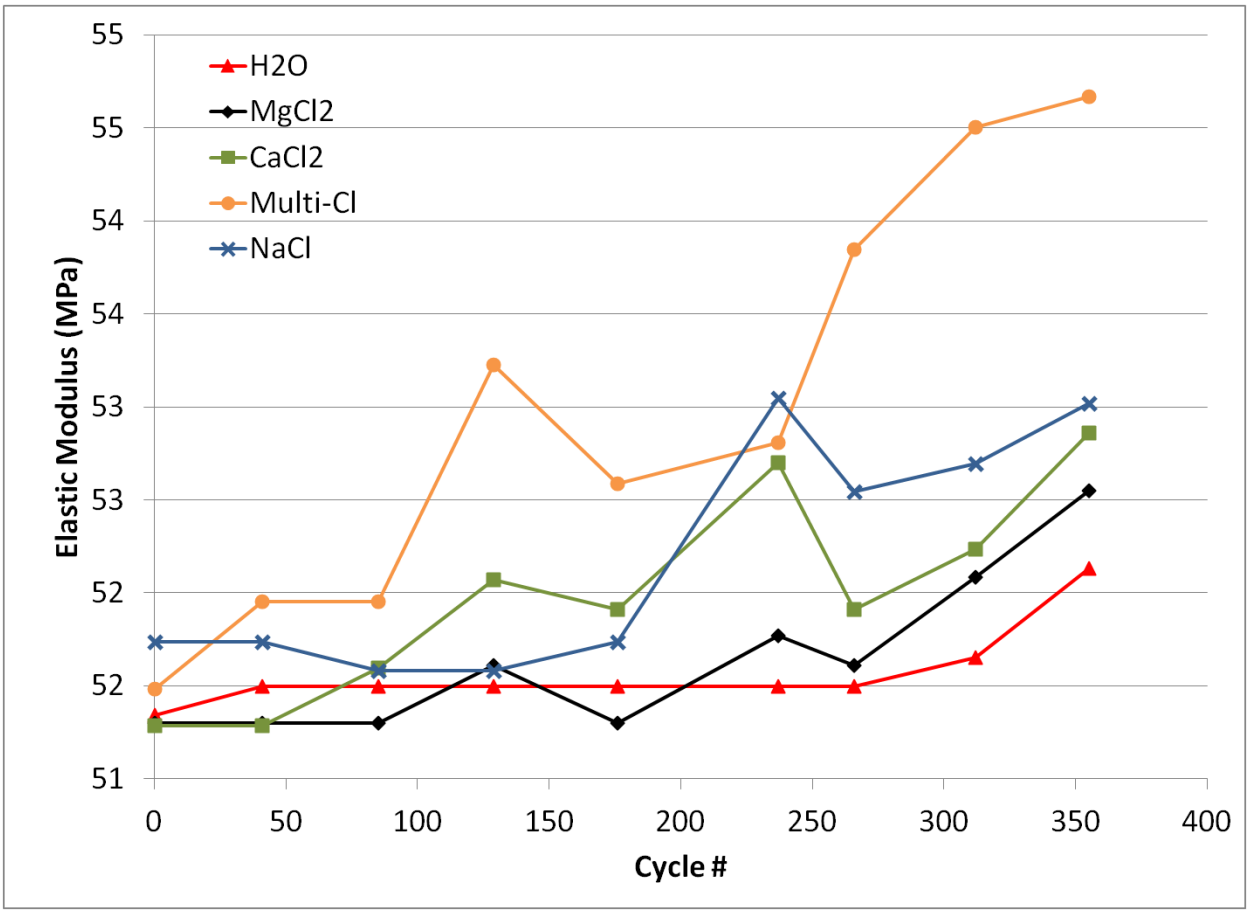

Figure 4.1-3 – Average elastic modulus of prisms in solutions diluted to 1/3-as-received as a function of freezing and thawing cycles

A similar trend to the full-strength testing is seen with the second set when the lower concentration solutions are used; however the period of increase is longer, and less steep. Unlike the first set of prisms, the samples exposed to water did not deteriorate at the same rate, but were able to be measured for the entire period of testing. While there are various factors including the small differences in concrete composition and temperature cycling, it is postulated that this is predominantly the effects of using a vibrating table to consolidate the samples in the second set of prisms instead of a vibrating rod as used for the first set. The use of the vibrating table provides a more effective consolidation, thus resulting in better surface quality. The similarity of results is seen more clearly when the data are plotted on the same axes, as seen in Figure 4.1-4.

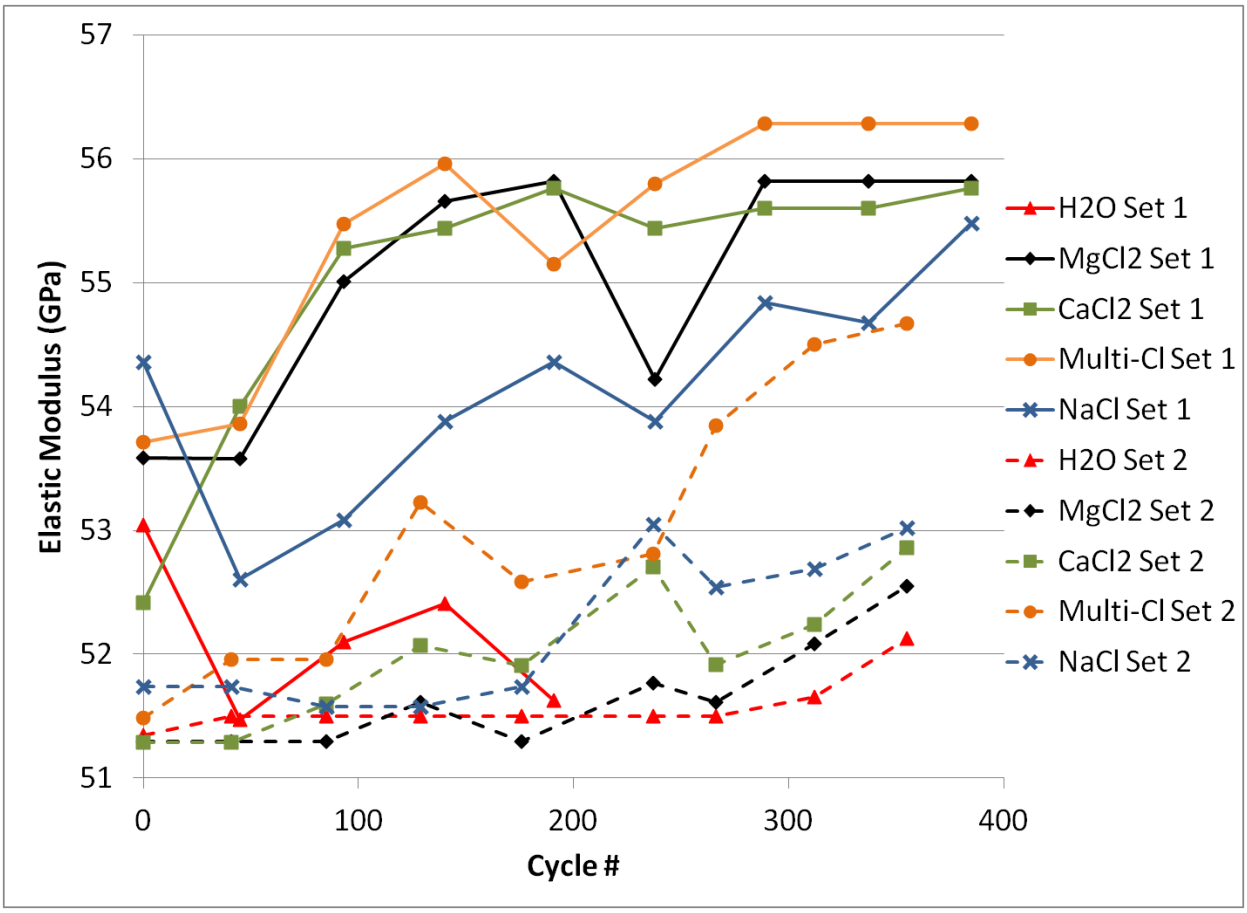

Figure 4.1-4 - Freeze and thaw average elastic modulus per solution, comparison

From these data it can be seen that there is a common increase, however, the second set of prisms exhibited a much slower rate of increase, and do not appear to reach the plateau over the period of testing.

The average mass change data are given in Figure 4.1-5 and present some interesting perspectives with respect to solution penetration. Prior to immersion in the solutions in the test containers, the prisms dried in the laboratory atmosphere for eleven weeks, which accounts for the large initial increase in mass: the first measurements were made while the

samples were dry, and the second after one week wet and cycling. The samples absorbed a significant amount of solution during this time, as indicated by the sharp initial increase in mass shown in Figure 4.1-6. The pre-testing mass values were subtracted from the results for each prism each week for the corresponding prism. The data points for each set of replicate prisms were then averaged. The results of this can be seen in Figure 4.1-5. After the initial increase, there was very little change in mass except for the prisms exposed to water which exhibited significant scaling.

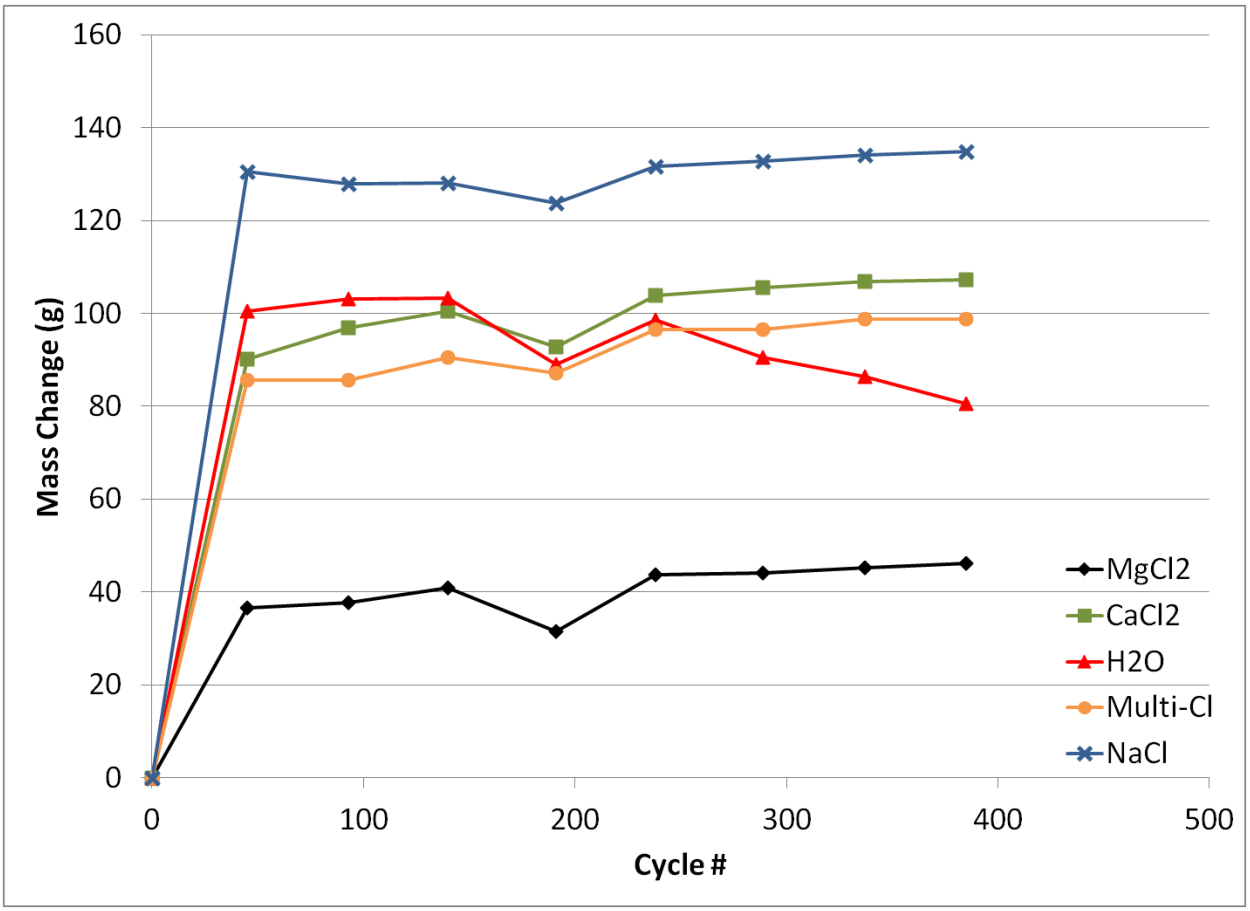

Figure 4.1-5 - Cumulative average mass change of freeze and thaw prisms, Set 1, exposed to as-received solutions

During the second set of freeze and thaw testing there was a notably different trend. In the second set, after a slight initial increase, the mass of the samples exposed to all salt solutions except magnesium chloride decreased similar to the water samples. Aside from the difference in consolidation method, the preparation procedure remained the same; this included using the same mix design and curing process as the first set. The change indicates that the solutions are, in fact, freezing and damage is occurring at the surface of the prisms. This is shown in Figure 4.1-6.

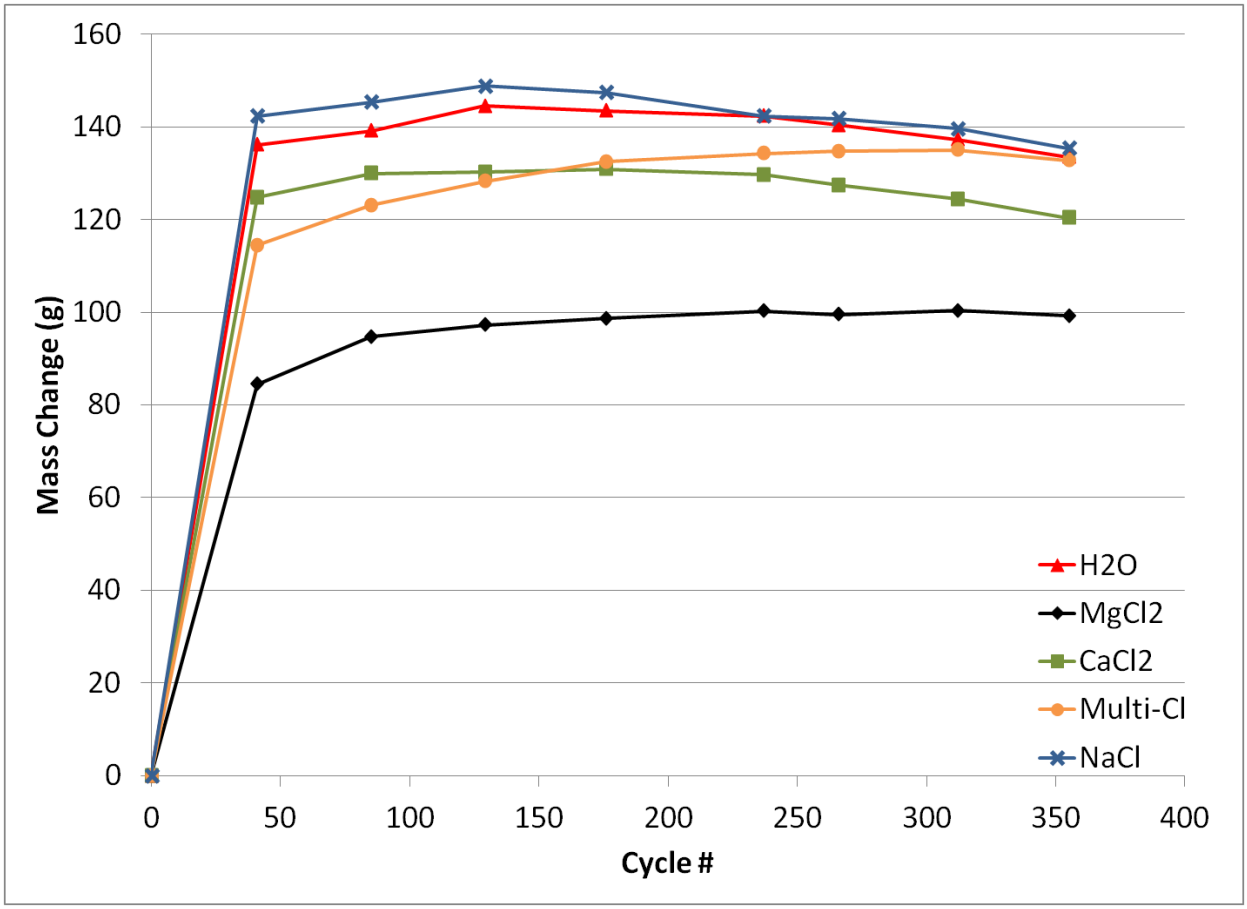

Figure 4.1-6 – Cumulative average mass change of freeze and thaw prisms, Set 2, exposed to diluted solutions

The differences in trends between the two sets of samples are shown most clearly in Figure 4.1-7.

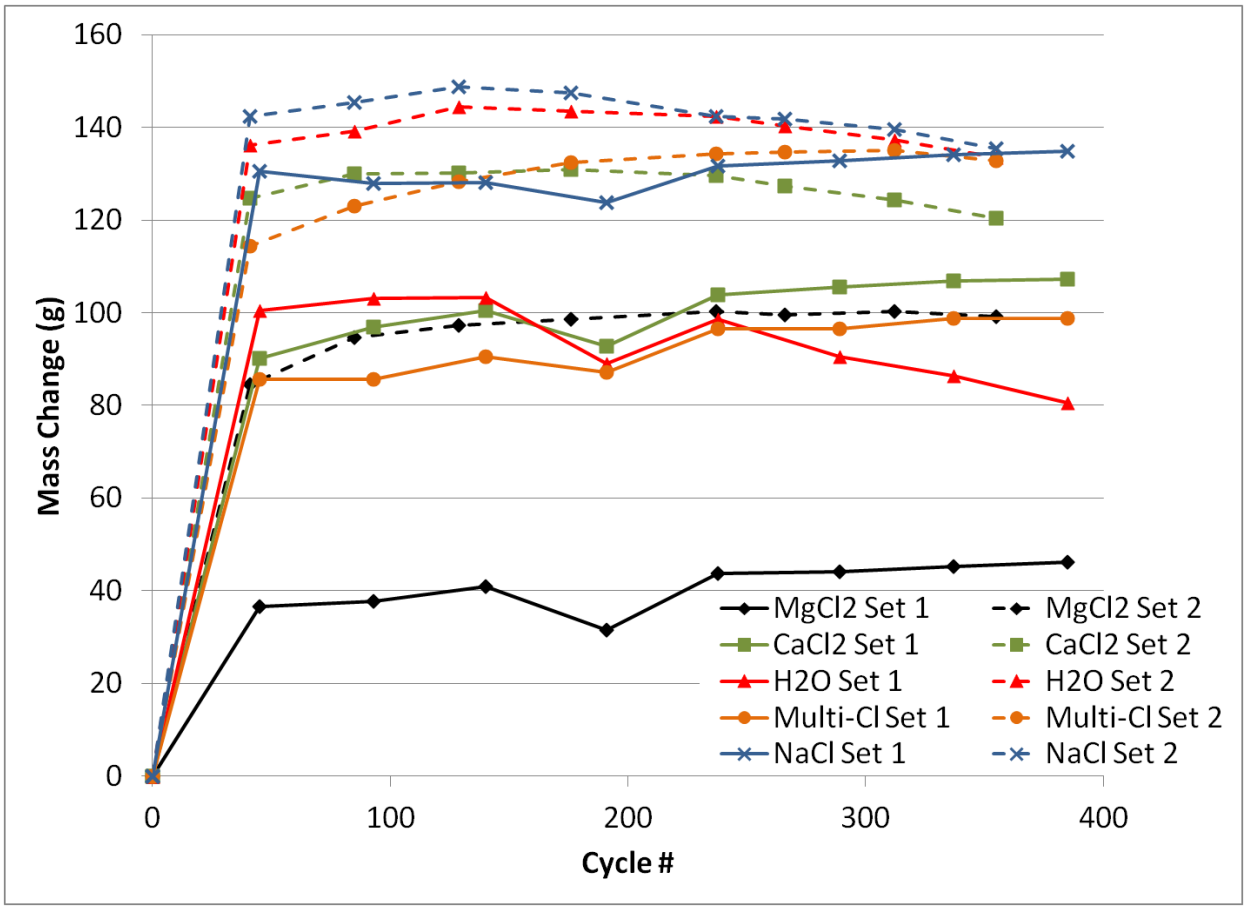

Figure 4.1-7 – Cumulative average mass change of freeze thaw specimens, comparison

The mass loss, measured by capturing the debris from the specimen trays at the end of each week, gives a clear indication of the damaged being cause by the freezing and thawing, the salts, or the combination of the two. The debris is collected, allowed to dry and then weighed. The results for Set 1 are shown in Figure 4.1-8. As expected due to the freezing temperature of the salt solutions, there is minimal debris from any samples other than those exposed to water.

Values represent the debris collected at each particular measurement period, not the summation.

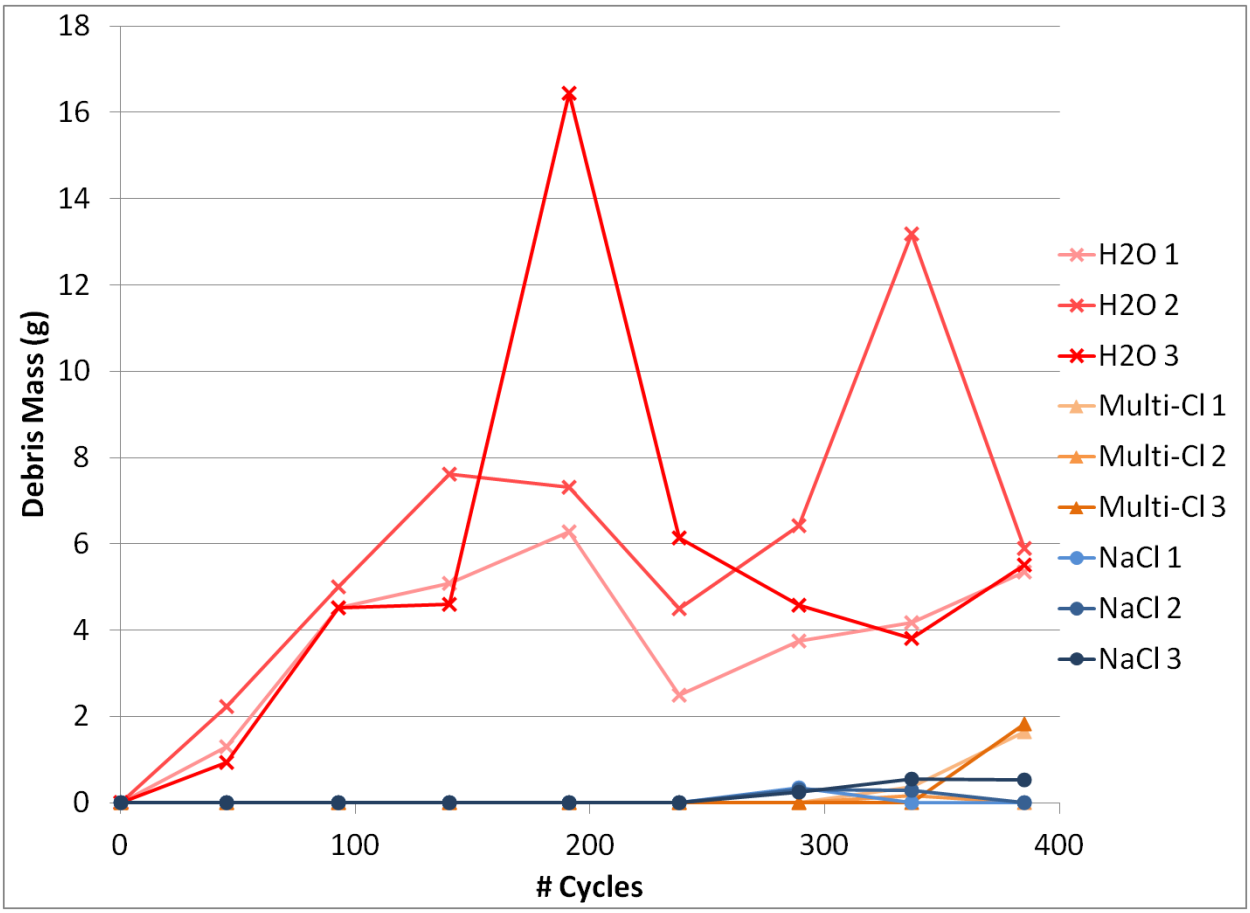

Figure 4.1-8 - Freeze and thaw Set 1, as-received solutions, prism debris for each of the three individual prisms in those solutions where scaling occurred

In Set 2, the diluted solutions were not able to provide the same freezing and thawing protection as in Set 1 due to their more positive liquidus temperatures. In the freezing cycle, each of the solutions, based upon the phase diagrams shown in Figure 2.2-1, Figure 2.2-3, and Figure 2.2-4, ice should form in each of the solutions, which should result in an increase in debris – that is, the samples exposed to salt solution should have debris in amounts similar to

the prisms exposed to water, unlike in Set 1. This effect may be compounded by the effects of salt scaling. The debris results of Set 2 in diluted solutions is shown in Figure 4.1-9.

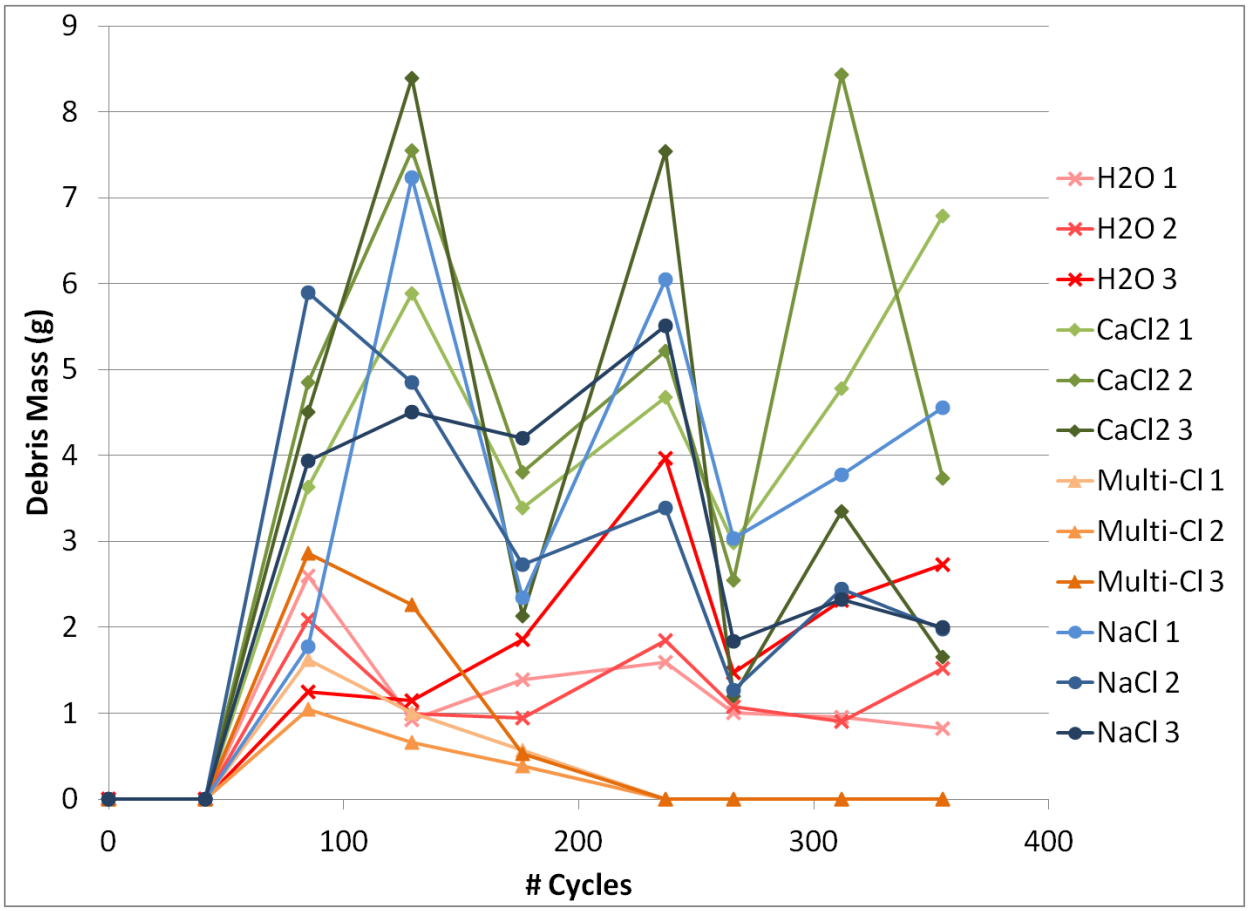

Figure 4.1-9 - Freeze and thaw Set 2, diluted solutions, prism debris for each of the three individual prisms in those solutions where scaling occurred

Comparison of the average debris collected from each solution type from both Set 1 and Set 2 is shown in Figure 4.1-10.

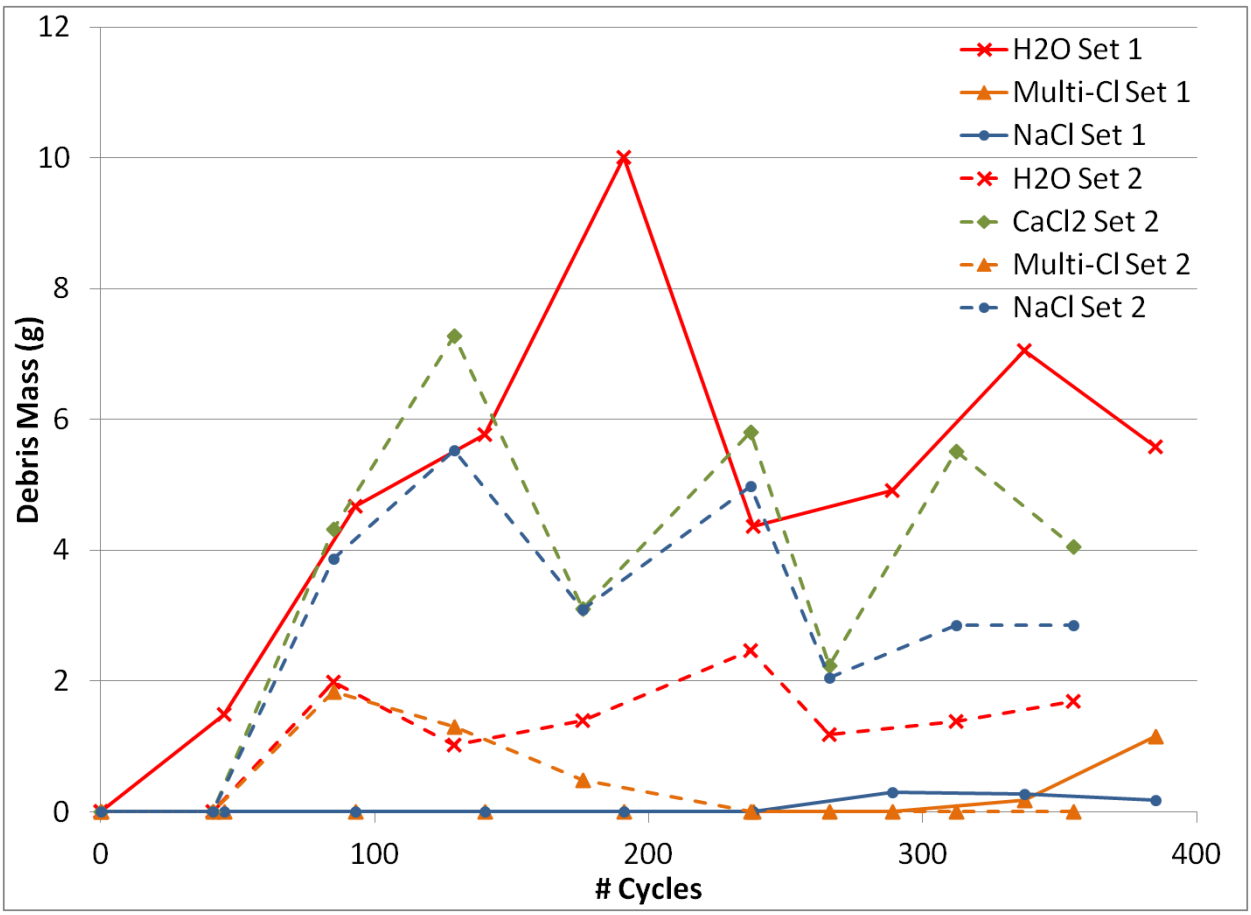

Figure 4.1-10 - Freeze and thaw Set 1 and Set 2 average debris mass

4.2 Internal strain

The outdoor slab testing yields two values for each measurement, the strain and temperature, for each gauge every hour. Though this results in a large volume of data, it is this consistency of measurement that allows not only general trends but also the day to day trends with changes in climate to be determined. Figure 4.2-1 shows the adjusted strain such that the first measurement has been subtracted from each subsequent measurement according to Equation 4.2-1.

$$Adjusted\ Strain_i = Raw\ Value_i - First\ Value$$

Equation 4.2-1

Figure 4.2-2 represents the results for the slab exposed to magnesium chloride, showing strain of the top gauge in blue, the middle gauge in red, and the bottom gauge in green with the temperature measurement from the top gauge shown in purple. The strain measurements are corrected to eliminate pre-exposure strain caused during curing of the concrete. This is accomplished by subtracting the first recorded value from each measurement, thus leaving only the effects of solution and climate. These data are representative of all of the data for the different solutions, although the magnesium chloride has shown the highest strains. As expected the strain is highest in concrete at the level of the top gauge because this would have the highest salt content. Moreover, the effect of allowing the ponding wells to remain empty for nine weeks is reflected in the decrease in strain in the top gauge over this period (from week 11 to week 20). This decrease is not observed as severely in the strain measured deeper in the concrete indicating that the concrete at these depths remained saturated. In the cases where the pond is able to dry due to unusually high temperatures, as seen clearly near week 20 and again between weeks 70 and 80, the strain at each of the three gauges get closer together as the outer and middle gauge experience the compressive effects of the concrete drying, while the effect does not seem to reach the deepest gauge. The loss of data for the top gauge exposed to $MgCl_2$ around week 45 was caused by a rabbit eating the cable connecting the gauge to the data logger. Since data are only collected every 2-3 weeks, it was some time before the issue was found and corrected.

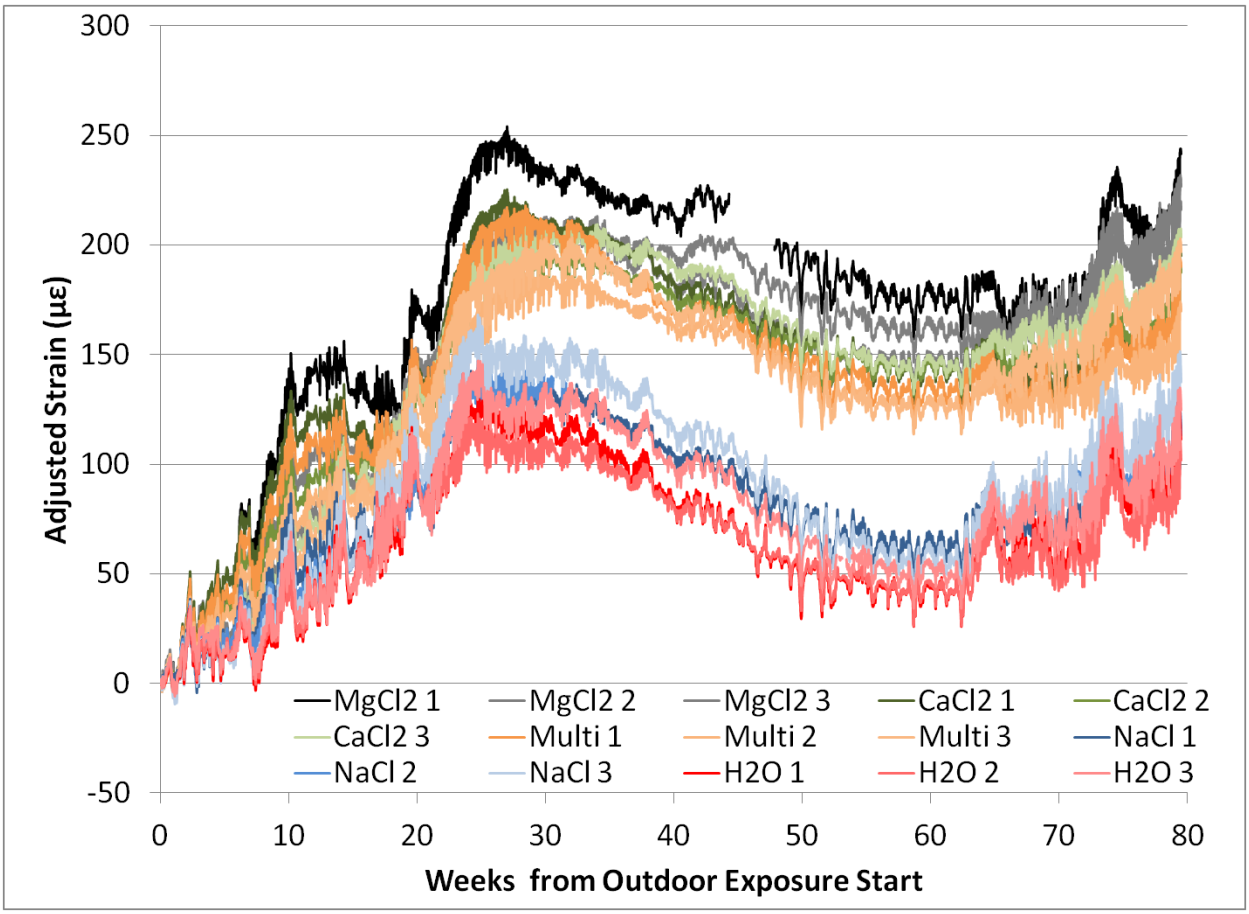

Figure 4.2-1 - Adjusted strain from all gauges such that the first value from each data set has been subtracted from all subsequent raw values

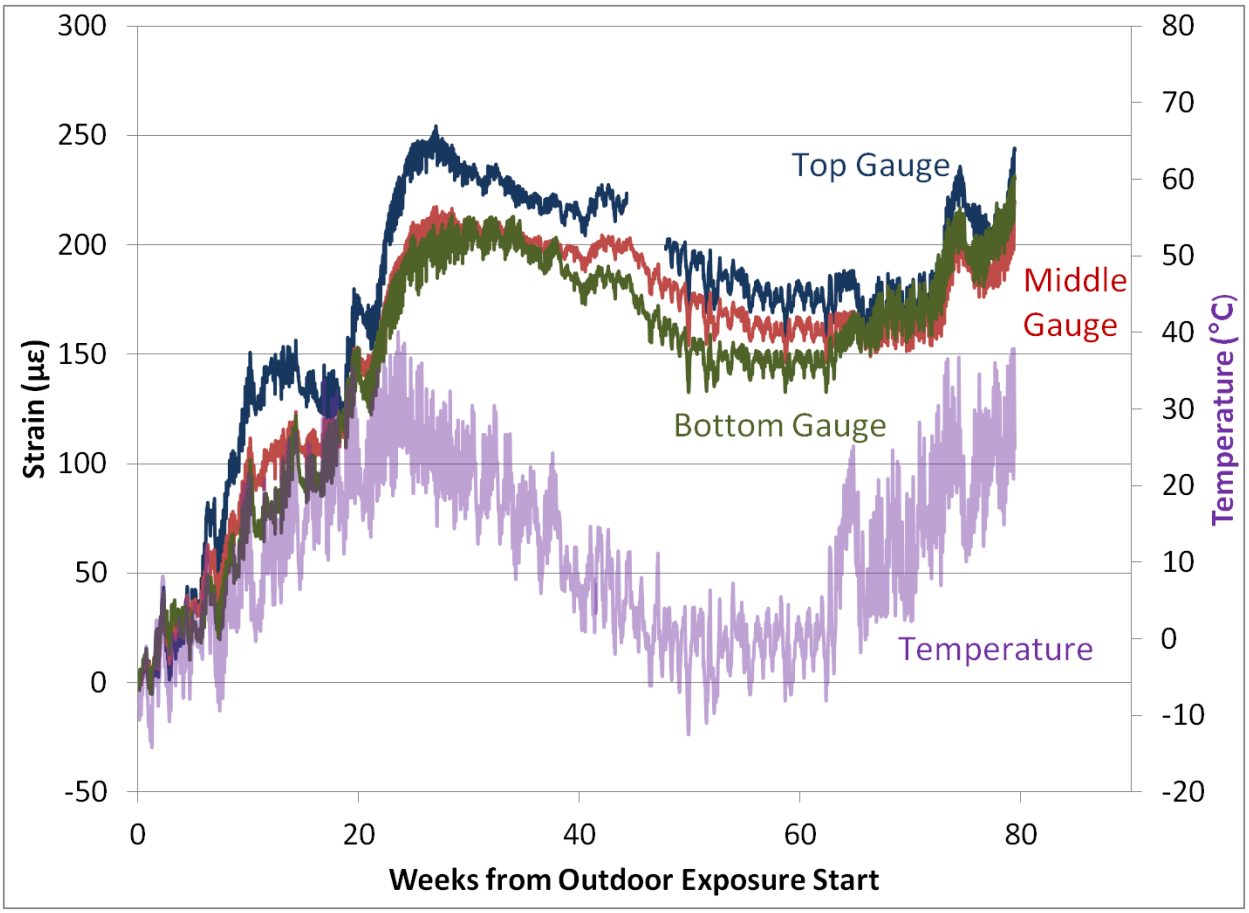

Figure 4.2-2 – Water corrected strain in $MgCl_2$ at three levels on the primary ordinate and temperature on the secondary ordinate

Figure 4.2-3 shows the strain due only to the effects of the anti-icing agents in the top gauge for each of the four solutions. These data have been adjusted in the same manner as those in Figure 4.2-2, followed by subtracting the corresponding measurement from the control slab at the same gauge location and time from the corrected value to remove the effects of temperature changes. This is seen in Equation 4.2-2. The decrease in strains over the 11 week to 20 week period is again attributed to the concrete drying out in the period without salt solution.

$$Water\ Corrected_i = Raw\ Value_i - First\ Value - Control\ Value_i$$

Equation 4.2-2

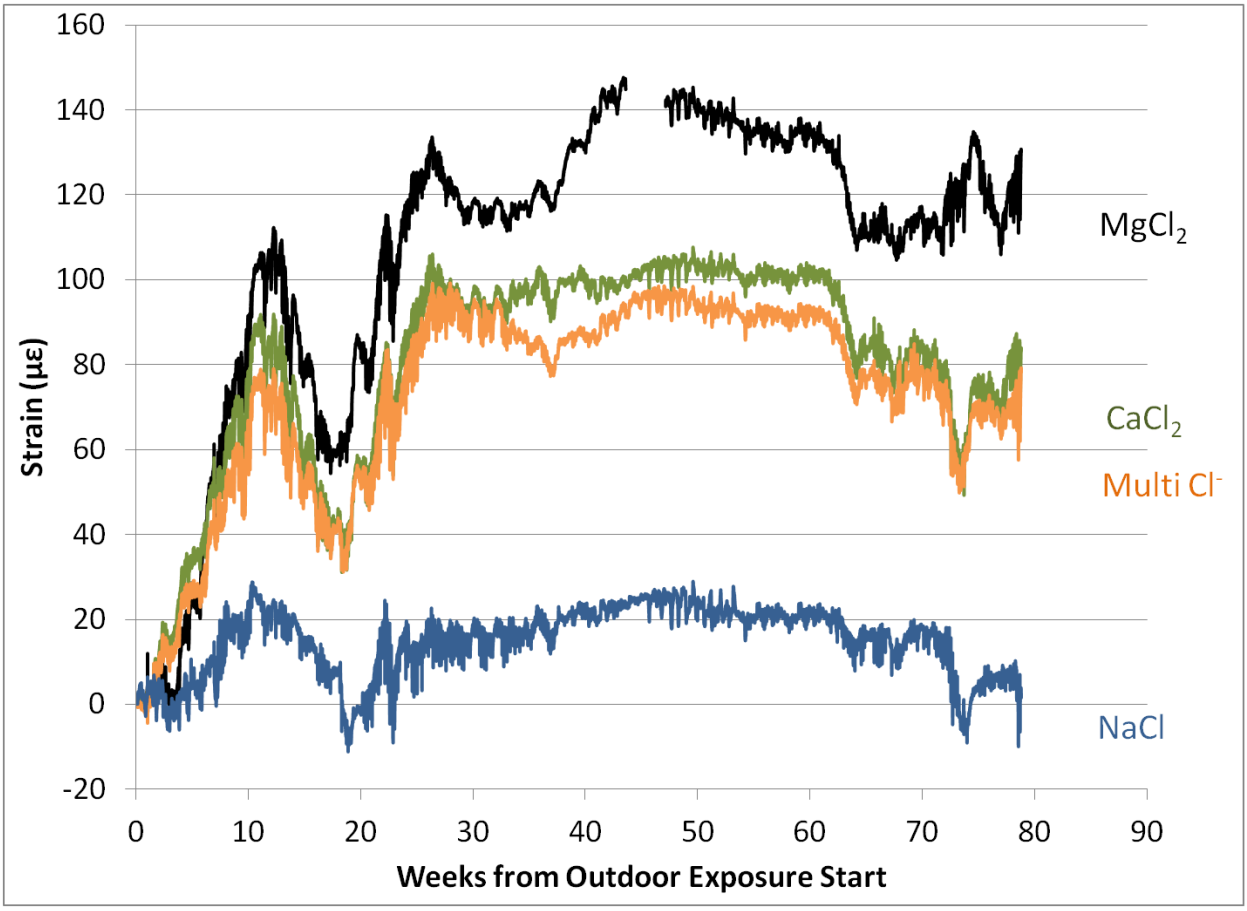

Figure 4.2-3 - Water corrected strain from the top-most gauge in each of the four solution samples

Each of the samples shows similar trends with respect to the strain in the sample, with the variation being the magnitude of the strain as seen in Figure 4.2-3. Figure 4.2-4 through Figure 4.2-7 show the slab comparison for each of the four salt solution exposed slabs after the results are water corrected.

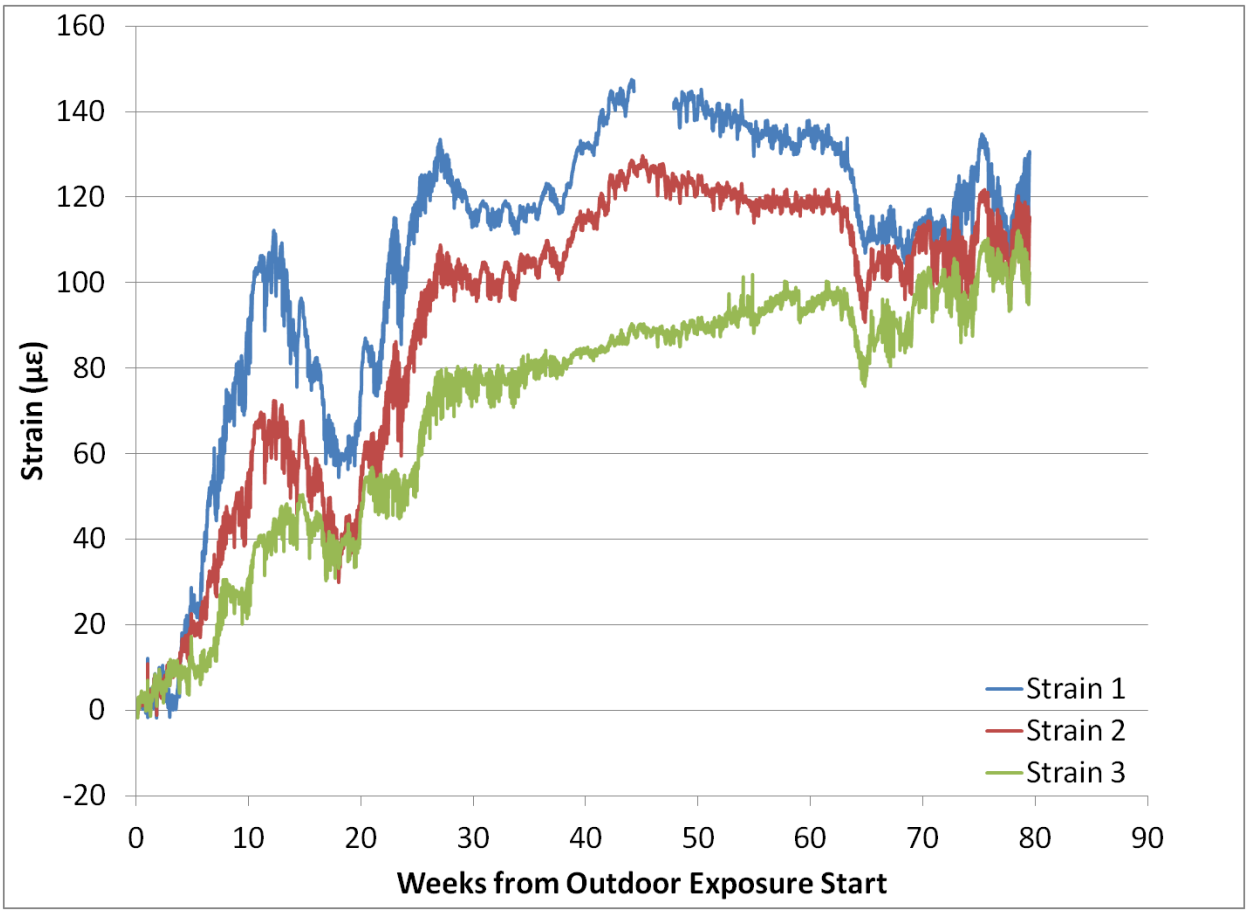

Figure 4.2-4 - Water corrected strain from the $MgCl_2$ slab

The data for the $MgCl_2$ sample most clearly shows the trends which occur over the period of testing the outdoor slabs. This is due to the fact that the magnitude of the strain is greatest for this sample as compared to the others, as seen in Figure 4.2-3. The decreases at 11 and 70 weeks are most clearly identified here, especially when the adjustment is made to subtract the control values, as is represented in Figure 4.2-4.

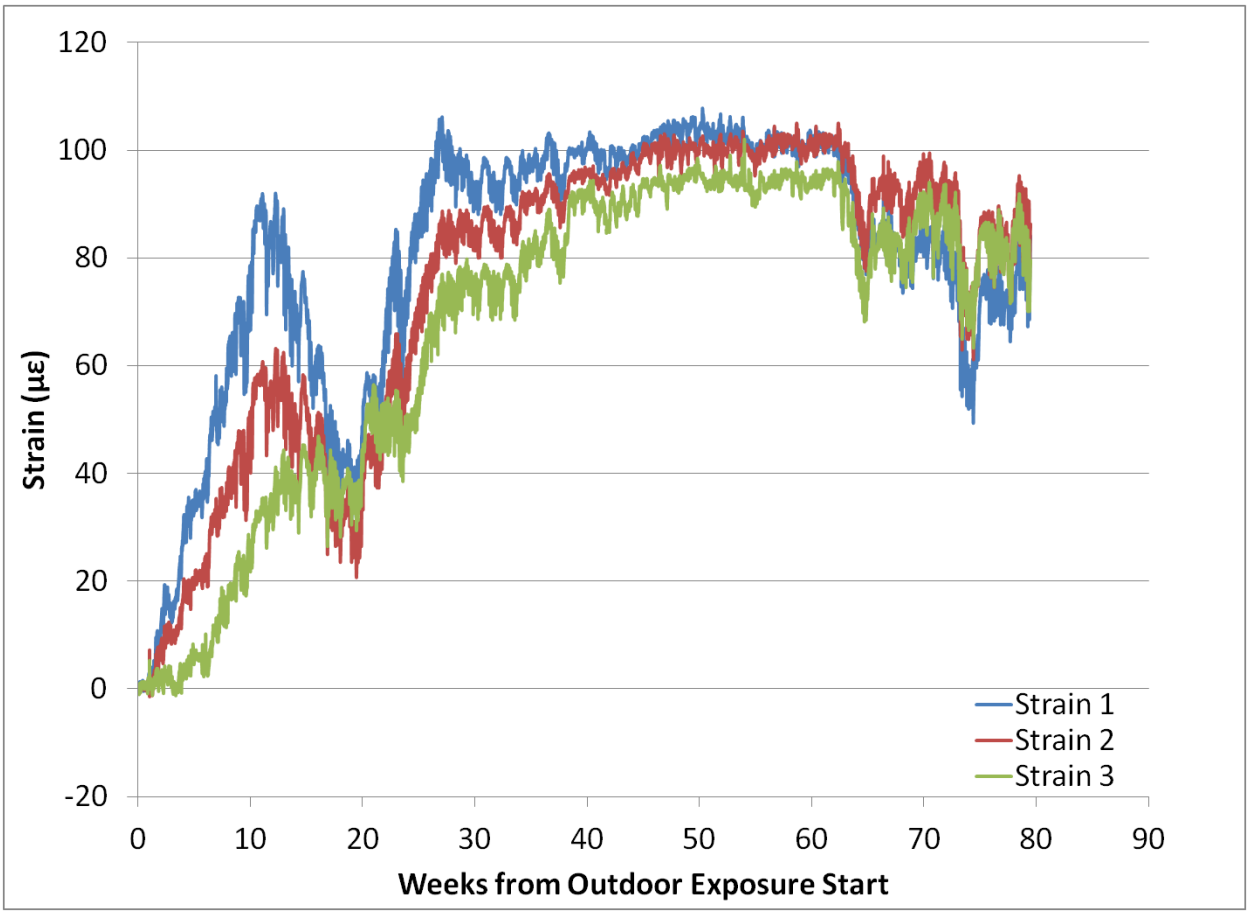

Figure 4.2-5 - Water corrected strain from the $CaCl_2$ slab

Compared to the $MgCl_2$ data from Figure 4.2-4, the data for $CaCl_2$, shown in Figure 4.2-5, shows both a smaller magnitude for equivalent measurements, and less variation between the three gauges. While this latter trend is clear throughout, it becomes most clear in the two periods where there is a reduced strain due to temperature and moisture levels. In these regions, the $CaCl_2$ data almost overlap, where the $MgCl_2$ data get closer but have minimal overlap.

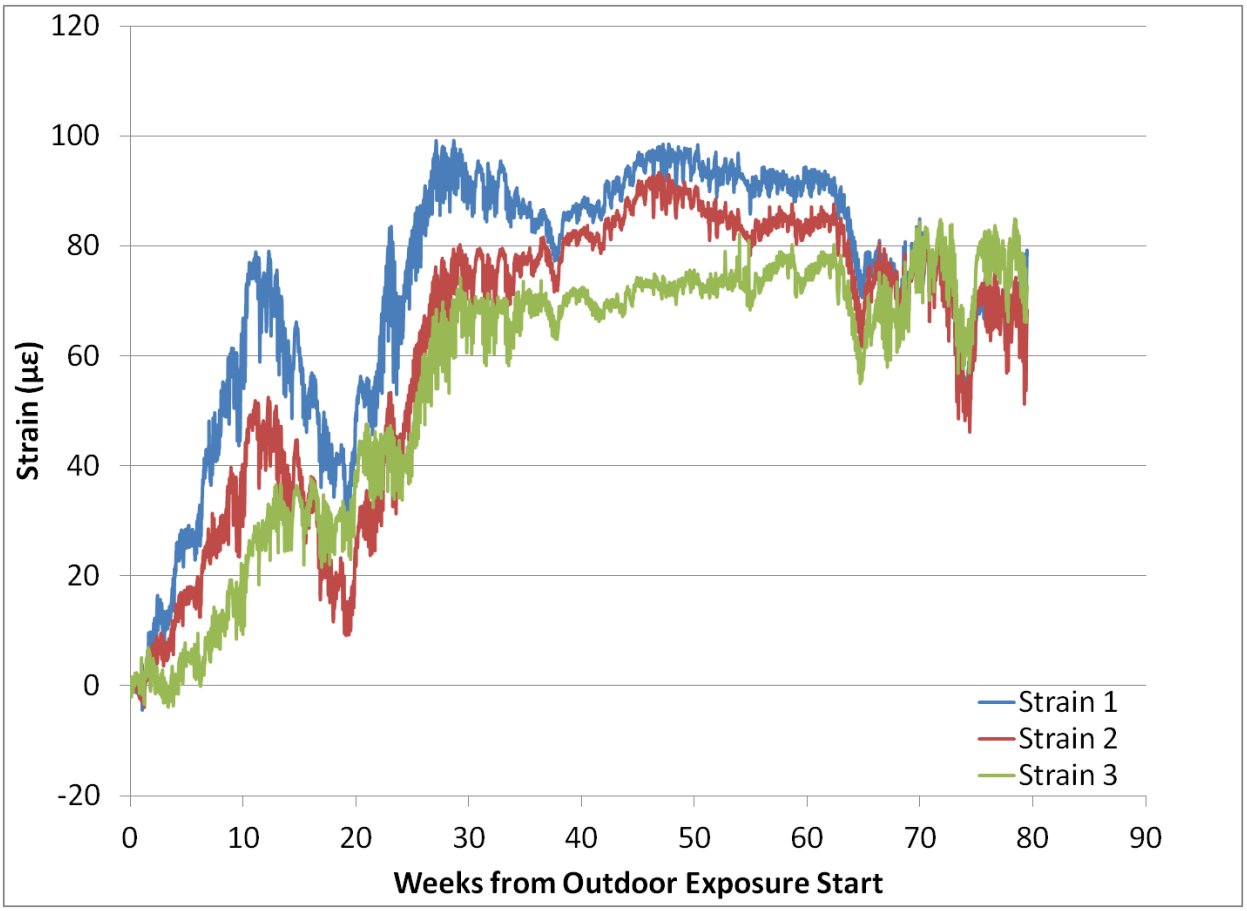

Figure 4.2-6 - Water and corrected strain from the Multi-Cl^- slab

The multi-Cl^- data, as seen in Figure 4.2-6, trends in a very similar manner to that of $CaCl_2$ with respect to strain. The magnitude of the data are slightly less than that of the $CaCl_2$ data and also shows greater spread between gauges, similar to the $MgCl_2$ as opposed to the $CaCl_2$.

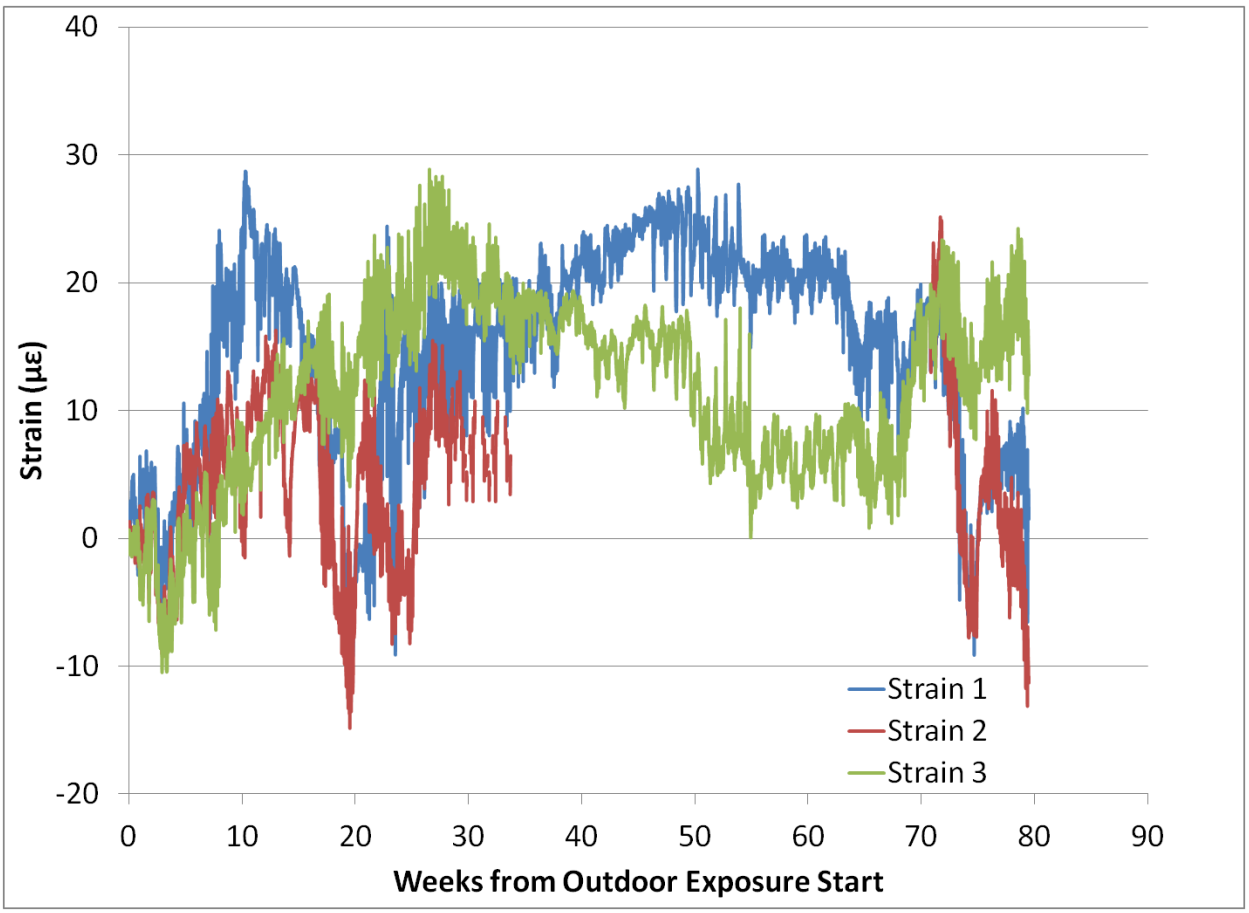

Figure 4.2-7 - Water corrected strain from the NaCl slab

The NaCl strain data, shown in Figure 4.2-7, do not appear similar to any of the other data sets from salt-solution exposed samples. As compared to the control sample, there is almost no difference, with the water corrected strain staying between 10 and 20με the majority of the time. This is equal to only 10-20% of the strain seen in the other salt-exposed samples.

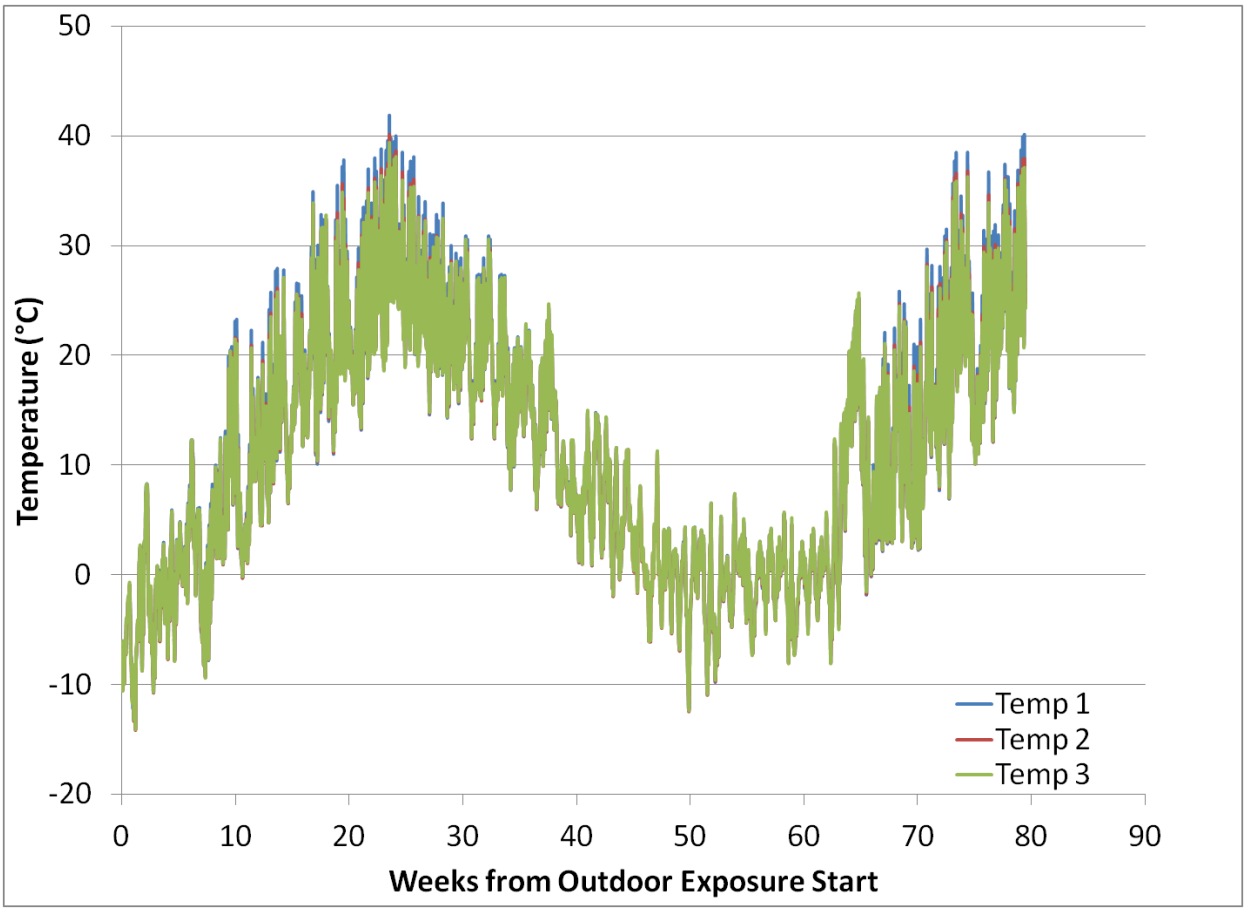

Figure 4.2-8 – Temperature profiles from the $MgCl_2$ slab

Collected with the strain measurements are a temperature measurement at each gauge, the curves for which are shown in Figure 4.2-8. As can be seen, there is almost perfect overlap of the temperature for all three gauges. For the majority of the measurements made, there is 0.25°C to 0.5°C difference from gauge to gauge, with the top gauge being closest to the ambient temperature, and the middle and bottom gauge trailing it. This is to say, if the temperature is dropping, the middle gauge is generally about 0.25°C warmer than the top gauge, and the bottom gauge about 0.25°C warmer than the middle. The exception to this trend is during the summer months when the effects of temperature have been compounded

by the additional effects of the sun. Above about 20°C, the temperature spread between gauges begins to increase, which is postulated to be the additional effects of the sun causing the concrete surface to be warmer than ambient temperature. As seen around 25 and 75 weeks, where the temperature is at the peaks, there is a visually discernible difference between the top and bottom gauge temperatures. At these peak times, there is up to 5°C between the top and bottom gauges, which is split as about 3.5°C between the top and middle gauge, and 1.5°C between the middle and bottom gauge. This temperature variation can have a significant effect on the moisture in the concrete and, thus, the strain.

4.3 Compressive Strength

The most commonly used method in understanding variations or changes in concrete is to consider the compressive strength over time of the concrete. Due to batch size constraints, in order to produce an ideal sample size two batches of concrete were cast using as identical a process as possible. Nevertheless, the 28 day strengths of the two batches differed by approximately 20%. Due to the variation in 28 day strength, compressive tests were conducted at two week intervals using three cylinders from alternating batches each test week. The raw data from Set 1 and Set 2 are in Appendix B in Table B.3-1 through Table B.3-5 and Table B.3-11 through Table B.3-15 in the appendices, respectively. The raw data were then normalized to account for differences in the 28 day strength of the concrete. This was done by dividing each value by the 28-day strength average from the corresponding batch, and then multiplying by the average 28 day strength of batch 2. This calculation is defined in Equation 4.3-1.

$$Strength_{norm} = \left[\frac{Strength_{measured,i}}{Strength_{28-day\ average,i}}\right] \times Strength_{28-day\ average,2}$$

Equation 4.3-1

The results of this normalizing are shown in Figure 4.3-1 and Figure 4.3-2 for Set 1 and Set 2, respectively. The first value in each set is the 28-day strength, and each following column represents the strength two weeks later. The normalized raw data for Set 1 and Set 2 are shown in Appendix B in Table B.3-6 through Table B.3-10 and Table B.3-16 through Table B.3-20, respectively.

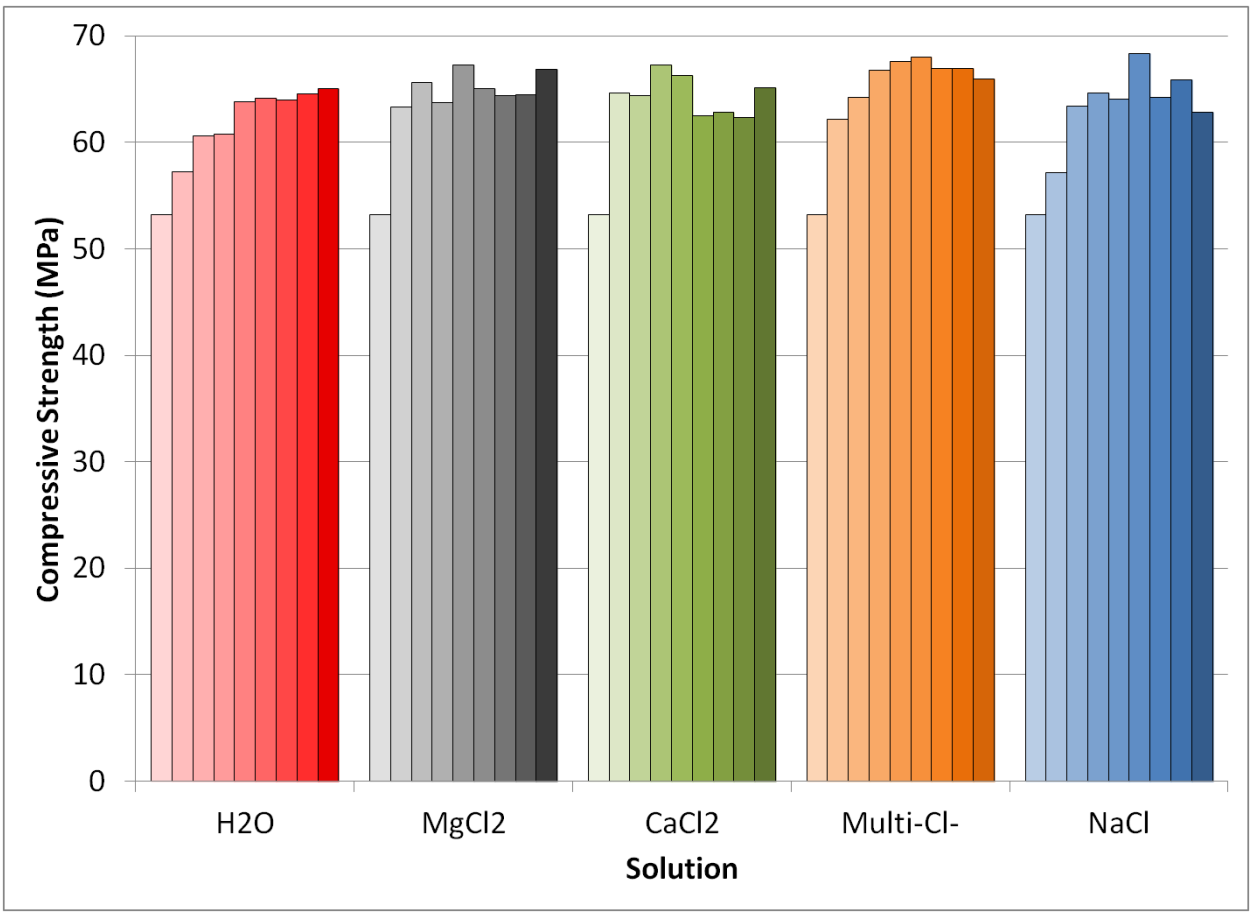

Figure 4.3-1 – Average compressive strength for continuously soaked samples starting at 28 day strength and measured every 2 weeks

The test was repeated using the same preparation procedure and mixture design except consolidation method, but instead of continuous soaking, the cylinders were alternated between ten days dry and four days wet, with measurement of compressive strength completed after the wet cycle. These cylinders were consolidated using a vibrating table as opposed to being using the rod method to manually consolidate the samples. Larger batches were used so that the cylinders could be kept in solution for a longer period of time. In order to accommodate this and the maximum batch size of the mixer, the extra specimens were split three each between the salt solutions, thus providing an extra two weeks of exposure. Due to

this, there is one more data set for each of the salt solutions, than the control specimens. As seen in Figure 4.3-2, there is significantly less change in the compressive strengths of the samples. There is no initial spike as seen in the first set of compressive testing, nor are there as large variations between measurements. The purpose of using wet and dry cycles was to increase the ingress of solutions into the specimens to maximize the effect; however, it would appear that the reverse has shown true, as there is less effect seen. The samples exhibit almost no change, with the exception of the NaCl samples, which exhibit a general continuous increasing trend.

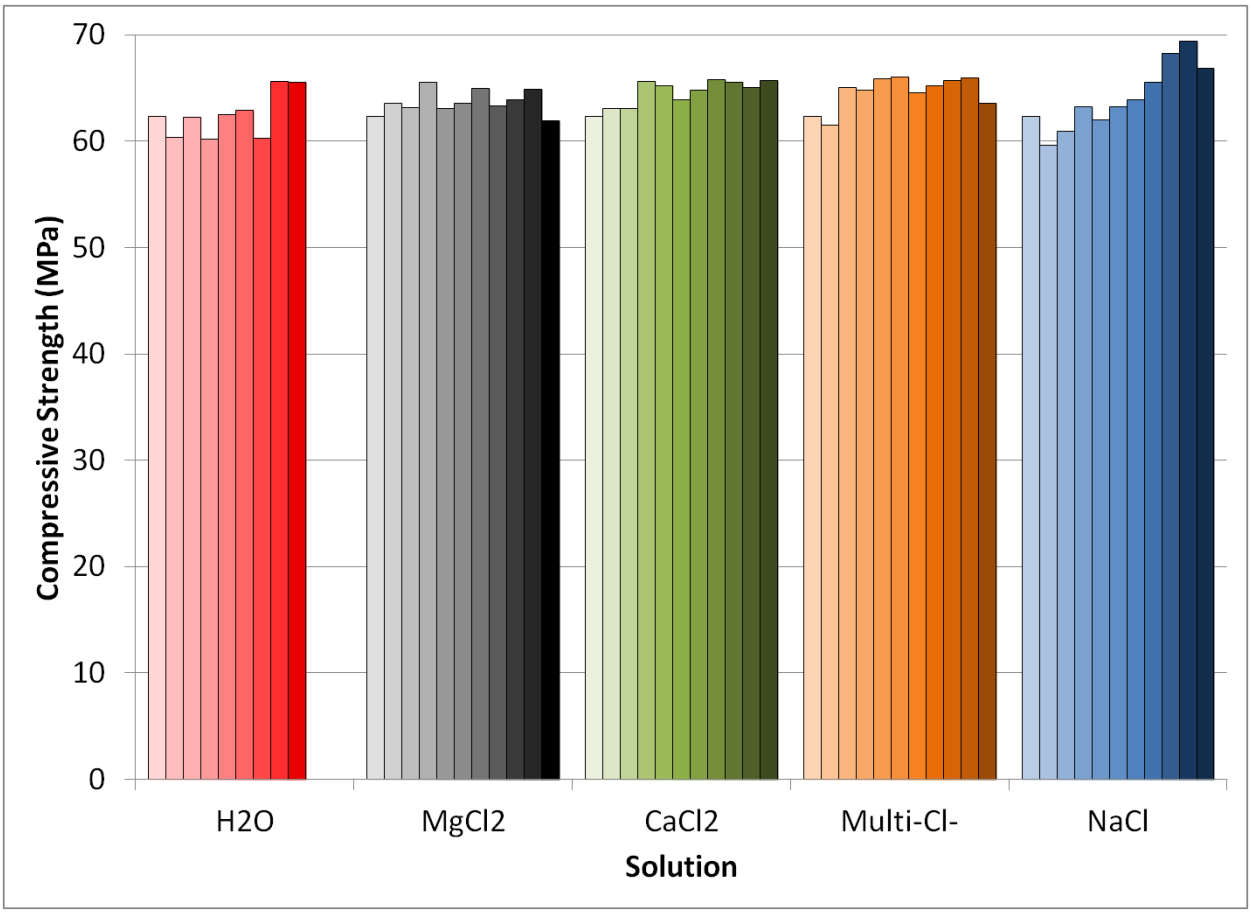

Figure 4.3-2 - Average compressive strength for alternating wet and dry samples starting at 28 day strength and measured every 2 weeks

At the end of the measurement period for the first set of testing there was a statistically insufficient number of cylinders left from each sample set. These cylinders were measured after 37 weeks of soaking (21 more than those recorded above) to see if any trends could be ascertained from them. These data are shown in Figure 4.3-3.

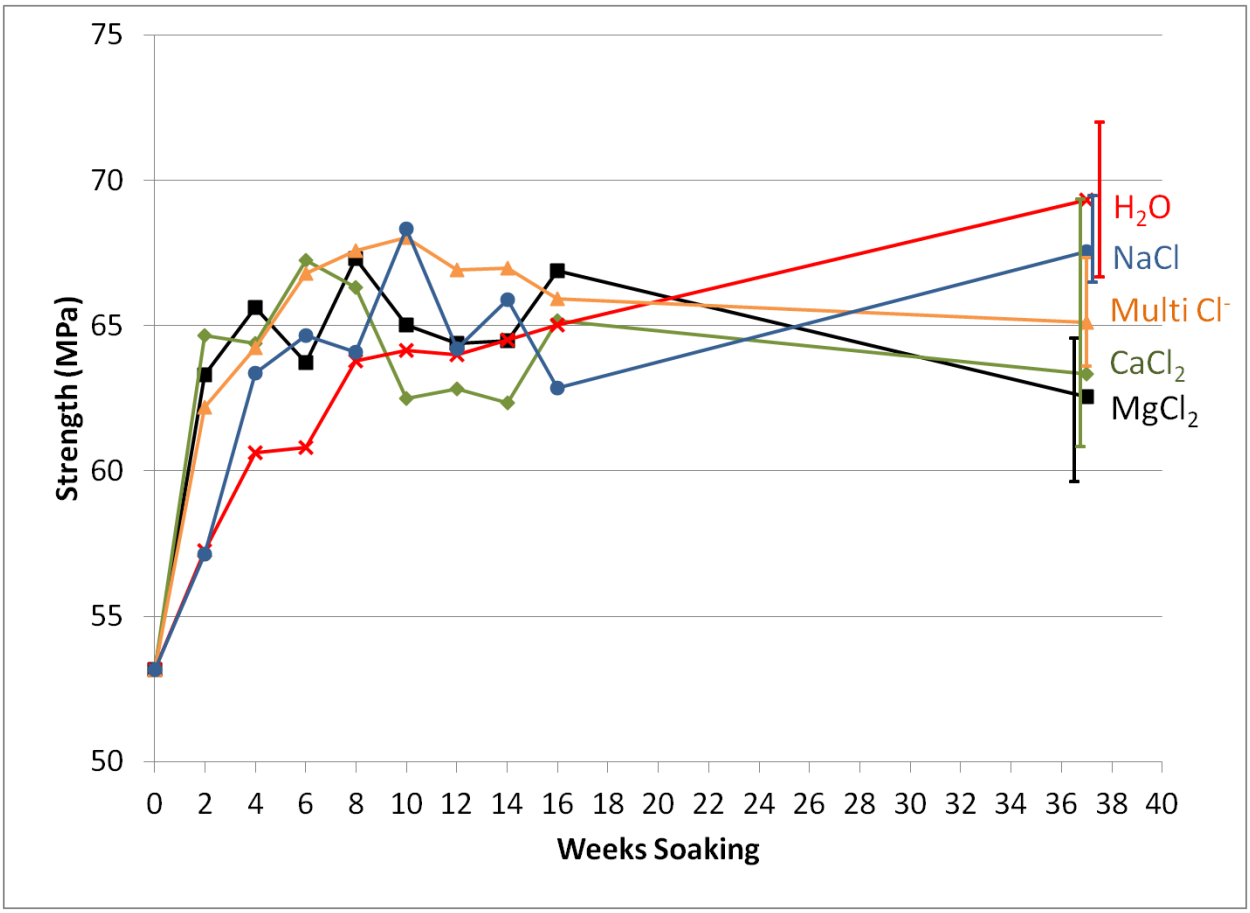

Figure 4.3-3 – Average compressive strength results from Set 1 including statistically insufficient measurements at 37 weeks with associated error bars

As related to durability, the changes in strength due to exposure can be a good measure of the improvement or detrimental effects of the solutions. If the results imply a close relationship to the control samples or exhibit little to no change, this is positive in terms of the specific ability for the concrete to continue to meet its intended purpose. If there is an excessive increase or decrease in strength, the durability would be negatively affected by the solution as there becomes risk of the structure becoming too brittle or incapable of meeting its designed purpose.

4.4 Tensile Strength

The tensile strength testing measured applied load in three point bending and displacement of the crosshead through which the load was applied. The result of this is a load-displacement curve which can be used to obtain the stress, strain, modulus of rupture and modulus of elasticity of the sample. The load-displacement curves obtained are shown in Figure 4.4-1. It is important to note that with a constant load application rate, the load-displacement curves should be linear assuming elastic deformation is occurring. The initial curve is due to settling of the equipment as the rubber stops and any connections are pushed tight, allowing excess displacement not related to the concrete. From these curves, the linear portion can be used to model the true load-displacement lines.

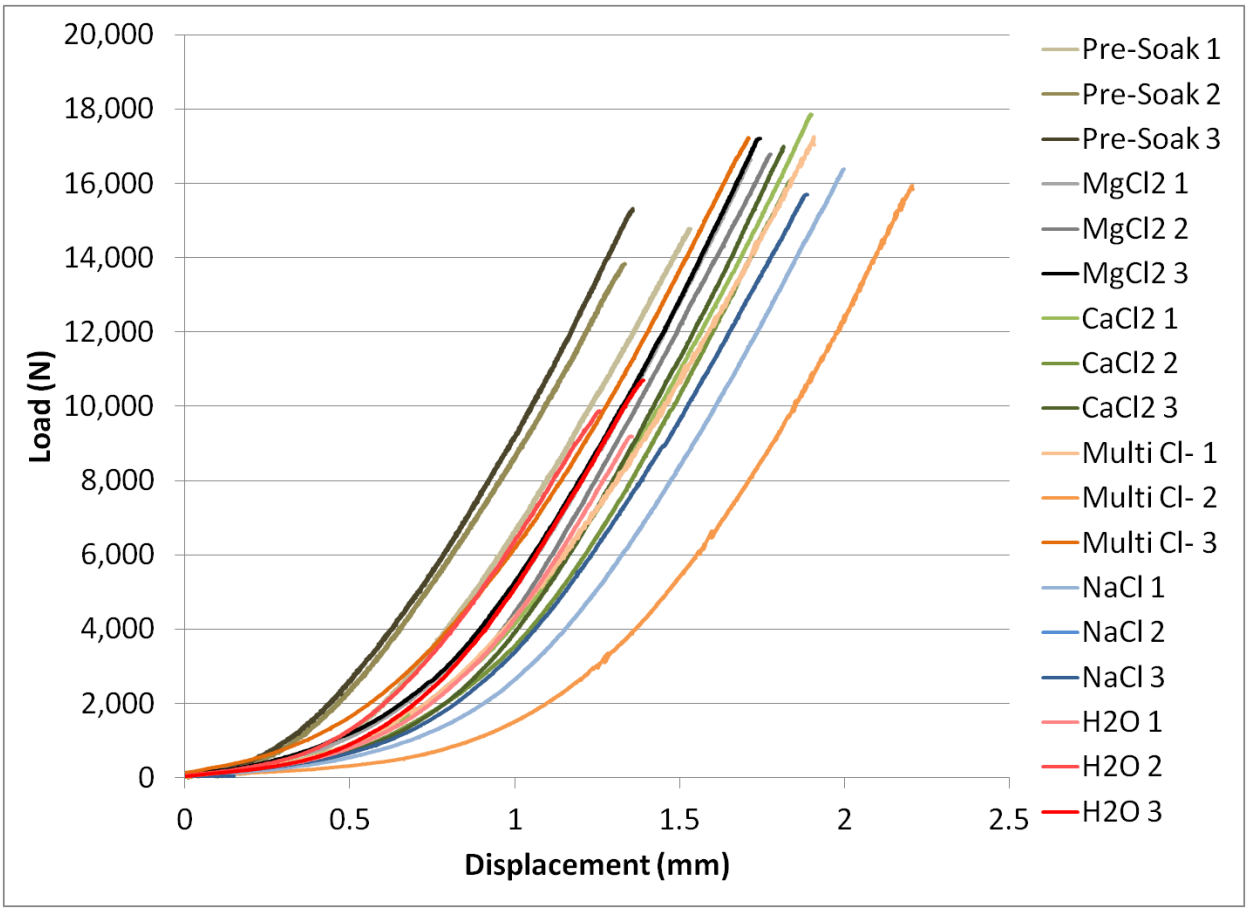

Figure 4.4-1 - Load versus displacement curves obtained from 3-point bend tensile testing

The curves in Figure 4.4-1 show a number of interesting results. The most notable result is the lower fracture load and displacement achieved by the control prisms which were only exposed to water. As opposed to increasing in strength as is normally expected when water is present to promote hydration, the samples decrease in strength. All prisms exposed to salt solution showed higher strength and displacement with generally similar results across each of the four solutions. A simplified version of Figure 4.4-1 is seen Figure 4.4-2 showing the median curve from each set since an average is not possible.

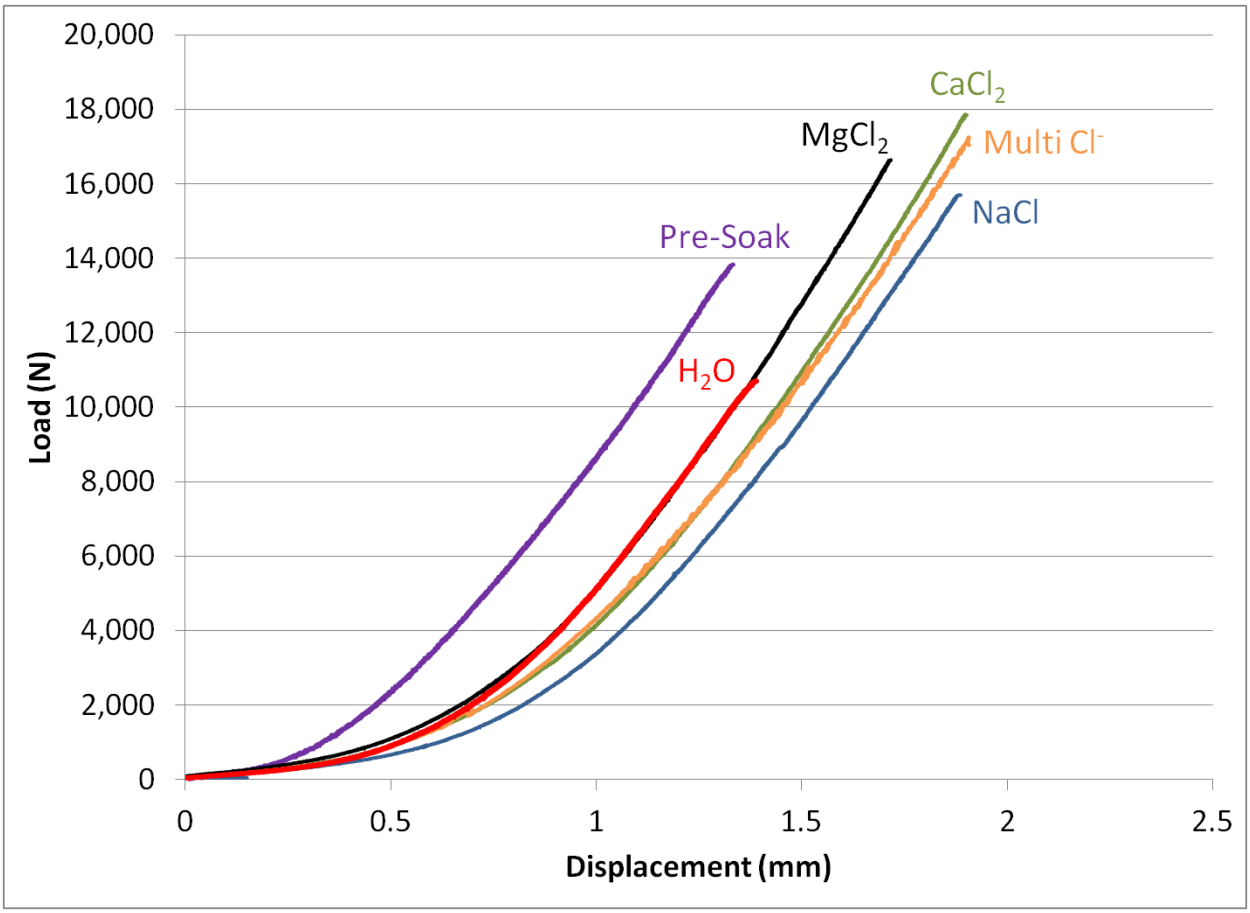

Figure 4.4-2 - Median curves for load versus displacement from tensile testing

The linear portions of the curves present the true data as related to the material properties. By applying a trend line to the linear section and acquiring the equation for the trend line, the effects of equipment settling can be removed and a true load-displacement curve for the concrete can be established. The load versus displacement for all samples measured is given in Figure 4.4-3, while the median values are shown in Figure 4.4-4.

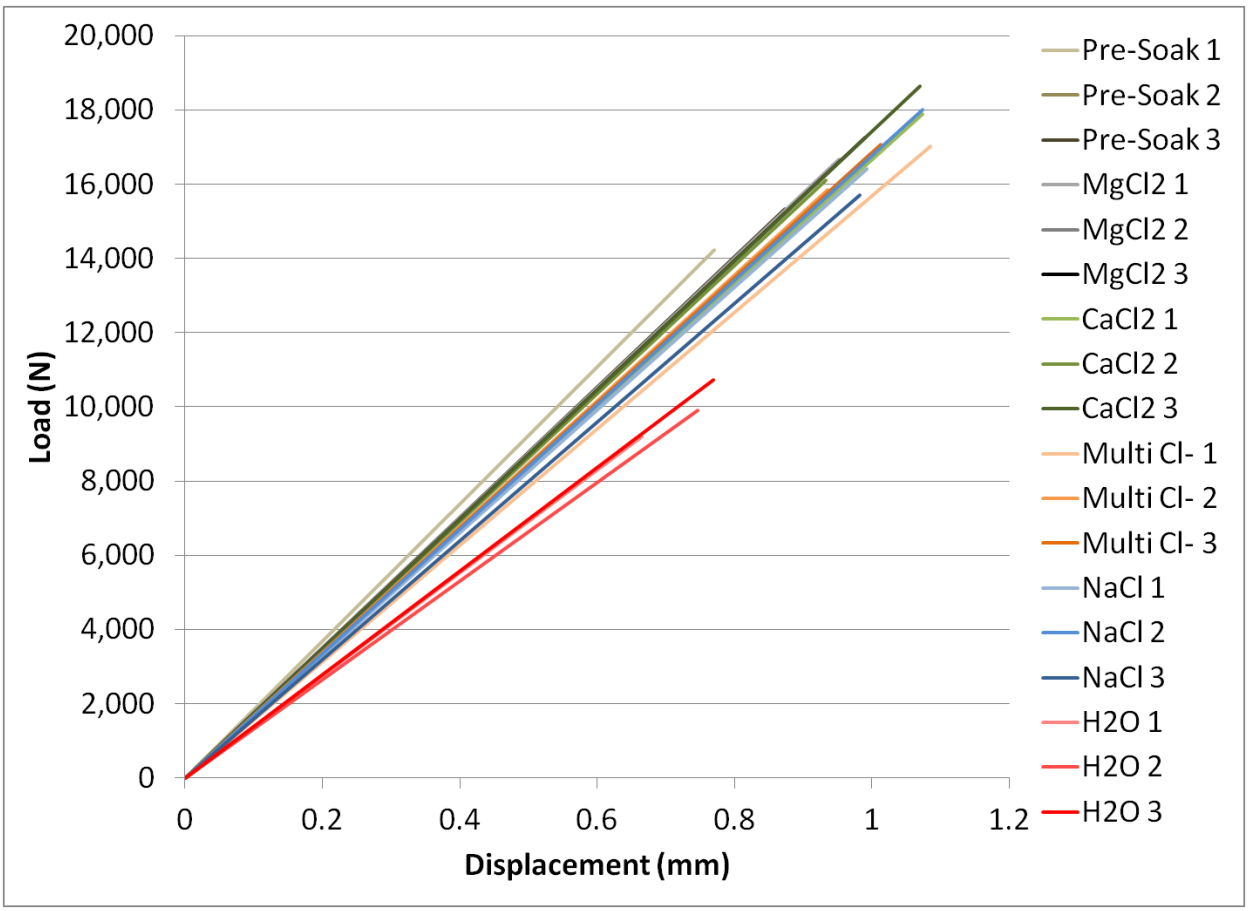

Figure 4.4-3 – True (adjusted) load versus displacement curves obtained from 3-point bend tensile testing

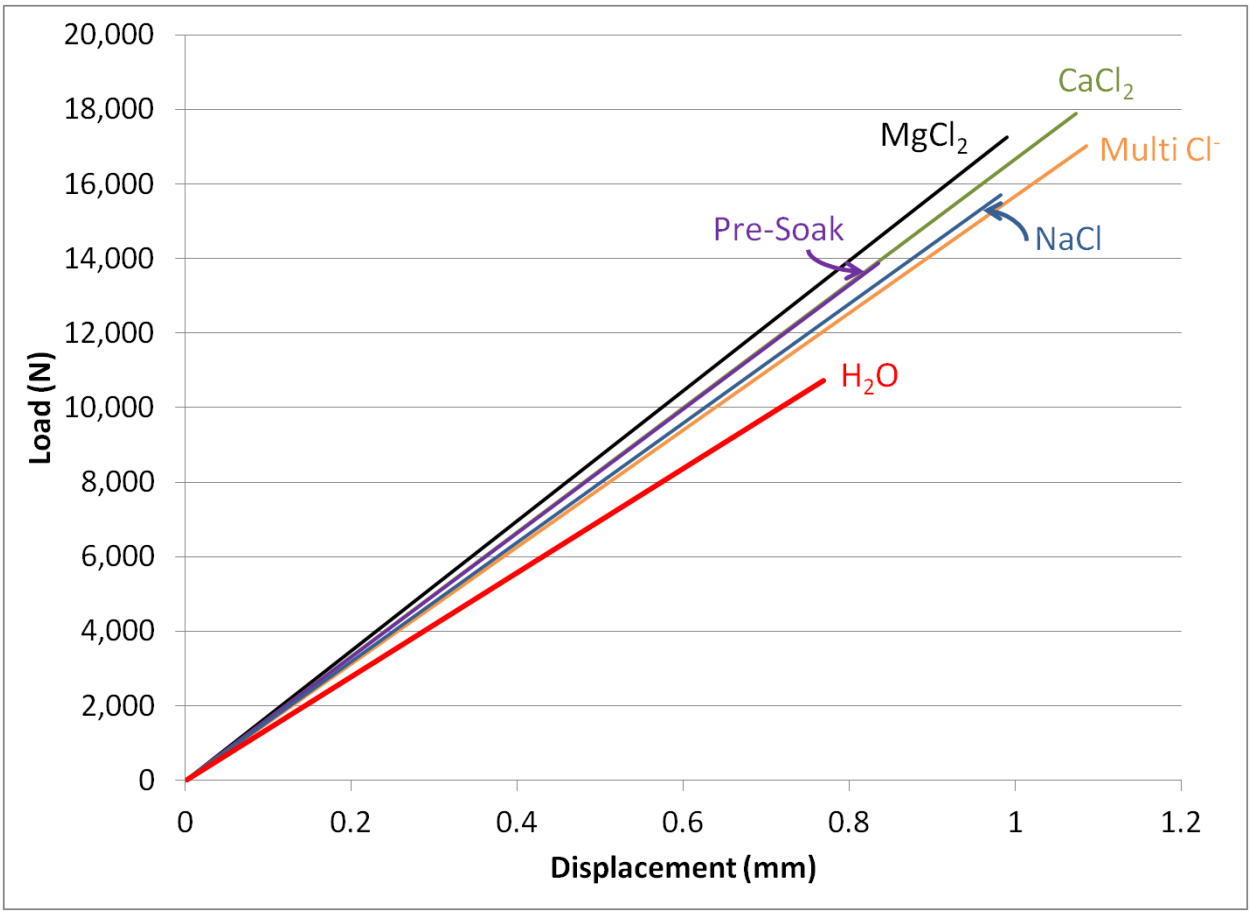

Figure 4.4-4 – True (adjusted) median curves for load versus displacement from tensile testing

Once the effects of the equipment are removed it can be seen that the results are actually quite similar for each of the different exposure conditions, except for the control set exposed to water. From the linear approximations of the true load-displacement curves, the material properties can be calculated. The results of this are shown in Table 4.4-1.

Table 4.4-1 - Results and material properties calculations from three-point bend tensile testing

Sample	Maximum load (Adjusted)			Modulus of Rupture (MPa)	Modulus of Elasticity (GPa)	Peak Adjusted Strength (Mpa)
	Axial Force (N)	Axial Displacement (mm)	Time (sec)			
Pre-Soak 1	14232.3	0.771	865.9	11.386	1.620	1.820
Pre-Soak 2	13882.9	0.835	841.7	10.581	1.447	1.764
Pre-Soak 3	15330.7	0.873	929.6	11.700	1.526	1.957
$MgCl_2$ 1	16670.2	0.952	1011.0	12.835	1.539	2.142
$MgCl_2$ 2	16804.2	0.997	1021.7	12.659	1.445	2.118
$MgCl_2$ 3	17250.2	0.990	1047.0	12.740	1.470	2.125
$CaCl_2$ 1	17889.6	1.073	1089.2	13.486	1.433	2.252
$CaCl_2$ 2	16095.7	0.933	980.6	12.386	1.514	2.069
$CaCl_2$ 3	18649.2	1.070	1136.0	13.938	1.487	2.327
Multi-Cl^- 1	17020.7	1.086	1032.3	12.654	1.323	2.124
Multi-Cl^- 2	15837.9	0.935	961.1	11.881	1.444	1.992
Multi-Cl^- 3	17063.0	1.013	1032.4	12.449	1.394	2.091
NaCl 1	16402.5	0.993	998.3	12.244	1.391	2.067
NaCl 2	18018.5	1.074	1094.8	13.837	1.465	2.318
NaCl 3	15708.7	0.983	956.6	12.002	1.387	2.012
H_2O 1	9208.3	0.666	559.9	7.156	1.235	1.186
H_2O 2	9901.2	0.747	600.6	7.349	1.129	1.221
H_2O 3	10728.7	0.769	651.3	8.165	1.212	1.363

Using three samples per solution allows for statistical variance to be minimized. By taking the average of the values, a reasonable representation of the data can be obtained. The results of this can be seen in Table 4.4-2.

Table 4.4-2 - Average material properties calculated from three-point bend tensile testing

Sample	Avg Displacement (mm)	Avg Mod of Rupture (MPa)	Modulus of Elasticity (GPa)	Avg Strength (MPa)
Pre-Soak 1	0.831	11.025	1.500	1.847
Pre-Soak 2				
Pre-Soak 3				
$MgCl_2$ 1	0.980	12.745	1.485	2.128
$MgCl_2$ 2				
$MgCl_2$ 3				
$CaCl_2$ 1	1.025	13.270	1.478	2.216
$CaCl_2$ 2				
$CaCl_2$ 3				
Multi-Cl^- 1	1.011	12.328	1.387	2.069
Multi-Cl^- 2				
Multi-Cl^- 3				
NaCl 1	1.017	12.694	1.414	2.133
NaCl 2				
NaCl 3				
H_2O 1	0.727	7.557	1.192	1.257
H_2O 2				
H_2O 3				

The two key results obtained from this testing are the elastic modulus and modulus of rupture of the concrete in tension. The elastic modulus is calculated using Equation 4.4-1 [**34**].

$$E = \frac{-PL^3}{48000I\delta_{max}}$$

Equation 4.4-1 [34]

where:

E = modulus of elasticity (GPa)

P = axial force (N)

L = span length (mm)

I = moment of inertia (mm^4)

δ_{max} = maximum displacement (mm)

The modulus of rupture is calculated using Equation 4.4-2 [**32**].

$$R = \frac{3PL}{2wd^2}$$

Equation 4.4-2 [32**]**

where:

R = modulus of rupture (MPa)

P = axial load (N)

L = span length (mm)

w = width (mm)

d = depth (mm)

From the modulus of rupture calculations, the results in Figure 4.4-5 are obtained.

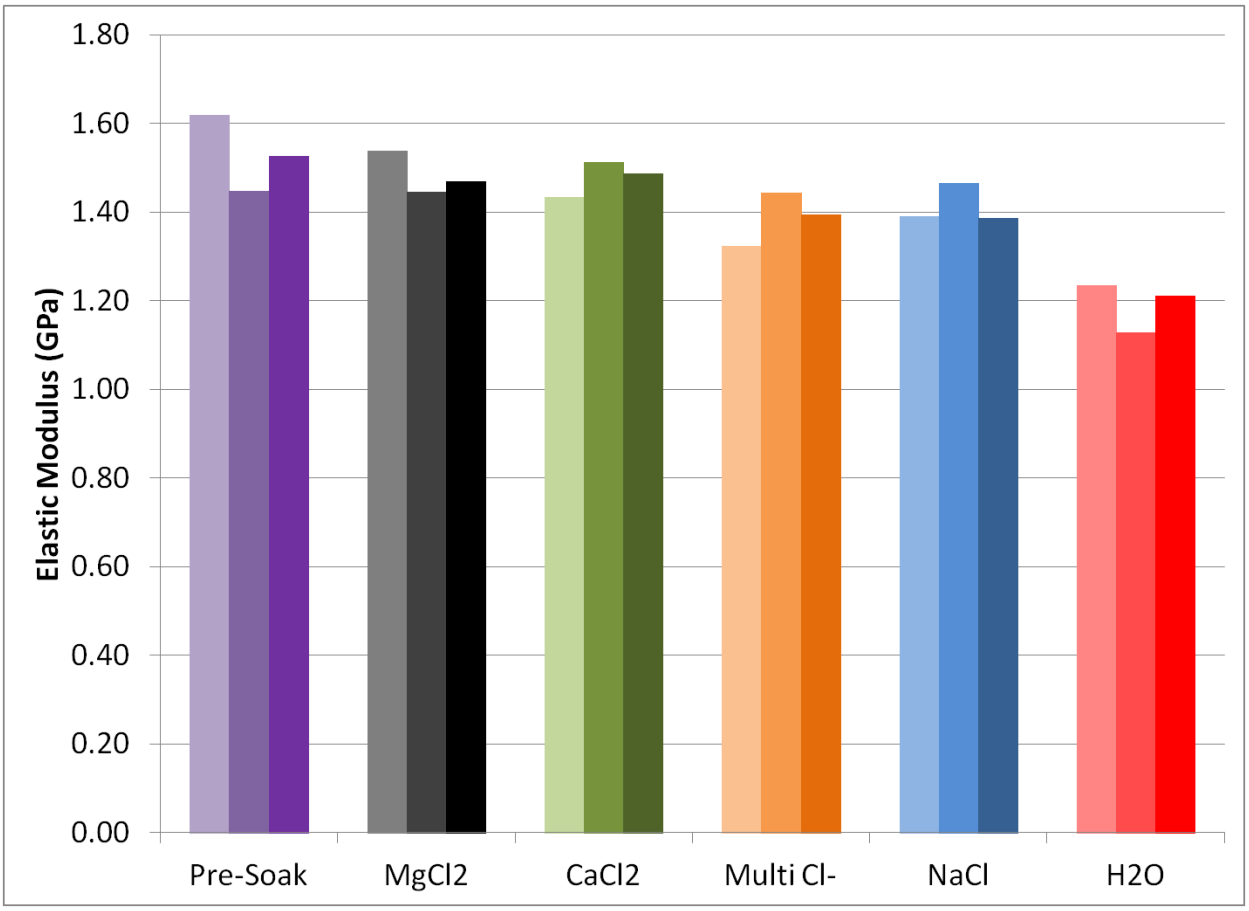

Figure 4.4-5 - Calculated elastic modulii in tension from three-point bend tensile testing

From these results it can be seen that there is no change or a decrease in elastic modulus when the prisms are exposed either salt solutions or water. From Figure 4.4-5 it can be seen that there is essentially no difference in elastic modulus after five months of wet dry cycling in either $MgCl_2$ or $CaCl_2$ solutions as compared to the pre-exposure results. The prisms exposed to multi-Cl^- and NaCl are slightly lower on average compared to the pre-exposure samples. The most surprising result was the control samples which were exposed to water in the same wet and dry cycling. These samples exhibited, on average, a 20% lower elastic modulus than the pre-exposure prisms.

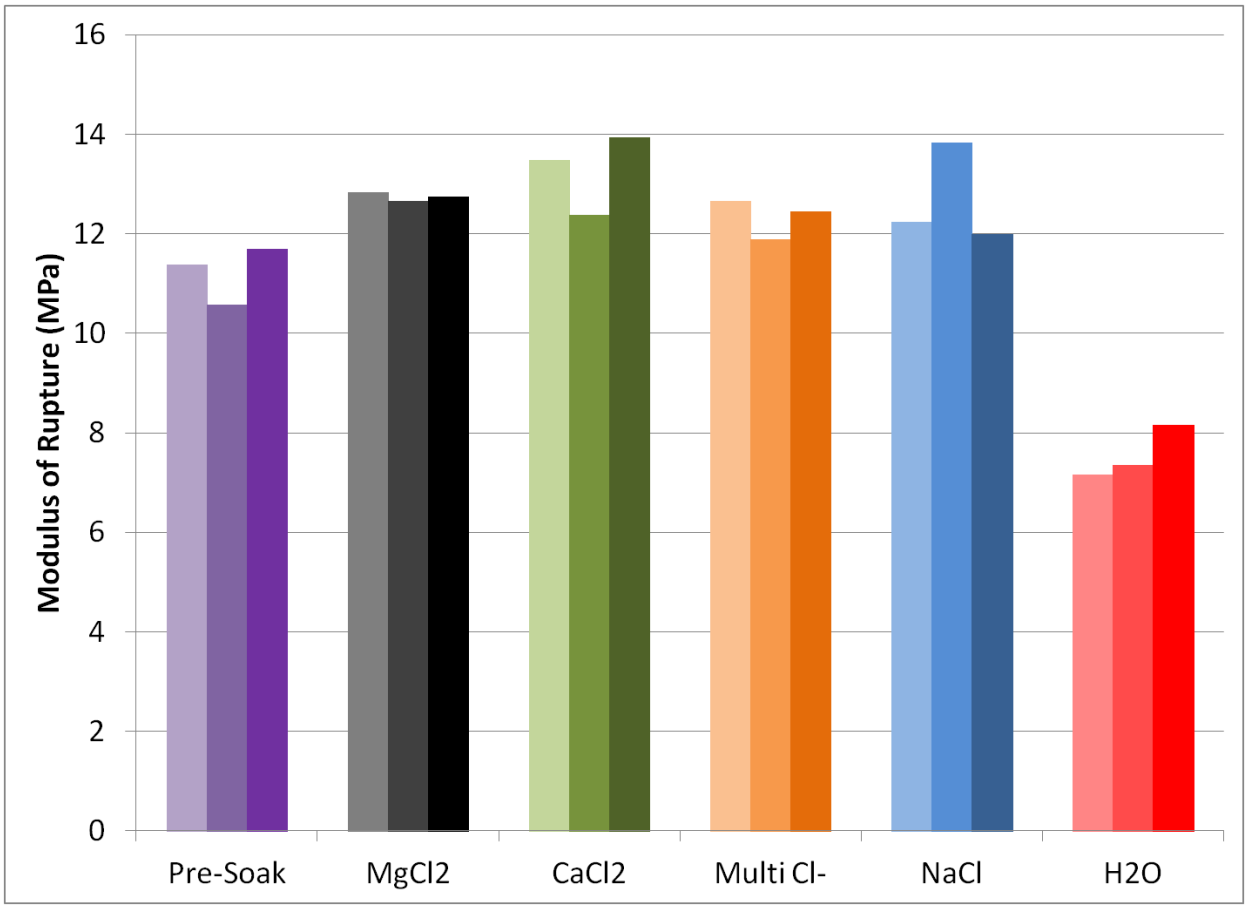

Figure 4.4-6 - Modulii of rupture calculated from results of three-point bend tensile testing

Figure 4.4-6 shows the modulii of rupture for each prism measured. Contrary to the elastic modulus results, the modulii of rupture for the samples exposed to salt solution are all greater than the pre-exposure results. This is generally a reflection of the strength increase in the samples after salt solution exposure. Prisms exposed to $CaCl_2$ exhibited the greatest strength on average, followed by the prisms exposed to $MgCl_2$ and NaCl, and finally by those exposed to the multi-Cl^-. Similar to the elastic modulus results, there was a lower modulus of rupture of the control samples. The modulii of rupture was over 30% lower.

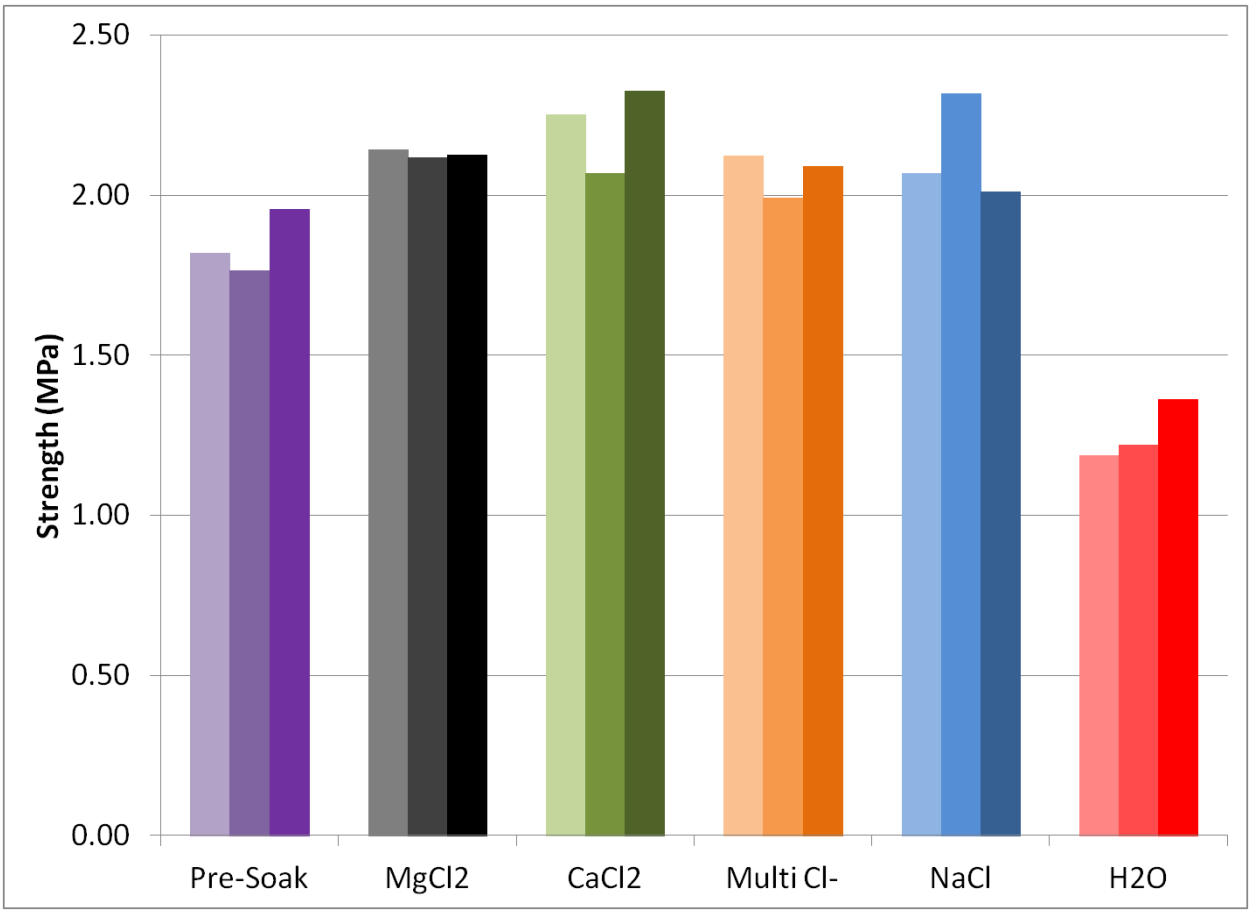

Figure 4.4-7 - Peak strength of prisms tested in tension by three-point bending

The peak strength in tension, shown in Figure 4.4-7, presents the results for tensile strength of concrete in tension under 3-point bending conditions. While there is reinforcing steel which primarily carries tensile loads in concrete structures, the concrete of a bridge deck is still being loaded in tension. From the results, it can be seen that the strength of the $CaCl_2$-exposed prisms were the highest, but at only just above 2.2 MPa. This is approximately one-thirtieth the compressive strength of concrete exposed to the same solutions measured in compression, highlighting the significant difference. The pre-soak prisms data indicated an average tensile strength just under 1.85 MPa with a reasonably large spread of data. All prisms exposed to salt

solutions displayed a higher tensile strength than that of the pre-soak prisms. The prisms exposed to multi-Cl^-, NaCl, and $MgCl_2$ all displayed similar peak strengths with an average around 2.1 MPa. The $MgCl_2$ and multi-Cl^- prisms showed good consistency in the variability of results, while the prisms exposed to $CaCl_2$, NaCl and the control specimens showed much higher variability from one measurement to the next. The control prisms, contrary to those exposed to salt solutions, exhibited a lower strength than the pre-soak prisms, with an average just under 1.3 MPa – almost half that of the samples exposed to salt solutions.

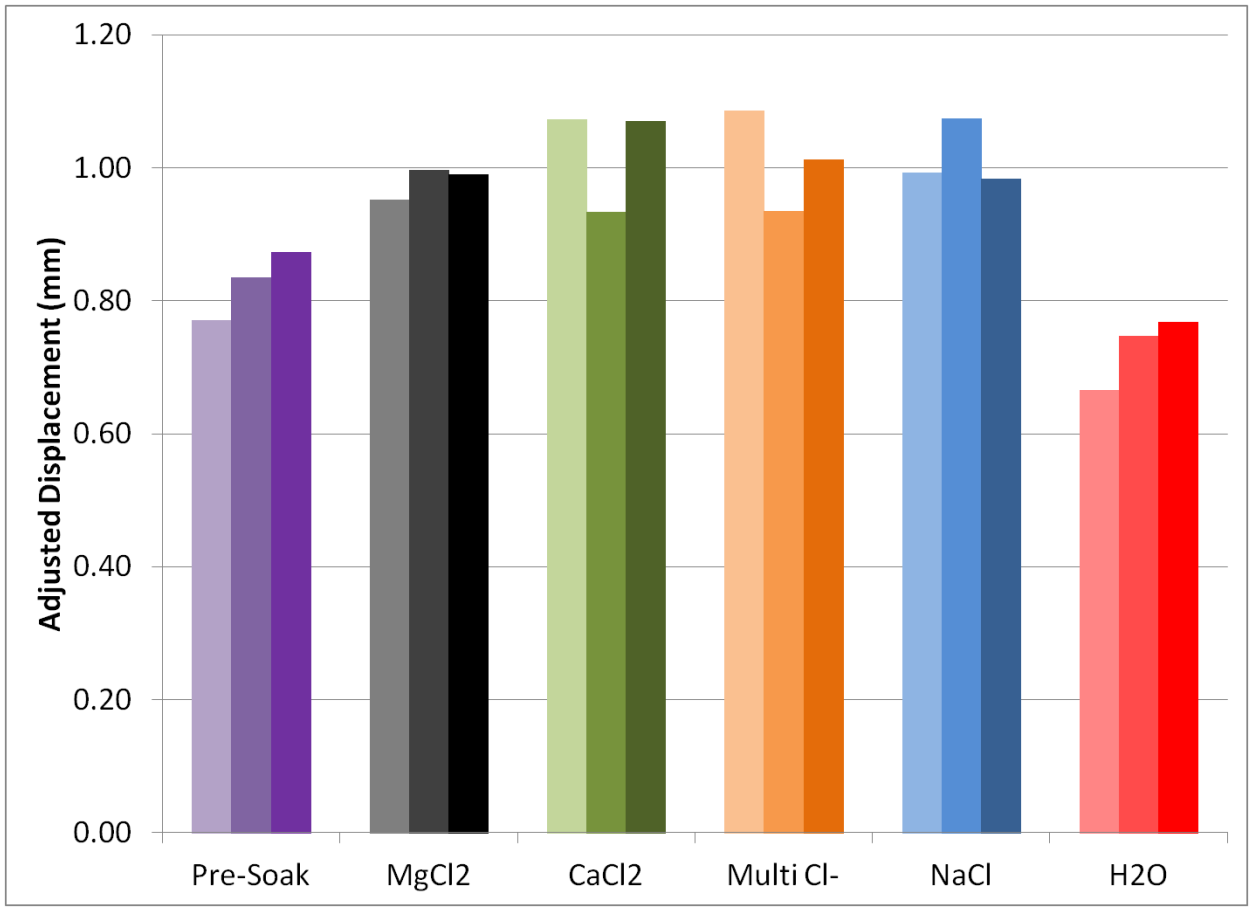

Figure 4.4-8 - Maximum displacement adjusted to remove effects of equipment settling for tension testing by three-point bend

The maximum displacements, adjusted to remove the effects of equipment settling, are shown in Figure 4.4-8. These data represent the distance that the ram moved during the application of force on the concrete, or the amount that the top surface of the concrete displaced from its original position. The pre-soak data show a reasonably wide spread of results, all around 0.80 mm of displacement. Similar to the peak strength, all prisms exposed to salt solutions exhibited a higher displacement than the pre-soak prisms. The prisms exposed to $CaCl_2$, multi-Cl^-, and NaCl each exhibited similar average displacements just over 1.0 mm. For each of these three sets, there was a reasonably high degree of variability between data. The $MgCl_2$-exposed prisms exhibited less displacement than the prisms exposed to $CaCl_2$, multi-Cl^-, and NaCl, with an average just less than 1.0 mm. Similar to the peak strength data, the data agreement for prisms exposed to $MgCl_2$ was high. The control prisms exhibited a lower displacement than the pre-soak prisms by an average of 0.1 mm or about 12.5%.

4.5 Chloride Penetration

The chloride concentration profiles were determined after two weeks soaking and again after 19 weeks soaking. From this, an understanding of chloride penetration and an effective diffusion coefficient can be calculated. The data in Figure 4.5-1 represent the percent chloride by weight of cementitious materials at given depths from the penetration surface.

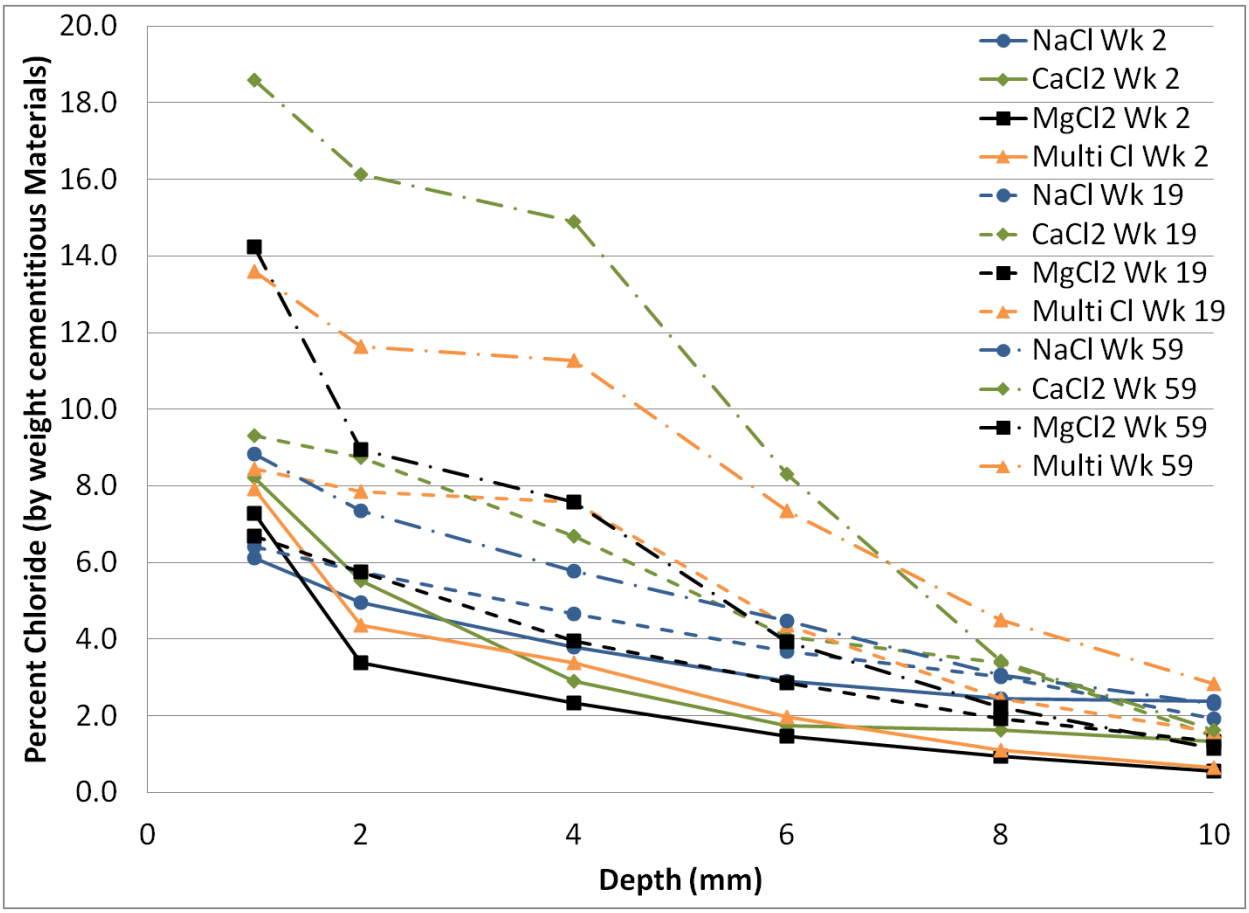

Figure 4.5-1 - Chloride penetration into concrete from one direction measured after 2, 19, and 59 weeks soaking by weight of cementitious materials

From Figure 4.5-1, a number of trends can be noted. Considering first with respect to time, there is a clear difference in the chloride concentration at the surface (less than 2 mm deep) versus greater than 2 mm deep. There is a much greater concentration gradient in the $MgCl_2$ and multi-Cl^- samples from one to two millimeters than there is from two to four millimeters. For the $CaCl_2$ sample, there is a sharper gradient from one to two millimeters, but from two to four and four to six millimeters, the gradient is still relatively large. The NaCl sample shows little surface effect, instead appearing more linear. Comparing solutions, magnesium chloride has the lowest chloride concentration while other than at the surface, NaCl is highest.

Reviewing the measurements from 19 weeks exposure, there exists much lower gradient between each measurement depth and instead more linear trends. There still exists a notable gradient between the surface and ten millimeters within the sample, though it appears to be slightly less than at two weeks. Specimens exposed to $MgCl_2$ exhibit the lowest chloride concentration, while those exposed to $CaCl_2$ and multi-Cl^- have the highest concentration of chloride, at similar levels. There appears to be very little change in the NaCl ingress. There are about 0.7% increases over this period of time at most points, which is small compared to the 3-4% changes seen in samples from the other solutions.

The results from 59 weeks show different trends than those seen at 19 weeks. The $CaCl_2$ and multi-Cl^- show significant increases in chloride concentration, especially at the surface where an increase of 5-7% is seen. These samples also both exhibit greater slopes which appear less linear than after 19 weeks. There is also a much more significant increase in the magnesium chloride sample, which suggests that the $Mg(OH)_2$ (brucite) layer expected to have formed is being penetrated at an increasing rate. The sodium chloride penetration shows a similar increase to that at 19 weeks, but with a greater magnitude. The profile of the NaCl curve is nearly the same as at 19 weeks. The 2 week, 19 week, and 59 week profiles by solution are shown in Figure B.4-1 through Figure B.4-4.

From the penetration data, effective diffusion coefficients can be modeled. In order to calculate the diffusion coefficients, Equation 1 from ASTM C1556.11 [**35**] is applied in

combination with the measured concentrations and extrapolated surface concentration. The equation is shown in .

$$C_{(x,t)} = C_s - (C_s - C_i) \cdot \text{erf}\left(\frac{x}{\sqrt{4 \cdot D_{eff} \cdot t}}\right)$$

Figure 4.5-2 - Fick's second law for diffusion [35**]**

where:

$C_{(x,t)}$ = concentration at depth, x, and time, t

C_s = surface concentration

C_i = initial concentration

x = depth (m)

D_{eff} = effective diffusion coefficient (m^2/s)

t = time (s)

The diffusion coefficient profiles for the salt solutions by measured data are shown in Figure B.4-5 through Figure B.4-9. From these results it can be seen that the values are continuously decreasing. The results for single-diffusion coefficient analysis shown in Figure B.4-10 through Figure B.4-13 and Figure B.4-14 through Figure B.4-17 for chloride selective electrode and EDS methods, respectively, apply the same equations for a best fit curve as opposed to point-by-point analysis. The effective diffusion coefficients for the four solutions established through this approach are shown in Table 4.5-1 for both sets of data, i.e by chloride selective electrode

measurements of ground powders and by energy dispersive x-ray spectroscopy of cross sections.

Table 4.5-1 - Effective diffusion coefficients by curve approximation

	D (m^2/s)	
	Cl^- SE	**EDS**
NaCl	$9.00x10^{-13}$	$3.50x10^{-13}$
$CaCl_2$	$4.00x10^{-13}$	$2.50x10^{-12}$
$MgCl_2$	$4.50x10^{-13}$	$1.10x10^{-12}$
Multi-Cl^-	$7.00x10^{-13}$	$2.60x10^{-13}$

From Table 4.5-1 it can be seen that the effective diffusion coefficient is higher by chloride selective electrode than by EDS analysis for the $CaCl_2$ and $MgCl_2$ solutions, but lower for the NaCl and multi-Cl^- solutions.

4.6 pH and Chloride Penetration by Spray Methods

As seen in Figure 3.2-12, the spray indicators cause a colour change in the surface of the material. In the top row, samples sprayed with the pH indicator solution, appears predominantly green, purple, or blue in colour which represents pH of 9, 11, and 13, respectively. The lower row, samples sprayed with the 0.1M $AgNO_3$ solution, shows a white rim around the outside of the specimens. This colour change border represents the limit of chloride penetration where the soluble chlorides are equal to 0.15% Cl^- by weight of cement [**33**] which is indicative of approximately 0.5% Cl^- total chlorides by weight of cement. The width of the colour change area is taken three times on each side of the sample for statistical

accuracy and averaged to find the associated penetration depth from each exposed surface of the concrete.

The chemical changes in concrete specimens can provide a background in understanding changes that are happening with respect to physical properties of the concrete. While the focus of this report is on the changes of the concrete, it is important to consider that the vast majority of concrete used in civil infrastructure will contain embedded reinforcing steel, which is highly susceptible to damage due to chlorides, but also requires a high pH to remain passive. Changes in pH can also provide insight into reactions occurring between the salt solutions and paste, as the pH of the reaction products will tend to cause an increase or decrease in pH of the concrete, depending on the reaction.

The analysis using spray methods yields two results – one from the pH spray, indicating the pH profile of the sample, and one from the $AgNO_3$ spray, indicating the depth to which a minimum of 0.15% Cl^- by weight of cement has penetrated.

Considering the pH analysis, the majority of results indicated there was little change in the pH of the specimens. Some specimens exhibited slight changes in colour and thus pH near the edges, but there was relatively little difference between the edges and centre. Figure 4.6-1 through Figure 4.6-5 show the pH images taken from the testing. It can be seen that all samples appear the same colour, including the sample exposed only to potable tap water.

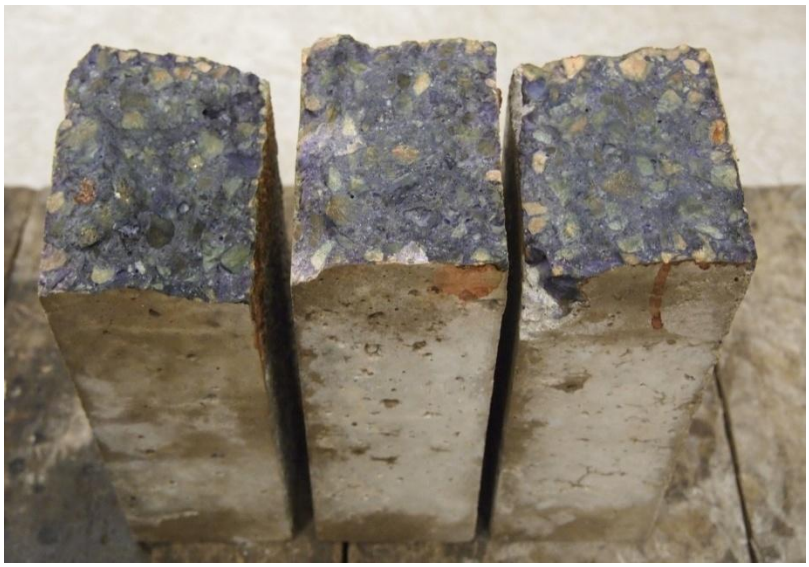

Figure 4.6-1 - $MgCl_2$ pH results by spray method

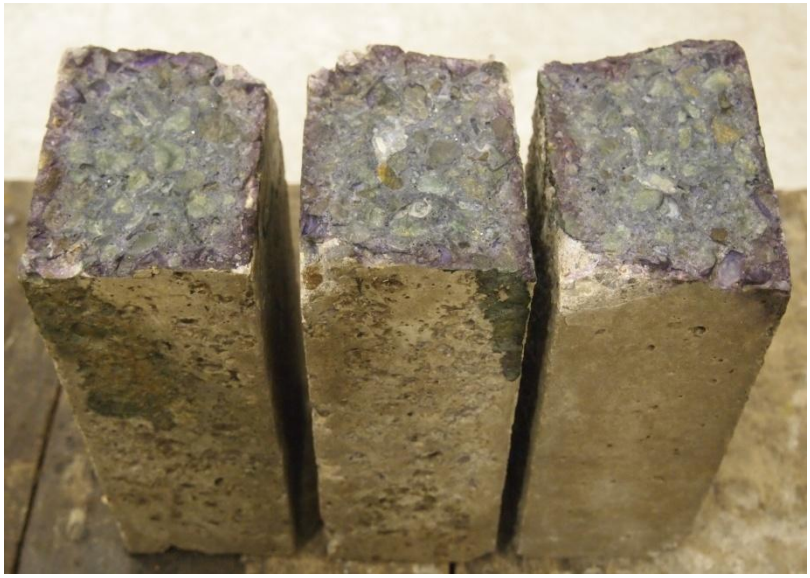

Figure 4.6-2 - $CaCl_2$ pH results by spray method

Figure 4.6-3 - Multi-Cl^- pH results by spray method

Figure 4.6-4 - NaCl pH results by spray method

Figure 4.6-5 - H_2O pH results by spray method

In order to establish the chloride penetration depth by spray method, the samples must all be photographed one by one from a top view and then chords drawn to measure the depth of penetration. An example of the chord implementation is shown in Figure 4.6-6.

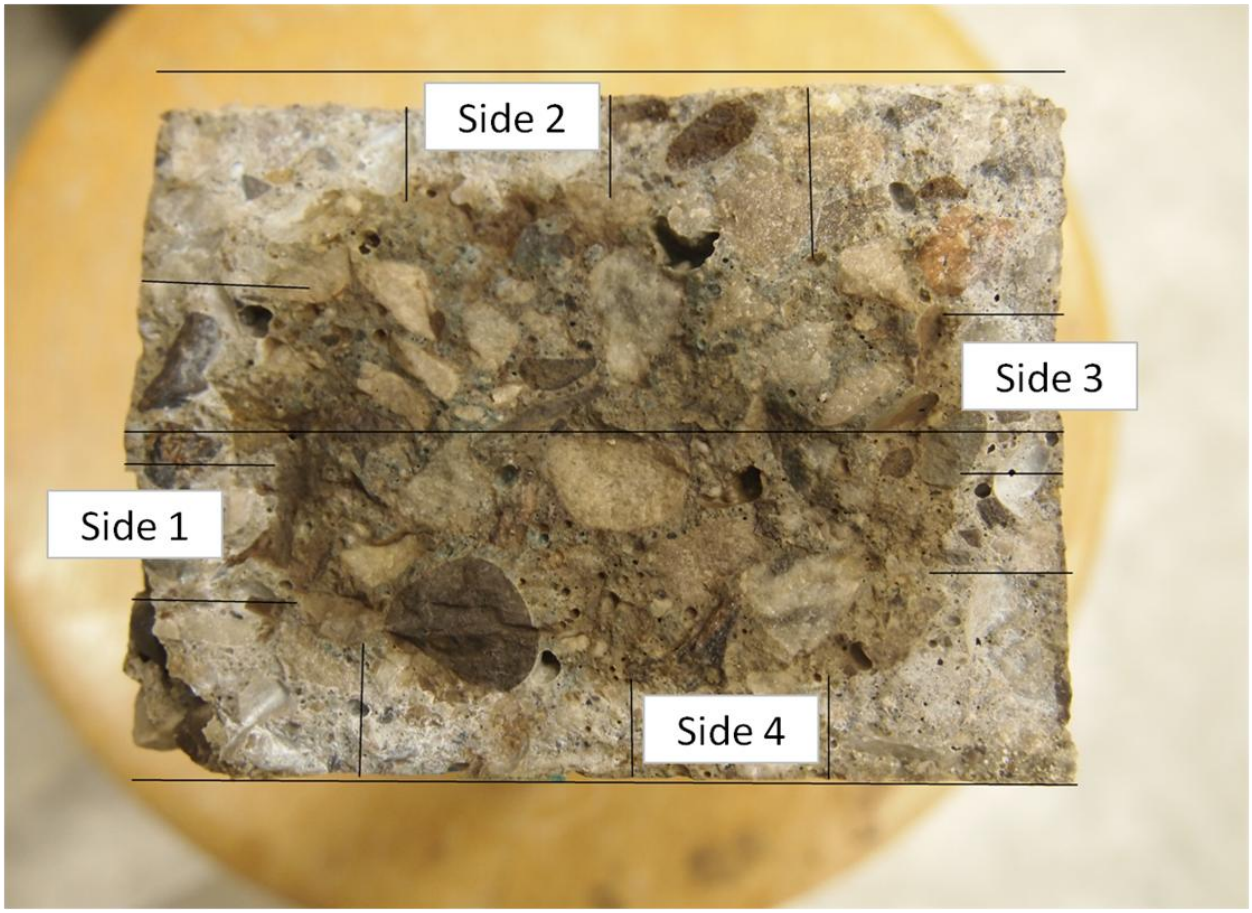

Figure 4.6-6 - Chloride penetration by $AgNO_3$ sample chord measurement layout

All samples are analyzed using the method shown in Figure 4.6-6, and the lengths recorded. The chord locations were selected for each specimen to avoid extraneous effects of aggregates close to the surface. The three long horizontal chords were used to calibrate the dimensions of the specimen in pixels. The resulting data from this analysis are shown in Table 4.6-1. Side one and side three are each 76.2 mm (3 in), while sides two and four are 101.6 mm (4 in). Samples are rotated such that side one and side three alternated being at the top and bottom of the container during testing, such that penetration should be reasonably consistent.

Table 4.6-1 - Chloride penetration by $AgNO_3$ spray method results

Sample	Side 1	Cast Top (Side 2)	Side 3	Cast Bottom (Side 4)	Average (76.2mm)	Average (101.6mm)	Average (All)
CaCl2 1	12.88	12.57	18.49	12.12	15.69	12.34	**14.02**
CaCl2 2	14.23	11.30	15.57	13.77	14.90	12.54	**13.72**
CaCl2 3	14.81	10.90	17.21	13.39	16.01	12.15	**14.08**
MgCl2 1	9.75	8.76	9.44	6.79	9.59	7.77	**8.68**
MgCl2 2	10.25	5.68	11.59	9.28	10.92	7.48	**9.20**
MgCl2 3	8.91	7.70	10.29	10.74	9.60	9.22	**9.41**
Multi 1	25.63	14.20	8.84	13.58	17.23	13.89	**15.56**
Multi 2	13.18	16.00	14.55	12.10	13.87	14.05	**13.96**
Multi 3	13.76	10.12	14.22	10.77	13.99	10.45	**12.22**
NaCl 1	16.68	15.39	13.33	16.21	15.01	15.80	**15.40**
NaCl 2	16.89	16.76	20.21	13.88	18.55	15.32	**16.93**
NaCl 3	15.39	13.19	15.26	13.78	15.32	13.48	**14.40**

From the data in Table 4.6-1 the results can be averaged to get a single result for each of the salt solutions. These data are presented in Table 4.6-2. From these results it can be seen that the sodium chloride shows the greatest average penetration, with the average of all sides being 15.58 mm of penetration for 0.15% Cl^- by weight of cement. The multi-Cl^- and $CaCl_2$ are almost identical with an average of 13.91 mm and 13.94 mm, respectively. As would be expected when considering the formation of brucite ($Mg(OH)_2$), the $MgCl_2$ samples show the least penetration, with only 9.10 mm for a concentration of 0.15% Cl^- by weight of cement.

Table 4.6-2 - Data averages for chloride penetration by $AgNO_3$ spray method

Sample	Avg(76.2mm)	Avg(101.6mm)	Avg(All)
CaCl2 1	15.53	12.34	13.94
CaCl2 2			
CaCl2 3			
MgCl2 1	10.04	8.16	9.10
MgCl2 2			
MgCl2 3			
Multi 1	15.03	12.79	13.91
Multi 2			
Multi 3			
NaCl 1	16.29	14.87	15.58
NaCl 2			
NaCl 3			

4.7 Energy Dispersive X-Ray Spectroscopy (EDS)

Energy dispersive x-ray spectroscopy (EDS) is an analysis tool often paired with environmental scanning electron microscopy (ESEM) which are a preferential tool set for analyzing and imaging of non-conductive materials, such as concrete. The samples for ESEM/EDS analysis, cut from the chloride penetration blocks, were analyzed each millimeter, with the composition of Na, Mg, Al, Si, Cl, K, Ca, and Fe being measured at each point. With these results a profile of the composition, and specifically the chloride profile, can be accurately measured and recorded, while observing the differences between paste and aggregates with respect to composition. Care was given to select sample paths that would present a majority of paste or fine aggregate so that an accurate chloride profile could be developed, which included repetition of the $MgCl_2$ measurements with a second sample to obtain better data. To understand this change, Figure 4.7-1 is presented showing the results of the first analysis set for the $MgCl_2$ sample where there is essentially only Ca, Si, and Mg present.

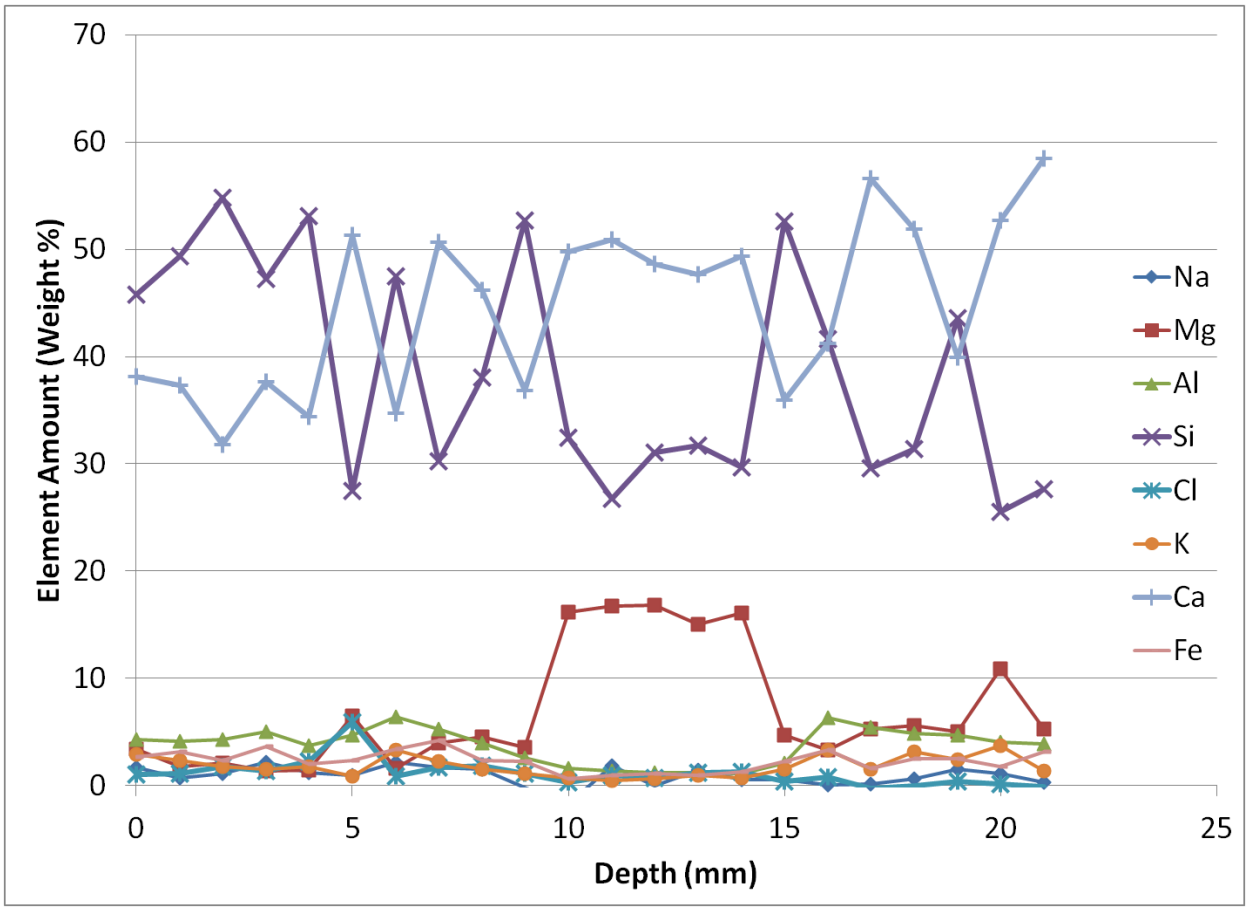

Figure 4.7-1 - Energy dispersive x-ray spectroscopy composition profile for the first $MgCl_2$ sample

After plotting these results and seeing that there appeared to be predominantly aggregate in the path of analysis, a second sample was cut and analyzed. The results of this analysis are presented in Figure 4.7-2.

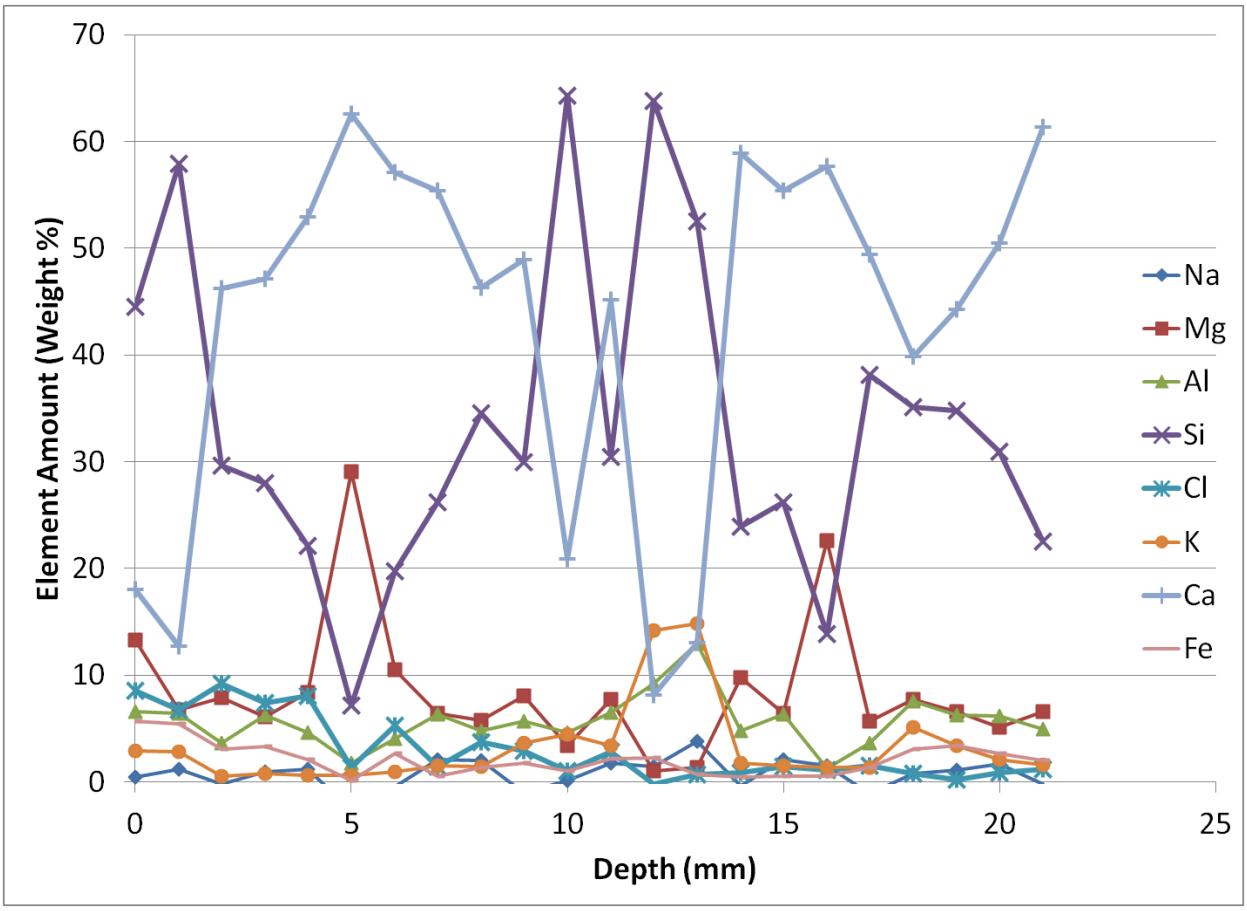

Figure 4.7-2 - Energy dispersive x-ray spectroscopy composition profile for the second $MgCl_2$ sample

From Figure 4.7-2 it can be seen that most of the surface analyzed is paste and fine aggregates as there are a multitude of other elements present. This is most clearly seen through the chloride trend which is high at the surface and decreases with increasing depth. This is the expected result as the surface has the shortest diffusion distance to cross. Areas of silicon-based aggregates can be clearly seen by spikes in the Si profile and corresponding dips in the Ca profile – the primary element in the paste. Presence of Ca-Mg aggregates can also be seen at 5 mm and 16 mm where there are corresponding peaks of Mg and Ca and decreases in all other elements at these locations.

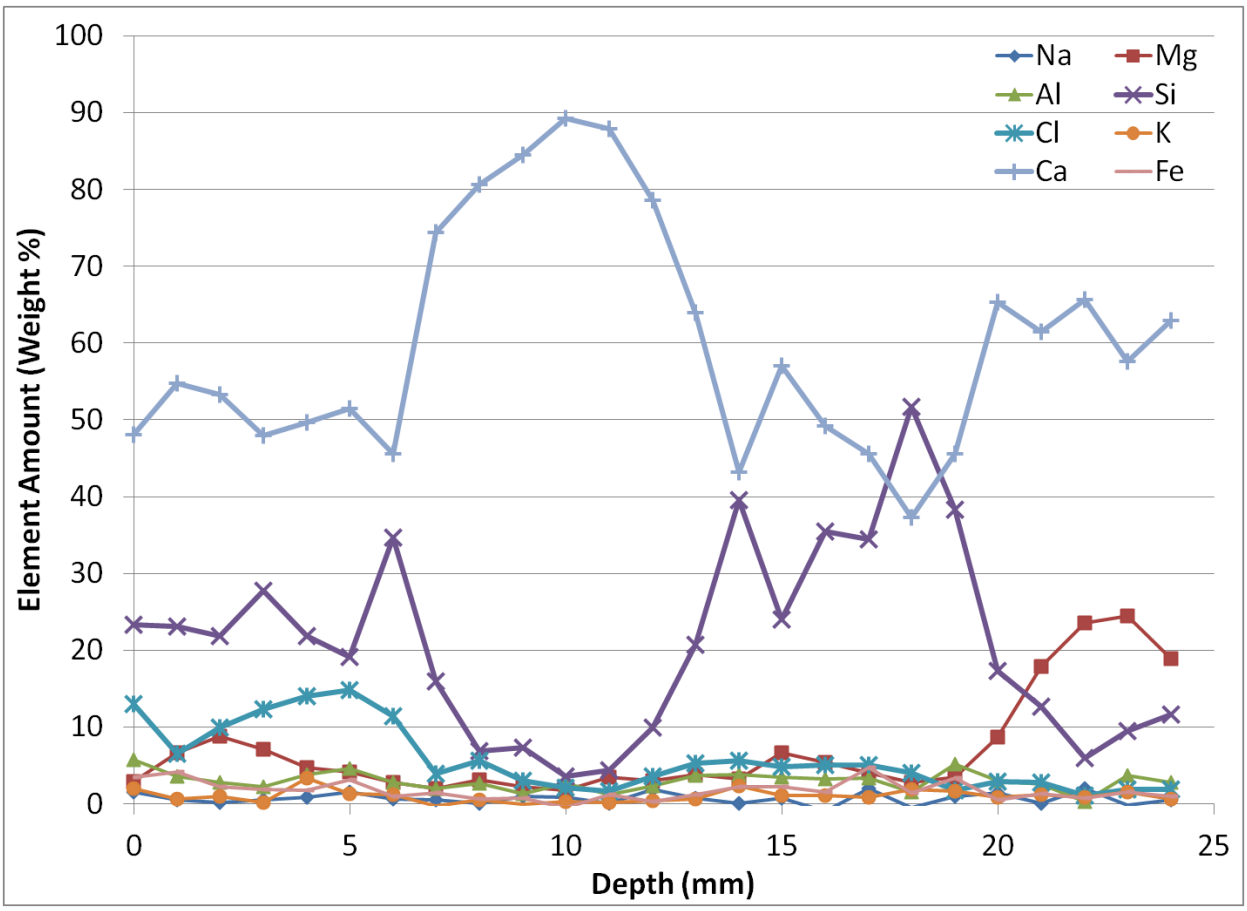

Figure 4.7-3 - Energy dispersive x-ray spectroscopy composition profile for the $CaCl_2$ sample

The composition profile for $CaCl_2$ can be seen in Figure 4.7-3, and shows similar results to the second $MgCl_2$ profile. Areas of paste and aggregate can be clearly differentiated, and the chloride profile is as-expected. The dip in the chloride profile at one millimeter is likely due to a higher presence of aggregate at this location, which appears to extend to about 5 mm into the sample. The aggregate likely occupies a decreasing percentage of the area analyzed as there as a steadily increasing Cl^- content from 1 mm to 5 mm depth.

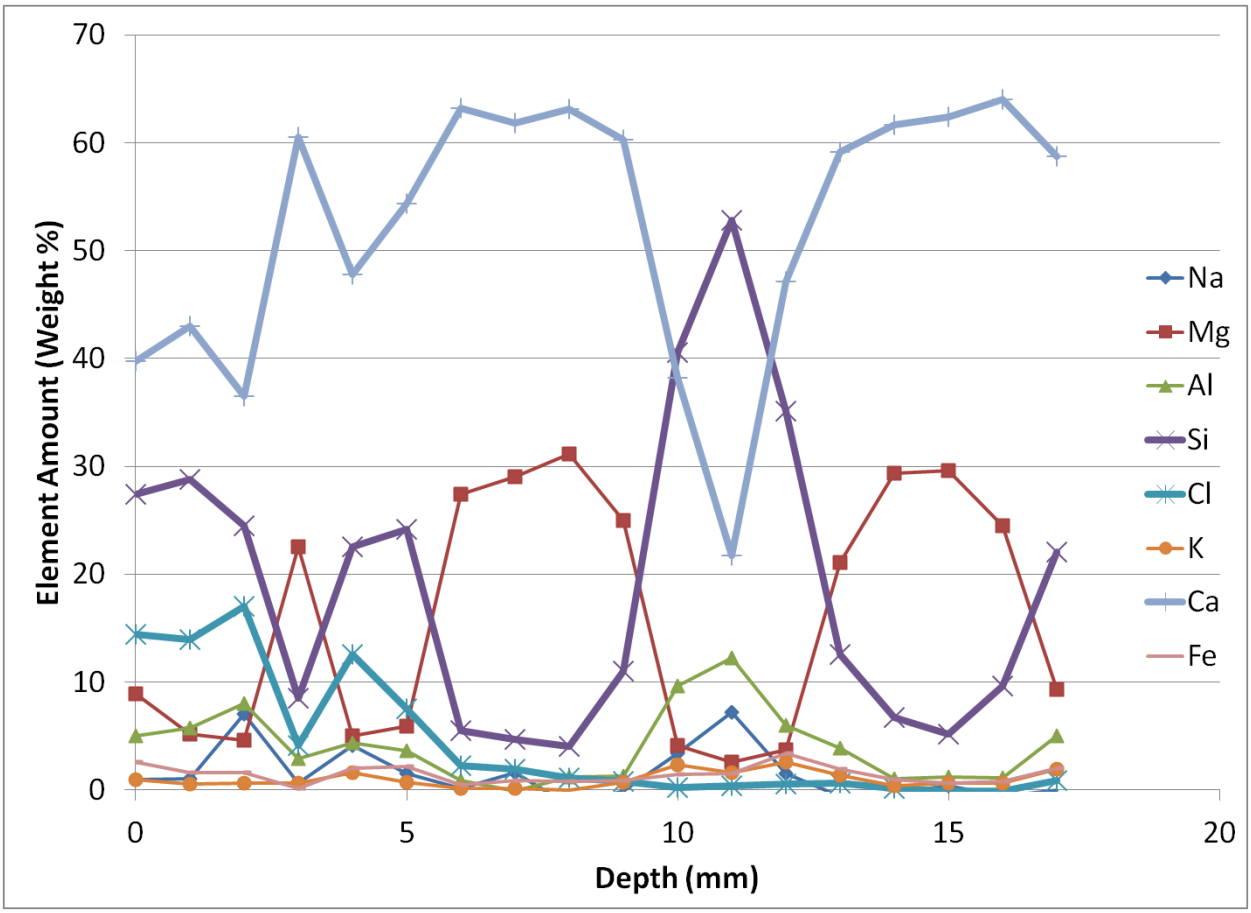

Figure 4.7-4 - Energy dispersive x-ray spectroscopy composition profile for the multi-Cl^- sample

The composition profile for the multi-Cl^- sample is presented in Figure 4.7-4. The results are very similar to the other samples, with the exception of a higher amount of Mg-based aggregates. Similar to the $CaCl_2$ sample, the chloride content near the surface is approximately 15%, which is quite high. It appears that an aggregate at 6 mm has significantly reduced the ingress of chlorides past its depth.

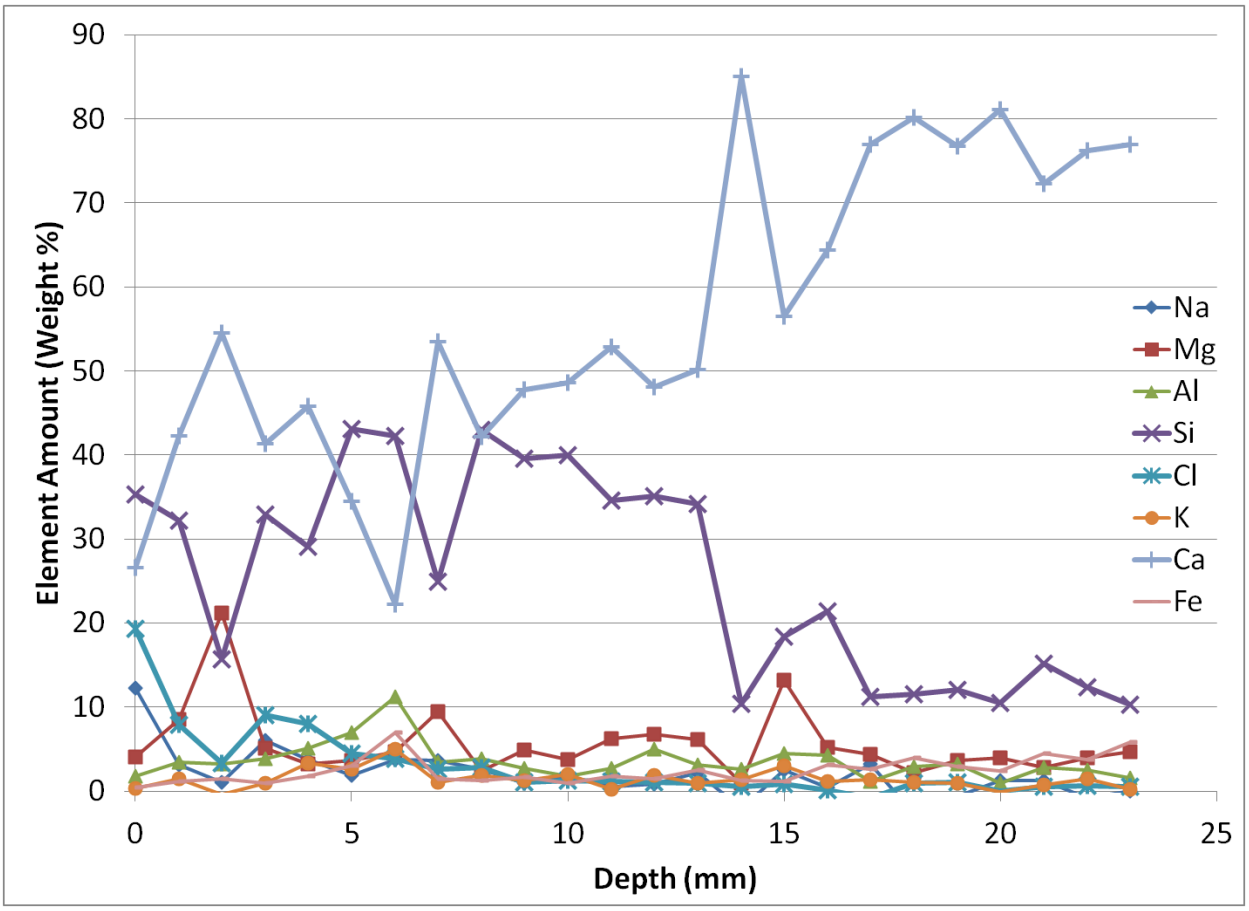

Figure 4.7-5 - Energy dispersive x-ray spectroscopy composition profile for the NaCl sample

The NaCl sample composition profile, shown in Figure 4.7-5, shows the same trends as the other samples except with a higher volume of Ca-based aggregates. The chloride profile has the highest surface concentration at almost 20%, and appears as though it would slowly decrease to about 5% at 5 mm depth.

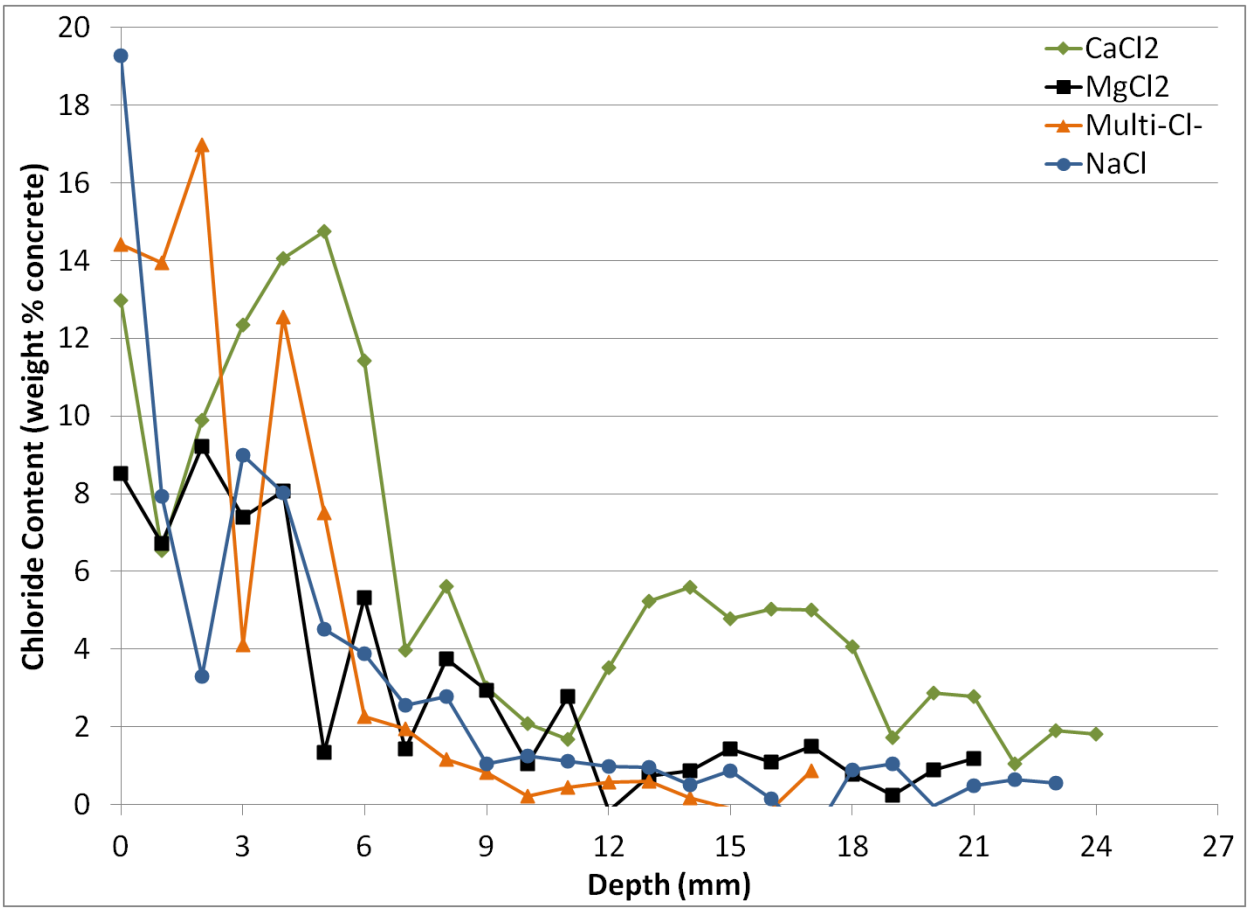

Figure 4.7-6 – Energy dispersive x-ray spectroscopy chloride profile for each of the four samples

The chloride profiles of the samples are the key deliverables from the ESEM testing, and these profiles are shown in Figure 4.7-6. These profiles show that the samples have reached 5% Cl^- by weight of concrete to a minimum of 5mm depth after 59 weeks of soaking. All samples seem to taper off to approximately 1% Cl^- shortly thereafter, with the exception of $CaCl_2$ which appears to essentially maintain a level of 5% Cl^- to 18 mm, and decrease to about 2% at 24 mm.

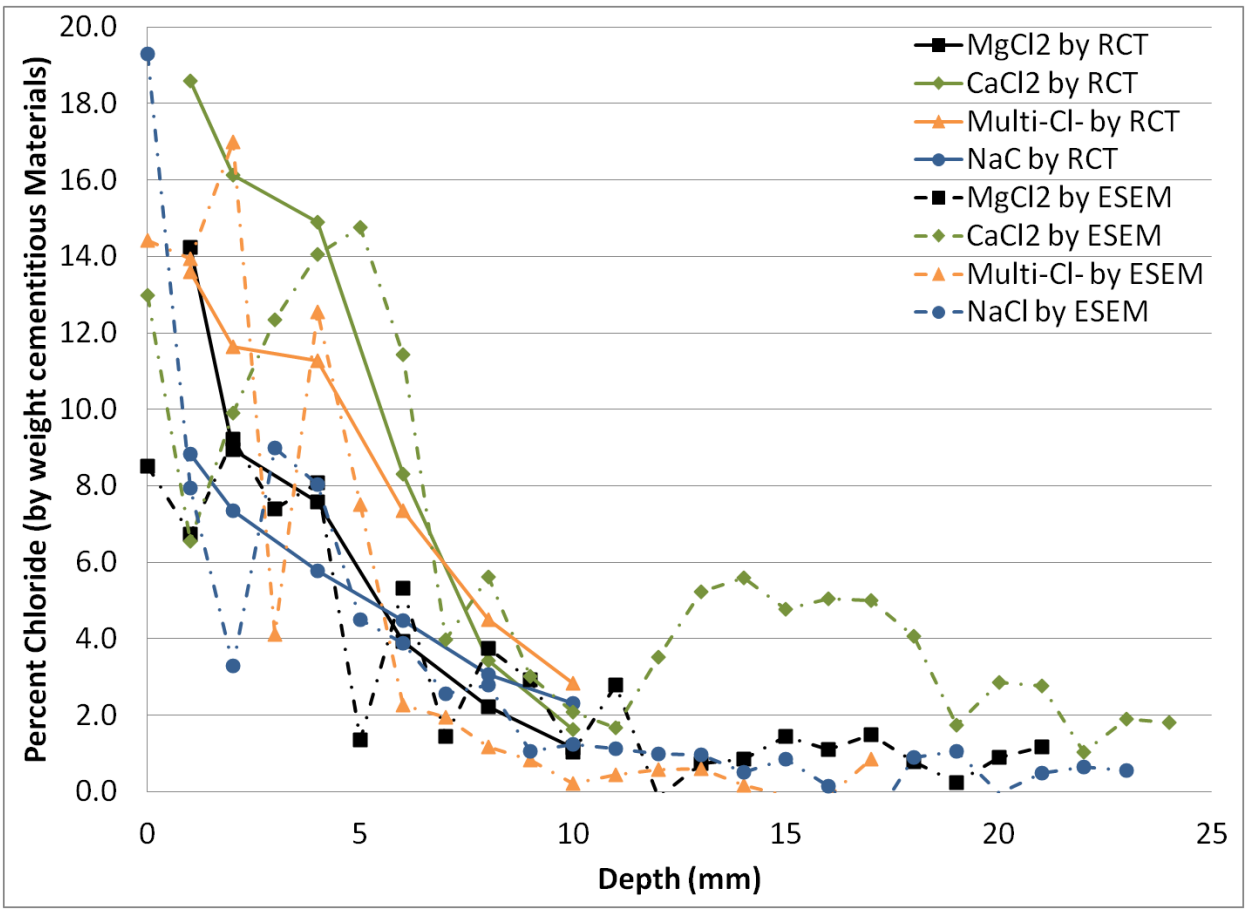

Figure 4.7-7 - Comparison of chloride selective electrode testing and energy dispersive x-ray spectroscopy results from the same samples after 59 weeks soaking in salt solutions

The data in Figure 4.7-7 shows the results of rapid chloride testing (solid lines) and environmental scanning electron microscopy (dashed lines) for samples cut from the same specimen after 59 weeks of the specimen soaking in salt solution. While there is some similarity, there appears notable difference between most individual measurements.

4.8 Air Void Analysis

Air void analysis was conducted for the purpose of both collecting the air void data as well as to inspect the sample for internal cracks. The polished surface shows any imperfections which will

include both air voids and cracks if any are present. The results of the air void analysis were highly variable, which is unexpected since all samples were from a single batch of concrete. The key results of the air void analysis are shown in Table 4.8-1. The full set of raw data can be found in Appendix B in Table B.6-1 and Table B.6-2 following ASTM C457 [**36**].

Table 4.8-1 - Air void analysis results

All Chords		Part 1	Part 2	Average
Air Content (%):	H2O	3.33	3.13	3.23
	$CaCl_2$	5.43	3.22	4.33
	$MgCl_2$	5.05	4.04	4.55
	Multi	9.51	7.45	8.48
	NaCl	3.97	4.37	4.17
Specific Surface (mm^{-1}):	H2O	27.57	28.78	28.18
	$CaCl_2$	53.13	35.44	44.29
	$MgCl_2$	40.38	46.51	43.45
	Multi	58.85	48.02	53.44
	NaCl	46.05	44.54	45.30
Spacing Factor (mm):	H2O	0.213	0.210	0.211
	$CaCl_2$	0.088	0.168	0.128
	$MgCl_2$	0.120	0.116	0.118
	Multi	0.050	0.078	0.064
	NaCl	0.118	0.117	0.117
Void Frequency (mm^{-1}):	H2O	0.229	0.225	0.227
	$CaCl_2$	0.721	0.285	0.503
	$MgCl_2$	0.509	0.469	0.489
	Multi	1.399	0.895	1.147
	NaCl	0.457	0.486	0.472
Average Chord Length (mm):	H2O	0.145	0.139	0.142
	$CaCl_2$	0.075	0.113	0.094
	$MgCl_2$	0.099	0.086	0.093
	Multi	0.068	0.083	0.076
	NaCl	0.087	0.090	0.089

These results also suggest that 4 out of 5 prisms would not meet the requirement of a minimum of 5.5% air content in concrete, as specified by the Canadian Standards Association [**37**]. This means that the concrete would have been deemed sub-standard. Due to the size of the specimens and limitations of the analysis equipment, the samples had to be analyzed in two passes, and the results are the average of the two sides of each sample.

The samples, cut from freeze and thaw specimens which had been exposed to full strength solutions, did not exhibit any cracking visible in the collected micrographs.

5 Discussion:

5.1 Freezing and Thawing

The freezing and thawing testing provided an understanding of the effects of the anti-icing solutions not only on the properties, but also the likelihood of freezing. As discussed, the testing was repeated a second time with solutions diluted to one-third the as-received concentration in order to reach a concentration where all solutions would freeze according to their respective phase diagrams, in Figure 2.2-1 through Figure 3.1-1, Figure 3.2-3, and Figure 3.2-4. The freezing points of the eutectic solutions (-51°C for $CaCl_2$, -33.9°C for $MgCl_2$, and -21.1°C for NaCl) are all more negative than the minimum temperature of the chamber, -18°C. Though not specifically known, the freezing temperature of the multi-Cl^- is expected to be between that of NaCl and $CaCl_2$ since it is primarily a combination of the two.

While the eutectic temperatures are all lower than -18°C, the actual liquidus temperatures of the as-received solutions are about -5°C for the NaCl solution, -16°C for the $MgCl_2$ solution, and +4°C for the $CaCl_2$ solution. It is estimated that the multi-Cl^- would have a liquidus temperature of approximately 0°C considering the liquidus curves for the NaCl and $CaCl_2$ solutions. This means that all solutions are expected to cross the liquidus (or be below it the entire time in the case of $CaCl_2$) during the freezing cycle of the testing. In this case, the solutions would be in the hydro-halite plus brine region, where solid crystals of hydrated halites would form from the solution while the remainder would stay liquid brine. Since all solutions are hypereutectic in nature, the liquid will always approach the eutectic point as the hydro-halites precipitate from it, thus reducing the freezing temperature of the liquid during this process. The

transformations that would occur would result in the formation of hydro-halite crystals as well as more dilute liquid brine.

For the second set of freezing and thawing testing, the solution concentrations were reduced to one-third the as-received resulting in the concentrations indicated in Figure 3.2-4. At these compositions, the solutions surrounding the samples will partially freeze resulting in a combination of ice and more concentrated liquid brine. Solidification theory predicts that a solid is most likely to precipitate at existing solid surfaces, indicating that the ice formation will occur at the sample surface and/or the container walls. As seen by the damage to the surface of the control samples which froze during each freezing cycle, the freezing of the sample cause significant scaling of the surface. This scaling was seen on all samples in the second set of testing except for those exposed to $MgCl_2$.

Since none of the solutions is a pure mixture of the primary salt and water, the actual reactions are likely to be slightly different. A strong indicator of this is the $MgCl_2$ solution, which did not appear to exhibit notable solidification at the minimum temperature in any of the cases where samples were checked. According to Figure 2.2-1, below -16.4°C, a second reaction should occur resulting in complete solidification by Equation 5.1-1.

$$MgCl_2\ Brine \rightarrow (MgCl_2 \cdot 8H_2O)_s + (MgCl_2 \cdot 12H_2O)_s$$

Equation 5.1-1

According to Equation 5.1-1, which represents a second eutectic reaction for $MgCl_2$ at about 31.6% $MgCl_2$ in solution, the entire solution should solidify into the two hydrated halite solids, creating a complete solid instead of a solid-liquid mixture. Since it has been observed that this complete solidification does not, in fact, occur it can be assumed that the impurities and other contents of the solution create a shift in the liquidus curves and eutectic point, and/or that the time for at the low temperatures was not sufficient to allow for the transformation. This seems especially true of $MgCl_2$, which also remained liquid at the -18°C temperature minimum during the second set of freezing and thawing cycles. This suggests that the impurities have sufficient effect to move the liquidus temperature of the solutions and combined with the extremely fast temperature cycles, the solutions are not able to transform before the temperature rises again.

From the elastic modulus results presented in Figure 4.1-2 through Figure 4.1-4 it can be seen that there is a clear and consistent trend of increasing in the samples exposed to salt solutions as compared to the control samples. In Set 1, with the as-received solutions, the increase was fairly rapid, and followed by what appeared to be a plateau. In Set 2, the increase was much more gradual. No plateau appeared to be reached, though this may be the result of the period of testing. Such a plateau as seen in the Set 1 data may have been reached over a longer testing period. It is predicted that the cause of this change in elastic modulus is the ingress of chlorides which result in two effects: filling of the pores with crystals and expansive reaction of the salt with the cement paste components, thus increasing molecular binding. As seen through the tensile strength testing, the addition of the salt solutions results in a small increase in strain and a more significant increase in strength, which is consistent with the freezing and

thawing test results. The pores in concrete act to weaken it by reducing the cross-sectional area through which the load can be transferred while also allowing easier crack propagation. In the case of filling the pores as the crystallized salts do, thus reducing their ability to allow strain, while simultaneously increasing the strength by increasing the surface area over which an applied force could be distributed and reducing the ease of crack propagation. The equation for elastic modulus is given in Equation 5.1-2 [**34**].

$$E = \frac{\sigma}{\varepsilon}$$

Equation 5.1-2 [34**]**

where:

E = elastic modulus (MPa)

σ = strength (MPa)

ε = strain (m/m)

The filling of pores by precipitates causes both stress and strain at fracture to increase simultaneously. As shown by MacGregor and Bartlett [**38**], there is a correlation between increasing compressive strength and stiffness of concrete seen in Figure 5.1-1.

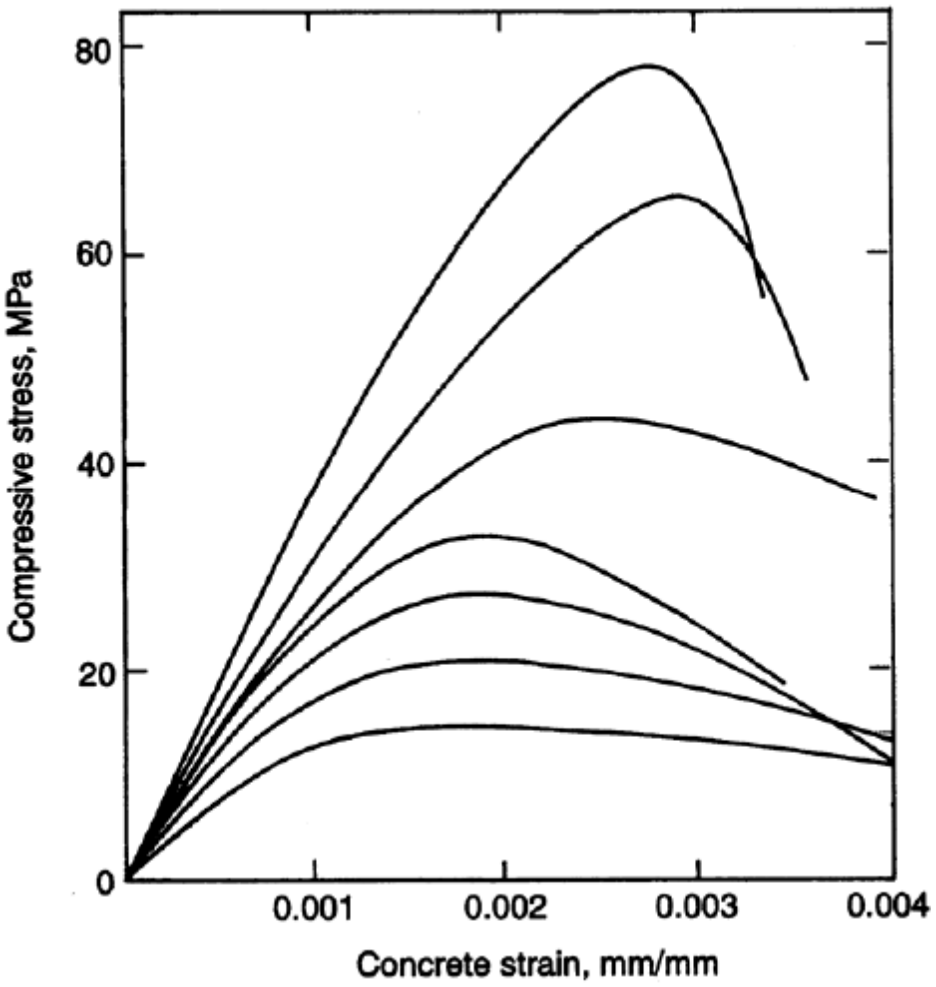

Figure 5.1-1 - Stress versus strain profiles for concrete of increasing compressive strength [38**]**

The elastic modulus of concrete can be estimated by Equation 5.1-3 [**39**].

$$E_c = \left(3300\sqrt{\sigma} + 6900\right) \cdot \left(\frac{\rho}{2300}\right)^{1.5}$$

Equation 5.1-3 [39**]**

where:

E_c = elastic modulus (MPa)

σ = compressive strength (MPa)

ρ = concrete density (kg/m^3)

Knowing that the compressive strength of the concrete increases with the exposure to salt solution and considering both Figure 5.1-1 and Equation 5.1-3 an increase in elastic modulus is expected.

The presence of NaCl is not known to cause reaction with the cement paste components. The reactions of the $MgCl_2$, $CaCl_2$, and multi-Cl^- solutions with the cement paste components would be based primarily around the $CaCl_2$ reaction with $Ca(OH)_2$ as defined by Equation 2.2-3 [**2**]. While this is a secondary reaction in $MgCl_2$, it will still occur. There is a slightly higher elastic modulus for the three groups of prisms exposed to these salt solutions than for those exposed to NaCl for the as-received solution application. For the specimens exposed to the diluted solutions, the elastic modulii of the specimens exposed to NaCl are, on average, higher than the specimens exposed to $CaCl_2$ or $MgCl_2$, suggesting that if there is an effect seen from the reactions with the cement paste, it is too small to cause an effect in these samples over this short period of time because of the lower solution concentrations.

An explanation for the higher elastic modulus of the samples exposed to the diluted NaCl solution can be had from a review of chloride penetration data in Figure 4.5-1. At early stages of exposure, the NaCl had a more linear concentration profile and higher concentrations at deeper levels than seen for the other three solutions. The elevated levels of NaCl deeper into

the specimens suggest there will be more crystallization in the pores at these depths, thus causing the increase in strength. The compressive strength data of Figure 4.3-1 and Figure 4.3-2 do not show agreement with a higher strength than the other samples, but cannot verify nor deny the possibility of a decrease in achievable strain.

An interesting aspect of the freezing and thawing Set 2 results using diluted solutions, in Figure 4.1-3, is the change in elastic modulii of the control samples around 275 cycles. Up to 275 cycles there appears to be no change in the elastic modulus of the control samples, after the increase over the first week which is associated with the initial absorption of water. These results show that it took about 275 cycles for the effects of the freezing and thawing to cause a change in the elastic modulus, after which the elastic modulii of prisms exposed only to water increase. This effect is not seen in the first set due to the damage and scaling of the control prism and inconsistency of results; however, this observation implies that the increases in elastic modulii over the first 200-300 cycles seen in the samples exposed to salt solutions are due to the solutions themselves rather than the effects of freezing. For the Set 2 data, it is possible that there would be compounding effects of the freezing of the concrete and the effects of the salt solutions on the concrete found near the end of the test period, which may help to explain the significant increase in elastic modulus of the prisms exposed to multi-Cl^- at about 275 cycles – similar to the control samples.

While the elastic modulii give insight into the changes in physical properties of the concrete, the mass data give a better perspective on the damaging effects of freezing and thawing. In Set

1, where unlike the prisms exposed to water there was relatively little scaling of the samples exposed to salts due to the lack of freezing. Instead, there is a slight increase or no change in mass with respect to time indicating that the salt solutions actually benefit the concrete by helping prevent mass loss. This is quite evident in the first set where the elastic modulii of the control samples could not be measured after only 200 cycles while the prisms exposed to salt solutions, based on final appearance, could have been measured long after the completion at about 400 cycles. At a minimum, the salt solutions doubled the period of time over which the surface of the concrete remained in good condition. Photographs of a control prism and one exposed to $MgCl_2$ are shown in Figure 5.1-2 and Figure 5.1-3, respectively. It is important to note that both samples were in the same orientations when the images were taken and that both were marked in the same manner prior to the initial submersion. It can be seen by the complete loss of material due to scaling of the H_2O prism that there has been such severe damage the initial markings are completely removed.

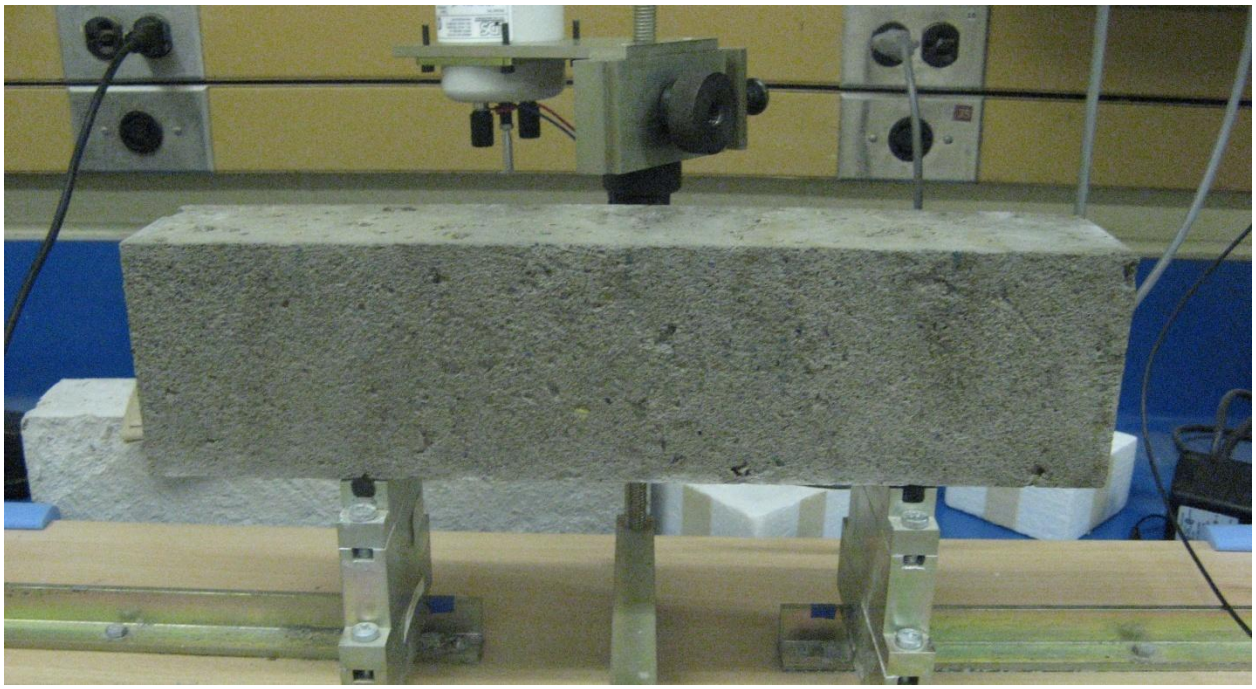

Figure 5.1-2 - H_2O freeze and thaw prism number one front after 385 freeze and thaw cycles

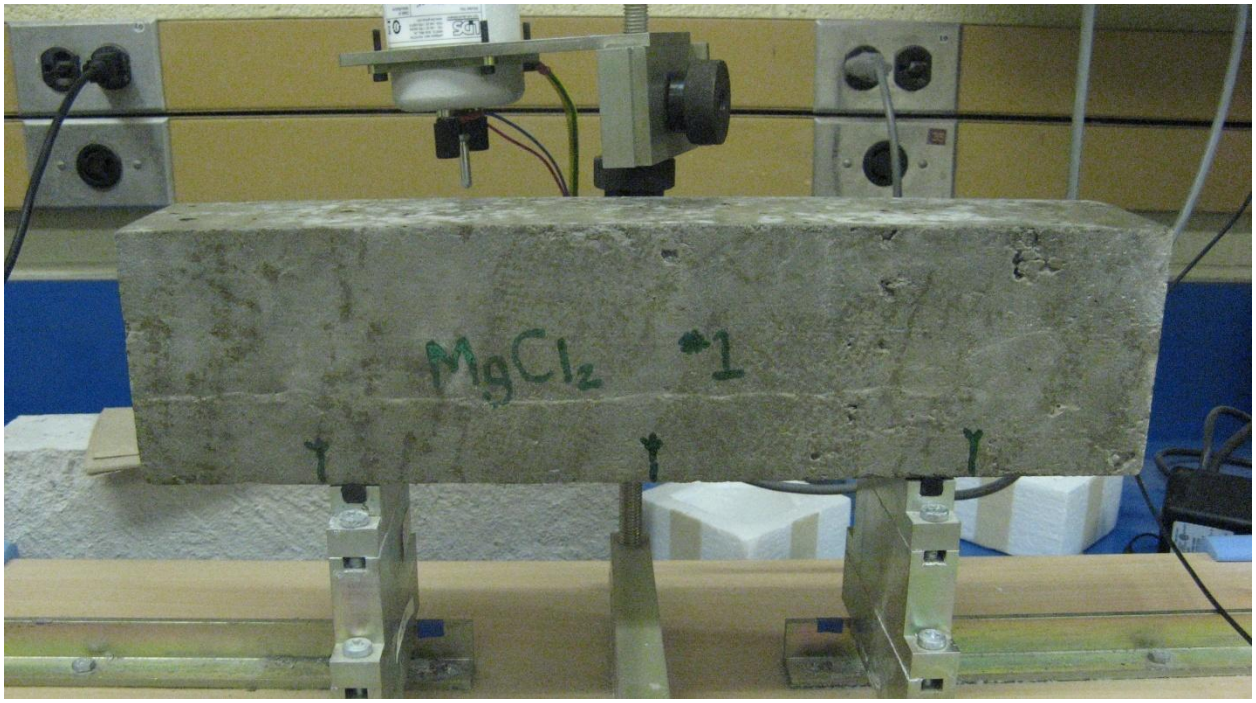

Figure 5.1-3 - $MgCl_2$ freeze and thaw prism number one front after 385 freeze and thaw cycles

In Set 2, the masses of all samples except for those exposed to $MgCl_2$ exhibited a decreasing trend following their initial increase, Figure 4.1-6. This result, which can be strongly correlated with debris measurements, indicates the inability of the solutions to prevent freezing of the samples. While the reduction of effects of the concrete freezing is not the direct purpose of the solutions, it is an indirect benefit of the solutions on the quality of the concrete surface. Continued exposure to freezing and thawing will not only lead to continued damage, however, it will be compounded by the effects of salt scaling, which was not found in the freeze and thaw testing of the samples exposed to as-received solutions, though may be with prolonged exposure. This damage can be clearly seen when comparing the NaCl prism pre-exposure to the same prism after 355 freezing and thawing cycles as seen in Figure 5.1-4 and Figure 5.1-5, respectively.

Figure 5.1-4 - freezing and thawing set 2, diluted solutions, NaCl prism one prior to exposure

Figure 5.1-5 - freezing and thawing set 2, diluted solutions, NaCl prism one after 355 freezing and thawing cycles

The mass of debris is consistent with the mass change of the prism for each measurement. There is not a direct agreement since the prisms will absorb water and salts. In the first set of freeze and thaw testing the specimens exhibited an initial average increase of 36.5 g for the $MgCl_2$ specimens up to 130.5 g for the NaCl specimens. Over the course of the 8 weeks of freezing and thawing exposure, average mass change for prisms exposed to $CaCl_2$ and $MgCl_2$ solutions increased week over week, with the exception of week four when the chamber remained in the freeze cycle and, thus, the prisms exhibited lower masses for that measurement. The prisms exposed to the multi-Cl^- solution increased each week except for the sixth and eighth weeks, equivalent to about 300 and 400 cycles, respectively. For those two weeks the decrease was negligible (0.033 g) and may have been caused by equipment variances or slight temperature differences. The samples exposed to NaCl solution exhibited a decrease for two of the three weeks following the initial increase, and increases all other weeks, again with the exception of week four, around 200 cycles. In the case of NaCl the decrease was 2.7 g and 4.2 g, respectively, which cannot be attributed to debris due to the lack thereof. In this case it may be a result of surface drying since the NaCl solution had a tendency to wick over the specimen container edges thus leaving the top surface uncovered and able to dry out.

The agreement between specimen mass and debris mass is more clearly seen through the data from freeze and thaw Set 2, exposure to diluted solutions, where there was appreciable and consistent mass decrease correlated to debris collection. Although there was debris in the second week, the mass loss from debris was offset by the mass gain due to the solution absorption. This offset is reflected in the measurements following 140 cycles, as the average

mass of debris was greater than the average decrease in prism mass for each solution. This reflects the continued absorption and diffusion of solution into the sample.

In addition to mass loss by scaling, the freezing and thawing cycles can induce cracking. However, such cracks were not detected by the microscopy associated with the air void analysis on the first set of freezing and thawing prisms exposed to as-received solutions. However, the temperature control sample was completely split due to the effects of freezing during the last week of temperature cycling as shown in Figure 5.1-6.

Figure 5.1-6 - Severe crack in freezing and thawing Set 1 temperature control prism

Three of the four solutions in this study do not begin to form ice until well below the minimum temperature of the test. The sodium chloride, with 25.5% NaCl, is more concentrated than the eutectic composition and, under equilibrium conditions at –18°C, it would be only about 3.3% solid and the solid would be crystalline hydrated halite, as defined in Figure 2.2-4, not ice. In the non-equilibrium temperature conditions of the test, the solution would have likely remained

fully liquid at -18°C because there would not be time for nucleation and growth of the NaCl crystals to any significant size. Under equilibrium conditions, the $CaCl_2$ and $MgCl_2$ solutions would experience similar hydro-halite formation reactions during the testing, and it is expected that the multi-chloride solution would do the same. However, with a three-hour cycle, equilibrium is never reached. Consequently, these results do not present useful data for elastic modulii relating to the freezing and thawing aspect. The tests in diluted solutions more realistically reflect the combination of effects of salt solution and freezing, though biased by the lower concentrations.

5.2 Internal Strain

The long-term testing of outdoor slabs exposed to the elements under almost continuous exposure to the salt solutions provides data on (i) the changes in the strain in the concrete due to salt solution, and (ii) the added effects of temperature change. In general, there is about a quarter of a degree Celsius difference between the top and middle gauges, and the same between the middle and bottom gauges. When ambient temperature exceeds 20°C and there is minimal cloud coverage, this temperature spread tends to increase, up to about 4°C difference in the 40°C ambient temperature range. The lag is minimal at lower temperatures, but shows difference in effects.

The strains in the slab exposed to the $MgCl_2$ solution are consistently higher than those in the other slabs (over 100% higher than in the control slab). The slabs exposed to $CaCl_2$ and multi-Cl^- show similar results to the $MgCl_2$ slab with the former tending to be the slightly higher of the

two (as expected because of the higher $CaCl_2$ content), while the strains in the slab exposed to NaCl is consistently only about 10-20% higher than those in the control slab. The samples show up to 150 με, over and above the peak of 140 με seen in the control sample. This means that penetration of the $MgCl_2$ solution caused double the strain in the concrete. This is most likely due to the formation of both brucite ($Mg(OH)_2$) and calcium hydroxy-chloride causing internal expansion in the concrete.

While the results of this testing show the effects of the solution, exposure through summer months does not accurately replicate the real-world conditions. The weekly application of the solution prevents the drying of the concrete and, as seen in the data from eleven to twenty weeks, this effect can be significant. The drying process – especially after salt solution exposure – causes significant contraction of the concrete, enough that near the surface the strain is reduced by half. Cracking and other damage would be caused during this shrinkage process due to the changes in the concrete chemistry and/or the drying itself. The data around 65 and 75 weeks show a decrease again due to a single hot week causing the specimens to dry. Since the $MgCl_2$ solution has tended to evaporate at a slower rate, it was not completely dry like the other specimens, hence it did not decrease in the same manner. This is immediately followed by a return to increase when the ponds were refilled with solution. While the effects of solution penetration are important to see, limiting the conditions to constant exposure may cover up some of the changes which would occur during hot summer months when the concrete is dry.

There are clear differences in the trends for the different slabs. The data in Figure 4.2-4 for the slab exposed to $MgCl_2$ show a difference in strain between the three gauges with a peak value of 20 με difference between the top and the middle gauges and 40 με between the middle gauge and the bottom gauges. The cause of these differences is postulated to be the effects of the formation of brucite ($Mg(OH)_2$), which causes strain and also limits the penetration of solution further into the concrete. The $CaCl_2$ strain data, shown in Figure 4.2-5, have much less variation in strain from gauge to gauge. After from the first 11 weeks, the maximum difference is about 15 με from top-most to middle gauge, and about 10 με from middle to bottom gauge. This can be explained by the chloride penetration and ESEM analysis shown in Figure 4.5-1 and Figure 4.7-3, respectively, which show high amounts of chloride penetration deep into the $CaCl_2$ sample. More consistent penetration would allow for the reactions and changes taking place at the surface to also take place deeper inside the sample, thus limiting the variation in strain between any two points. The gauges in the slab exposed to multi-Cl^- show slightly more variation than the $CaCl_2$ slab, though less than the $MgCl_2$ slab. As the summer months approach (at about 30 week exposure), the middle and bottom gauges show similar results with a difference of only 5-10 με, while the middle and top gauges have much greater variation, with about 25 με difference. The hot summer months cause these variations to switch. It is postulated that this difference is due to reduction of moisture near the surface, while the interior better maintains its moisture content. Finally, the NaCl-exposed slab shows almost no discernible trend in the water-adjusted results as seen in Figure 4.2-7. A function of the lack of effects of the salt on the concrete chemistry and almost linear penetration trends, the NaCl slab shows no consistency with respect to which gauge is highest or lowest.

The variations in strain of the control and NaCl slabs closely follow those of the temperature, while the $MgCl_2$, $CaCl_2$, and multi-Cl^- slabs do not. It is probably that the different behaviour is caused by the formation of brucite ($Mg(OH)_2$) and calcium hydroxy-chlorides, which have been shown to cause expansive internal pressures [**7**].

The slabs used for outdoor strain measurement have had a period of about 19 months of exposure to salt solution at the time of this writing. Though the primary focus is internal strain measurement, the exposure to natural climate allows for a more realistic understanding of effects. One key aspect of this is the effects of salt scaling on the concrete surface. While the ponding wells are unlikely to exhibit scaling since they are unlikely to have frozen due to the low freezing temperatures of the solutions, the surface of the concrete which creates the pond walls is exposed to small amounts without being fully submerged. Following the 19 months of exposure, only the slab exposed to $MgCl_2$ solution has show effects of salt scaling, which can be seen in Figure 5.2-1. Not only was there scaling of the $MgCl_2$ slab, but the damage was quite severe with large sections of surface damage found.

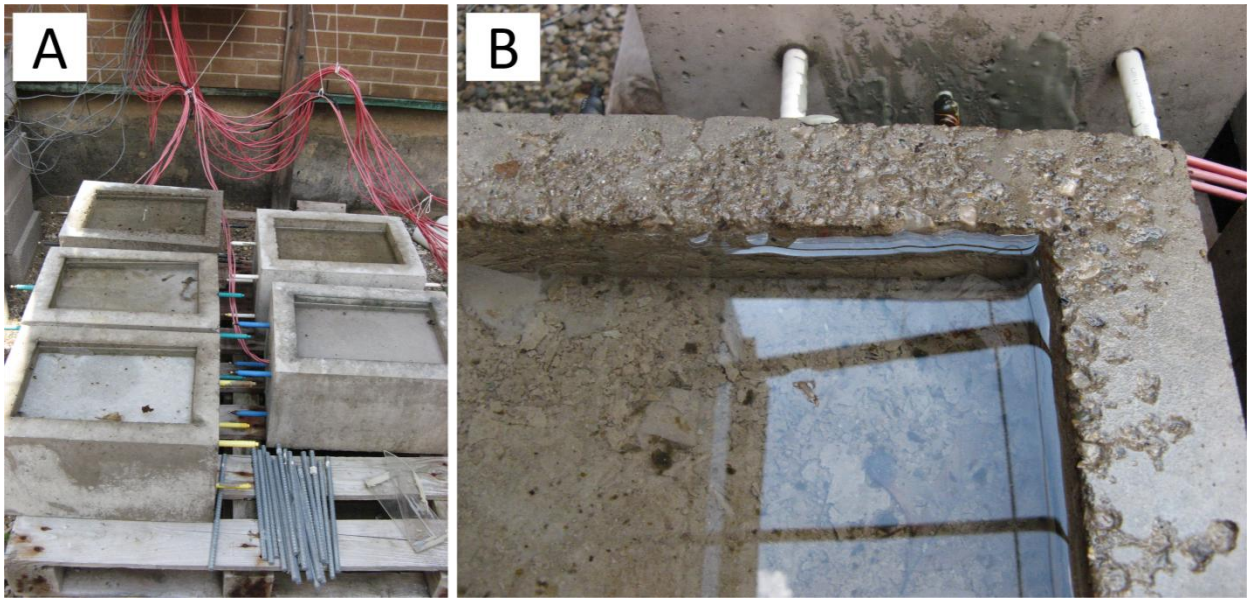

Figure 5.2-1 - Surface images of slabs after 19 months outdoor exposure (A), and surface damage to $MgCl_2$ slab after 19 months outdoor exposure (B)

While the occurrence of scaling in this location is not particularly surprising, the fact that it occurred on the slab exposed to $MgCl_2$ solution is. From the results of the freezing and thawing testing, the $MgCl_2$ sample showed the least effect of the testing in terms of scaling, with no debris collected in either of the two tests. Contrary to this, the concrete exposed to the three other solutions all exhibited scaling to some degree during the freezing and thawing tests. While the latter occurred in lab exposure, there were no signs of scaling damage on the slabs exposed outdoors to $CaCl_2$, multi-Cl^-, or NaCl.

The presence of elevated strain in the samples exposed to salt solutions can have a number of effects long-term. The most clear long term effect is the gradual increase of internal stresses as a result of the strain. The strain itself is indicative of changes either in the cement paste chemistry or in the free space volume of air voids in the concrete. Since the air voids are key

elements in minimizing the damaging effects of freezing and thawing, filling of these voids with solution and/or crystallized salts decreases the ability of the voids to provide room for the expansion and contraction of moisture as it freezes and thaws. This will lead to increasing levels of damage due to freezing and thawing of the concrete, which will lead to more penetration and more internal strain.

With respect to the cement paste chemistry, the reactions of components – especially $CaCl_2$ with the cement paste to form calcium hydroxy-chlorides (hydrated form) or calcium oxy-chlorides (dehydrated form) – will cause increases in strain due to their expansive nature. At low strain levels these are not likely to have significant effect on the physical properties of the concrete. However, as more reaction occurs, the stresses increase. As shown by Poursaee et al. [**1**], these reactions can cause enough stress (and strain) within the concrete to cause it to crack severely. Such cracking in a bridge structure could catastrophically reduce the capability of the concrete to withstand its design service load. The mortar specimens used in reference [**1**] did not contain large aggregates or blast furnace slag, which is known to reduce the diffusion rate through the cement paste and mortar; however, the results still indicate significant deterioration of the specimen leading to what could be catastrophic failure in practical application [**8**]. A further factor that has not been taken into account in the current project is the time of exposure. As diffusion through and reaction with concrete is a naturally slow process, the time of exposure can play a significant role on any effects of the salts on the concrete. The period of exposure that resulted in catastrophic failure in reference [**1**] was 126 weeks in 3% $CaCl_2$ solution and 6 weeks in 30% $CaCl_2$ solution – longer than any exposure time

yet reached for the testing associated with the current project [**1**]. While the differences in the composition of the samples will help to slow the ingress of the salts, it is expected that eventually the same results will occur given sufficient exposure time.

5.3 Compressive Strength

Though it is a common misconception that high strength means high durability, the changes in the compressive strength of concrete – a key indicator when assessing concrete quality – can provide a clear understanding of changes due to external factors. While the exposure conditions varied between the two sets, so too did the consolidation method as previously described. As seen in the freeze and thaw results, the consolidation method can have a notable effect on the surface of the concrete. It is possible that, in the second set, the improved surface quality of the cylinders helped to slow the penetration of salt solutions into the concrete. While this would be a beneficial result, in practice large vibrating tables cannot be placed in the field, thus making it an impractical process.

5.3.1 Cylinders Set 1 - Continuous Soaking

The Set 1 results, shown in Figure 4.3-1, provide an interesting perspective on the effects of the solutions on the concrete as compared to the control cylinders. The concrete exposed only to water, displays a relatively smooth logarithmic trend with continuous increase becoming more gradual over time. This is the expected trend of strength gain over time for concrete, which is expected to continue to increase “indefinitely” barring other factors interrupting that growth.

The strength profiles for the cylinders exposed to salt solutions do not follow the same smooth but, instead, have sharp increases and what appears to be a peak value.

The cylinders exposed to $MgCl_2$ show a significant gain in the first week of soaking over the 28-day strength, which is the first value in each set shown in Figure 4.3-1. This first measurement is almost three times higher on average over the first week compared to the control specimens. The week over week changes are also more sporadic since the batch from which the cylinders originated is alternated at each measurement, this results in the zigzag trend seen. The average strength at week eight for the $MgCl_2$ samples appears as a peak in the data set, with a plateau effect following this point. Similar plateaus were seen after six weeks for $CaCl_2$, and ten weeks for the prisms exposed to the multi-Cl^- and NaCl solutions.

5.3.2 Cylinders Set 2 – Wet and Dry Cycles

The results from the second set of compressive strength testing, in Figure 4.3-2, were much less clear than those from the first set. Even the control cylinders exhibited less consistency in the results. Although the data do not show significant changes over the 20 weeks of testing (16 for the control samples), the general trend seems to be similar to that seen in the first set, minus the large initial jump in strength following the 28-day strength measurement.

The cylinders exposed to salt solutions showed similar trends in the second set, with one key difference: the plateaus seen for the cylinders exposed to salt solutions came much later in the testing, though their timing with respect to each other was consistent with the first set. It is

likely that the differences in these results are due to two factors: (i) the improved consolidation providing better resistance to penetration, and (ii) the differences in exposure.

The data, as a whole, suggest that the presence of the salt solutions causes a higher rate of strength development following exposure than is seen in cylinders exposed only to water, but that the peak strength is relatively unchanged. The major long-term difference between concrete exposed to salt solution and concrete exposed only to water with respect to strength plateau following the peak.

5.4 Tensile Strength

The tensile strength testing was intended to provide another perspective on the changes in elastic modulus of the concrete as well as understanding the modulus of rupture in tension. While the raw results give the impression that there is a difference between the different measurements, once the linear approximations are plotted it can be seen that all except for the control set exposed to potable tap water are similar. The data in Table 4.4-1 and Table 4.4-2 show that there is an improvement in mechanical properties in tension when the prisms have been exposed to salt solution, and conversely a decrease when only exposed to potable tap water.

Considering the calculated results for the elastic modulii of the prisms in Figure 4.4-5, the prisms exposed to $MgCl_2$ and $CaCl_2$ for five months of wetting and drying show almost no change from the baseline data (i.e. that of prisms prior to exposure to the solutions), with

similar results for all prisms. This implies that there is no benefit or detriment in terms of elastic modulus. The multi-Cl^- and NaCl prisms all showed similar results to each other, with average elastic modulus for both solutions being slightly lower than the baseline average, though it is not significant. The greatest change in elastic modulus was found for the prisms exposed to water which show a much lower elastic modulii than the baseline results. This implies that it is beneficial to have salt solution exposure as opposed to just water exposure for short-term exposure as it results in a higher elastic modulus. Compared to the freezing and thawing data, there is an agreement considering the salt-exposed results as compared to the prisms not exposed to salt solutions. The elastic modulii of the freezing and thawing prisms increased from their baseline data with time in the salt solution while the control samples remained the same or lower. In the tensile testing, all data were lower than the baseline data. Certainly the freezing and thawing will affect this, and the freezing/thawing data suggest that there is an increase in elastic modulus associated with the freezing and thawing. Overall, it can be seen that there is an improvement in elastic modulus in tension for concrete after short-term salt solution exposure.

As expected, the modulii of rupture, as seen in Figure 4.4-6, show a different trend than the elastic modulii since it is a function of strength but not strain. The baseline data shows a somewhat consistent set of data with an average around 11 MPa. For all samples exposed to salt solutions, the resultant modulii of rupture was greater than the baseline results. This improvement is due to the crystallization in the pores which helps to reduce crack propagation while increasing the area over which load is transferred within the concrete. Conversely, all

control samples exhibited a decrease in modulus of rupture, with an average modulus of rupture of about 7.56 MPa - 30% lower modulus of rupture than baseline prisms.

The peak tensile strengths of the samples – the basis from which the modulus of rupture is calculated – are shown in Figure 4.4-7. The prisms exposed to $CaCl_2$ exhibited the highest strength, followed by the prisms exposed to $MgCl_2$ and NaCl, then the multi-Cl^--exposed samples, followed by the control samples, which again exhibited a decrease as compared to baseline results. Though highest, the difference in strength was minimal, which is in reasonable agreement with the compressive strength results. All prisms exposed to salt solutions exhibited higher peak strength than both the baseline prisms and those exposed to water. Caused by crystallization of the salts in the pores of the concrete, these results show that there is benefit to tensile strength and elastic modulus of the concrete with short-term exposure to salt solutions.

The displacement prior to failure is the final important set of data collected from these tests. The maximum displacement gives an indication of the amount of strain that the sample can withstand prior to failure. The ability of the concrete to flex slightly during loading is important in, for example, bridge deck applications where the loading can be tensile, and the applied load should not cause structure failure. The reinforcing steel will carry most of the tensile load, but will also flex. Allowing the concrete to flex without significant cracking will help to maximize the life of the structure as well as avoid excess penetration of salt solution through the cracks. As seen in Figure 4.4-8 the general trend is again the same, where all samples exposed to salt

solution exhibit greater displacement before failure as compared to the baseline prisms while the control samples exhibit lower displacements. Once again, the results suggest that with the short exposure period, the salt solutions have resulted in an increase in the properties of the concrete.

5.5 Chloride Penetration

The results of the chloride penetration analysis have given some insight into some of the chemical reactions expected to take place during exposure to different salt solutions. After two weeks of wet curing followed by nine weeks drying at approximately 23°C and 50% RH, the subsequent soaking allowed a high rate of absorption of liquid into the concrete, leading to the high chloride contents after only two weeks. Figure 4.5-1 shows that the two week penetration data from magnesium chloride exhibits high concentration near the surface, but a sharp drop and low concentrations past about 2 mm depth into the concrete. It is postulated that this is due to the precipitation of magnesium hydroxide in the capillary pores, thereby limiting penetration of chlorides deeper into the sample as observed previously by Kurdowski [**7**]. A similar profile was determined for the concrete exposed for two weeks to $CaCl_2$ solution and, to a lesser extent, that exposed the multi-Cl^- solution, attributed to the precipitation of calcium oxy-chloride. In contrast, the concrete exposed sodium chloride showed a lower chloride content in the near-surface region and relatively high chloride levels deeper in the concrete, presumably because there is little reaction between this solution and the cementitious materials.

Subsequent ingress of chlorides is by diffusion, a much slower process than absorption. Consequently, there was only a small increase in chloride penetration in the first 2 mm of the concrete after exposure to the salts for an additional 17 week period, but all the concretes exhibited much higher chloride concentrations beyond this depth. This was particularly noticeable for the concrete exposed to magnesium chloride, indicating that the chloride had penetrated the magnesium hydroxide layer. The trend for concrete exposed to the multi-Cl^- shows almost no change to 4mm depth, followed by much more rapid decrease. The chloride profiles also appear much more linear than the measurements at two weeks.

The third set of measurements, performed 40 weeks after the second set (a total of week 59 of soaking), saw a change from the previous set. There were significant increases in the surface concentration of chloride for the $MgCl_2$-, $CaCl_2$-, and multi-Cl^--soaked samples. This increase seems reasonable given the long period of exposure between measurements. While the surface concentrations have significantly increased, the decrease in concentration with depth has become steeper, with the concentrations at 10mm depth having changed by less than 1%. The most consistent of the profiles with respect to time is the NaCl profile. While there is an increase in concentration, the curve itself is quite similar to that at 19 weeks. This further suggests that the lack of reactions between the NaCl solution and the concrete compared with the more reactive $CaCl_2$ and $MgCl_2$ salts.

There are two key pieces of information which can be gathered about the cation presence based upon chloride penetration. First, the depth of chloride penetration is a reasonable

indicator of the expected depth of penetration of the cations. While this is less concerning for the NaCl solution, knowing how deep the chloride has penetrated in the other three solutions will give an idea of how deep reaction between $MgCl_2$ or $CaCl_2$ and the cement paste is occurring. This is especially important where $CaCl_2$ is present, as the deeper the penetration has occurred, the more calcium oxy-chloride that can be expected in the concrete. While M-S-H formation is much more concerning with respect to strength loss, all $Ca(OH)_2$ must be consumed by $Mg(OH)_2$ formation before the M-S-H reaction will occur. Due to the large amount of $Ca(OH)_2$ in concrete, the immediate effects of reaction with $CaCl_2$ to form calcium hydroxy-chloride is of much greater concern. While this reaction may be less harmful at the surface, reactions deeper within the concrete can cause significant internal stresses which may result in damage as seen in the work of Poursaee et al. [**1**]. The second benefit of understanding chloride penetration as related to cations is understanding the nature of the products of reaction between $MgCl_2$ and $Ca(OH)_2$. Though it was not obvious at week 19, the presence of $Mg(OH)_2$ (brucite) can be somewhat predicted by the penetration curves of chloride. The sharp drops in concentration from 1 mm to 2 mm at week 2 and 1 mm to 6 mm at week 59 are likely partially due to a layer of $Mg(OH)_2$ formation while the drop between 4 mm and 6 mm at week 59 is likely predominantly due to the effects of $Mg(OH)_2$ in limiting the penetration of ions.

Figure B.4-5 and Figure B.4-6 represent the apparent diffusion coefficients of the concrete with respect to depth and with respect to time, respectively. The initial penetration was absorption-controlled, rather than diffusion-controlled. As can be seen in both figures, as exposure period

increases, the apparent diffusion coefficients approach a constant value. These values can be used as an initial approximation for the effective diffusion coefficient, which is established by fitting the curve of predicted Cl^- concentration to the measured Cl^- concentration. The results in Table 4.5-1 show that the effective diffusion coefficients of the NaCl- and multi-Cl^-–exposed samples are lower by EDS analysis of cross-sections, while the effective diffusion coefficients of samples exposed to $MgCl_2$ and $CaCl_2$ are lower by chloride selective electrode measurement of ground powder. The EDS measures total chlorides while the chloride selective electrode method only measures acetic acid-soluble chlorides. Due to the chemical binding of chlorides in the formation of calcium hydroxy-chloride, some of the chlorides in the $CaCl_2$- and $MgCl_2$-exposed samples may not be detected with a chloride selective electrode. The effects of pH on calcium hydroxy-chloride solubility are also unknown, which may affect the formation of calcium hydroxy-chloride in the sample exposed to multi-Cl^-. Since NaCl will react with $Ca(OH)_2$ to form a higher pH $Na(OH)_2$, if calcium hydroxy-chloride is less stable in high pH, it may not form at the same rate as in concrete exposed to $CaCl_2$ or $MgCl_2$.

5.6 pH and Chloride Penetration by Spray Methods

The results of the pH analysis are visual and are seen in Figure 4.6-1 through Figure 4.6-5. In all cases, most of the surface has turned purple indicating that the pH is between 11 and 13. This suggests that, over the exposure period of eight weeks under freeze and thaw conditions, there is insufficient effect of the salt solutions on pH to cause a detectable change by this technique. Due to the short exposure period, this is a reasonable result, however, a longer exposure period

is likely to yield different results as the reactions of the solutions with the concrete will cause shifts in pH given enough time.

The chloride penetration by spray method can offer numerical results of the changes occurring in terms of penetration depth. Table 4.6-1 which shows each of the penetration depth measurements as well as the average for the two sides that are 76.2 mm (3 in), the a average for the sides that are 101.6 mm (4 in), and the average of all four sides for each prism. When in the solution, the 101.6 mm sides are always parallel to the sides of the container while the 76.2 mm sides are either at the top or bottom of the container. While solution surrounds the prism, it can be seen from Table 4.6-1 that there is a clear difference between short and long sides. The 76.2 mm sides – at the top or bottom, depending on the week – exhibit higher penetration in 10 of 12 prisms measured. The difference between the average of 76.2 mm sides and 101.6 mm sides is as high as 3.86 mm. This indicates that some aspect of the prism orientation, likely the free surface at the top, allows for increased penetration. The cast surface is one of the two 101.6 mm surfaces, which would alternate sides as the vertical surface during testing.

The data averages in Table 4.6-1 and Table 4.6-2 give a clear perspective as to the differences in penetration. As discussed, the penetration of the $MgCl_2$ is likely to be limited by the formation of $Mg(OH)_2$, and this is represented clearly, with a lower average penetration by nearly 5 mm than seen in prisms exposed to the $CaCl_2$ or multi-Cl^- solutions, and 6.5mm less than those exposed to NaCl. These results also correlate with the results of chloride penetration by

chloride selective electrode which indicated a clear similarity between the $CaCl_2$ and multi-Cl^- penetration. The average for all sides for these two solutions were the same with the $CaCl_2$ and the multi-Cl^- averaging 13.9 mm. This further agrees with the postulation that the penetration of the multi-Cl^- acts predominantly by the $CaCl_2$. The prisms exposed to NaCl exhibited the highest penetration depth, averaging 15.6 mm. The ionic mobility of each of the four ions relative to potassium (K) are presented in Table 5.6-1 [**40**].

Table 5.6-1 - Ionic mobility relative to potassium (K) for Na^+, Ca^{2+}, Mg^{2+}, and Cl^- [40]

Ion	Relative Mobility (vs. Potassium)
Na^+	0.682
Ca^{2+}	0.405
Mg^{2+}	0.361
Cl^-	1.039

While it seems reasonable that the two-to-one ratio of chloride ions in $CaCl_2$ and $MgCl_2$ would mean that more Cl^- would be able to penetrate faster, this is not the case. Based upon the ionic mobility, Na^+ ions are able penetrate at almost twice the rate of Ca^{2+} or Mg^{2+} ions. The chloride profiles shown in Figure 4.5-1 indicate a reasonable agreement between the two sets of data as in the early stages of exposure the NaCl solution results in higher Cl^- concentration deeper within the concrete while $MgCl_2$ results in the lowest Cl^- penetration.

5.7 Energy Dispersive X-Ray Spectroscopy (EDS)

The use of EDS in conjunction with the ESEM in the analysis of the concrete samples provided a similar understanding of chloride penetration as the previous two methods, but also provided a measurement of other elements present and allowed for analysis of the distribution of those elements. Seen in Figure 4.7-2 through Figure 4.7-5, the composition profiles of each sample analyzed clearly break down different major elements and contrast them. Significant increases in levels of silicon, calcium, or magnesium, especially when one or both of the other two elements exhibit a simultaneous decrease, is a key indicator that the area of analysis contains a high proportion of aggregate. This is further reflected by the chloride which tends to have significantly lower levels in these areas. Figure 4.7-6 shows the chloride profile for each of the four samples analyzed. While there are peaks and valleys throughout due to the other components present, especially the aggregate, the general trends can be compared to other chloride penetration analysis to understand the accuracy of each and develop a clear understanding of the penetration of the solutions through the concrete. While these results help to shape the perspective, the results in Figure 4.7-1 as compared to Figure 4.7-5 clearly indicate how easily results can change or skew. The data from both figures were measured from separate slices of the same sample. Due to the high aggregate content of the first set of measurements, a second slice was taken to understand the chloride penetration, since the chloride does not penetrate the aggregate. Ideally this testing would be repeated on multiple slices from each sample; however, at a full day of measurements per slice, time did not permit further analysis. It should also be noted that while the results in Figure 4.7-6 suggest that the concentrations are by weight of concrete, it is likely more reasonable to think of them as by

weight of cementitious materials. Due to the small area which is analyzed, the results often reflect little or no aggregate presence, and thus are essentially a measurement of the hardened cement paste contents.

Each of the four solutions shows similar trends in terms of element amounts. The biggest difference, aside from aggregates, is the chloride profile. In order to isolate this information, the four chloride profiles have been shown together in Figure 4.7-6. Contrary to the chloride selective electrode results, the surface of the NaCl sample exhibited the highest chloride content of the four samples at over 19%. The $CaCl_2$ and multi-Cl^- were similar to each other at the surface, with about 13% and 14% Cl^-, respectively. The $MgCl_2$ sample exhibited the lowest surface concentration, with about 8.5% Cl^- at the surface. Again, it is important to consider that these are not statistical averages, and thus may not be representative of the entire specimen. The only major variation was at 12 mm to 19 mm depth where the $CaCl_2$ sample exhibited about 4% higher chloride concentration than the other samples. This is an unexpected peak in concentration, which may be caused by high diffusion rates or possibly micro-cracking within the concrete allowing higher penetration rates. Other than the $CaCl_2$ sample, the results of the other three specimens are about equal deeper than 6mm, and all lower than 2% at depths from the surface greater than 12 mm.

The results of the chloride selective electrode analysis for chloride concentration and those from the EDS did not appear to be as consistent on a measurement-by-measurement basis as would have been ideal. Due to the single measurement nature of this testing, this result is not

surprising. Nevertheless, the general trends appear to be reasonably similar to each other when comparing the two methods.

Through the use of environmental scanning electron microscopy (ESEM), images were collected to accompany the EDS analysis. Near the surface of the $CaCl_2$, $MgCl_2$, and multi-Cl^- samples, cracks were found as seen in Figure 5.7-1 through Figure 5.7-3. Conversely, Figure 5.7-4 shows an absence of cracking at the surface of the NaCl specimen. While the goal of air void analysis was to inspect for cracks across the sample surface, none were found as seen in Appendix B in Figure B.6- through Figure B.6-5. This agrees with the postulation that a longer test period is required as the samples where cracking was found were exposed to salt solutions for fifty-nine weeks whereas those analyzed using the air void measurement equipment and only nine weeks exposure.

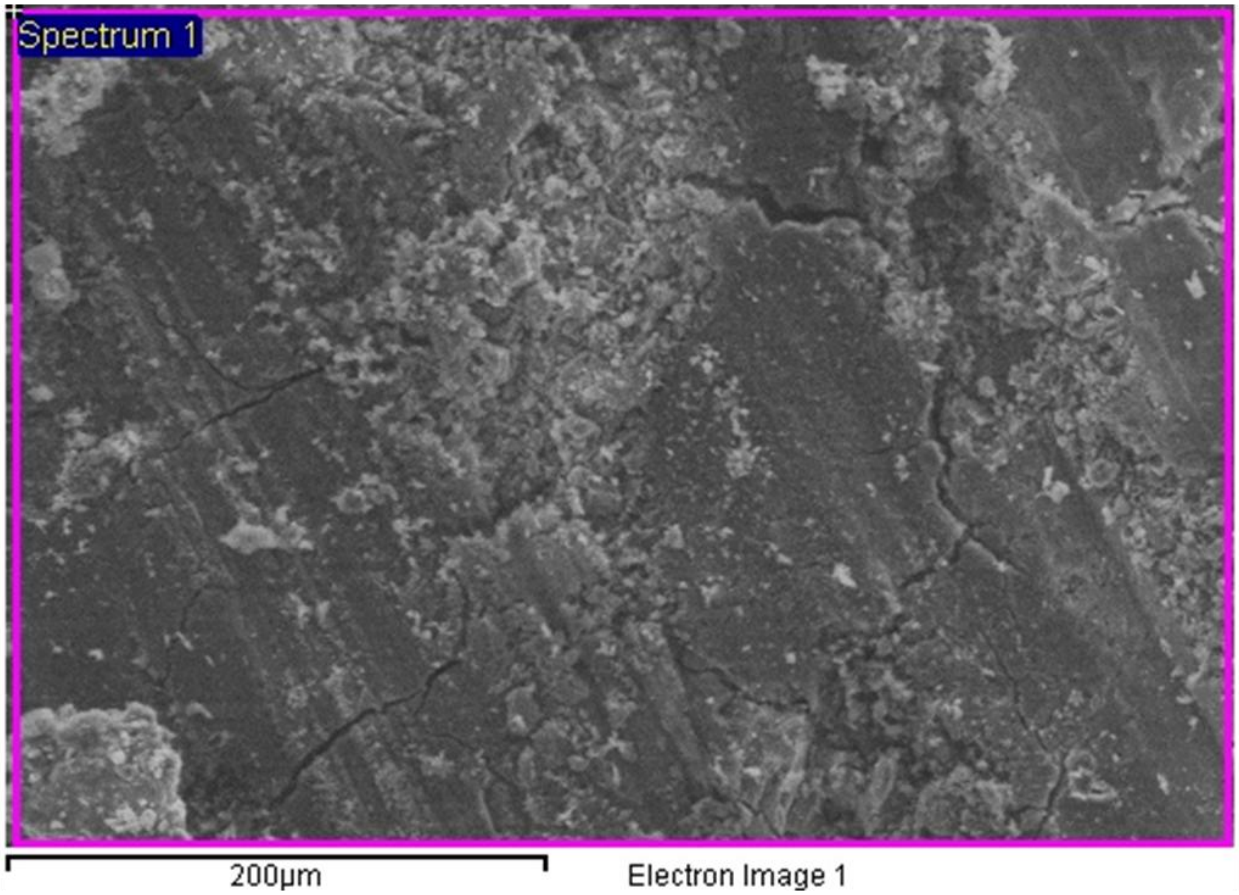

Figure 5.7-1 - Cracks found after 59 weeks exposure to $CaCl_2$ using environmental scanning electron microscopy

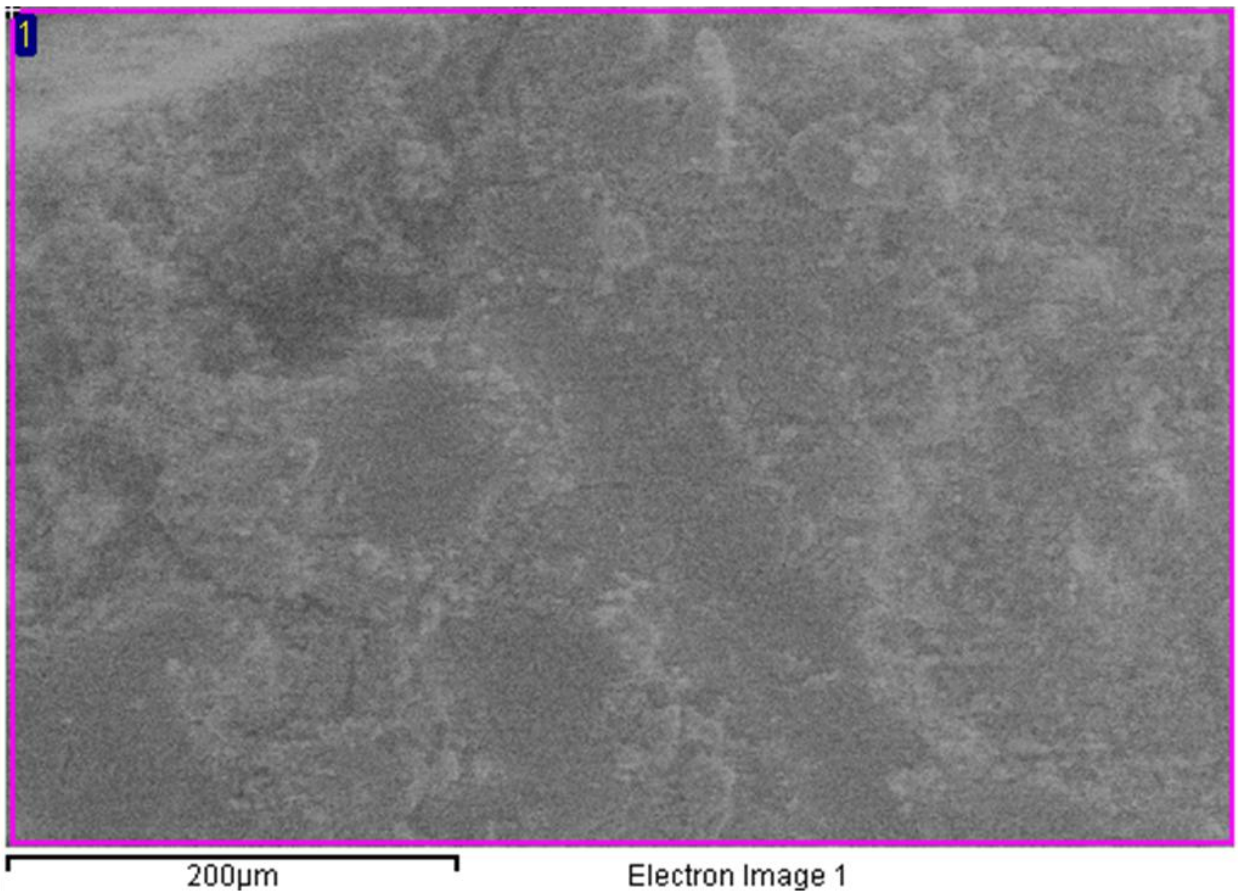

Figure 5.7-2 - Cracks found after 59 weeks exposure to $MgCl_2$ using environmental scanning electron microscopy

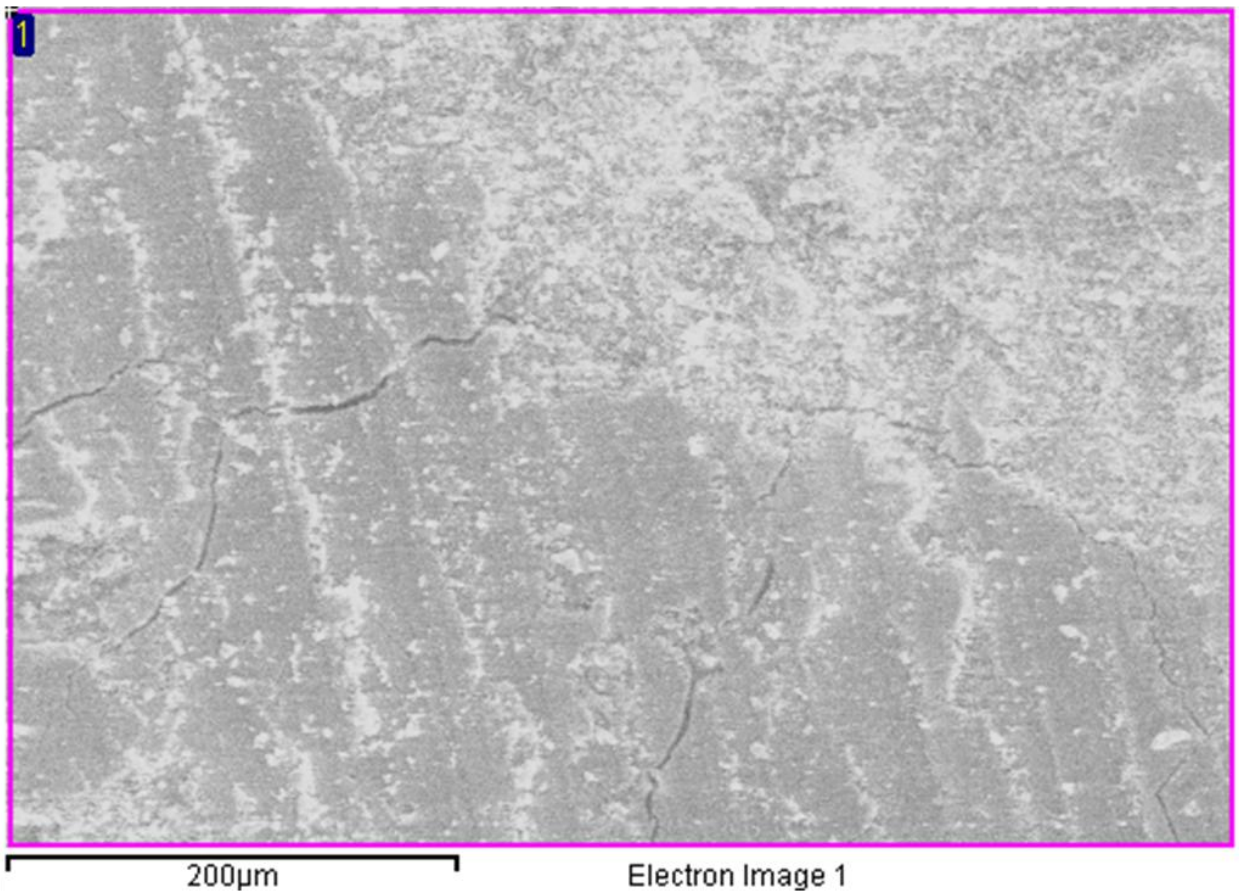

Figure 5.7-3 - Cracks found after 59 weeks exposure to multi-Cl^- using environmental scanning electron microscopy

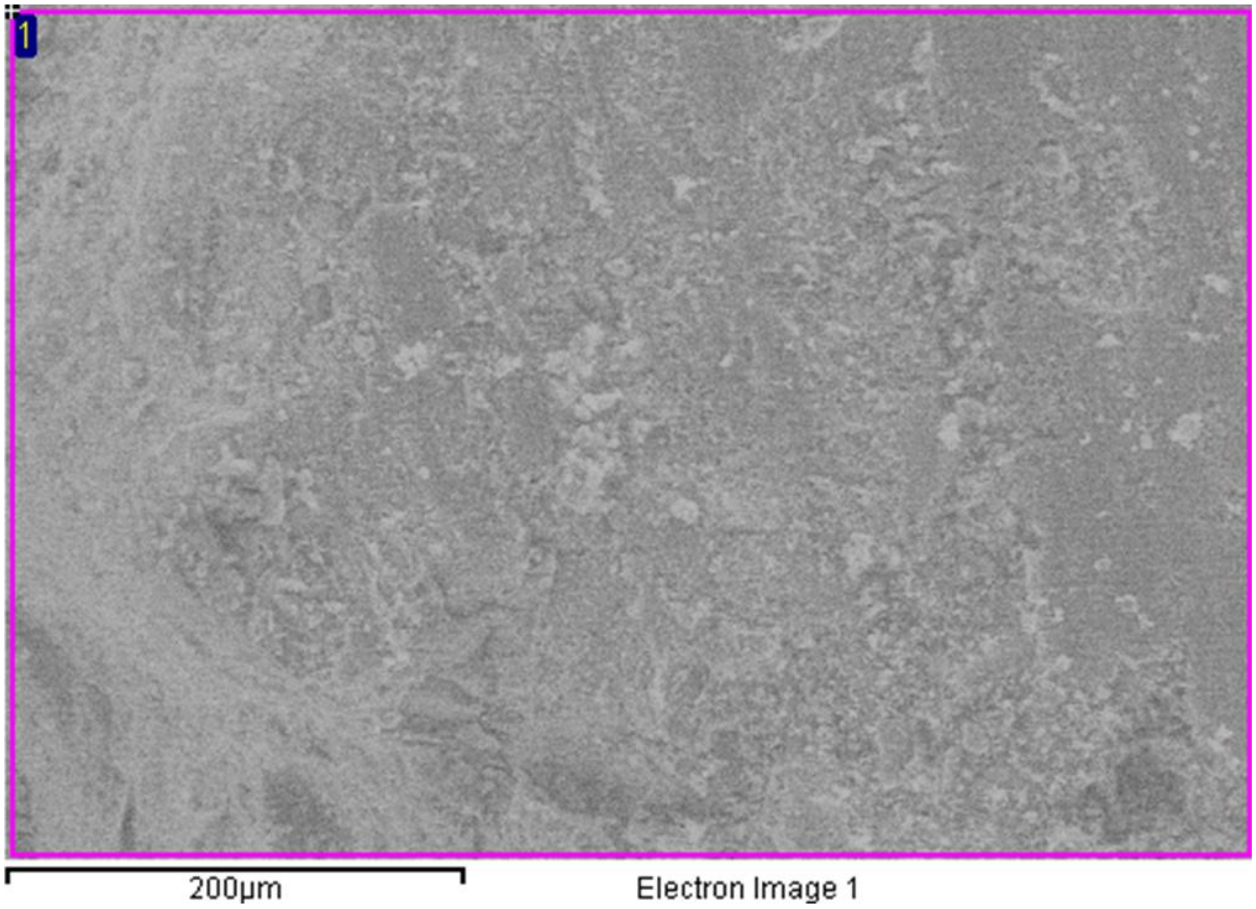

Figure 5.7-4 – Absence of cracks after 59 weeks exposure to NaCl using environmental scanning electron microscopy

5.8 General Observations and Discussion

Although not all of the data gathered have yielded clearly analyzable results, there has been a reasonably high level of agreement between comparable aspects of various tests. One of the most notable was between the compressive test results and the strain measurements from the outdoor slab testing samples. The highest strains were seen in the slab exposed to magnesium chloride solution, and similarly high strengths (though not consistently highest) were seen from the compressive strength testing. While this relationship seems unlikely, it is postulated that the formation of precipitates in the pores of the concrete help to add strength by removing

pore volume, which normally decreases the compressive strength of concrete. There were similar results from the multi-chloride solution and calcium chloride when compared between the two testing methods, as both sets of specimens showed reasonably high strains and high strengths, respectively. The clearest indication of the trends was when these are compared with the specimens exposed to sodium chloride solution, which showed consistently lower strengths and strains than the other sets of specimens, and were generally not significantly different from the water-soaked control samples. This difference was also noted audibly in the compression testing: specimens exposed to magnesium chloride solution failed with a much louder popping noise than the samples those exposed to sodium chloride or water. Even when the strength only varied by a small margin, the cylinders exposed to the same solutions as the slabs exhibiting the highest strains were much more audible during fracture.

Previous work of Kurdowski [**7**] as well as Frigione and Sersale [**8**] have indicated that both $MgCl_2$ and $CaCl_2$ react with the constituents of the hardened cement paste. The results of these reactions, predominantly $Mg(OH)_2$ and calcium hydroxy-chloride respectively, are known to cause changes in various properties of the concrete. The changes attributed to brucite ($Mg(OH)_2$) production have been seen across the various chemical tests for chloride content.

Likely the most important consistency in data is the magnitude of effect seen in different test methods when considering the salt solution the specimens were exposed to. Across most tests with the exception of internal strain, the $CaCl_2$ caused the greatest changes in the properties of the concrete. The $MgCl_2$ and multi-Cl^- tended to have similar results to the $CaCl_2$ though they

generally exhibited slightly lower magnitudes of change. In general the NaCl caused the least effect, in some cases barely more than exposure to potable tap water. Regardless of the situation, the salt solutions always caused some change in properties, even if slight. This implies that there is a clear effect of the salt solutions on the concrete itself and not just as a result of their effects on the reinforcing steel. However, the effect varies. In some cases such as freezing and thawing resistance or tensile loading, the exposure to salt solution caused an improvement to the properties – at least in the short term. In other tests, such as internal strain measurement or compressive strength testing, the exposure to salt solutions ultimately caused a reduction of properties compared with those of the control specimens exposed to water. These variations between benefit and detriment make defining the effects on concrete a difficult task. Adding to this difficulty is the different periods of exposure. ASTM C666, defines 300 cycles as a standard test period. From the results of testing it can be seen that for salt solutions longer exposure time would significantly improve the quality of results. The same is likely true for compressive strength testing, where the exposure period of 16-20 weeks reached only the cusp of what appeared to be change to a plateau. By increasing this period to a full year or more, a much clearer understanding of the effects on a long-term basis could be achieved. Without this long-term exposure, it is difficult to truly predict the long-term effects. There is clearly an effect, and based upon the results observed, it is slow to develop but can be detrimental in long-term exposure scenarios.

When considering the results of the study in all aspects, it is important to note the accelerated effects of the testing methods. For example, while testing such as the compressive test lasted

only 16 weeks, the exposure is representative of a much greater period of time, because the specimens were continuously exposed to solution or to wet and dry cycles. This is not a realistic scenario, as the only time long term soaking of concrete in salt solution occurs is in seawater, which has a much lower salt concentration. In essence, a 16 week period of accelerated testing may be more indicative of several years of application. Though it is difficult to correlate the data to actual results due to variations in exposure in practice, it is expected that these results will reflect much longer periods of time, as the laboratory exposure was much more severe than normal exposure. Furthermore, the exposure was to the maximum concentration of the salts. It is most likely that, in practice, the solutions would be rapidly diluted by precipitation.

While these tests are more severe in the exposure conditions, there is no replacement for the effects of time on exposure. While continuous soaking can replicate the amount of salt exposure of much longer periods of time, it cannot replace the effect of time in terms of diffusion or time for reaction. The diffusion of the salt will be much more effective with more time, and there will be less limitation on the amount of reaction which can occur due to time in practice, which could not be replicated in the short-term lab studies. Even in these tests, it would have been beneficial to continue the testing for longer periods of time. In a number of the situations, particularly freezing and thawing testing and compressive strength testing, the results indicated that a test period at least twice as long would be likely to yield much clearer results. The data suggested that the samples in these sets of testing were on the cusp of

changing as the end of the testing neared, and a longer test period would allow for the trends to be clearer.

6 Conclusions:

The results have shown a mixture of benefit and detriment by applying chloride-based anti-icing agents to concrete structures. Certainly the solutions provide benefits in terms of inhibiting ice formation and adhesion, but the lack of freezing of the prisms exposed to magnesium chloride, calcium chloride, and the multi-chloride also provided benefit. Over almost 400 cycles between +4°C and -18°C with the as-received solutions, the lack of freezing resulted in their showing negligible amounts of scaling, which is prevalent in practice in concretes exposed to sodium chloride in freezing conditions [**22**]. When exposed to solutions diluted to one-third the as-received concentrations, the ability to provide some protection during freezing and thawing has been eliminated, and the damage of scaling is worse for the prisms exposed to $CaCl_2$, multi-Cl^-, and NaCl prisms than those exposed to water. Elastic modulus data were quite similar over the two tests, with a general increase in elastic modulus of all prisms exposed to salt solutions. The main difference was the rate of increase – where the prisms in the as-received solution caused a rapid increase in elastic modulus, those in the diluted solutions exhibited a much slower rate of increase. The fact that none of the solutions was likely to freeze in the first test using as-received solutions suggests that these data are not necessarily realistic, because the solutions are likely to be diluted by snow and ice in practice and, thus, freezing of the solutions and concrete is likely to occur.

The strain and temperature measurements show the effects caused by the solutions more clearly, as noted by the significantly higher strains in the concretes exposed to the $MgCl_2$, $CaCl_2$, and multi-Cl^- solutions than in the control concrete not exposed to salt solution and the

concrete exposed to NaCl solution. In the long term perspective, these can have deleterious effects, as the internal strains will reduce the load that can be carried prior to failure. The increase in internal energy can mean that the failure is more dynamic and explosive as seen in the compressive testing, should the concrete fail.

The compressive tests showed that exposure of hardened concrete to salt solutions resulted in an increase in early strength and strength development relative to that of the control samples not exposed to salt solution in soaking exposure. For wet and dry cycles, it seems that there is much less difference in strength development between cylinders exposed to salt solutions and those exposed to water. While there is an increase in early strength development, there appears to be a peak in strength achieved in both the soaking and wet/dry cycle exposure types, followed by a plateau. A further important difference in the concrete behaviour was attributed to the consolidation method. While the consolidation was better in the second set, the first set is likely more accurate to real life conditions since vibrating tables cannot be used in practice.

The results of the tensile strength testing suggested improvements or minimal decrease in all key mechanical properties calculated. The salt solutions resulted in a small or negligible change in elastic modulus, an increase in the modulus of rupture, increase in peak strength, and an increase in displacement to failure. All of these results suggest that with respect to tensile properties the application of salt solutions is, in fact, beneficial to the mechanical properties of the concrete.

Though not related specifically to mechanical properties, the chloride penetration results suggested that NaCl penetrated the concrete deeper and more quickly than the other solutions, but, following the initial penetration, showed little change. The $MgCl_2$ solution was slow to penetrate, likely due to the limiting nature of the $Mg(OH)_2$ formed in reaction with the $Ca(OH)_2$. However, once this limiting layer was penetrated, the chloride content increase quite rapidly. The $CaCl_2$ and multi-Cl^- solutions showed similar penetration results with a slower initial penetration rate than NaCl, but quickly overtaking the NaCl to have the highest concentrations of Cl^- in the concrete. These results suggest that early in exposure the NaCl is more likely to have effects on both the concrete and reinforcing steel, but over the longer exposure periods $CaCl_2$ and multi-Cl^- are likely to have a more severe effect on these components as seen in the work of Poursaee et al. [**1**].

Due to the inability to accelerate time in testing, it is important to keep in mind that the conclusions drawn are based upon short-term testing. To truly understand long-term effects, much longer exposure times would be required. This considered, from the results there are two separate conclusions drawn. The first is that with a 75 year service life requirement [**37**] and the common use of black steel – a plain carbon steel often fabricated from melted scrap steel - for concrete reinforcement, the results of the testing conducted do not appear to show significant cause for concern with respect to the change in properties of the concrete. Though there are both positive and negative effects found the negatives do not seem to be seriously deleterious to the concrete. The decreases in strength after the peak and the internal strains found both seem insufficient to be cause for concern based upon the short-term studies.

Especially with the use of black reinforcing steel, it is postulated that the damage to the steel will have caused much greater damage to the concrete over the code dictated 75 years of service [**37**] than the salt solutions. Over a prolonged period of time, with regular exposure to the solutions, a black reinforcing steel structure would require repair and rehabilitation due to the effects of the salt solutions – a process which would require replacement of both reinforcement and the cover concrete. This implies that over that period, the concrete will not be a concern, and if this service life is the limit of use of the structure, there does not appear to be reason for serious concern about the salt-affected properties of the concrete.

The second side to the conclusions considers two factors: the likely actual service life of a structure, and the possibility of improved reinforcement. The use of alternative reinforcement, especially stainless steel, can significantly increase the achievable service life of the structure. If appropriate grades of stainless steel are used, then the effects of the salt solutions on the concrete become much more concerning. The reactions of the $CaCl_2$ and $MgCl_2$ with the cement paste constituents have been shown to have deleterious effects [**1**], [**3**], [**2**], and a long period of exposure is expected to allow for the full damage of these reactions to be realized. This would require significantly more longer term testing be conducted to better understand the true long-term effects of the solutions, but based upon the results of this testing and others, significant damage can be projected.

With respect to comparing the effects of the salt solutions to each other, considering only the effects on the concrete, there are clear differences between the solutions. It was found that

the $CaCl_2$ had the greatest effect on the properties of the concrete. Combining this and the formation of expansive calcium hydroxy-chloride as defined by Shi [**2**] and observed by others, the long-term effects of $CaCl_2$ are predicted to be most severe. This correlates to some degree with the $CaCl_2$ solution also being the most effective to the lowest temperatures – a trade off between benefit and detriment. The $MgCl_2$ and multi-Cl^- tend to have similar effects to those of the $CaCl_2$ solution, each displaying significant effect, sometimes greater than that of $CaCl_2$. Based upon this testing they would be considered more safe than $CaCl_2$ long term. However, consideration of the work of Frigione and Sersale [**8**] and Kurdowski [**7**] cannot be overlooked as pertaining to $MgCl_2$. Should the $MgCl_2$ be applied in sufficient amounts to completely consume the $Ca(OH)_2$ in the concrete, the $MgCl_2$ becomes the most damaging as it forms magnesium-silicate-hydrate, known to have no strength or binding properties. In this case, the concrete loses its strength and its ability to carry load. The NaCl solution, especially seen in the strain analysis, has much less effect on the concrete than the other solutions. Over long-term exposure, there is not predicted to be any severe deterioration other than surface scaling. While NaCl will not provide some of the benefits with respect to tensile properties and freeze and thaw resistance, the lack of reactions between the NaCl and cement paste constituents makes it the least deleterious. Considering only the concrete itself, the NaCl solution is the only one of the four that can be used without causing concern of long-term damage.

In summary, based upon the results of the short-term tests performed in this study, it is postulated that the effects of salt solutions on concrete will not be sufficiently deleterious to cause concern with respect to the concrete quality. Though there are deleterious effects, the

effects seen in short term testing do not suggest that there will be significant or concerning damage over that period, especially if the effects of the salt solutions on the reinforcing steel are considered. While this is based upon short-term testing and data collection, it should be maintained that proper long-term testing would be required to truly understand the long-term effects of the solutions on the concrete. The accelerated exposure conditions help to replicate some of the long-term effects, but there is most certainly a lot that cannot be understood from this period of testing, namely with respect to the effect of time itself. As mentioned, the effects of the chloride on standard black reinforcing steel appear to be significantly more deleterious and of concern than the effects of the salt solutions on the concrete. The degradation of the reinforcing steel is expected to take effect long before the concrete becomes a concern. This being considered, for structures intended to serve a long service life, especially with the application of stainless steel as reinforcement in key areas, the concrete may become the focal point for concern of damaging effects. In a structure where appropriate grades of stainless steel have been used to partially or completely replace the black reinforcing steel, it is the belief of the author that the effects of the salt solutions on the concrete itself becomes the greatest concern in terms of degradation of mechanical properties.

7 Recommendations

7.1 Testing Methods

There are a number of recommendations that can be made from the results of this work regarding both the testing procedures associated with and practical application of salt solutions as anti-icing agents. Though some of the effects have been identified through these tests, there is much more to be learned through more in-depth testing and analysis.

7.1.1 Freezing and Thawing Testing

The most obvious short-coming in testing methods is the application of ASTM C666 [**29**] as the freezing and thawing test method. This test method, intended to be used for analyzing different concrete mixtures, does not provide severe enough parameters to test the effects of anti-icing agents accurately. In order to understand the effects of the anti-icing agents as-received during freezing and thawing, much lower temperatures would be necessary. It is recommended that for salt-solution analysis, the freezing temperature be shifted to -40°C, a temperature low enough that all but the $CaCl_2$ would be expected to have some ice formation. This would allow for the effects of the salt solutions and of the freezing and thawing to be evaluated. The difficulty in this will likely lie in the capability of the chambers to bring the temperature low enough for freezing to occur, which would result in increased requirements and thus increased cost of equipment.

With respect to length of testing for ASTM C666, the standard specifies 300 cycles as the limit of testing for this procedure [**29**]. Since the salt solutions reduce the effects of freezing and thawing to some degree, it would be beneficial to increase the number of cycles sufficiently enough to allow for effects to set in. If the temperature range remains unchanged or similar to that currently specified in ASTM C666, a test period of 1000 cycles is recommended as a more appropriate analysis period. This length of testing should allow both the effects of the anti-icing agents as well as the effects of the freezing and thawing to be observed in as-received solutions. Should the temperature range be increased to reach -30°C or -40°C, it is recommended that the number of cycles still be increased to 600 to allow for the effects to be fully realized. The test period of 8 weeks allowed for approximately 375 cycles, and seemed to be right around an inflection point where the well compacted concrete exposed to water was starting to see change. With more cycles for effects to build, a clearer understanding of these effects can be achieved.

The freeze and thaw results provided insight into the effects of the solutions and temperature cycles, but it was unclear which results were caused by which factors. To better understand this in the future, exposure of a set of concrete to the solutions without temperature variation is recommended. These exposure conditions will help to identify changes in mass or elastic modulus caused by the solutions, which can then be used to adjust results of freeze and thaw testing to only show the additional effects realized from the freezing and thawing.

7.1.2 Compressive Testing

The ideal situation based upon this testing would be a single batch of concrete of sufficient volume to cast 400 or more cylinders. This would allow for three cylinders exposed to each salt solution and three exposed to water as a control to be measured every second week for one year. It is postulated that this would provide a more true understanding of the long-term effects of the solution on the strength of concrete.

7.1.3 pH Analysis

The spray methods provide a quick understanding of the changes which have occurred within the cement paste, however, the pH analysis yielded very little understanding. In order to understand if there are changes in pH over a long period of time, it would be beneficial to conduct long-term exposure (minimum one to two years, as oppose to nine weeks) and measurements made periodically during exposure to understand if changes are being caused by the salt solutions. In this case a more accurate method of pH analysis would be beneficial as the changes are unlikely to be detectable by spray methods.

7.1.4 Chemical Composition Analysis

While the presence of $Mg(OH)_2$ and calcium oxy-chloride are the postulated results of any reactions occurring, they cannot be confirmed in the concrete. If aggregate were not used and hardened cement paste samples were exposed to the solutions it would allow for chemical analysis as well as pH determination.

7.1.5 Chloride Penetration

It would be beneficial to continue the analysis of chloride penetration and subsequent diffusion coefficient calculation using the remaining blocks in solution. Measurement of these blocks after 10-12 months will provide further perspective on chloride penetration as well as in the trends of the diffusion coefficients. It is also recommended that a slice of the blocks be taken and analyzed using the air void imaging to inspect for any cracks that may have occurred in the concrete. This analysis should also be applied to the blocks measured at 59 weeks.

In ASTM C1152 [**41**] the standard solution used for acid-soluble chloride analysis is nitric acid; however, the procedure for the chloride selective electrode analysis equipment recommends acetic acid. The relative effectiveness of the two acids at breaking down calcium hydroxy-chlorides is not known. A comparison of the two would be beneficial in establishing the stability of the calcium hydroxy-chlorides and, thus, the proportion of the total chlorides available in solution to cause corrosion. It is known that the pH of the concrete pore solution is increased by NaCl and decreased by CaCl2 and MgCl2 so understanding the effect of pH on the formation of the calcium hydroxy-chloride would provide additional insight into the overall effects of these salts.

7.2 Salt-Based Anti-Icing Application

The application of salt solutions as anti-icing agents provides clear benefit in the prevention of ice formation as well as minimizing adhesion to the pavement thereby making it easier to

remove if it does form. While this is, obviously, beneficial, there are detrimental effects on concrete structures which must be considered also. The following are recommendations with respect to use of salt solutions as anti-icing agents strictly considering the effects on concrete. There are clear detrimental effects on reinforcing steel but these will not be addressed here.

7.2.1 $MgCl_2$

Though one of the more effective solutions, it is recommended that $MgCl_2$ not be used as an anti-icing solution. Though it did not represent the most severe effects in short-term testing, the products of reaction during long-term exposure can have the most severe results. The reactions of the $MgCl_2$ with the hardened cement paste [**3**] present serious concern with respect to the mechanical properties long-term.

7.2.2 $CaCl_2$

During the course of testing in support of this writing the $CaCl_2$ solution, on average, cause the greatest effect on mechanical properties. While it caused the greatest effect, the changes which were found did not cause significant concern short-term. It would be advisable not to use $CaCl_2$ solution as an anti-icing agent without conducting long-term testing of its effects. There is a distinct possibility that if applied consistently for anti-icing to a structure the degradation of the concrete due to calcium hydroxy-chloride formation [**2**] will cause sufficient reduction in mechanical properties to render the structure incapable of supporting its design load [**1**].

7.2.3 Multi-Cl^-

While the multi-Cl^- solution showed similar results to the $CaCl_2$ solution in most tests, the magnitude was generally less than that of the $CaCl_2$. A combination primarily of $CaCl_2$ and NaCl, the multi-Cl^- benefits from not having as high a concentration of $CaCl_2$ as the $CaCl_2$ solution which will help to slow the effects of the $CaCl_2$ on the concrete. It would be advisable not to use this solution without more detailed analysis of the solution phases and analysis of long-term effects.

7.2.4 NaCl

The NaCl solution was not found to have significant effects on a number of the mechanical properties. Of the four solutions tested, it consistently caused the least amount of change regardless of whether the change was beneficial or detrimental. With this understanding, The use of NaCl solution as an anti-icing agent over any period of time appears to be reasonable when only considering its effects on the concrete.

References

[1] A. Poursaee, A. Laurent, and C. M. Hansson, "Corrosion of Steel Bars in OPC Mortar Exposed to NaCl, MgCl2, and CaCl2: Macro- and Micro-Cell Corrosion Perspective," *Cement and Concrete Research*, vol. 40, pp. 426-430, 2010.

[2] Caijun Shi, "Formation and Stability of 3CaO•CaCl2•12H2O," *Cement and Concrete Research*, pp. 1373-1375, 2001.

[3] Lawrence Sutter, Karl Peterson, Sayward Touton, Tom Van Dam, and Dan Johnston, "Petrographic Evidence of Calcium Oxychloride Formation in Mortars Exposed to Magnesium Chloride Solution," *Cement and Concrete Research*, vol. 36, pp. 1533-1541, 2006.

[4] M. Saeed Mirza and Murtaza Haider. (2003) The State of Infrastructure in Canada: Implications for Infrastructure Planning and Policy. [Online]. www.regionomics.com/infra/Draft-July03.pdf

[5] Les Perreaux and Bill Curry. (2011, October) Ottawa announces 10-year plan to replace Montreal's Champlain Bridge. Newsprint. [Online]. http://www.theglobeandmail.com/news/politics/ottawa-announces-10-year-plan-to-replace-montreals-champlain-bridge/article4199259/

[6] David Darwin, JoAnn Browning, Lien Gong, and Sean R. Hughes, "Effects of Deicers on Concrete Deterioration," *ACI Materials Journal*, vol. 105, no. 6, pp. 622-627, December 2008.

[7] Wieslaw Kurdowski, "The Protective Layer and Decalcification of the C-S-H in the

mechanism of Chloride Corrosion of Cement Paste," *Cement and Concrete Research*, vol. 34, pp. 1555-1559, 2004.

[8] G. Frigione and R. Sersale, "The Action of Some Aggressive Solutions on Portland, Pozzolanic, and Blastfurnace Slag Cement Mortars," *Cement and Concrete Research*, vol. 19, pp. 885-993, 1989.

[9] Steven H. Kosmatka, Beatrix Kerkhoff, William C. Panarese, Norman F. MacLeod, and Richard J. McGrath, *Design and Control of Concrete Mixtures*, 7th ed. Ottawa, Canada: Cement Association of Canada, 2002.

[10] A. M. Neville, *Properties of Concrete*, 3rd ed. New York, United States: John Wiley and Sons Inc., 1981.

[11] Cement Association of Canada, "Canadian Cement Industry Sustainability Report," Industry Report 2008.

[12] P. Kumar Mehta, *Concrete Structure, Properties, and Materials*. Englewood Cliffs, United States of America: Prentice-Hall, 1986.

[13] Patrick L. Maier and Stephan A. Durham, "Beneficial Use of Recycled Materials in Concrete Mixtures," *Construction and Building Materials*, vol. 29, pp. 428-437, 2012.

[14] Robert F.M. Bakker, "Permeability of Blended Cement Concretes," in *Proceedings of the CANMET/ACI First International Conference on the Use of Fly Ash, Silica Fume, Slag, and Other Mineral By-Products in Concrete*, Montebello, 1983, pp. 589-605.

[15] Shahzma J. Jaffer and Carolyn M. Hansson, "Chloride-induced corrosion products of steel in cracked-concrete subjected to different loading conditions," *Cement and Concrete*

Research, vol. 39, pp. 116-125, November 2008.

[16] John B. Brady, "Magma in a Beaker: Analog Experiments with Water and Various Salts or Sugar for Teaching Igneous Petrology," *The Canadian Mineralogist*, vol. 47, pp. 457-471, 2009.

[17] Hyomin Lee, Robert D. Cody, Anita M. Cody, and Paul G. Spry, "Effects of Various Deicing Chemicals on Pavement Concrete Deterioration," in *Mid-Continent Transportation Symposium*, Ames, pp. 151-155.

[18] Benjamin D. Kosbab and Kimberly E. Kurtis, "Effect of Calcium Chloride and Initial Curing Temperature on Expansion Caused by Sulfate Exposure," *ACI Materials Journal*, pp. 632-639, 2010.

[19] V S Ramachandran, "Calcium Chloride in Concrete - Applications and Ambiguities," *Canadian Journal of Civil Engineering*, pp. 213-221, 1978.

[20] C. M. Hansson, Th. Frolund, and J. B. Markussen, "The Effect of Chloride Cation Type on the Corrosion of Steel in Concrete by Chloride Salts," *Cement and Concrete Research*, pp. 65-73, 1985.

[21] Fay et al., "Evaluation of Alternative Anti-Icing and Deicing Compounts using Sodium Chloride and Magnesium Chloride as Baseline Deicers - Phase I," Colorado Department of Transportation, Denver, Technical Report CDOT-2009-1, 2009.

[22] John J. Valenza II and George W. Scherer, "Mechanism for Salt Scaling of a Cementitious Surface," *Materials and Structures*, vol. 40, pp. 259-268, October 2007.

[23] John J. Valenza II and George W. Scherer, "A Review of Salt Scaling: I. Phenomenology,"

Cement and Concrete Research, vol. 37, pp. 1007-1021, 2007.

[24] John J. Valenza II and George W. Scherer, "A Review of Salt Scaling: II. Mechanisms," *Cement and Concrete Research*, vol. 37, pp. 1022-1034, 2007.

[25] George W. Scherer, "Crystallization in Pores," *Cement and Concrete Research*, vol. 29, pp. 1347-1358, 1999.

[26] American Society for Testing and Materials, "ASTM C192 - Standard Practice for Making and Curing Concrete Test Specimens in the Laboratory," pp. 1-8, December 2010.

[27] Ontario Provincial Standard Specification, "OPSS 1350 - Material Specification for Concrete - Materials and Production," pp. 1-14, February 1996.

[28] U.S. Department of Transportation - Federal Highway Administration, "Manual of Practice for an Effective Anti-icing Program: A Guide For Highway Winter Maintenance Personnel," Turner-Fairbank Highway Research Center, Maclean, FHWA-RD-95-202, 1996.

[29] American Society for Testing and Materials, "ASTM C666 - Standard Test Method for Resistance of Concrete to Rapid Freezing and Thawing," pp. 1-6, November 2008.

[30] CNS Farnell Limited, "Operating Instructions - Erudite MKIV (PC1004)," Borehamwood, Instructional 2004.

[31] American Society for Testing and Materials, "ASTM C39 - Standard Test Method for Compressive Strength of Cylindrical Concrete Specimens," pp. 1-7, September 2011.

[32] American Society for Testing and Materials, "ASTM C293M-10 Standard Test Method for Flexural Strength of Concrete (Using Simple Beam with Center-Point Loading)," pp. 1-3, 2010.

[33] Nobuaki Otsuki, Shigeyoshi Nagataki, and Kenji Nakashita, "Evaluation of the AgNO3 solution spray method for measurement of chloride penetration into hardened cementitious matrix materials," *Construction and Building Materials*, vol. 7, no. 4, pp. 195-201, January 1993.

[34] Donald R. Askeland and Pradeep P. Phule, *The Science and Engineering of Materials, 5th Edition*. Toronto: Thomson Canada Limited, 2006.

[35] American Society for Testing and Materials, "ASTM C1556-11a - Standard Test Method for Determining the Apparent Chloride Diffusion Coefficient of Cementitious Mixtures by Bulk Diffusion," pp. 1-7, January 2012.

[36] American Society for Testing and Materials, "ASTM C457 - Standard Test Method for Microscopical Determination of Parameters of the Air-Void System in Hardened Concrete," pp. 1-14, November 2011.

[37] Standards Council of Canada, "Canadian Highway Bridge Design Code," Canadian Standards Association, Mississauga, Design Code CAN/CSA-S6-06, 2006.

[38] J. G. MacGregor and Fred Michael Pierce Bartlett, *Reinforced Concrete: Mechanics and Design*. Canada: Pearson Education Canada, 2000.

[39] Standards Council of Canada, "Design of Concrete Structures," Canadian Standards Association, Standard CAN/CSA-A23.3-04, 2004.

[40] P. H. Barry. (2012, February) Ionic Mobility Tables. Website. [Online]. http://web.med.unsw.edu.au/phbsoft/mobility_listings.htm

[41] American Society for Testing and Materials, "ASTM C1152 - Standard Test Method for Acid-

Soluble Chloride in Mortar and Concrete," pp. 1-4, February 2006.

[42] Ervin Poulsen, "Chloride Profiles: Analysis and Interpretation of Observations," AEClaboratory, Vadbaek, 1995.

Appendix A Background

Appendix A.1 Casting Information

The following tables, Table A.1-1 through Table A.1-9, present the information and process specific to each batch of concrete cast for the testing associated with this writing.

Table A.1-1 - Freeze and thaw testing Set 1 prisms casting information

Cast Date:	Monday, December 10, 2010 (cast indoors)
Specimen Types:	20 prisms, five cylinders
Curing Conditions:	In lab, under wet burlap and vapour barrier
Slump:	50mm
Air Volume:	5.50%
Aggregate Water Volume:	0.2113%

CAST RECIPE	Quantity	Type
Gravel:	140.98kg	12.7mm crush
Sand:	101.46kg	
Cement:	42.74kg	Holcim GU 10
Slag:	14.10kg	Holcim Grancem
Air Entrainer:	34.11mL	Euclid ExtraAir
Water Reducer:	115.13mL	Euclid Water Reducer
Super Plasticizer:	0mL	Glenium 7700
Water:	22.84L	

Cast Procedure:

- Fill mould to half full
- Rod 32 times (as per ASTM C192)
- Fill mould to full
- Rod 32 times (as per ASTM C192)
- vibrate exterior mould walls to ensure consolidation and smooth surface

Cure Procedure:

- In lab under wet burlap and vapour barrier
- maintained in this configuration for two weeks, then sat dry 9 weeks

Table A.1-2 - Freeze and thaw testing Set 2 prisms casting information

Cast Date:	Thursday, November 24, 2011 (cast indoors)
Specimen Types:	20 prisms, five cylinders
Curing Conditions:	In lab, under wet burlap and vapour barrier for 4 days, followed by 17 days in humidity chamber @ 25°C, 100% relative humidity
Slump:	95mm (post super-p)
Air Volume:	4.90%
Aggregate Water Volume:	0.2113%

CAST RECIPE	Quantity	Type
Gravel:	150.39kg	12.7mm crush
Sand:	101.46kg	
Cement:	42.74kg	Holcim GU 10
Slag:	14.10kg	Holcim Grancem
Air Entrainer:	34.11mL	Euclid ExtraAir
Water Reducer:	115.13mL	Euclid Water Reducer
Super Plasticizer:	80mL	Glenium 7700
Water:	22.84L	

Cast Procedure:

-Fill half full
- Vibrate table for 10-20 seconds
- Fill to full
- Vibrate table for 10-20 seconds
- Smooth top, place the lid on

Cure Procedure:

- 4 days in lab, under wet burlap and vapour barrier
- Moulds removed after 96 hours (4 days)
- 17 days in humidity chamber @ 25°C, 100% relative humidity
- 9 weeks dry in laboratory prior to exposure

Table A.1-3 - Internal strain slabs casting information

Cast Date:	Wednesday, December 12, 2010 (cast indoors)
Specimen Types:	Five slabs with gauges and rebar, one slab just rebar, five cylinders
Curing Conditions:	In lab, under wet burlap and vapour barrier
Slump:	N/A
Air Volume:	5.50%
Aggregate Water Volume:	0.2113%

CAST RECIPE	Quantity	Type
Gravel:	241.50kg	12.7mm crush
Sand:	162.93kg	
Cement:	68.64kg	Holcim GU 10
Slag:	22.65kg	Holcim Grancem
Air Entrainer:	54.77 mL	Euclid ExtraAir
Water Reducer:	184.88mL	Euclid Water Reducer
Super Plasticizer:	660mL	Glenium 7700
Water:	36.68L	

Cast Procedure:

- Concrete was extremely workable to begin (slump test not possible)
- Cocnrete scooped/poured into moulds and pushed into all gaps with fingers
- Carefully press concrete in around gauges by hand ensure not to disrupt gauge orientation
- Fill to top of mould
- Tap sides to ensure consolidation and smooth surface

Cure Procedure:

- In lab under wet burlap and vapour barrier
- maintained in this configuration for two weeks, then placed outdoors and exposed

Table A.1-4 - Compressive strength testing Set 1, batch "X" cylinder casting information

Cast Date:	Tuesday, February 22, 2011 (cast indoors)
Specimen Types:	Seventy-five 101.6mm x 203.2mm (4in x 8in) cylinders
Curing Conditions:	humidity chamber @ 25°C, 100% relative humidity
Slump:	40mm (pre-super plasticizer)
Air Volume:	9.00%
Aggregate Water Volume:	0.2113%

CAST RECIPE	Quantity	Type
Gravel:	174.62kg	12.7mm crush
Sand:	117.80kg	
Cement:	49.63kg	Holcim GU 10
Slag:	22.65kg	Holcim Grancem
Air Entrainer:	39.60mL	Euclid ExtraAir
Water Reducer:	133.68mL	Euclid Water Reducer
Super Plasticizer:	190mL	Glenium 7700
Water:	26.52L	

Cast Procedure:

- Fill 1/3 full
- Rod 21 times
- Tap the outside of the mould with rod (all around)
- Fill to 2/3 full
- Rod 21 times
- Tap the outside of the mould with rod (all around)
- Fill to full
- Rod 21 times
- Tap the outside of the mould with rod (all around)
- Smooth top, place the lid on

Cure Procedure:

- Removed from moulds after 24 hours

Notes:

- Cylinders marked with an X

Table A.1-5 - Compressive strength testing Set 1, batch "O" cylinder casting information

Cast Date:	Friday, February 25, 2011 (cast indoors)
Specimen Types:	Seventy-seven 101.6mm x 203.2mm (4in x 8in) cylinders
Curing Conditions:	humidity chamber @ 25°C, 100% relative humidity
Slump:	6.5mm (pre-super plasticizer)
Air Volume:	6.00%
Aggregate Water Volume:	0.2113%

CAST RECIPE	Quantity	Type
Gravel:	174.62kg	12.7mm crush
Sand:	117.80kg	*
Cement:	49.63kg	Holcim GU 10
Slag:	22.65kg	Holcim Grancem
Air Entrainer:	39.60mL	Euclid ExtraAir
Water Reducer:	133.68mL	Euclid Water Reducer
Super Plasticizer:	190mL	Glenium 7700
Water:	26.52L	

Cast Procedure:

- Fill 1/3 full
- Rod 21 times
- Tap the outside of the mould with rod (all around)
- Fill to 2/3 full
- Rod 21 times
- Tap the outside of the mould with rod (all around)
- Fill to full
- Rod 21 times
- Tap the outside of the mould with rod (all around)
- Smooth top, place the lid on

Cure Procedure:

- Removed from moulds after 96 hours

Notes:

- Cylinders maked with an O
- * The mixer was found to be out of alignment and after casting it was noticed that a notable amount of sand was in the bottom of the mixer

Table A.1-6 - Compressive strength testing Set 2, batch "X" cylinder casting information

Cast Date:	Thursday, November 24, 2011 (cast indoors)
Specimen Types:	Seventy-five 101.6mm x 203.2mm (4in x 8in) cylinders
Curing Conditions:	humidity chamber @ 25°C, 100% relative humidity
Slump:	45mm (post super-p)
Air Volume:	4.50%
Aggregate Water Volume:	0.2113%

CAST RECIPE	Quantity	Type
Gravel:	174.62kg	12.7mm crush
Sand:	117.80kg	
Cement:	49.63kg	Holcim GU 10
Slag:	22.65kg	Holcim Grancem
Air Entrainer:	39.60mL	Euclid ExtraAir
Water Reducer:	133.68mL	Euclid Water Reducer
Super Plasticizer:	150mL	Glenium 7700
Water:	26.52L	

Cast Procedure:

- Fill 1/3 full
- Vibrate table for 10-20 seconds
- Fill to 2/3 full
- Vibrate table for 10-20 seconds
- Fill to full
- Vibrate table for 10-20 seconds
- Smooth top, place the lid on

Cure Procedure:

- molds removed after 96 hours
- 3 weeks cure in humidity chamber followed by 3 weeks dry in laboratory

Notes:

- Cylinders marked "X"

Table A.1-7 - Compressive strength testing Set 2, batch "O" cylinder casting information

Cast Date:	Wednesday, December 12, 2010 (cast indoors)
Specimen Types:	Seventy-five 101.6mm x 203.2mm (4in x 8in) cylinders
Curing Conditions:	humidity chamber @ 25°C, 100% relative humidity
Slump:	75mm (post super-p)
Air Volume:	5.40%
Aggregate Water Volume:	0.2113%

CAST RECIPE	Quantity	Type
Gravel:	174.62kg	12.7mm crush
Sand:	117.80kg	
Cement:	49.63kg	Holcim GU 10
Slag:	22.65kg	Holcim Grancem
Air Entrainer:	39.60mL	Euclid ExtraAir
Water Reducer:	133.68mL	Euclid Water Reducer
Super Plasticizer:	125mL	Glenium 7700
Water:	26.52L	

Cast Procedure:

- Fill 1/3 full
- Vibrate table for 10-20 seconds
- Fill to 2/3 full
- Vibrate table for 10-20 seconds
- Fill to full
- Vibrate table for 10-20 seconds
- Smooth top, place the lid on

Cure Procedure:

- molds removed after 96 hours
- 3 weeks cure in humidity chamber followed by 3 weeks dry in laboratory

Notes:

- Cylinders marked "O"

Table A.1-8 - Tensile strength testing prisms casting information

Cast Date:	Friday, April 1, 2011 (cast indoors)
Specimen Types:	20 prisms, five cylinders
Curing Conditions:	humidity chamber @ 25°C, 100% relative humidity
Slump:	65mm post-super plasticizer
Air Volume:	7.00%
Aggregate Water Volume:	0.2113%

CAST RECIPE	Quantity	Type
Gravel:	150.39kg	12.7mm crush
Sand:	101.46kg	
Cement:	42.74kg	Holcim GU 10
Slag:	14.10kg	Holcim Grancem
Air Entrainer:	34.11mL	Euclid ExtraAir
Water Reducer:	115.13mL	Euclid Water Reducer
Super Plasticizer:	235mL	Glenium 7700
Water:	22.84L	

Cast Procedure:

- Fill mould to half full
- Rod 32 times (as per ASTM C192)
- Fill mould to full
- Rod 32 times (as per ASTM C192)
- vibrate exterior mould walls to ensure consolidation and smooth surface

Cure Procedure:

- Cured in humidity chamber @ 25°C, 100% relative humidity
- maintained in this configuration for two weeks, then sat dry 9 weeks

Table A.1-9 - Chloride penetration block casting information

Cast Date:	Monday, December 10, 2010 (cast indoors)
Specimen Types:	20 prisms, five cylinders
Curing Conditions:	In lab, under wet burlap and vapour barrier
Slump:	50mm
Air Volume:	5.50%
Aggregate Water Volume:	0.2113%

CAST RECIPE	Quantity	Type
Gravel:	140.98kg	12.7mm crush
Sand:	101.46kg	
Cement:	42.74kg	Holcim GU 10
Slag:	14.10kg	Holcim Grancem
Air Entrainer:	34.11mL	Euclid ExtraAir
Water Reducer:	115.13mL	Euclid Water Reducer
Super Plasticizer:	0mL	Glenium 7700
Water:	22.84L	

Cast Procedure:

- Fill mould to half full
- Rod 32 times (as per ASTM C192)
- Fill mould to full
- Rod 32 times (as per ASTM C192)
- vibrate exterior mould walls to ensure consolidation and smooth surface

Cure Procedure:

- In lab under wet burlap and vapour barrier
- maintained in this configuration for two weeks, then sat dry 9 weeks

Appendix B Results

Appendix B.1 28-Day Strengths

The data in Table B.1-1 are the measurements taken for 28-day strength of each set of concrete cast.

Table B.1-1 - 28-day strength data for all concrete batches cast for testing purposes

Specimen Type	Sample #	Peak Force (kN)	Diameter (mm)	Peak Stress (Measured, MPa)	Peak Stress (Actual, MPa)	Cast Date
Prisms 1 (freeze/thaw)	1	418.729	101	53.317	52.264	Friday, December 10, 2010
Prisms 1 (freeze/thaw)	2	438.732	101	55.862	54.760	
Prisms 1 (freeze/thaw)	3	449.106	101	57.185	56.055	
Prisms 1 (freeze/thaw)	4	416.140	101	52.987	51.941	
Prisms 1 (freeze/thaw)	5	405.291	101	51.601	50.586	
Slabs	1	423.840	101	53.966	52.902	Wednesday, December 22, 2010
Slabs	2	431.384	101	54.924	53.843	
Slabs	3	415.677	101	52.924	51.883	
Slabs	4	411.189	101	52.352	51.323	
Slabs	5	436.041	101	55.517	54.425	
Cylinders 1-1 (X)	1	407.386	101	51.870	50.848	Tuesday, February 22, 2011
Cylinders 1-1 (X)	2	379.789	101	48.353	47.403	
Cylinders 1-1 (X)	3	379.798	101	48.360	47.405	
Cylinders 1-1 (X)	4	395.785	101	50.394	49.400	
Cylinders 1-1 (X)	5	352.001	101	44.816	43.935	
Cylinders 1-2 (O)	1	487.009	101	62.005	60.786	Friday, February 25, 2011
Cylinders 1-2 (O)	2	457.984	101	58.309	57.163	
Cylinders 1-2 (O)	3	463.562	101	59.026	57.860	
Cylinders 1-2 (O)	4	477.463	101	60.791	59.595	
Cylinders 1-2 (O)	5	459.688	101	58.530	57.376	
Prisms 2 (3-point)	1	513.765	101	65.418	64.126	Friday, April 1, 2011
Prisms 2 (3-point)	2	532.350	101	67.783	66.445	
Prisms 2 (3-point)	3	502.444	101	63.977	62.713	
Prisms 2 (3-point)	4	532.661	101	67.824	66.484	
Prisms 2 (3-point)	5	514.472	101	65.507	64.214	
Cylinders 2-1 (X)	1	521.478	101	66.397	65.088	Thursday, November 24, 2011
Cylinders 2-1 (X)	2	515.553	101	65.645	64.349	
Cylinders 2-1 (X)	3	514.419	101	65.501	64.207	
Cylinders 2-2 (O)	1	484.331	101	61.667	60.452	Thursday, November 24, 2011
Cylinders 2-2 (O)	2	489.954	101	62.384	61.154	
Cylinders 2-2 (O)	3	471.195	101	59.992	58.812	
Prisms 3 (freeze/thaw)	1	440.534	101	56.089	54.985	Thursday, November 24, 2011
Prisms 3 (freeze/thaw)	2	447.429	101	56.972	55.846	
Prisms 3 (freeze/thaw)	3	443.212	101	56.434	55.320	
Prisms 3 (freeze/thaw)	4	438.190	101	55.793	54.693	
Prisms 3 (freeze/thaw)	5	424.529	101	54.055	52.988	

Appendix B.2 Freeze and Thaw Results

Appendix B.2.1 Freezing and Thawing Temperature Data

In order to ensure the temperature in the freeze and thaw chamber matches the temperatures specified in ASTM C666 [**29**] the temperature is controlled with an embedded thermistors and logged with a second embedded thermistor. The temperature profile for freeze and thaw testing set 1 (full strength solutions), and Set 2 (diluted solutions) are shown in Figure B.2-1 and Figure B.2-2, respectively.

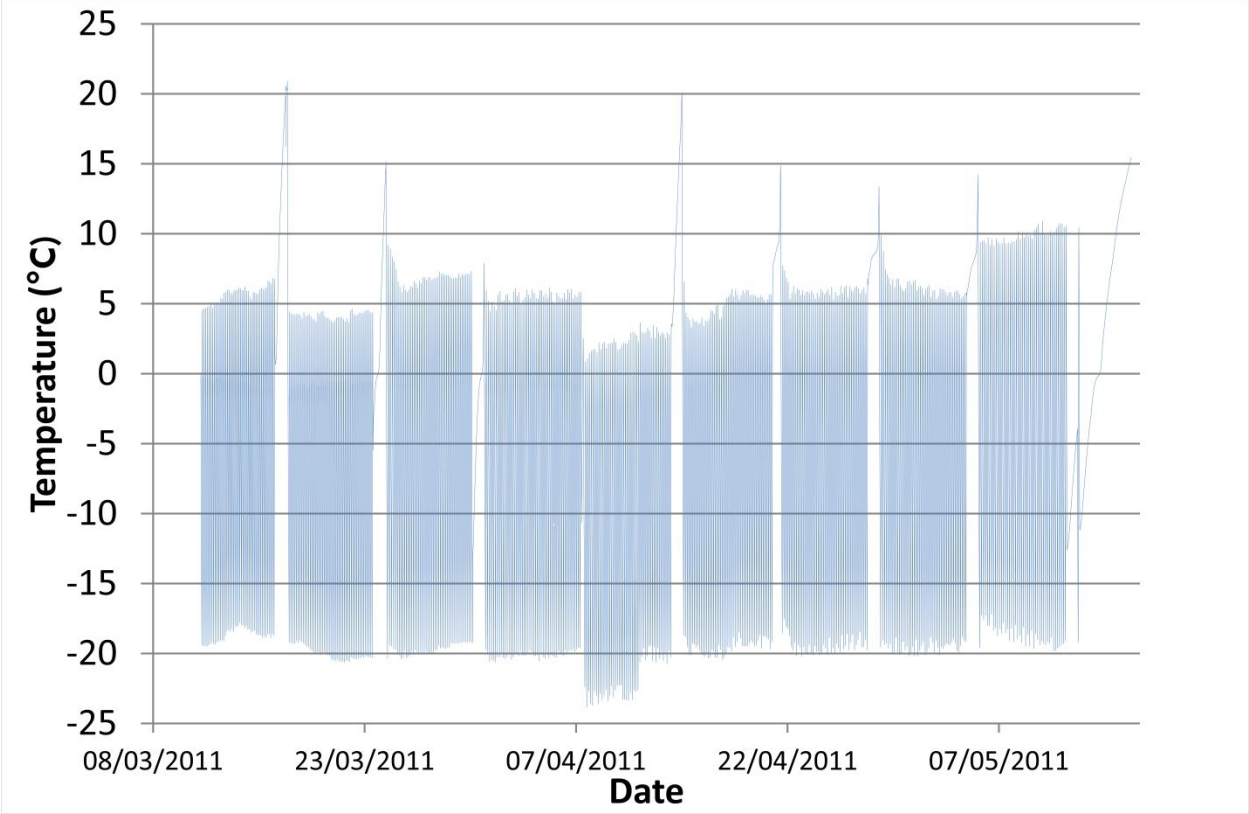

Figure B.2-1 - Freeze and thaw Set 1, full strength solutions, temperature profile

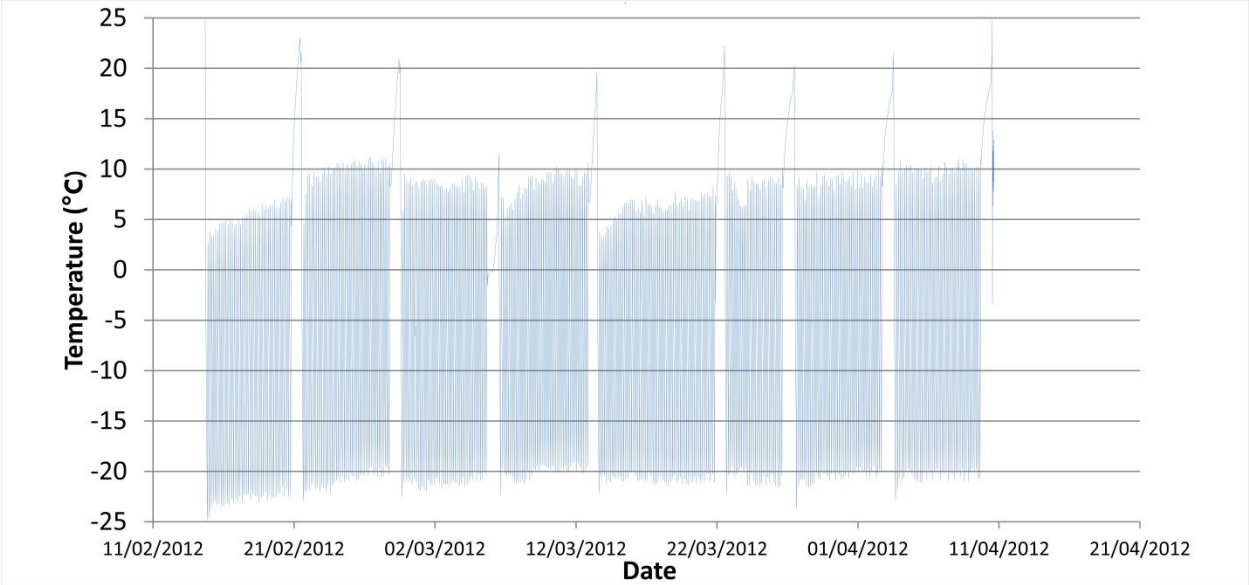

Figure B.2-2 - Freeze and thaw Set 2, diluted solutions, temperature profile

Appendix B.2.2 Freezing and Thawing Set 1 Data

The data in Table B.2-1 through Table B.2-4 represent all data collected during the freeze and thaw testing with respect to the prism characteristics for set 1 which was subjected to the full strength solutions.

Table B.2-1 - Freeze and thaw data from Set 1, full strength solutions, for $MgCl_2$, $CaCl_2$, and H_2O for the first 35 days

		$MgCl_2$ 1	$MgCl_2$ 2	$MgCl_2$ 3	$CaCl_2$ 1	$CaCl_2$ 2	$CaCl_2$ 3	H_2O 1	H_2O 2	H_2O 3
Initial	Mass (lb)	16.8	16.6	16.5	16.5	16.4	16.5	16.6	16.4	16.6
	Mass (g)	7618.9	7548.1	7477.2	7505.5	7448.8	7470.1	7526.8	7434.7	7526.8
	Debris (g)	0.00	0.00	0.00	0.00	0.00	0.00	0.00	0.00	0.00
	F_r	2.29	2.21	2.22	2.24	2.22	2.22	2.20	2.25	2.26
	F_l	2.25	2.20	2.20	2.20	2.20	2.20	2.20	2.20	2.20
	F_h	2.58	2.50	2.51	2.54	2.51	2.51	2.49	2.54	2.55
	Q	6.94	7.37	7.16	6.59	7.16	7.16	7.59	6.62	6.46
7 Days	Mass (lb)	16.9	16.7	16.6	16.7	16.6	16.7	16.8	16.6	16.8
	Mass (g)	7650.6	7588.1	7515.0	7587.1	7543.8	7564.1	7622.1	7540.8	7626.8
	Debris (g)	0.00	0.00	0.00	0.00	0.00	0.00	1.29	2.24	0.94
	F_r	2.28	2.21	2.23	2.28	2.26	2.24	2.20	2.20	2.21
	F_l	2.22	2.20	2.20	2.20	2.20	2.20	2.17	2.19	2.20
	F_h	2.57	2.50	2.52	2.56	2.55	2.53	2.49	2.49	2.49
	Q	6.52	7.37	6.97	6.34	6.46	6.79	6.88	7.34	7.62
14 Days	Mass (lb)	16.9	16.7	16.6	16.7	16.6	16.7	16.8	16.6	16.8
	Mass (g)	7654.8	7589.4	7513.0	7592.5	7551.8	7570.7	7627.5	7541.2	7628.9
	Debris (g)	0.00	0.00	0.00	0.00	0.00	0.00	4.52	5.01	4.51
	F_r	2.29	2.25	2.27	2.29	2.28	2.29	2.20	2.21	2.24
	F_l	2.26	2.20	2.20	2.20	2.26	2.21	2.20	2.20	2.20
	F_h	2.59	2.55	2.57	2.59	2.57	2.57	2.49	2.50	2.53
	Q	6.94	6.43	6.14	6.94	6.34	6.94	7.59	7.57	6.79
21 Days	Mass (lb)	16.9	16.7	16.6	16.7	16.7	16.7	16.8	16.6	16.8
	Mass (g)	7657.5	7592.9	7516.7	7597.4	7555.3	7573.1	7625.8	7540.7	7631.7
	Debris (g)	0.00	0.00	0.00	0.00	0.00	0.00	5.09	7.62	4.61
	F_r	2.29	2.27	2.29	2.29	2.29	2.29	2.20	2.22	2.25
	F_l	2.27	2.20	2.24	2.27	2.26	2.26	2.19	2.20	2.20
	F_h	2.59	2.56	2.57	2.59	2.59	2.59	2.49	2.50	2.54
	Q	7.16	6.31	6.94	7.16	6.94	6.94	7.34	7.40	6.62
28 Days	Mass (lb)	16.9	16.7	16.6	16.7	16.6	16.7	16.8	16.6	16.8
	Mass (g)	7651.7	7576.7	7510.2	7586.0	7544.6	7572.4	7617.6	7522.6	7615.1
	Debris (g)	0.00	0.00	0.00	0.00	0.00	0.00	6.28	7.31	16.45
	F_r	2.30	2.27	2.29	2.30	2.29	2.30	2.20	2.20	2.22
	F_l	2.28	2.20	2.26	2.27	2.26	2.27	2.18	2.20	2.20
	F_h	2.59	2.56	2.59	2.59	2.59	2.59	2.49	2.49	2.50
	Q	7.42	6.31	6.94	7.19	6.94	7.19	7.10	7.59	7.40
35 Days	Mass (lb)	16.9	16.7	16.6	16.8	16.7	16.7	16.8	16.6	16.8
	Mass (g)	7659.3	7596.3	7519.8	7600.4	7558.3	7577.3	7626.9	7538.8	7618.2
	Debris (g)	0.00	0.00	0.00	0.00	0.00	0.00	2.49	4.49	6.13
	F_r	2.29	2.23	2.24	2.29	2.29	2.29			
	F_l	2.24	2.20	2.20	2.26	2.25	2.25			
	F_h	2.58	2.52	2.53	2.59	2.57	2.57			
	Q	6.74	6.97	6.79	6.94	7.16	7.16			

Table B.2-2 - Freeze and thaw data from Set 1, full strength solutions, for $MgCl_2$, $CaCl_2$, and H_2O for days 36 to 56

		$MgCl_2$ 1	$MgCl_2$ 2	$MgCl_2$ 3	$CaCl_2$ 1	$CaCl_2$ 2	$CaCl_2$ 3	H_2O 1	H_2O 2	H_2O 3
42 Days	Mass (lb)	16.9	16.7	16.6	16.8	16.7	16.7	16.8	16.6	16.8
	Mass (g)	7660.4	7597.0	7518.9	7600.9	7561.1	7579.3	7619.6	7529.6	7610.4
	Debris (g)	0.00	0.00	0.00	0.00	0.00	0.00	3.74	6.43	4.59
	F_r	2.30	2.28	2.28	2.30	2.29	2.29			
	F_l	2.27	2.21	2.24	2.28	2.25	2.26			
	F_h	2.59	2.56	2.57	2.59	2.58	2.59			
	Q	7.19	6.52	6.91	7.42	6.94	6.94			
49 Days	Mass (lb)	16.9	16.7	16.6	16.8	16.7	16.7	16.8	16.6	16.8
	Mass (g)	7661.2	7597.2	7521.4	7602.5	7562.5	7580.3	7619.2	7517.7	7610.5
	Debris (g)	0.00	0.00	0.00	0.00	0.00	0.00	4.17	13.19	3.82
	F_r	2.30	2.28	2.28	2.30	2.29	2.29			
	F_l	2.27	2.22	2.23	2.28	2.26	2.26			
	F_h	2.59	2.56	2.57	2.59	2.59	2.59			
	Q	7.19	6.71	6.71	7.42	6.94	6.94			
56 Days	Mass (lb)	16.9	16.8	16.6	16.8	16.7	16.7	16.8	16.6	16.8
	Mass (g)	7661.1	7599.2	7522.1	7602.2	7563.4	7580.7	7616.1	7508.9	7604.8
	Debris (g)	0.00	0.00	0.00	0.00	0.00	0.00	5.35	5.90	5.51
	F_r	2.30	2.28	2.28	2.30	2.29	2.30			
	F_l	2.27	2.23	2.24	2.28	2.26	2.27			
	F_h	2.59	2.57	2.56	2.59	2.59	2.59			
	Q	7.19	6.71	7.13	7.42	6.94	7.19			

Table B.2-3 - Freeze and thaw data from Set 1, full strength solutions, for Multi-Cl^- and NaCl for the first 35 days

		Multi-Cl 1	Multi-Cl 2	Multi-Cl 3	NaCl 1	NaCl 2	NaCl 3
Initial	Mass (lb)	16.6	16.8	16.7	16.6	16.8	16.6
	Mass (g)	7526.8	7604.8	7569.3	7526.8	7597.7	7512.6
	Debris (g)	0.00	0.00	0.00	0.00	0.00	0.00
	F_r	2.22	2.28	2.22	2.26	2.29	2.22
	F_l	2.20	2.21	2.20	2.20	2.26	2.20
	F_h	2.51	2.57	2.51	2.55	2.58	2.50
	Q	7.16	6.52	7.16	6.46	7.16	7.37
7 Days	Mass (lb)	16.8	16.9	16.9	16.9	17.0	16.9
	Mass (g)	7619.6	7673.9	7664.1	7657.2	7721.8	7649.7
	Debris (g)	0.00	0.00	0.00	0.00	0.00	0.00
	F_r	2.22	2.26	2.25	2.20	2.26	2.20
	F_l	2.20	2.20	2.20	2.20	2.20	2.18
	F_h	2.50	2.55	2.54	2.49	2.55	2.49
	Q	7.40	6.46	6.62	7.59	6.46	7.10
14 Days	Mass (lb)	16.8	16.9	16.9	16.9	17.0	16.9
	Mass (g)	7625.5	7676.6	7655.6	7662.8	7713.7	7644.1
	Debris (g)	0.00	0.00	0.00	0.00	0.00	0.00
	F_r	2.26	2.29	2.28	2.22	2.27	2.20
	F_l	2.20	2.25	2.20	2.20	2.20	2.19
	F_h	2.54	2.57	2.56	2.50	2.56	2.49
	Q	6.65	7.16	6.34	7.40	6.31	7.34
21 Days	Mass (lb)	16.8	16.9	16.9	16.9	17.0	16.9
	Mass (g)	7631.3	7682.6	7658.4	7660.4	7713.0	7647.8
	Debris (g)	0.00	0.00	0.00	0.00	0.00	0.00
	F_r	2.28	2.29	2.29	2.24	2.29	2.21
	F_l	2.22	2.26	2.25	2.20	2.24	2.20
	F_h	2.56	2.59	2.57	2.52	2.56	2.49
	Q	6.71	6.94	7.16	7.00	7.16	7.62
28 Days	Mass (lb)	16.8	16.9	16.9	16.9	17.0	16.8
	Mass (g)	7633.6	7673.2	7655.3	7658.1	7715.3	7635.3
	Debris (g)	0.00	0.00	0.00	0.00	0.00	0.00
	F_r	2.29	2.23	2.29	2.26	2.29	2.22
	F_l	2.23	2.23	2.25	2.20	2.23	2.20
	F_h	2.58	2.59	2.59	2.56	2.58	2.50
	Q	6.55	7.19	6.74	6.28	6.55	7.40
35 Days	Mass (lb)	16.8	16.9	16.9	16.9	17.0	16.9
	Mass (g)	7638.4	7687.7	7664.2	7663.9	7718.1	7650.1
	Debris (g)	0.00	0.00	0.00	0.00	0.00	0.00
	F_r	2.28	2.29	2.28	2.23	2.29	2.22
	F_l	2.21	2.23	2.20	2.20	2.25	2.20
	F_h	2.55	2.57	2.56	2.50	2.56	2.49
	Q	6.71	6.74	6.34	7.44	7.39	7.66

Table B.2-4 - Freeze and thaw data from Set 1, full strength solutions, for Multi-Cl- and NaCl for days 36 to 56

		Multi-Cl 1	Multi-Cl 2	Multi-Cl 3	NaCl 1	NaCl 2	NaCl 3
42 Days	Mass (lb)	16.8	16.9	16.9	16.9	17.0	16.9
	Mass (g)	7639.8	7687.6	7662.8	7664.9	7719.6	7651.2
	Debris (g)	0.00	0.00	0.00	0.35	0.30	0.25
	F_r	2.29	2.30	2.29	2.27	2.29	2.24
	F_l	2.25	2.27	2.25	2.20	2.26	2.20
	F_h	2.57	2.59	2.59	2.54	2.58	2.53
	Q	7.16	7.19	6.74	6.68	7.16	6.79
49 Days	Mass (lb)	16.8	17.0	16.9	16.9	17.0	16.9
	Mass (g)	7641.9	7690.1	7665.4	7666.2	7721.3	7651.9
	Debris (g)	0.36	0.16	0.00	0.00	0.29	0.55
	F_r	2.29	2.30	2.29	2.27	2.29	2.23
	F_l	2.25	2.27	2.25	2.20	2.26	2.20
	F_h	2.57	2.59	2.57	2.54	2.59	2.50
	Q	7.16	7.19	7.16	6.68	6.94	7.44
56 Days	Mass (lb)	16.9	17.0	16.9	16.9	17.0	16.9
	Mass (g)	7643.2	7689.3	7664.8	7666.7	7721.9	7652.9
	Debris (g)	1.63	0.00	1.83	0.00	0.00	0.53
	F_r	2.29	2.30	2.29	2.28	2.30	2.26
	F_l	2.26	2.27	2.26	2.20	2.26	2.20
	F_h	2.58	2.59	2.58	2.56	2.59	2.55
	Q	7.16	7.19	7.16	6.34	6.97	6.46

Appendix B.2.3 Freezing and Thawing Set 2 Data

The data in Table B.2-5 through Table B.2-8 represent all data collected during the freeze and thaw testing with respect to the prism characteristics for set 2 which was subjected to diluted solutions.

Table B.2-5 - Freeze and thaw data from Set 2, diluted solutions, for $MgCl_2$, $CaCl_2$, and H_2O for the first 35 days

		$MgCl_2$ 1	$MgCl_2$ 2	$MgCl_2$ 3	$CaCl_2$ 1	$CaCl_2$ 2	$CaCl_2$ 3	H_2O 1	H_2O 2	H_2O 3
Initial	Mass (lb)	16.4	16.0	16.6	16.5	16.1	16.1	16.3	16.6	16.0
	Mass (g)	7435.9	7269.4	7523.8	7473.0	7321.2	7308.2	7375.6	7533.9	7251.9
	Debris (g)	0.00	0.00	0.00	0.00	0.00	0.00	0.00	0.00	0.00
	F_r	2.20	2.20	2.20	2.20	2.19	2.21	2.20	2.20	2.19
	F_l	2.20	2.18	2.20	2.20	2.15	2.20	2.19	2.19	2.17
	F_h	2.49	2.48	2.48	2.49	2.44	2.49	2.49	2.48	2.49
	Q	7.59	7.34	7.86	7.59	7.56	7.62	7.34	7.59	6.85
7 Days	Mass (lb)	16.6	16.2	16.8	16.8	16.3	16.4	16.6	16.9	16.3
	Mass (g)	7515.2	7361.3	7605.9	7627.0	7394.1	7455.5	7513.8	7666.8	7389.1
	Debris (g)	0.00	0.00	0.00	0.00	0.00	0.00	0.00	0.00	0.00
	F_r	2.20	2.20	2.20	2.20	2.19	2.21	2.20	2.20	2.20
	F_l	2.18	2.17	2.17	2.20	2.15	2.20	2.19	2.13	2.16
	F_h	2.44	2.44	2.44	2.45	2.39	2.46	2.48	2.48	2.49
	Q	8.47	8.15	8.15	8.80	9.13	8.50	7.59	6.29	6.67
14 Days	Mass (lb)	16.6	16.2	16.8	16.8	16.3	16.4	16.6	16.9	16.3
	Mass (g)	7529.2	7368.9	7615.1	7632.9	7398.3	7460.9	7516.1	7670.5	7392.3
	Debris (g)	0.00	0.00	0.00	3.64	4.85	4.50	2.60	2.10	1.25
	F_r	2.20	2.20	2.20	2.20	2.20	2.22	2.20	2.20	2.20
	F_l	2.20	2.18	2.19	2.20	2.17	2.20	2.18	2.17	2.17
	F_h	2.47	2.44	2.49	2.46	2.45	2.49	2.44	2.44	2.49
	Q	8.15	8.47	7.34	8.47	7.86	7.66	8.47	8.15	6.38
21 Days	Mass (lb)	16.6	16.3	16.8	16.8	16.3	16.4	16.6	16.9	16.3
	Mass (g)	7532.3	7371.9	7616.5	7634.9	7398.2	7459.9	7520.0	7675.9	7399.1
	Debris (g)	0.00	0.00	0.00	5.88	7.55	8.40	0.92	0.99	1.14
	F_r	2.21	2.20	2.21	2.22	2.20	2.23	2.20	2.20	2.20
	F_l	2.20	2.19	2.20	2.20	2.17	2.20	2.19	2.18	2.17
	F_h	2.46	2.44	2.47	2.45	2.44	2.47	2.44	2.44	2.43
	Q	8.50	8.80	8.19	8.88	8.15	8.26	8.80	8.47	8.47
28 Days	Mass (lb)	16.6	16.3	16.8	16.8	16.3	16.4	16.6	16.9	16.3
	Mass (g)	7536.1	7371.4	7617.6	7635.0	7398.4	7461.5	7520.0	7676.5	7395.2
	Debris (g)	0.00	0.00	0.00	3.39	3.81	2.13	1.39	0.95	1.85
	F_r	2.20	2.20	2.20	2.21	2.20	2.23	2.20	2.20	2.20
	F_l	2.20	2.19	2.20	2.20	2.17	2.20	2.19	2.18	2.19
	F_h	2.46	2.44	2.49	2.45	2.44	2.49	2.47	2.45	2.48
	Q	8.47	8.80	7.59	8.84	8.15	7.69	7.86	8.15	7.59
35 Days	Mass (lb)	16.6	16.3	16.8	16.8	16.3	16.4	16.6	16.9	16.3
	Mass (g)	7537.3	7372.5	7619.9	7635.0	7395.2	7461.3	7521.0	7675.3	7392.2
	Debris (g)	0.00	0.00	0.00	4.68	5.22	7.54	1.59	1.85	3.96
	F_r	2.22	2.20	2.21	2.22	2.20	2.27	2.20	2.20	2.20
	F_l	2.20	2.20	2.20	2.20	2.18	2.20	2.19	2.20	2.20
	F_h	2.47	2.49	2.49	2.49	2.47	2.49	2.46	2.45	2.45
	Q	8.23	7.59	7.62	7.66	7.59	7.83	8.15	8.80	8.80

Table B.2-6 - Freeze and thaw data from Set 2, diluted solutions, for $MgCl_2$, $CaCl_2$, and H_2O for days 36 through 56

		$MgCl_2$ 1	$MgCl_2$ 2	$MgCl_2$ 3	$CaCl_2$ 1	$CaCl_2$ 2	$CaCl_2$ 3	H_2O 1	H_2O 2	H_2O 3
42 Days	Mass (lb)	16.6	16.3	16.8	16.8	16.3	16.4	16.6	16.9	16.3
	Mass (g)	7537.0	7371.9	7618.7	7631.8	7393.2	7459.5	7515.0	7677.7	7389.7
	Debris (g)	0.00	0.00	0.00	2.98	2.55	1.20	1.01	1.08	1.47
	F_r	2.20	2.21	2.21	2.22	2.20	2.22	2.20	2.20	2.20
	F_l	2.20	2.20	2.20	2.20	2.17	2.20	2.20	2.18	2.19
	F_h	2.46	2.45	2.47	2.48	2.44	2.45	2.44	2.41	2.42
	Q	8.54	8.84	8.23	7.93	8.15	8.88	9.17	9.57	9.57
49 Days	Mass (lb)	16.6	16.3	16.8	16.8	16.3	16.4	16.6	16.9	16.3
	Mass (g)	7538.1	7372.1	7620.0	7629.9	7386.5	7459.3	7513.8	7672.4	7386.9
	Debris (g)	0.00	0.00	0.00	4.78	8.43	3.34	0.95	0.90	2.32
	F_r	2.23	2.20	2.22	2.24	2.19	2.23	2.21	2.20	2.20
	F_l	2.20	2.20	2.20	2.20	2.16	2.20	2.20	2.20	2.20
	F_h	2.47	2.44	2.46	2.47	2.45	2.47	2.46	2.46	2.46
	Q	8.26	9.17	8.54	8.30	7.56	8.26	8.50	8.47	8.47
56 Days	Mass (lb)	16.6	16.2	16.8	16.8	16.3	16.4	16.6	16.9	16.3
	Mass (g)	7537.3	7369.8	7619.5	7623.7	7383.6	7456.2	7511.1	7668.6	7382.1
	Debris (g)	0.00	0.00	0.00	6.79	3.74	1.66	0.82	1.52	2.73
	F_r	2.23	2.22	2.23	2.22	2.20	2.28	2.22	2.22	2.20
	F_l	2.20	2.20	2.20	2.20	2.18	2.21	2.20	2.20	2.19
	F_h	2.49	2.49	2.49	2.49	2.47	2.52	2.49	2.49	2.49
	Q	7.69	7.66	7.69	7.66	7.59	7.36	7.66	7.66	7.34

Table B.2-7 - Freeze and thaw data from Set 2, diluted solutions, for Multi-Cl- and NaCl for the first 35 days

		Multi-Cl 1	Multi-Cl 2	Multi-Cl 3	NaCl 1	NaCl 2	NaCl 3
Initial	Mass (lb)	16.1	16.4	16.5	16.6	16.1	16.2
	Mass (g)	7301.8	7438.4	7479.8	7513.3	7317.1	7348.5
	Debris (g)	0.00	0.00	0.00	0.00	0.00	0.00
	F_r	2.20	2.20	2.20	2.21	2.20	2.20
	F_l	2.17	2.20	2.19	2.20	2.19	2.19
	F_h	2.48	2.49	2.49	2.49	2.48	2.49
	Q	7.10	7.59	7.34	7.62	7.59	7.34
7 Days	Mass (lb)	16.4	16.6	16.7	16.9	16.4	16.5
	Mass (g)	7425.4	7547.9	7590.1	7656.2	7458.3	7491.5
	Debris (g)	0.00	0.00	0.00	0.00	0.00	0.00
	F_r	2.20	2.22	2.21	2.21	2.20	2.20
	F_l	2.17	2.20	2.20	2.20	2.13	2.18
	F_h	2.48	2.49	2.49	2.49	2.45	2.47
	Q	7.10	7.66	7.62	7.62	6.88	7.59
14 Days	Mass (lb)	16.4	16.7	16.8	16.9	16.5	16.5
	Mass (g)	7433.1	7558.1	7597.9	7659.1	7461.8	7494.0
	Debris (g)	1.63	1.04	2.86	1.78	5.89	3.94
	F_r	2.20	2.22	2.21	2.20	2.20	2.20
	F_l	2.18	2.20	2.20	2.18	2.19	2.20
	F_h	2.45	2.47	2.48	2.45	2.47	2.47
	Q	8.15	8.23	7.90	8.15	7.86	8.15
21 Days	Mass (lb)	16.4	16.7	16.8	16.9	16.5	16.5
	Mass (g)	7439.3	7564.8	7600.7	7664.9	7463.5	7497.1
	Debris (g)	1.00	0.66	2.26	7.23	4.85	4.51
	F_r	2.21	2.27	2.23	2.20	2.20	2.20
	F_l	2.20	2.20	2.20	2.19	2.19	2.19
	F_h	2.46	2.49	2.49	2.42	2.45	2.43
	Q	8.50	7.83	7.69	9.57	8.47	9.17
28 Days	Mass (lb)	16.4	16.7	16.8	16.9	16.5	16.5
	Mass (g)	7443.4	7568.7	7605.2	7664.8	7463.2	7493.2
	Debris (g)	0.57	0.38	0.52	2.35	2.73	4.20
	F_r	2.21	2.24	2.22	2.21	2.20	2.20
	F_l	2.19	2.20	2.20	2.18	2.18	2.18
	F_h	2.49	2.51	2.49	2.49	2.47	2.47
	Q	7.37	7.23	7.66	7.13	7.59	7.59
35 Days	Mass (lb)	16.4	16.7	16.8	16.9	16.4	16.5
	Mass (g)	7445.7	7572.0	7605.1	7659.3	7458.2	7488.3
	Debris (g)	0.00	0.00	0.00	6.05	3.39	5.51
	F_r	2.22		2.24	2.25		2.20
	F_l	2.20		2.20	2.20		2.04
	F_h	2.49		2.49	2.49		2.40
	Q	7.66		7.73	7.76		6.11

Table B.2-8 - Freeze and thaw data from Set 2, diluted solutions, for Multi-Cl- and NaCl for days 36 to 56

		Multi-Cl 1	Multi-Cl 2	Multi-Cl 3	NaCl 1	NaCl 2	NaCl 3
42 Days	Mass (lb)	16.4	16.7	16.8	16.9	16.4	16.5
	Mass (g)	7445.6	7572.7	7605.9	7657.8	7457.7	7488.6
	Debris (g)	0.00	0.00	0.00	3.04	1.26	1.84
	F_r	2.27	2.23	2.25	2.26	2.20	2.20
	F_l	2.21	2.20	2.21	2.19	2.17	2.21
	F_h	2.51	2.49	2.50	2.49	2.46	2.49
	Q	7.57	7.69	7.76	7.54	7.59	8.07
49 Days	Mass (lb)	16.4	16.7	16.8	16.9	16.4	16.5
	Mass (g)	7446.4	7572.6	7606.1	7654.7	7456.3	7486.7
	Debris (g)	0.00	0.00	0.00	3.78	2.45	2.32
	F_r	2.23	2.29	2.27	2.25	2.22	2.20
	F_l	2.20	2.22	2.20	2.20	2.20	2.19
	F_h	2.49	2.55	2.54	2.51	2.49	2.49
	Q	7.69	6.94	6.68	7.26	7.66	7.34
56 Days	Mass (lb)	16.4	16.7	16.8	16.9	16.4	16.5
	Mass (g)	7444.1	7571.3	7603.0	7649.2	7454.0	7482.0
	Debris (g)	0.00	0.00	0.00	4.56	1.98	2.00
	F_r	2.23	2.29	2.28	2.27	2.21	2.21
	F_l	2.20	2.24	2.20	2.20	2.20	2.20
	F_h	2.49	2.55	2.55	2.53	2.49	2.49
	Q	7.69	7.39	6.52	6.88	7.62	7.62

Appendix B.3 Compressive Strength Testing Results

Appendix B.3.1 Set 1 Raw Compressive Testing Results

The data in Table B.3-1 through Table B.3-5 represent the raw data collected during the compressive strength testing for Set 1 where the cylinders were continuously soaked.

Table B.3-1 - Compressive strength testing results for Set 1, continuous soaking, weeks 0-2

Week	Solution	Cast Set	Sample #	Force (kN)	Average Force (kN)	Diameter (mm)	Measured Strength (MPa)	Calculated Strength (MPa)	Average Strength (MPa)
0	-	X	1	407.4	383.0	101.0	51.9	50.8	47.8
	-	X	2	379.8		101.0	48.4	47.4	
	-	X	3	379.8		101.0	48.4	47.4	
	-	X	4	395.8		101.0	50.4	49.4	
	-	X	5	352.0		101.0	44.8	43.9	
	-	O	1	487.0	469.1	101.0	62.0	60.8	58.6
	-	O	2	458.0		101.0	58.3	57.2	
	-	O	3	463.6		101.0	59.0	57.9	
	-	O	4	477.5		101.0	60.8	59.6	
	-	O	5	459.7		101.0	58.5	57.4	
2	$MgCl_2$	X	1	472.3	455.9	101.0	60.1	59.0	56.9
	$MgCl_2$	X	2	434.2		101.0	55.3	54.2	
	$MgCl_2$	X	3	461.1		101.0	58.7	57.6	
	$CaCl_2$	X	1	460.8	465.6	101.0	58.7	57.5	58.1
	$CaCl_2$	X	2	478.1		101.0	60.9	59.7	
	$CaCl_2$	X	3	457.9		101.0	58.3	57.2	
	H_2O	X	1	403.2	412.4	101.0	51.3	50.3	51.5
	H_2O	X	2	414.3		101.0	52.8	51.7	
	H_2O	X	3	419.8		101.0	53.4	52.4	
	Multi-Cl^-	X	1	444.0	447.8	101.0	56.5	55.4	55.9
	Multi-Cl^-	X	2	426.9		101.0	54.4	53.3	
	Multi-Cl^-	X	3	472.5		101.0	60.2	59.0	
	NaCl	X	1	430.6	411.5	101.0	54.8	53.7	51.4
	NaCl	X	2	396.6		101.0	50.5	49.5	
	NaCl	X	3	407.3		101.0	51.9	50.8	

Table B.3-2 - Compressive strength testing results for Set 1, continuous soaking, weeks 4-6

Week	Solution	Cast Set	Sample #	Force (kN)	Average Force (kN)	Diameter (mm)	Measured Strength (MPa)	Calculated Strength (MPa)	Average Strength (MPa)
4	$MgCl_2$	O	1	590.0	578.9	101.0	75.1	73.6	72.3
	$MgCl_2$	O	2	579.5		101.0	73.8	72.3	
	$MgCl_2$	O	3	567.1		101.0	72.2	70.8	
	$CaCl_2$	O	1	574.6	568.0	101.0	73.2	71.7	70.9
	$CaCl_2$	O	2	545.2		101.0	69.4	68.0	
	$CaCl_2$	O	3	584.2		101.0	74.4	72.9	
	H_2O	O	1	543.3	534.9	101.0	69.2	67.8	66.8
	H_2O	O	2	523.4		101.0	66.6	65.3	
	H_2O	O	3	538.0		101.0	68.5	67.1	
	Multi-Cl^-	O	1	574.5	566.7	101.0	73.2	71.7	70.7
	Multi-Cl^-	O	2	555.7		101.0	70.8	69.4	
	Multi-Cl^-	O	3	570.0		101.0	72.6	71.1	
	NaCl	O	1	550.0	559.1	101.0	70.0	68.6	69.8
	NaCl	O	2	557.3		101.0	71.0	69.6	
	NaCl	O	3	570.0		101.0	71.8	71.1	
6	$MgCl_2$	X	1	477.8	458.9	101.0	60.8	59.6	57.3
	$MgCl_2$	X	2	476.2		101.0	60.6	59.4	
	$MgCl_2$	X	3	422.6		101.0	53.8	52.7	
	$CaCl_2$	X	1	466.9	484.4	101.0	59.4	58.3	60.5
	$CaCl_2$	X	2	520.7		101.0	66.3	65.0	
	$CaCl_2$	X	3	465.6		101.0	59.3	58.1	
	H_2O	X	1	439.0	437.8	101.0	55.9	54.8	54.6
	H_2O	X	2	440.4		101.0	56.1	55.0	
	H_2O	X	3	434.1		101.0	55.3	54.2	
	Multi-Cl^-	X	1	484.9	481.0	101.0	61.7	60.5	60.0
	Multi-Cl^-	X	2	470.5		101.0	59.9	58.7	
	Multi-Cl^-	X	3	487.6		101.0	62.1	60.9	
	NaCl	X	1	470.6	465.7	101.0	59.9	58.7	58.1
	NaCl	X	2	477.5		101.0	55.7	59.6	
	NaCl	X	3	449.1		101.0	57.2	56.1	

Table B.3-3 - Compressive strength testing results for Set 1, continuous soaking, weeks 8-10

Week	Solution	Cast Set	Sample #	Force (kN)	Average Force (kN)	Diameter (mm)	Measured Strength (MPa)	Calculated Strength (MPa)	Average Strength (MPa)
8	$MgCl_2$	O	1	601.5	593.7	101.0	76.6	75.1	74.1
	$MgCl_2$	O	2	589.8		101.0	75.1	73.6	
	$MgCl_2$	O	3	589.8		101.0	75.1	73.6	
	$CaCl_2$	O	1	568.3	585.0	101.0	72.4	70.9	73.0
	$CaCl_2$	O	2	588.7		101.0	75.0	73.5	
	$CaCl_2$	O	3	597.9		101.0	76.1	74.6	
	H_2O	O	1	543.7	562.8	101.0	69.2	67.9	70.2
	H_2O	O	2	582.8		101.0	74.2	72.7	
	H_2O	O	3	562.0		101.0	71.6	70.1	
	Multi-Cl^-	O	1	583.9	596.2	101.0	74.3	72.9	74.4
	Multi-Cl^-	O	2	596.6		101.0	76.0	74.5	
	Multi-Cl^-	O	3	608.2		101.0	77.4	75.9	
	NaCl	O	1	576.3	565.4	101.0	73.7	71.9	70.6
	NaCl	O	2	546.0		101.0	69.5	68.1	
	NaCl	O	3	574.0		101.0	73.1	71.6	
10	$MgCl_2$	X	1	435.2	468.2	101.0	55.4	54.3	58.4
	$MgCl_2$	X	2	479.8		101.0	60.5	59.9	
	$MgCl_2$	X	3	489.6		101.0	61.4	61.1	
	$CaCl_2$	X	1	439.4	450.0	101.0	59.5	54.8	56.2
	$CaCl_2$	X	2	428.8		101.0	54.6	53.5	
	$CaCl_2$	X	3	481.8		101.0	61.3	60.1	
	H_2O	X	1	436.4	462.0	101.0	55.6	54.5	57.7
	H_2O	X	2	470.4		101.0	59.9	58.7	
	H_2O	X	3	479.1		101.0	61.0	59.8	
	Multi-Cl^-	X	1	470.7	489.9	101.0	59.9	58.8	61.1
	Multi-Cl^-	X	2	491.6		101.0	62.6	61.4	
	Multi-Cl^-	X	3	507.4		101.0	64.6	63.3	
	NaCl	X	1	453.4	492.0	101.0	57.7	56.6	61.4
	NaCl	X	2	492.9		101.0	56.4	61.5	
	NaCl	X	3	529.7		101.0	67.5	66.1	

Table B.3-4 - Compressive strength testing results for Set 1, continuous soaking, weeks 12-14

Week	Solution	Cast Set	Sample #	Force (kN)	Average Force (kN)	Diameter (mm)	Measured Strength (MPa)	Calculated Strength (MPa)	Average Strength (MPa)
12	$MgCl_2$	O	1	581.0	568.0	101.0	74.0	72.5	70.9
	$MgCl_2$	O	2	591.5		101.0	75.3	73.8	
	$MgCl_2$	O	3	531.5		101.0	67.7	66.3	
	$CaCl_2$	O	1	540.6	554.4	101.0	68.8	67.5	69.2
	$CaCl_2$	O	2	583.9		101.0	74.3	72.9	
	$CaCl_2$	O	3	538.6		101.0	68.6	67.2	
	H_2O	O	1	579.5	564.7	101.0	73.8	72.3	70.5
	H_2O	O	2	567.4		101.0	72.2	70.8	
	H_2O	O	3	547.2		101.0	69.7	68.3	
	Multi-Cl^-	O	1	578.4	590.5	101.0	73.6	72.2	73.7
	Multi-Cl^-	O	2	589.9		101.0	75.1	73.6	
	Multi-Cl^-	O	3	603.1		101.0	76.8	75.3	
	NaCl	O	1	579.8	566.3	101.0	73.8	72.4	70.7
	NaCl	O	2	560.0		101.0	71.3	69.9	
	NaCl	O	3	559.1		101.0	71.2	69.8	
14	$MgCl_2$	X	1	452.9	464.4	101.0	57.7	56.5	58.0
	$MgCl_2$	X	2	445.6		101.0	56.7	55.6	
	$MgCl_2$	X	3	494.8		101.0	63.0	61.8	
	$CaCl_2$	X	1	430.4	449.0	101.0	54.8	53.7	56.0
	$CaCl_2$	X	2	446.8		101.0	56.9	55.8	
	$CaCl_2$	X	3	469.9		101.0	59.8	58.6	
	H_2O	X	1	459.4	464.6	101.0	58.5	57.3	58.0
	H_2O	X	2	483.8		101.0	61.6	60.4	
	H_2O	X	3	450.7		101.0	57.4	56.3	
	Multi-Cl^-	X	1	507.8	482.3	101.0	64.7	63.4	60.2
	Multi-Cl^-	X	2	471.0		101.0	60.0	58.8	
	Multi-Cl^-	X	3	468.1		101.0	59.6	58.4	
	NaCl	X	1	487.6	474.4	101.0	62.1	60.9	59.2
	NaCl	X	2	480.8		101.0	61.2	60.0	
	NaCl	X	3	454.9		101.0	57.9	56.8	

Table B.3-5 - Compressive strength testing results for Set 1, continuous soaking, weeks 16-37

Week	Solution	Cast Set	Sample #	Force (kN)	Average Force (kN)	Diameter (mm)	Measured Strength (MPa)	Calculated Strength (MPa)	Average Strength (MPa)
16	$MgCl_2$	O	1	588.1	590.1	101.0	74.9	73.4	73.6
	$MgCl_2$	O	2	589.0		101.0	75.0	73.5	
	$MgCl_2$	O	3	593.1		101.0	75.5	74.0	
	$CaCl_2$	O	1	565.5	575.0	101.0	72.0	70.6	71.8
	$CaCl_2$	O	2	586.7		101.0	74.7	73.2	
	$CaCl_2$	O	3	572.6		101.0	72.9	71.5	
	H_2O	O	1	572.7	573.6	101.0	72.9	71.5	71.6
	H_2O	O	2	586.7		101.0	74.7	73.2	
	H_2O	O	3	561.5		101.0	71.5	70.1	
	Multi-Cl^-	O	1	590.6	581.7	101.0	75.2	73.7	72.6
	Multi-Cl^-	O	2	575.2		101.0	73.2	71.8	
	Multi-Cl^-	O	3	579.3		101.0	73.8	72.3	
	NaCl	O	1	584.3	554.5	101.0	74.4	72.9	69.2
	NaCl	O	2	553.3		101.0	70.5	69.1	
	NaCl	O	3	525.7		101.0	66.9	65.6	
37	$MgCl_2$	O	1	552.4	561.0	101.0	70.3	68.9	70.0
	$MgCl_2$	O	2	569.6		101.0	72.5	71.1	
	$MgCl_2$	X	1	456.8	443.1	101.0	58.2	57.0	55.3
	$MgCl_2$	X	2	429.4		101.0	54.7	53.6	
	$CaCl_2$	O	1	539.6	543.2	101.0	68.7	67.4	67.8
	$CaCl_2$	O	2	546.8		101.0	69.6	68.2	
	$CaCl_2$	X	1	499.4	468.7	101.0	63.6	62.3	58.5
	$CaCl_2$	X	2	438.1		101.0	55.8	54.7	
	H_2O	O	1	588.2	599.9	101.0	74.9	73.4	74.9
	H_2O	O	2	611.6		101.0	77.9	76.3	
	H_2O	X	1	518.6	518.6	101.0	66.0	64.7	64.7
	Multi-Cl^-	O	1	561.1	565.2	101.0	71.1	70.0	70.5
	Multi-Cl^-	O	2	569.3		101.0	72.5	71.1	
	Multi-Cl^-	X	1	484.9	476.4	101.0	61.7	60.5	59.5
	Multi-Cl^-	X	2	468.0		101.0	59.6	58.4	
	NaCl	O	1	586.6	590.3	101.0	74.7	73.2	73.7
	NaCl	O	2	581.7		101.0	74.1	72.6	
	NaCl	O	3	602.6		101.0	76.7	75.2	
	NaCl	X	1	500.4	500.4	101.0	66.0	62.5	62.5

Appendix B.3.2 Set 1 Normalized Compressive Testing Results

The data in Table B.3-6 through Table B.3-10 show the normalized data for the compressive strength testing from Set 1 where the cylinders were continuously soaked. The results are

normalized by Equation 4.3-1 so that difference in the two batches can be removed from the analysis.

Table B.3-6 – Normalized compressive strength testing results for Set 1, continuous soaking, weeks 0-2

Week	Solution	Cast Set	Sample #	Force (kN)	Calculated Strength (MPa)	Normalized Force Ratio	Avg Force (kN)	Avg Normalized Force (kN)	Avg Normalized Strength (MPa)
0	-	X	1	407.4	50.8	1.1	383.0	426.0	53.2
	-	X	2	379.8	47.4	1.0			
	-	X	3	379.8	47.4	1.0			
	-	X	4	395.8	49.4	1.0			
	-	X	5	352.0	43.9	0.9			
	-	O	1	487.0	60.8	1.0	469.1	426.0	53.2
	-	O	2	458.0	57.2	1.0			
	-	O	3	463.6	57.9	1.0			
	-	O	4	477.5	59.6	1.0			
	-	O	5	459.7	57.4	1.0			
2	$MgCl_2$	X	1	472.3	59.0	1.2	455.9	507.2	63.3
	$MgCl_2$	X	2	434.2	54.2	1.1			
	$MgCl_2$	X	3	461.1	57.6	1.2			
	$CaCl_2$	X	1	460.8	57.5	1.2	465.6	518.0	64.7
	$CaCl_2$	X	2	478.1	59.7	1.2			
	$CaCl_2$	X	3	457.9	57.2	1.2			
	H_2O	X	1	403.2	50.3	1.1	412.4	458.8	57.3
	H_2O	X	2	414.3	51.7	1.1			
	H_2O	X	3	419.8	52.4	1.1			
	Multi-Cl^-	X	1	444.0	55.4	1.2	447.8	498.2	62.2
	Multi-Cl^-	X	2	426.9	53.3	1.1			
	Multi-Cl^-	X	3	472.5	59.0	1.2			
	NaCl	X	1	430.6	53.7	1.1	411.5	457.8	57.1
	NaCl	X	2	396.6	49.5	1.0			
	NaCl	X	3	407.3	50.8	1.1			

Table B.3-7 – Normalized compressive strength testing results for Set 1, continuous soaking, weeks 4-6

Week	Solution	Cast Set	Sample #	Force (kN)	Calculated Strength (MPa)	Normalized Force Ratio	Avg Force (kN)	Avg Normalized Force (kN)	Avg Normalized Strength (MPa)
4	$MgCl_2$	O	1	590.0	73.6	1.3	578.9	525.7	65.6
	$MgCl_2$	O	2	579.5	72.3	1.2			
	$MgCl_2$	O	3	567.1	70.8	1.2			
	$CaCl_2$	O	1	574.6	71.7	1.2	568.0	515.8	64.4
	$CaCl_2$	O	2	545.2	68.0	1.2			
	$CaCl_2$	O	3	584.2	72.9	1.2			
	H_2O	O	1	543.3	67.8	1.2	534.9	485.8	60.6
	H_2O	O	2	523.4	65.3	1.1			
	H_2O	O	3	538.0	67.1	1.1			
	Multi-Cl^-	O	1	574.5	71.7	1.2	566.7	514.7	64.2
	Multi-Cl^-	O	2	555.7	69.4	1.2			
	Multi-Cl^-	O	3	570.0	71.1	1.2			
	NaCl	O	1	550.0	68.6	1.2	559.1	507.7	63.4
	NaCl	O	2	557.3	69.6	1.2			
	NaCl	O	3	570.0	71.1	1.2			
6	$MgCl_2$	X	1	477.8	59.6	1.2	458.9	510.5	63.7
	$MgCl_2$	X	2	476.2	59.4	1.2			
	$MgCl_2$	X	3	422.6	52.7	1.1			
	$CaCl_2$	X	1	466.9	58.3	1.2	484.4	538.9	67.3
	$CaCl_2$	X	2	520.7	65.0	1.4			
	$CaCl_2$	X	3	465.6	58.1	1.2			
	H_2O	X	1	439.0	54.8	1.1	437.8	487.1	60.8
	H_2O	X	2	440.4	55.0	1.1			
	H_2O	X	3	434.1	54.2	1.1			
	Multi-Cl^-	X	1	484.9	60.5	1.3	481.0	535.1	66.8
	Multi-Cl^-	X	2	470.5	58.7	1.2			
	Multi-Cl^-	X	3	487.6	60.9	1.3			
	NaCl	X	1	470.6	58.7	1.2	465.7	518.2	64.7
	NaCl	X	2	477.5	59.6	1.2			
	NaCl	X	3	449.1	56.1	1.2			

Table B.3-8 – Normalized compressive strength testing results for Set 1, continuous soaking, weeks 8-10

Week	Solution	Cast Set	Sample #	Force (kN)	Calculated Strength (MPa)	Normalized Force Ratio	Avg Force (kN)	Avg Normalized Force (kN)	Avg Normalized Strength (MPa)
8	$MgCl_2$	O	1	601.5	75.1	1.3	593.7	539.2	67.3
	$MgCl_2$	O	2	589.8	73.6	1.3			
	$MgCl_2$	O	3	589.8	73.6	1.3			
	$CaCl_2$	O	1	568.3	70.9	1.2	585.0	531.2	66.3
	$CaCl_2$	O	2	588.7	73.5	1.3			
	$CaCl_2$	O	3	597.9	74.6	1.3			
	H_2O	O	1	543.7	67.9	1.2	562.8	511.1	63.8
	H_2O	O	2	582.8	72.7	1.2			
	H_2O	O	3	562.0	70.1	1.2			
	Multi-Cl^-	O	1	583.9	72.9	1.2	596.2	541.5	67.6
	Multi-Cl^-	O	2	596.6	74.5	1.3			
	Multi-Cl^-	O	3	608.2	75.9	1.3			
	NaCl	O	1	576.3	71.9	1.2	565.4	513.5	64.1
	NaCl	O	2	546.0	68.1	1.2			
	NaCl	O	3	574.0	71.6	1.2			
10	$MgCl_2$	X	1	435.2	54.3	1.1	468.2	520.9	65.0
	$MgCl_2$	X	2	479.8	59.9	1.3			
	$MgCl_2$	X	3	489.6	61.1	1.3			
	$CaCl_2$	X	1	439.4	54.8	1.1	450.0	500.6	62.5
	$CaCl_2$	X	2	428.8	53.5	1.1			
	$CaCl_2$	X	3	481.8	60.1	1.3			
	H_2O	X	1	436.4	54.5	1.1	462.0	513.9	64.1
	H_2O	X	2	470.4	58.7	1.2			
	H_2O	X	3	479.1	59.8	1.3			
	Multi-Cl^-	X	1	470.7	58.8	1.2	489.9	545.0	68.0
	Multi-Cl^-	X	2	491.6	61.4	1.3			
	Multi-Cl^-	X	3	507.4	63.3	1.3			
	NaCl	X	1	453.4	56.6	1.2	492.0	547.4	68.3
	NaCl	X	2	492.9	61.5	1.3			
	NaCl	X	3	529.7	66.1	1.4			

Table B.3-9 – Normalized compressive strength testing results for Set 1, continuous soaking, weeks 12-14

Week	Solution	Cast Set	Sample #	Force (kN)	Calculated Strength (MPa)	Normalized Force Ratio	Avg Force (kN)	Avg Normalized Force (kN)	Avg Normalized Strength (MPa)
12	$MgCl_2$	O	1	581.0	72.5	1.2	568.0	515.8	64.4
	$MgCl_2$	O	2	591.5	73.8	1.3			
	$MgCl_2$	O	3	531.5	66.3	1.1			
	$CaCl_2$	O	1	540.6	67.5	1.2	554.4	503.4	62.8
	$CaCl_2$	O	2	583.9	72.9	1.2			
	$CaCl_2$	O	3	538.6	67.2	1.1			
	H_2O	O	1	579.5	72.3	1.2	564.7	512.8	64.0
	H_2O	O	2	567.4	70.8	1.2			
	H_2O	O	3	547.2	68.3	1.2			
	Multi-Cl^-	O	1	578.4	72.2	1.2	590.5	536.2	66.9
	Multi-Cl^-	O	2	589.9	73.6	1.3			
	Multi-Cl^-	O	3	603.1	75.3	1.3			
	NaCl	O	1	579.8	72.4	1.2	566.3	514.3	64.2
	NaCl	O	2	560.0	69.9	1.2			
	NaCl	O	3	559.1	69.8	1.2			
14	$MgCl_2$	X	1	452.9	56.5	1.2	464.4	516.7	64.5
	$MgCl_2$	X	2	445.6	55.6	1.2			
	$MgCl_2$	X	3	494.8	61.8	1.3			
	$CaCl_2$	X	1	430.4	53.7	1.1	449.0	499.5	62.4
	$CaCl_2$	X	2	446.8	55.8	1.2			
	$CaCl_2$	X	3	469.9	58.6	1.2			
	H_2O	X	1	459.4	57.3	1.2	464.6	516.9	64.5
	H_2O	X	2	483.8	60.4	1.3			
	H_2O	X	3	450.7	56.3	1.2			
	Multi-Cl^-	X	1	507.8	63.4	1.3	482.3	536.6	67.0
	Multi-Cl^-	X	2	471.0	58.8	1.2			
	Multi-Cl^-	X	3	468.1	58.4	1.2			
	NaCl	X	1	487.6	60.9	1.3	474.4	527.8	65.9
	NaCl	X	2	480.8	60.0	1.3			
	NaCl	X	3	454.9	56.8	1.2			

Table B.3-10 – Normalized compressive strength testing results for Set 1, continuous soaking, weeks 16-37

Week	Solution	Cast Set	Sample #	Force (kN)	Calculated Strength (MPa)	Normalized Force Ratio	Avg Force (kN)	Avg Normalized Force (kN)	Avg Normalized Strength (MPa)
16	$MgCl_2$	O	1	588.1	73.4	1.3	590.1	535.9	66.9
	$MgCl_2$	O	2	589.0	73.5	1.3			
	$MgCl_2$	O	3	593.1	74.0	1.3			
	$CaCl_2$	O	1	565.5	70.6	1.2	575.0	522.1	65.2
	$CaCl_2$	O	2	586.7	73.2	1.3			
	$CaCl_2$	O	3	572.6	71.5	1.2			
	H_2O	O	1	572.7	71.5	1.2	573.6	520.9	65.0
	H_2O	O	2	586.7	73.2	1.3			
	H_2O	O	3	561.5	70.1	1.2			
	Multi-Cl^-	O	1	590.6	73.7	1.3	581.7	528.3	65.9
	Multi-Cl^-	O	2	575.2	71.8	1.2			
	Multi-Cl^-	O	3	579.3	72.3	1.2			
	NaCl	O	1	584.3	72.9	1.2	554.5	503.5	62.8
	NaCl	O	2	553.3	69.1	1.2			
	NaCl	O	3	525.7	65.6	1.1			
37	$MgCl_2$	O	1	552.4	68.9	1.2	561.0	501.2	62.6
	$MgCl_2$	O	2	569.6	71.1	1.2			
	$MgCl_2$	X	1	456.8	57.0	1.2			
	$MgCl_2$	X	2	429.4	53.6	1.1			
	$CaCl_2$	O	1	539.6	67.4	1.2	543.2	507.4	63.3
	$CaCl_2$	O	2	546.8	68.2	1.2			
	$CaCl_2$	X	1	499.4	62.3	1.3			
	$CaCl_2$	X	2	438.1	54.7	1.1			
	H_2O	O	1	588.2	73.4	1.3	599.9	555.5	69.3
	H_2O	O	2	611.6	76.3	1.3			
	H_2O	X	1	518.6	64.7	1.4			
	Multi-Cl^-	O	1	561.1	70.0	1.2	565.2	521.7	65.1
	Multi-Cl^-	O	2	569.3	71.1	1.2			
	Multi-Cl^-	X	1	484.9	60.5	1.3			
	Multi-Cl^-	X	2	468.0	58.4	1.2			
	NaCl	O	1	586.6	73.2	1.3	590.3	541.2	67.6
	NaCl	O	2	581.7	72.6	1.2			
	NaCl	O	3	602.6	75.2	1.3			
	NaCl	X	1	500.4	62.5	1.3			

Appendix B.3.3 Set 2 Compressive Testing Results

The data in Table B.3-11 through Table B.3-15 represent the raw data collected during the compressive strength testing for Set 2 where the cylinders were exposed to wet and dry cycles.

Table B.3-11 - Compressive strength testing results for Set 2, wet and dry cycling, weeks 0-4

Week	Solution	Cast Set	Sample #	Force (kN)	Average Force (kN)	Diameter (mm)	Measured Strength (MPa)	Calculated Strength (MPa)	Average Strength (MPa)
0	-	X	1	521.5	517.2	101.0	66.4	65.1	64.5
	-	X	2	515.6		101.0	65.6	64.3	
	-	X	3	514.4		101.0	65.5	64.2	
	-	O	1	484.3	481.8	101.0	61.7	60.5	60.1
	-	O	2	490.0		101.0	62.4	61.2	
	-	O	3	471.2		101.0	60.0	58.8	
2	$MgCl_2$	X	1	529.5	527.7	101.0	67.4	66.1	65.9
	$MgCl_2$	X	2	526.9		101.0	67.1	65.8	
	$MgCl_2$	X	3	526.5		101.0	67.0	65.7	
	$CaCl_2$	X	1	519.6	523.2	101.0	66.2	64.9	65.3
	$CaCl_2$	X	2	527.4		101.0	67.2	65.8	
	$CaCl_2$	X	3	522.5		101.0	66.5	65.2	
	H_2O	X	1	505.6	500.9	101.0	64.4	63.1	62.5
	H_2O	X	2	504.2		101.0	64.2	62.9	
	H_2O	X	3	493.0		101.0	62.8	61.5	
	Multi-Cl^-	X	1	513.0	509.9	101.0	65.3	64.0	63.6
	Multi-Cl^-	X	2	491.7		101.0	62.6	61.4	
	Multi-Cl^-	X	3	525.1		101.0	66.9	65.5	
	NaCl	X	1	509.1	494.4	101.0	64.8	63.5	61.7
	NaCl	X	2	488.8		101.0	62.2	61.0	
	NaCl	X	3	485.1		101.0	61.8	60.6	
4	$MgCl_2$	O	1	499.9	488.0	101.0	63.6	62.4	60.9
	$MgCl_2$	O	2	484.7		101.0	61.7	60.5	
	$MgCl_2$	O	3	479.3		101.0	61.0	59.8	
	$CaCl_2$	O	1	497.3	487.4	101.0	63.3	62.1	60.8
	$CaCl_2$	O	2	496.9		101.0	63.3	62.0	
	$CaCl_2$	O	3	467.9		101.0	59.6	58.4	
	H_2O	O	1	474.0	481.1	101.0	60.3	59.2	60.0
	H_2O	O	2	477.8		101.0	60.8	59.6	
	H_2O	O	3	491.5		101.0	62.6	61.3	
	Multi-Cl^-	O	1	503.3	502.6	101.0	64.1	62.8	62.7
	Multi-Cl^-	O	2	483.3		101.0	61.5	60.3	
	Multi-Cl^-	O	3	521.3		101.0	66.4	65.1	
	NaCl	O	1	465.2	470.9	101.0	59.2	58.1	58.8
	NaCl	O	2	479.2		101.0	61.0	59.8	
	NaCl	O	3	468.4		101.0	59.6	58.5	

Table B.3-12 - Compressive strength testing results for Set 2, wet and dry cycling, weeks 6-8

Week	Solution	Cast Set	Sample #	Force (kN)	Average Force (kN)	Diameter (mm)	Measured Strength (MPa)	Calculated Strength (MPa)	Average Strength (MPa)
6	$MgCl_2$	X	1	545.2	544.0	101.0	69.4	68.0	67.9
	$MgCl_2$	X	2	545.3		101.0	69.4	68.1	
	$MgCl_2$	X	3	541.5		101.0	68.9	67.6	
	$CaCl_2$	X	1	543.8	544.1	101.0	69.2	67.9	67.9
	$CaCl_2$	X	2	538.4		101.0	68.6	67.2	
	$CaCl_2$	X	3	550.0		101.0	70.0	68.7	
	H_2O	X	1	487.7	499.1	101.0	62.1	60.9	62.3
	H_2O	X	2	514.7		101.0	65.5	64.2	
	H_2O	X	3	494.9		101.0	63.0	61.8	
	Multi-Cl^-	X	1	540.5	537.3	101.0	68.8	67.5	67.1
	Multi-Cl^-	X	2	535.2		101.0	68.1	66.8	
	Multi-Cl^-	X	3	536.1		101.0	68.4	66.9	
	NaCl	X	1	531.0	524.4	101.0	67.6	66.3	65.5
	NaCl	X	2	522.6		101.0	66.5	65.2	
	NaCl	X	3	519.6		101.0	66.2	64.9	
8	$MgCl_2$	O	1	473.1	487.7	101.0	60.2	59.0	60.9
	$MgCl_2$	O	2	497.5		101.0	63.3	62.1	
	$MgCl_2$	O	3	492.5		101.0	62.7	61.5	
	$CaCl_2$	O	1	491.5	503.7	101.0	62.6	61.3	62.9
	$CaCl_2$	O	2	516.4		101.0	65.7	64.4	
	$CaCl_2$	O	3	503.3		101.0	64.1	62.8	
	H_2O	O	1	476.6	483.3	101.0	60.7	59.5	60.3
	H_2O	O	2	490.5		101.0	62.4	61.2	
	H_2O	O	3	483.0		101.0	61.5	60.3	
	Multi-Cl^-	O	1	501.1	509.2	101.0	63.8	62.5	63.6
	Multi-Cl^-	O	2	504.9		101.0	64.3	63.0	
	Multi-Cl^-	O	3	521.7		101.0	66.4	65.1	
	NaCl	O	1	491.8	479.4	101.0	62.6	61.4	59.8
	NaCl	O	2	469.4		101.0	59.8	58.6	
	NaCl	O	3	476.9		101.0	60.7	59.5	

Table B.3-13 - Compressive strength testing results for Set 2, wet and dry cycling, weeks 10-12

Week	Solution	Cast Set	Sample #	Force (kN)	Average Force (kN)	Diameter (mm)	Measured Strength (MPa)	Calculated Strength (MPa)	Average Strength (MPa)
10	$MgCl_2$	X	1	518.6	527.5	101.0	66.0	64.7	65.8
	$MgCl_2$	X	2	516.3		101.0	65.7	64.4	
	$MgCl_2$	X	3	547.8		101.0	69.7	68.4	
	$CaCl_2$	X	1	541.9	530.4	101.0	69.0	67.6	66.2
	$CaCl_2$	X	2	527.9		101.0	67.2	65.9	
	$CaCl_2$	X	3	521.3		101.0	66.4	65.1	
	H_2O	X	1	531.5	521.8	101.0	67.7	66.3	65.1
	H_2O	X	2	512.7		101.0	65.3	64.0	
	H_2O	X	3	521.2		101.0	66.4	65.1	
	Multi-Cl^-	X	1	537.9	547.6	101.0	68.5	67.1	68.3
	Multi-Cl^-	X	2	559.5		101.0	71.2	69.8	
	Multi-Cl^-	X	3	545.4		101.0	69.4	68.1	
	NaCl	X	1	524.2	524.4	101.0	66.7	65.4	65.5
	NaCl	X	2	529.2		101.0	67.4	66.1	
	NaCl	X	3	519.9		101.0	66.2	64.9	
12	$MgCl_2$	O	1	501.0	502.3	101.0	63.7	62.5	62.7
	$MgCl_2$	O	2	512.2		101.0	65.2	63.9	
	$MgCl_2$	O	3	493.6		101.0	62.8	61.6	
	$CaCl_2$	O	1	500.8	501.0	101.0	63.8	62.5	62.5
	$CaCl_2$	O	2	496.9		101.0	63.3	62.0	
	$CaCl_2$	O	3	505.4		101.0	64.3	63.1	
	H_2O	O	1	475.7	465.8	101.0	60.6	59.4	58.1
	H_2O	O	2	470.4		101.0	59.9	58.7	
	H_2O	O	3	451.4		101.0	57.5	56.3	
	Multi-Cl^-	O	1	489.3	499.2	101.0	62.3	61.1	62.3
	Multi-Cl^-	O	2	498.7		101.0	63.5	62.2	
	Multi-Cl^-	O	3	509.5		101.0	64.9	63.6	
	NaCl	O	1	483.7	493.9	101.0	61.6	60.4	61.6
	NaCl	O	2	502.3		101.0	63.9	62.7	
	NaCl	O	3	495.8		101.0	63.1	61.9	

Table B.3-14 - Compressive strength testing results for Set 2, wet and dry cycling, weeks 14-16

Week	Solution	Cast Set	Sample #	Force (kN)	Average Force (kN)	Diameter (mm)	Measured Strength (MPa)	Calculated Strength (MPa)	Average Strength (MPa)
14	$MgCl_2$	X	1	533.1	525.6	101.0	67.9	66.5	65.6
	$MgCl_2$	X	2	526.0		101.0	67.0	65.7	
	$MgCl_2$	X	3	517.6		101.0	65.9	64.6	
	$CaCl_2$	X	1	547.2	545.7	101.0	69.7	68.3	68.1
	$CaCl_2$	X	2	543.4		101.0	69.2	67.8	
	$CaCl_2$	X	3	546.4		101.0	69.6	68.2	
	H_2O	X	1	547.3	544.6	101.0	69.7	68.3	68.0
	H_2O	X	2	537.5		101.0	68.4	67.1	
	H_2O	X	3	548.9		101.0	69.9	68.5	
	Multi-Cl^-	X	1	546.0	541.0	101.0	69.5	68.2	67.5
	Multi-Cl^-	X	2	531.3		101.0	67.6	66.3	
	Multi-Cl^-	X	3	545.8		101.0	69.5	68.1	
	NaCl	X	1	541.3	543.5	101.0	68.9	67.6	67.8
	NaCl	X	2	547.7		101.0	69.7	68.4	
	NaCl	X	3	541.6		101.0	69.0	67.6	
16	$MgCl_2$	O	1	492.7	493.9	101.0	62.7	61.5	61.6
	$MgCl_2$	O	2	504.4		101.0	64.2	63.0	
	$MgCl_2$	O	3	484.5		101.0	61.7	60.5	
	$CaCl_2$	O	1	506.0	506.6	101.0	64.4	63.2	63.2
	$CaCl_2$	O	2	498.1		101.0	63.4	62.2	
	$CaCl_2$	O	3	515.9		101.0	65.7	64.4	
	H_2O	O	1	511.3	506.4	101.0	65.1	63.8	63.2
	H_2O	O	2	488.7		101.0	62.2	61.0	
	H_2O	O	3	519.0		101.0	66.1	64.8	
	Multi-Cl^-	O	1	498.5	507.7	101.0	63.5	62.2	63.4
	Multi-Cl^-	O	2	501.2		101.0	63.8	62.6	
	Multi-Cl^-	O	3	523.5		101.0	66.7	65.3	
	NaCl	O	1	523.4	527.4	101.0	66.6	65.3	65.8
	NaCl	O	2	540.8		101.0	68.9	67.5	
	NaCl	O	3	518.0		101.0	66.0	64.7	

Table B.3-15 - Compressive strength testing results for Set 2, wet and dry cycling, weeks 18-20

Week	Solution	Cast Set	Sample #	Force (kN)	Average Force (kN)	Diameter (mm)	Measured Strength (MPa)	Calculated Strength (MPa)	Average Strength (MPa)
18	$MgCl_2$	X	1	492.7	493.9	101.0	62.7	61.5	61.6
	$MgCl_2$	X	2	504.4		101.0	64.2	63.0	
	$MgCl_2$	X	3	484.5		101.0	61.7	60.5	
	$CaCl_2$	X	1	506.0	506.6	101.0	64.4	63.2	63.2
	$CaCl_2$	X	2	498.1		101.0	63.4	62.2	
	$CaCl_2$	X	3	515.9		101.0	65.7	64.4	
	H_2O	X	1	511.3	506.4	101.0	65.1	63.8	63.2
	H_2O	X	2	488.7		101.0	62.2	61.0	
	H_2O	X	3	519.0		101.0	66.1	64.8	
	$Multi\text{-}Cl^-$	X	1	498.5	507.7	101.0	63.5	62.2	63.4
	$Multi\text{-}Cl^-$	X	2	501.2		101.0	63.8	62.6	
	$Multi\text{-}Cl^-$	X	3	523.5		101.0	66.7	65.3	
	NaCl	X	1	523.4	527.4	101.0	66.6	65.3	65.8
	NaCl	X	2	540.8		101.0	68.9	67.5	
	NaCl	X	3	518.0		101.0	66.0	64.7	
20	$MgCl_2$	O	1	535.6	538.0	101.0	68.2	66.8	67.2
	$MgCl_2$	O	2	535.8		101.0	68.2	66.9	
	$MgCl_2$	O	3	542.7		101.0	69.1	67.7	
	$CaCl_2$	O	1	551.0	539.9	101.0	70.2	68.8	67.4
	$CaCl_2$	O	2	533.5		101.0	67.9	66.6	
	$CaCl_2$	O	3	535.3		101.0	68.2	66.8	
	H_2O	O	1						
	H_2O	O	2						
	H_2O	O	3						
	$Multi\text{-}Cl^-$	O	1	533.2	547.4	101.0	67.9	66.5	68.3
	$Multi\text{-}Cl^-$	O	2	549.7		101.0	70.0	68.6	
	$Multi\text{-}Cl^-$	O	3	559.4		101.0	71.1	69.8	
	NaCl	O	1	573.0	575.6	101.0	73.0	71.5	71.8
	NaCl	O	2	577.5		101.0	73.5	72.1	
	NaCl	O	3	576.3		101.0	73.4	71.9	

Appendix B.3.4 Set 2 Normalized Compressive Testing Results

The data in Table B.3-16 through Table B.3-20 show the normalized data for the compressive strength testing from Set 2 where the cylinders were exposed to wet and dry cycles. The

results are normalized by Equation 4.3-1 so that difference in the two batches can be removed from the analysis.

Table B.3-16 – Normalized compressive strength testing results for Set 2, wet and dry cycling, weeks 0-4

Week	Solution	Cast Set	Sample #	Force (kN)	Calculated Strength (MPa)	Normalized Force Ratio	Avg Force (kN)	Avg Normalized Force (kN)	Avg Normalized Strength (MPa)
0	-	X	1	521.5	65.1	1.0	517.2	499.5	62.3
	-	X	2	515.6	64.3	1.0			
	-	X	3	514.4	64.2	1.0			
	-	O	1	484.3	60.5	1.0	481.8	499.5	62.3
	-	O	2	490.0	61.2	1.0			
	-	O	3	471.2	58.8	1.0			
2	$MgCl_2$	X	1	529.5	66.1	1.0	527.7	509.6	63.6
	$MgCl_2$	X	2	526.9	65.8	1.0			
	$MgCl_2$	X	3	526.5	65.7	1.0			
	$CaCl_2$	X	1	519.6	64.9	1.0	523.2	505.3	63.1
	$CaCl_2$	X	2	527.4	65.8	1.0			
	$CaCl_2$	X	3	522.5	65.2	1.0			
	H_2O	X	1	505.6	63.1	1.0	500.9	483.8	60.4
	H_2O	X	2	504.2	62.9	1.0			
	H_2O	X	3	493.0	61.5	1.0			
	Multi-Cl^-	X	1	513.0	64.0	1.0	509.9	492.5	61.5
	Multi-Cl^-	X	2	491.7	61.4	1.0			
	Multi-Cl^-	X	3	525.1	65.5	1.0			
	NaCl	X	1	509.1	63.5	1.0	494.4	477.5	59.6
	NaCl	X	2	488.8	61.0	0.9			
	NaCl	X	3	485.1	60.6	0.9			
4	$MgCl_2$	O	1	499.9	62.4	1.0	488.0	505.8	63.1
	$MgCl_2$	O	2	484.7	60.5	1.0			
	$MgCl_2$	O	3	479.3	59.8	1.0			
	$CaCl_2$	O	1	497.3	62.1	1.0	487.4	505.2	63.1
	$CaCl_2$	O	2	496.9	62.0	1.0			
	$CaCl_2$	O	3	467.9	58.4	1.0			
	H_2O	O	1	474.0	59.2	1.0	481.1	498.7	62.2
	H_2O	O	2	477.8	59.6	1.0			
	H_2O	O	3	491.5	61.3	1.0			
	Multi-Cl^-	O	1	503.3	62.8	1.0	502.6	521.1	65.0
	Multi-Cl^-	O	2	483.3	60.3	1.0			
	Multi-Cl^-	O	3	521.3	65.1	1.1			
	NaCl	O	1	465.2	58.1	1.0	470.9	488.2	60.9
	NaCl	O	2	479.2	59.8	1.0			
	NaCl	O	3	468.4	58.5	1.0			

Table B.3-17 – Normalized compressive strength testing results for Set 2, wet and dry cycling, weeks 6-8

Week	Solution	Cast Set	Sample #	Force (kN)	Calculated Strength (MPa)	Normalized Force Ratio	Avg Force (kN)	Avg Normalized Force (kN)	Avg Normalized Strength (MPa)
6	$MgCl_2$	X	1	545.2	68.0	1.1	544.0	525.4	65.6
	$MgCl_2$	X	2	545.3	68.1	1.1			
	$MgCl_2$	X	3	541.5	67.6	1.0			
	$CaCl_2$	X	1	543.8	67.9	1.1	544.1	525.5	65.6
	$CaCl_2$	X	2	538.4	67.2	1.0			
	$CaCl_2$	X	3	550.0	68.7	1.1			
	H_2O	X	1	487.7	60.9	0.9	499.1	482.1	60.2
	H_2O	X	2	514.7	64.2	1.0			
	H_2O	X	3	494.9	61.8	1.0			
	Multi-Cl^-	X	1	540.5	67.5	1.0	537.3	518.9	64.8
	Multi-Cl^-	X	2	535.2	66.8	1.0			
	Multi-Cl^-	X	3	536.1	66.9	1.0			
	NaCl	X	1	531.0	66.3	1.0	524.4	506.5	63.2
	NaCl	X	2	522.6	65.2	1.0			
	NaCl	X	3	519.6	64.9	1.0			
8	$MgCl_2$	O	1	473.1	59.0	1.0	487.7	505.6	63.1
	$MgCl_2$	O	2	497.5	62.1	1.0			
	$MgCl_2$	O	3	492.5	61.5	1.0			
	$CaCl_2$	O	1	491.5	61.3	1.0	503.7	522.2	65.2
	$CaCl_2$	O	2	516.4	64.4	1.1			
	$CaCl_2$	O	3	503.3	62.8	1.0			
	H_2O	O	1	476.6	59.5	1.0	483.3	501.1	62.5
	H_2O	O	2	490.5	61.2	1.0			
	H_2O	O	3	483.0	60.3	1.0			
	Multi-Cl^-	O	1	501.1	62.5	1.0	509.2	527.9	65.9
	Multi-Cl^-	O	2	504.9	63.0	1.0			
	Multi-Cl^-	O	3	521.7	65.1	1.1			
	NaCl	O	1	491.8	61.4	1.0	479.4	496.9	62.0
	NaCl	O	2	469.4	58.6	1.0			
	NaCl	O	3	476.9	59.5	1.0			

Table B.3-18 – Normalized compressive strength testing results for Set 2, wet and dry cycling, weeks 10-12

Week	Solution	Cast Set	Sample #	Force (kN)	Calculated Strength (MPa)	Normalized Force Ratio	Avg Force (kN)	Avg Normalized Force (kN)	Avg Normalized Strength (MPa)
10	$MgCl_2$	X	1	518.6	64.7	1.0	527.5	509.5	63.6
	$MgCl_2$	X	2	516.3	64.4	1.0			
	$MgCl_2$	X	3	547.8	68.4	1.1			
	$CaCl_2$	X	1	541.9	67.6	1.0	530.4	512.3	63.9
	$CaCl_2$	X	2	527.9	65.9	1.0			
	$CaCl_2$	X	3	521.3	65.1	1.0			
	H_2O	X	1	531.5	66.3	1.0	521.8	504.0	62.9
	H_2O	X	2	512.7	64.0	1.0			
	H_2O	X	3	521.2	65.1	1.0			
	Multi-Cl^-	X	1	537.9	67.1	1.0	547.6	528.9	66.0
	Multi-Cl^-	X	2	559.5	69.8	1.1			
	Multi-Cl^-	X	3	545.4	68.1	1.1			
	NaCl	X	1	524.2	65.4	1.0	524.4	506.5	63.2
	NaCl	X	2	529.2	66.1	1.0			
	NaCl	X	3	519.9	64.9	1.0			
12	$MgCl_2$	O	1	501.0	62.5	1.0	502.3	520.7	65.0
	$MgCl_2$	O	2	512.2	63.9	1.1			
	$MgCl_2$	O	3	493.6	61.6	1.0			
	$CaCl_2$	O	1	500.8	62.5	1.0	501.0	519.4	64.8
	$CaCl_2$	O	2	496.9	62.0	1.0			
	$CaCl_2$	O	3	505.4	63.1	1.0			
	H_2O	O	1	475.7	59.4	1.0	465.8	482.9	60.3
	H_2O	O	2	470.4	58.7	1.0			
	H_2O	O	3	451.4	56.3	0.9			
	Multi-Cl^-	O	1	489.3	61.1	1.0	499.2	517.4	64.6
	Multi-Cl^-	O	2	498.7	62.2	1.0			
	Multi-Cl^-	O	3	509.5	63.6	1.1			
	NaCl	O	1	483.7	60.4	1.0	493.9	512.0	63.9
	NaCl	O	2	502.3	62.7	1.0			
	NaCl	O	3	495.8	61.9	1.0			

Table B.3-19 – Normalized compressive strength testing results for Set 2, wet and dry cycling, weeks 14-16

Week	Solution	Cast Set	Sample #	Force (kN)	Calculated Strength (MPa)	Normalized Force Ratio	Avg Force (kN)	Avg Normalized Force (kN)	Avg Normalized Strength (MPa)
14	$MgCl_2$	X	1	533.1	66.5	1.0	525.6	507.6	63.4
	$MgCl_2$	X	2	526.0	65.7	1.0			
	$MgCl_2$	X	3	517.6	64.6	1.0			
	$CaCl_2$	X	1	547.2	68.3	1.1	545.7	527.0	65.8
	$CaCl_2$	X	2	543.4	67.8	1.1			
	$CaCl_2$	X	3	546.4	68.2	1.1			
	H_2O	X	1	547.3	68.3	1.1	544.6	526.0	65.7
	H_2O	X	2	537.5	67.1	1.0			
	H_2O	X	3	548.9	68.5	1.1			
	Multi-Cl^-	X	1	546.0	68.2	1.1	541.0	522.6	65.2
	Multi-Cl^-	X	2	531.3	66.3	1.0			
	Multi-Cl^-	X	3	545.8	68.1	1.1			
	NaCl	X	1	541.3	67.6	1.0	543.5	525.0	65.5
	NaCl	X	2	547.7	68.4	1.1			
	NaCl	X	3	541.6	67.6	1.0			
16	$MgCl_2$	O	1	492.7	61.5	1.0	493.9	512.0	63.9
	$MgCl_2$	O	2	504.4	63.0	1.0			
	$MgCl_2$	O	3	484.5	60.5	1.0			
	$CaCl_2$	O	1	506.0	63.2	1.1	506.6	525.2	65.6
	$CaCl_2$	O	2	498.1	62.2	1.0			
	$CaCl_2$	O	3	515.9	64.4	1.1			
	H_2O	O	1	511.3	63.8	1.1	506.4	524.9	65.5
	H_2O	O	2	488.7	61.0	1.0			
	H_2O	O	3	519.0	64.8	1.1			
	Multi-Cl^-	O	1	498.5	62.2	1.0	507.7	526.3	65.7
	Multi-Cl^-	O	2	501.2	62.6	1.0			
	Multi-Cl^-	O	3	523.5	65.3	1.1			
	NaCl	O	1	523.4	65.3	1.1	527.4	546.7	68.2
	NaCl	O	2	540.8	67.5	1.1			
	NaCl	O	3	518.0	64.7	1.1			

Table B.3-20 – Normalized compressive strength testing results for Set 2, wet and dry cycling, weeks 18-20

Week	Solution	Cast Set	Sample #	Force (kN)	Calculated Strength (MPa)	Normalized Force Ratio	Avg Force (kN)	Avg Normalized Force (kN)	Avg Normalized Strength (MPa)
18	$MgCl_2$	O	1	535.6	66.8	1.0	538.0	519.7	64.9
	$MgCl_2$	O	2	535.8	66.9	1.0			
	$MgCl_2$	O	3	542.7	67.7	1.0			
	$CaCl_2$	O	1	551.0	68.8	1.1	539.9	521.5	65.1
	$CaCl_2$	O	2	533.5	66.6	1.0			
	$CaCl_2$	O	3	535.3	66.8	1.0			
	H_2O	O	1						
	H_2O	O	2						
	H_2O	O	3						
	Multi-Cl^-	O	1	533.2	66.5	1.0	547.4	528.7	66.0
	Multi-Cl^-	O	2	549.7	68.6	1.1			
	Multi-Cl^-	O	3	559.4	69.8	1.1			
	NaCl	O	1	573.0	71.5	1.1	575.6	555.9	69.4
	NaCl	O	2	577.5	72.1	1.1			
	NaCl	O	3	576.3	71.9	1.1			
20	$MgCl_2$	X	1	473.1	59.0	0.9	489.6	496.4	62.0
	$MgCl_2$	X	2	498.0	62.2	1.0			
	$MgCl_2$	X	3	497.8	62.1	1.0			
	$CaCl_2$	X	1	506.5	63.2	1.1	507.7	526.3	65.7
	$CaCl_2$	X	2	507.5	63.3	1.1			
	$CaCl_2$	X	3	509.1	63.5	1.1			
	H_2O	X	1	0.0					
	H_2O	X	2	0.0					
	H_2O	X	3	0.0					
	Multi-Cl^-	X	1	494.8	61.8	1.0	491.2	509.2	63.6
	Multi-Cl^-	X	2	492.7	61.5	1.0			
	Multi-Cl^-	X	3	486.0	60.7	1.0			
	NaCl	X	1	511.8	63.9	1.1	516.6	535.5	66.8
	NaCl	X	2	522.9	65.3	1.1			
	NaCl	X	3	515.1	64.3	1.1			

Appendix B.4 Chloride Penetration

Appendix B.4.1 Chloride Penetration Curves by Exposure Solution

The curves in Figure B.4-1 through Figure B.4-4 show the chloride penetration at weeks 2, 19, and 59 by solution.

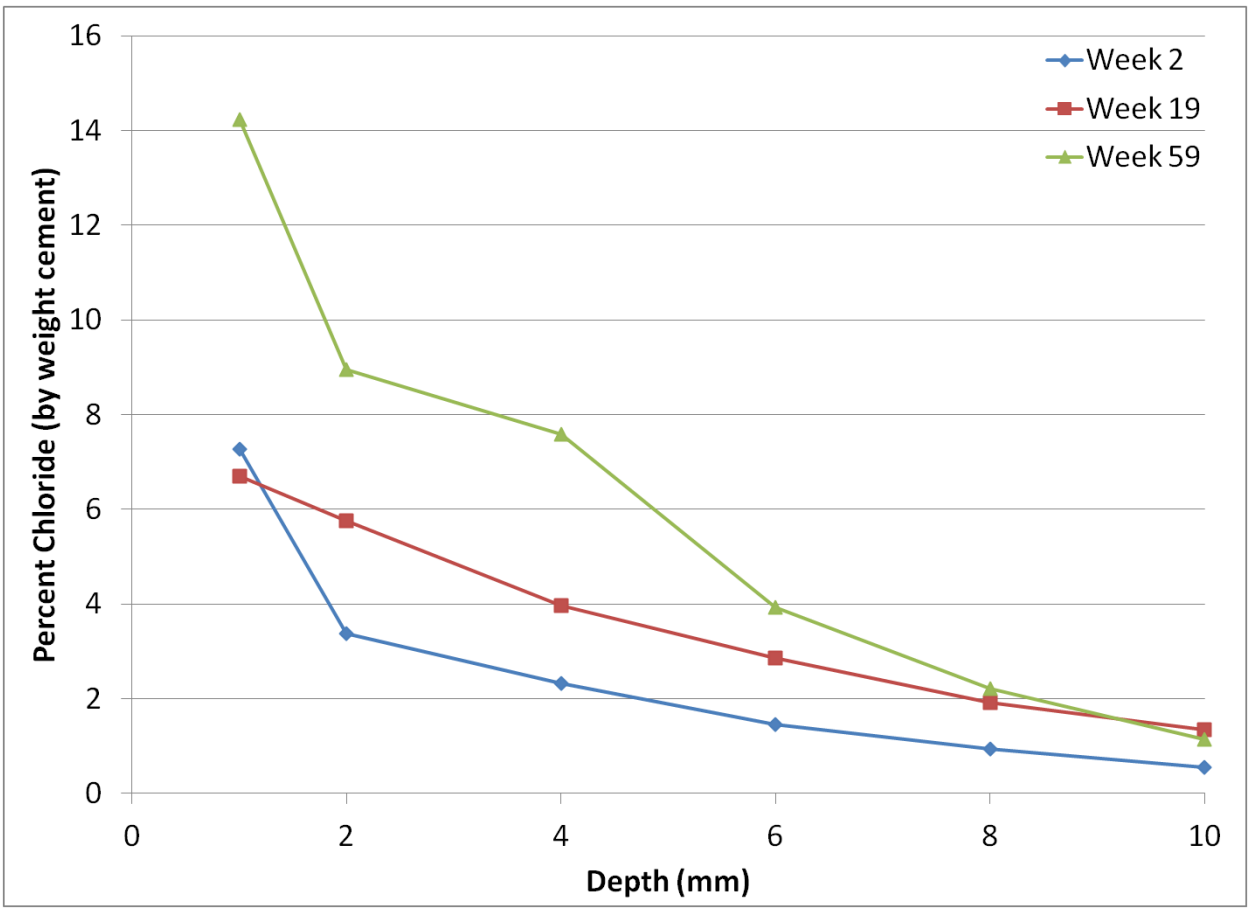

Figure B.4-1 - Chloride penetration curves from $MgCl_2$ samples at 2, 19, and 59 weeks soaking

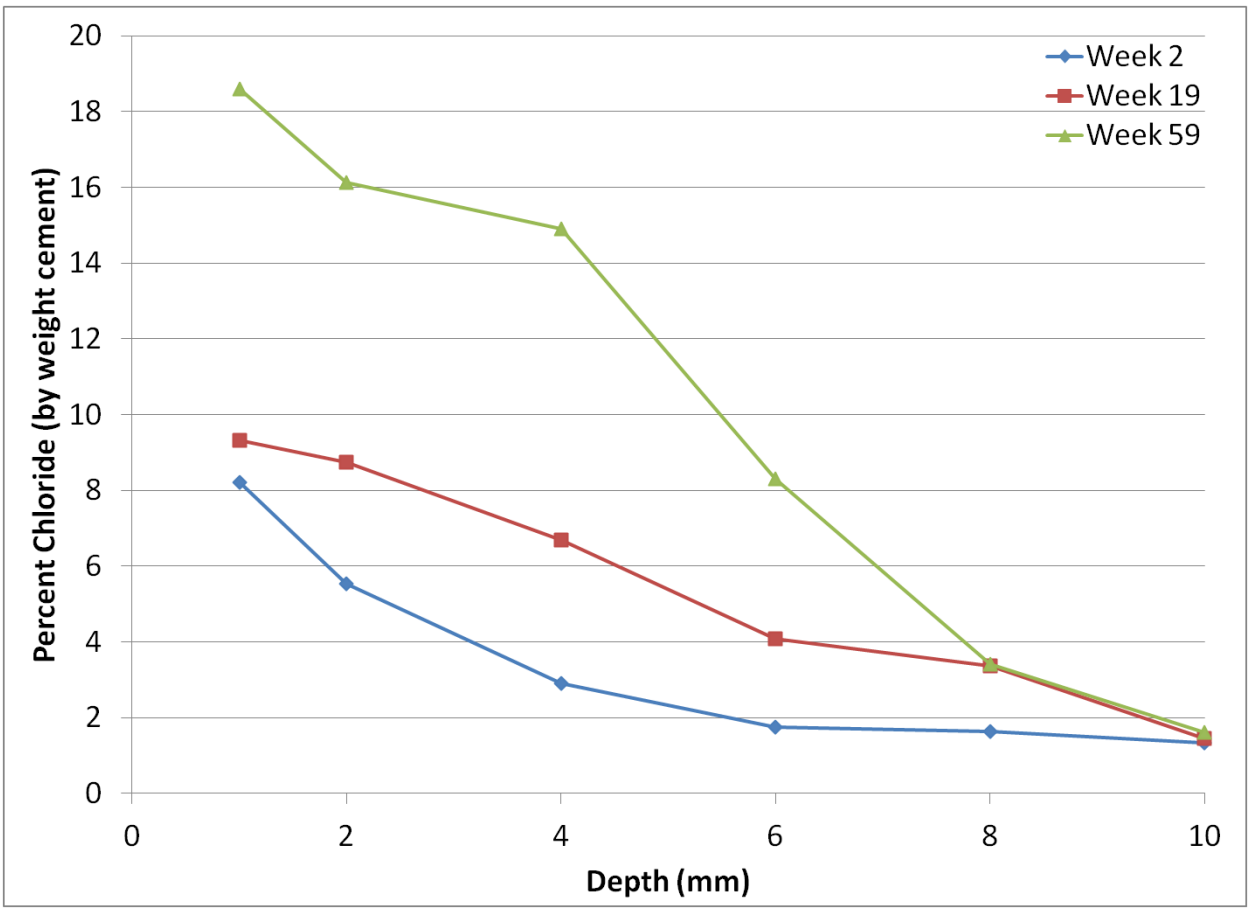

Figure B.4-2 - Chloride penetration curves from $CaCl_2$ samples at 2, 19, and 59 weeks soaking

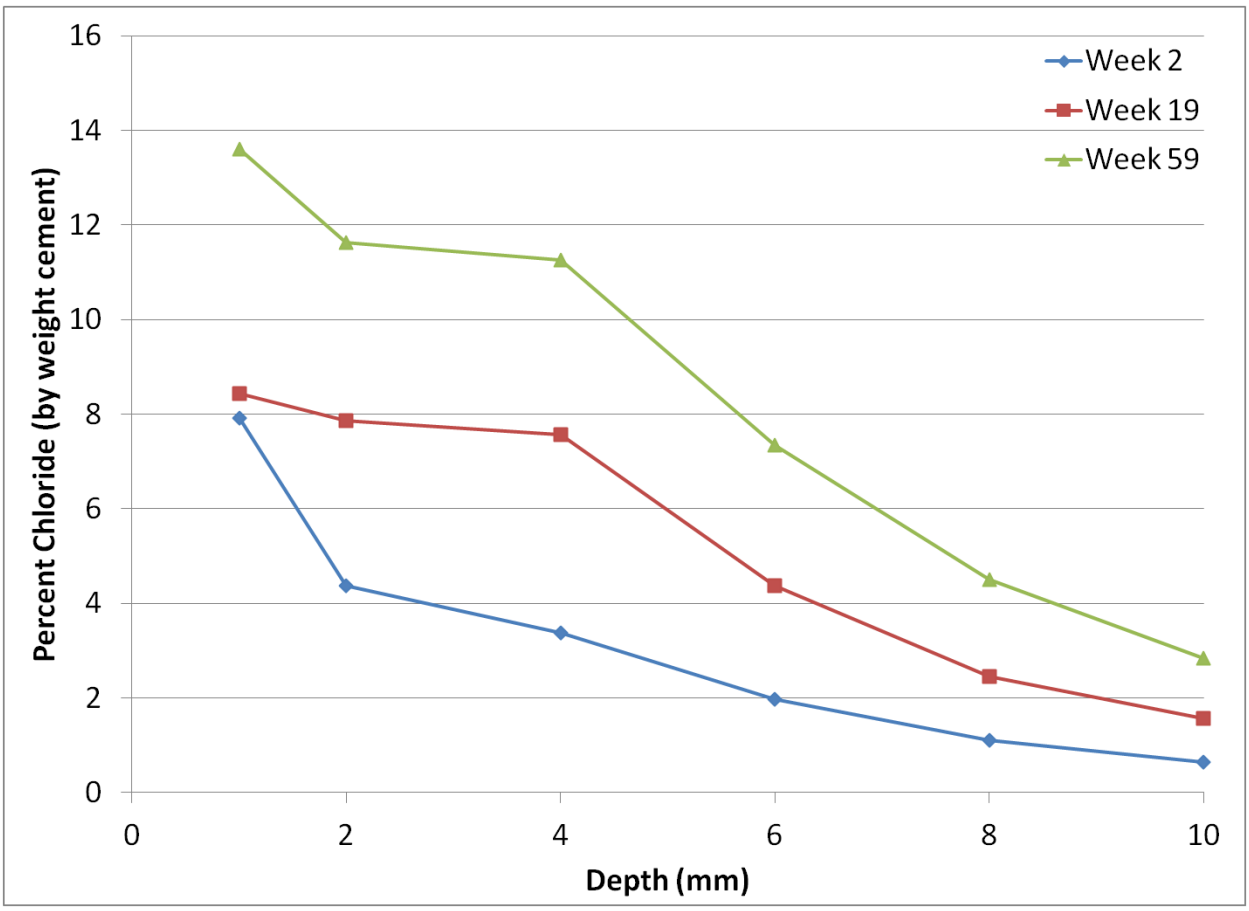

Figure B.4-3 - Chloride penetration curves from multi-Cl^- samples at 2, 19, and 59 weeks soaking

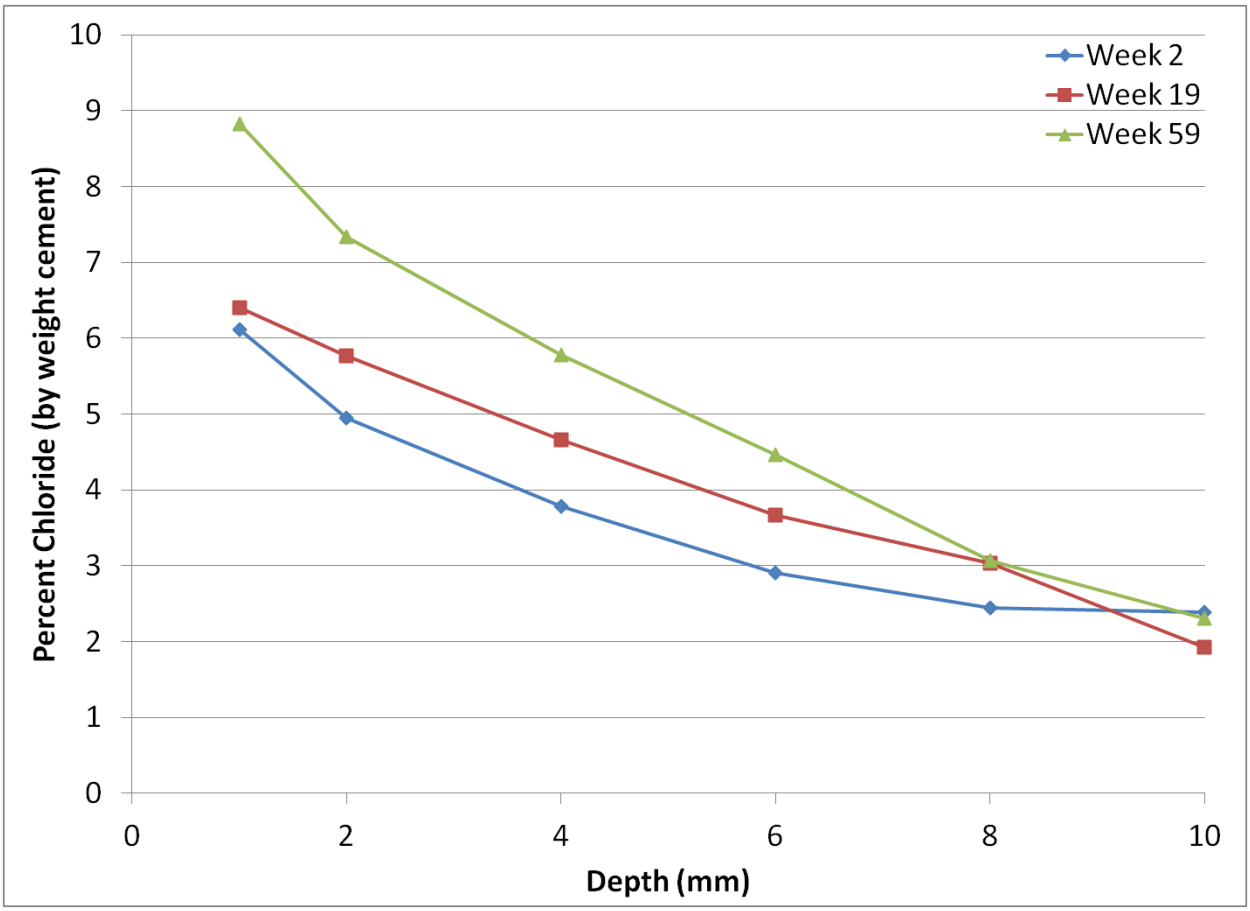

Figure B.4-4 - Chloride penetration curves from NaCl samples at 2, 19, and 59 weeks soaking

Appendix B.4.2 Chloride Penetration Diffusion Coefficients with Respect to Depth

Figure B.4-5 shows the diffusion coefficients calculated using Fick's second law applied to the raw data results. The results in Figure B.4-6 through Figure B.4-9 show the change in diffusion coefficient with respect to time for each depth measured during chloride penetration by the raw data.

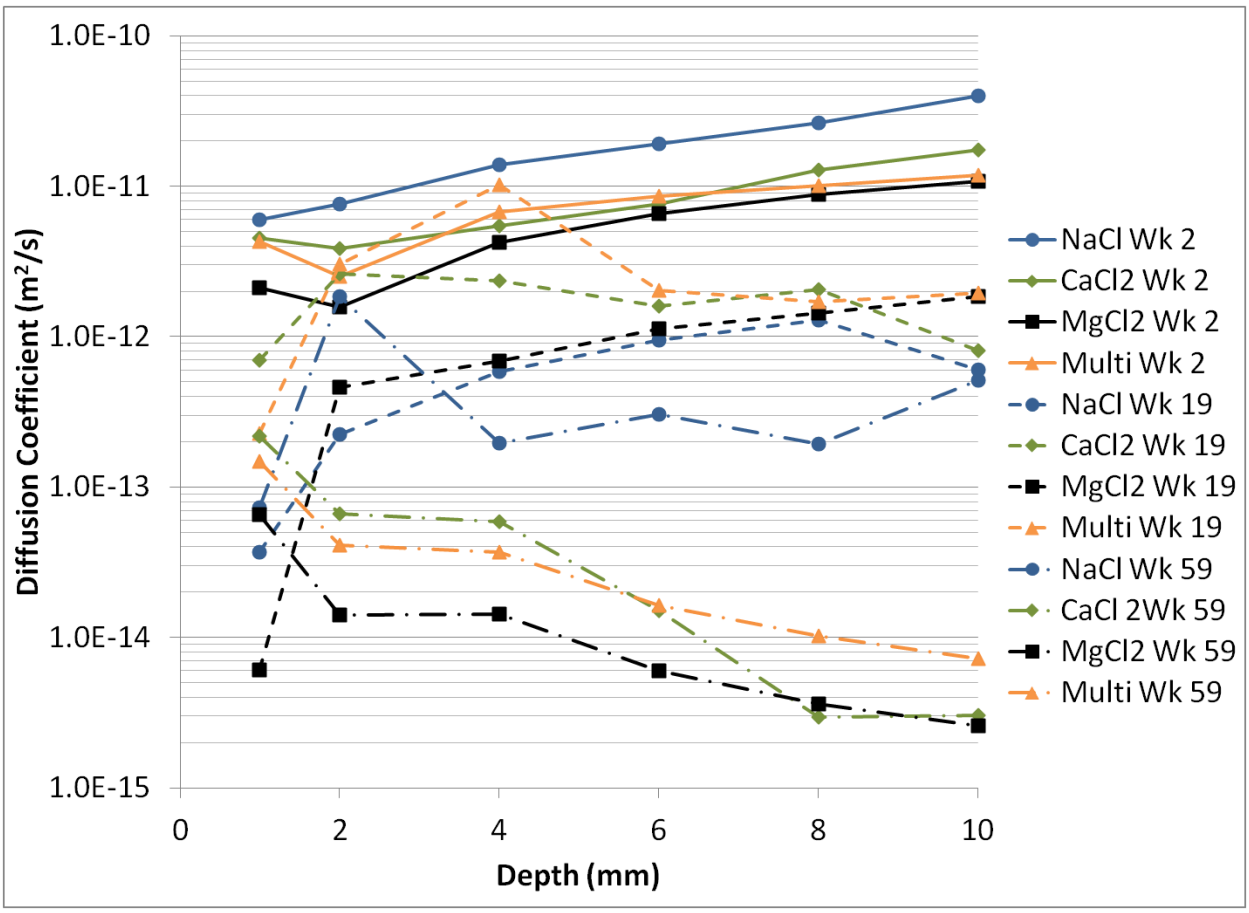

Figure B.4-5 - Diffusion Coefficients (m^2/s) for all four solutions at each depth at 2, 19, and 59 weeks soaking

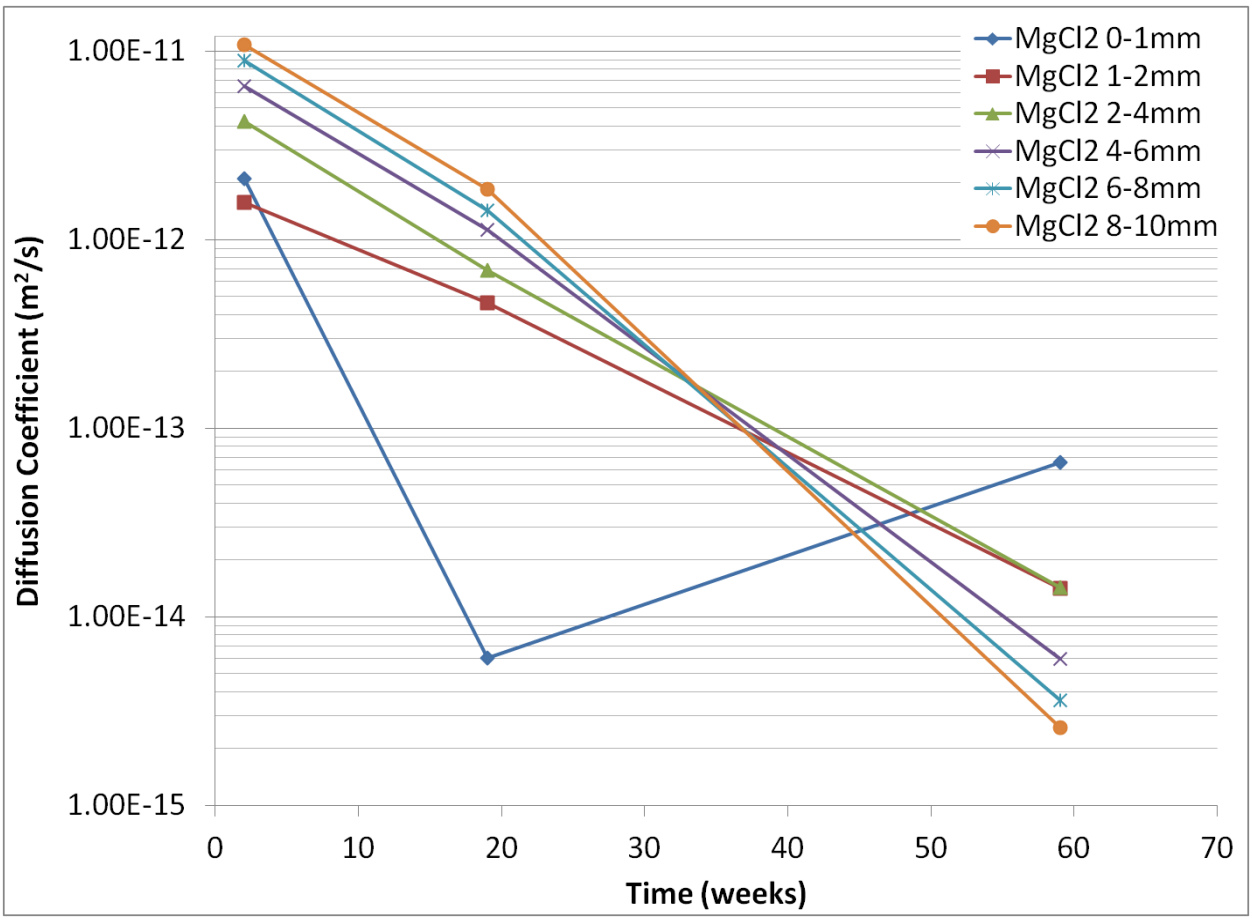

Figure B.4-6 - Diffusion coefficients versus time at each measurement depth from chloride penetration for $MgCl_2$

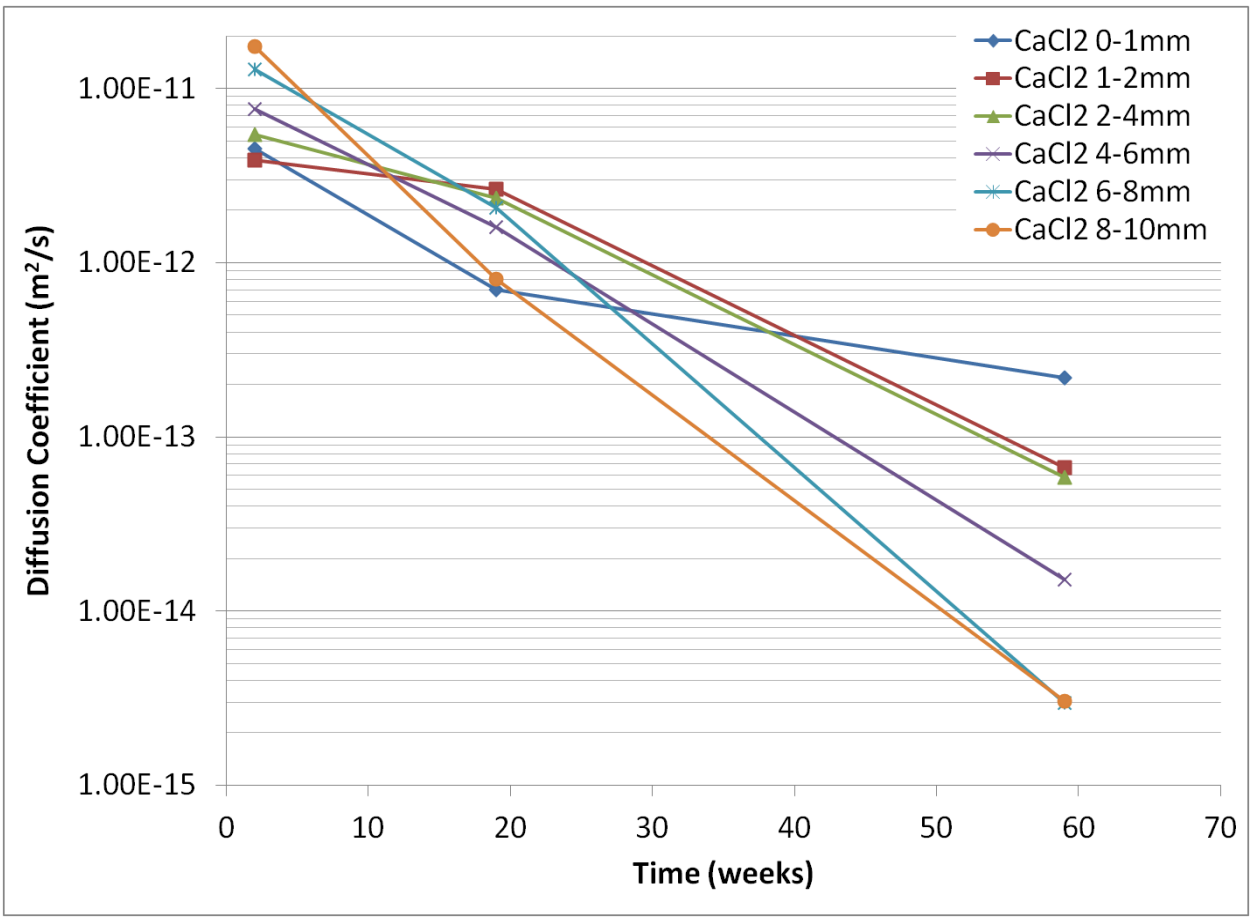

Figure B.4-7 - Diffusion coefficients versus time at each measurement depth from chloride penetration for $CaCl_2$

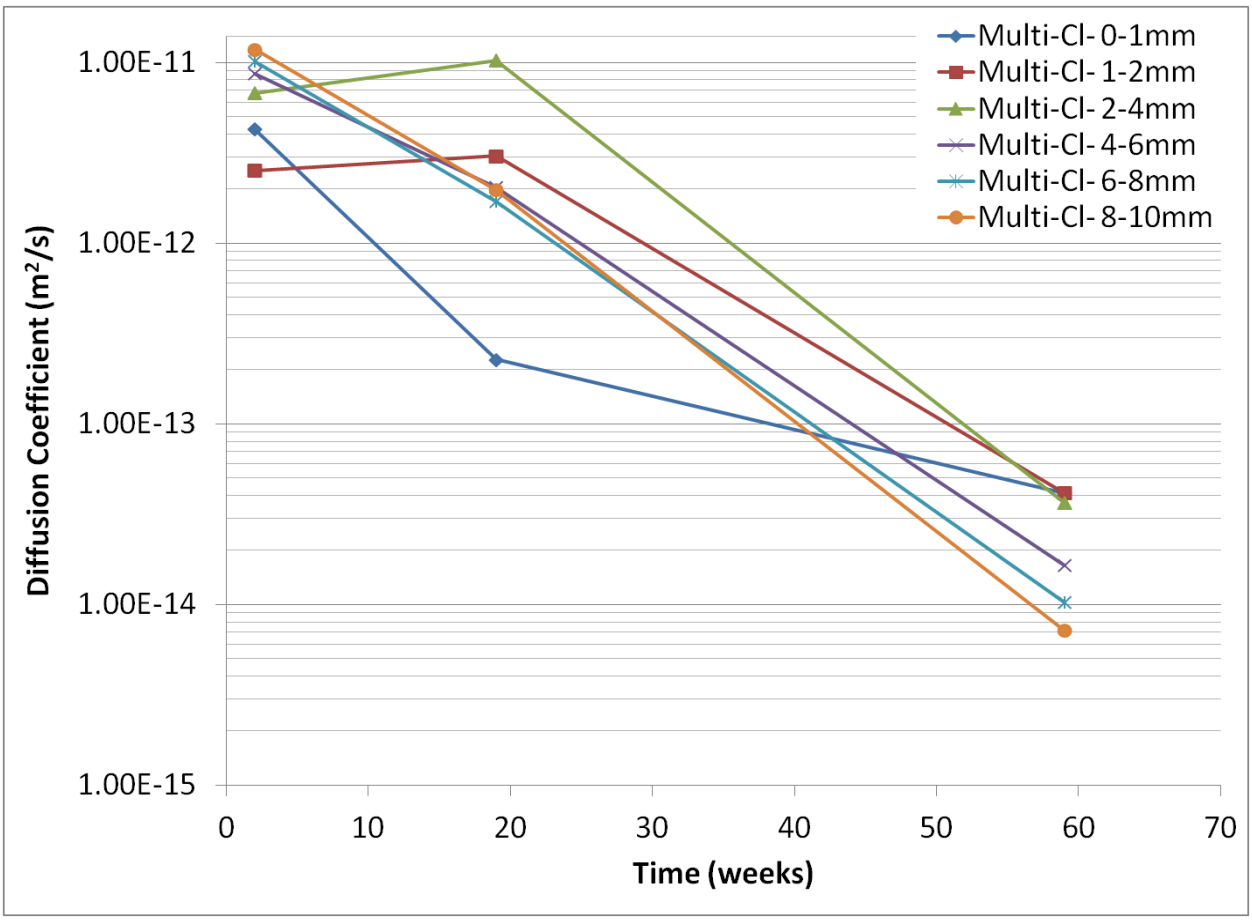

Figure B.4-8 - Diffusion coefficients versus time at each measurement depth from chloride penetration for multi-Cl^-

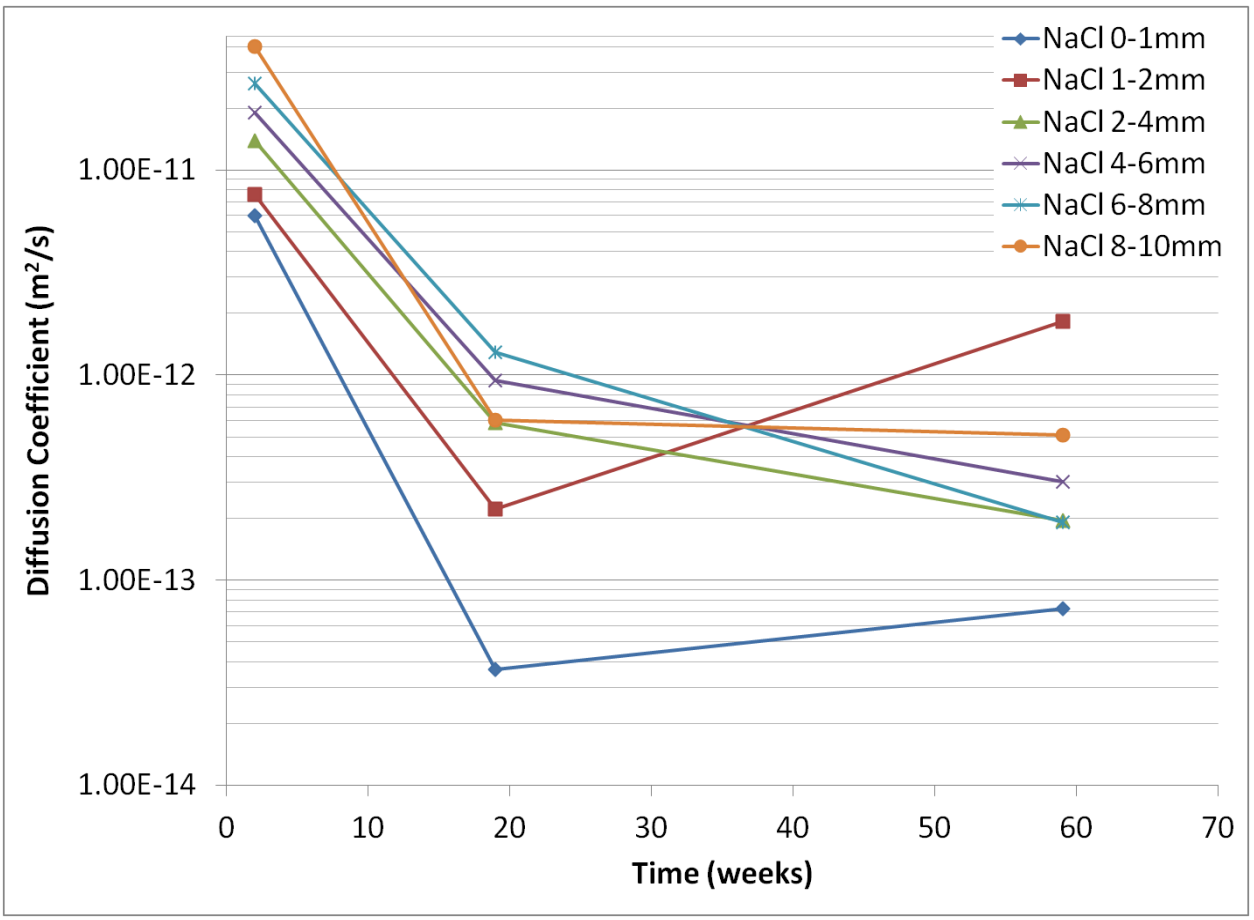

Figure B.4-9 - Diffusion coefficients versus time at each measurement depth from chloride penetration for NaCl

Appendix B.4.3 Diffusion Coefficient Analysis by Visual Approximation

To approximate a single diffusion coefficient from the chloride penetration curves, Fick's second law (equation 1 in [**35**]) is applied. The equation is used to calculate and plot the predicted chloride concentration of the concrete by adjusting the value of surface concentration, C_s, and effective diffusion coefficient, D, are adjust to optimize the solution to best match the penetration curves. Application of an automated solver yielded diverging results and, thus, the optimization was done manually. This is one of the recommended methods of Poulsen for determining diffusion coefficients from penetration data [**42**]. The

graphical results of this analysis are shown in Figure B.4-10 through Figure B.4-13 for the results by chloride selective electrode and in Figure B.4-14 through Figure B.4-17 for the results by EDS.

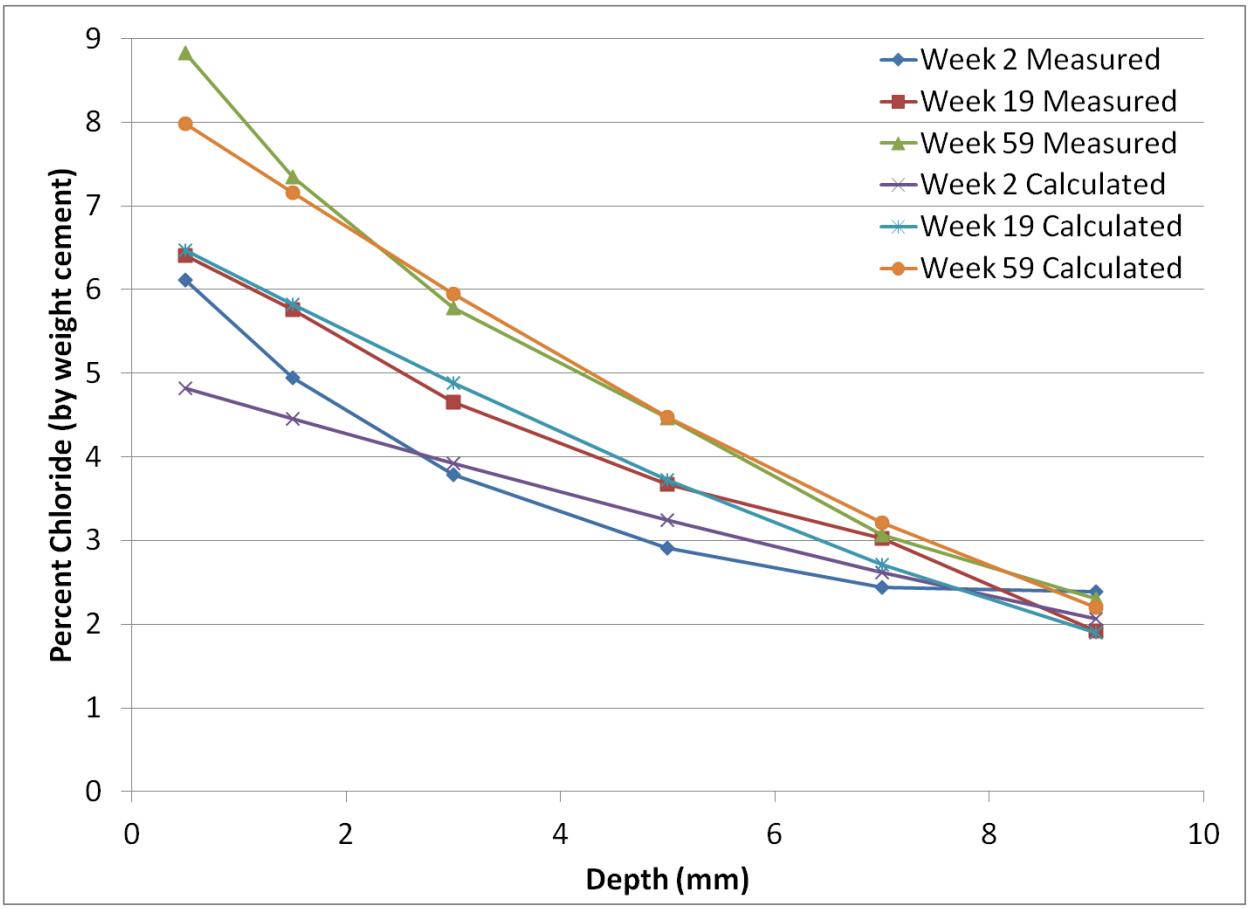

Figure B.4-10 - $MgCl_2$ penetration curves, measured and calculated, for effective diffusion coefficient determination by chloride selective electrode

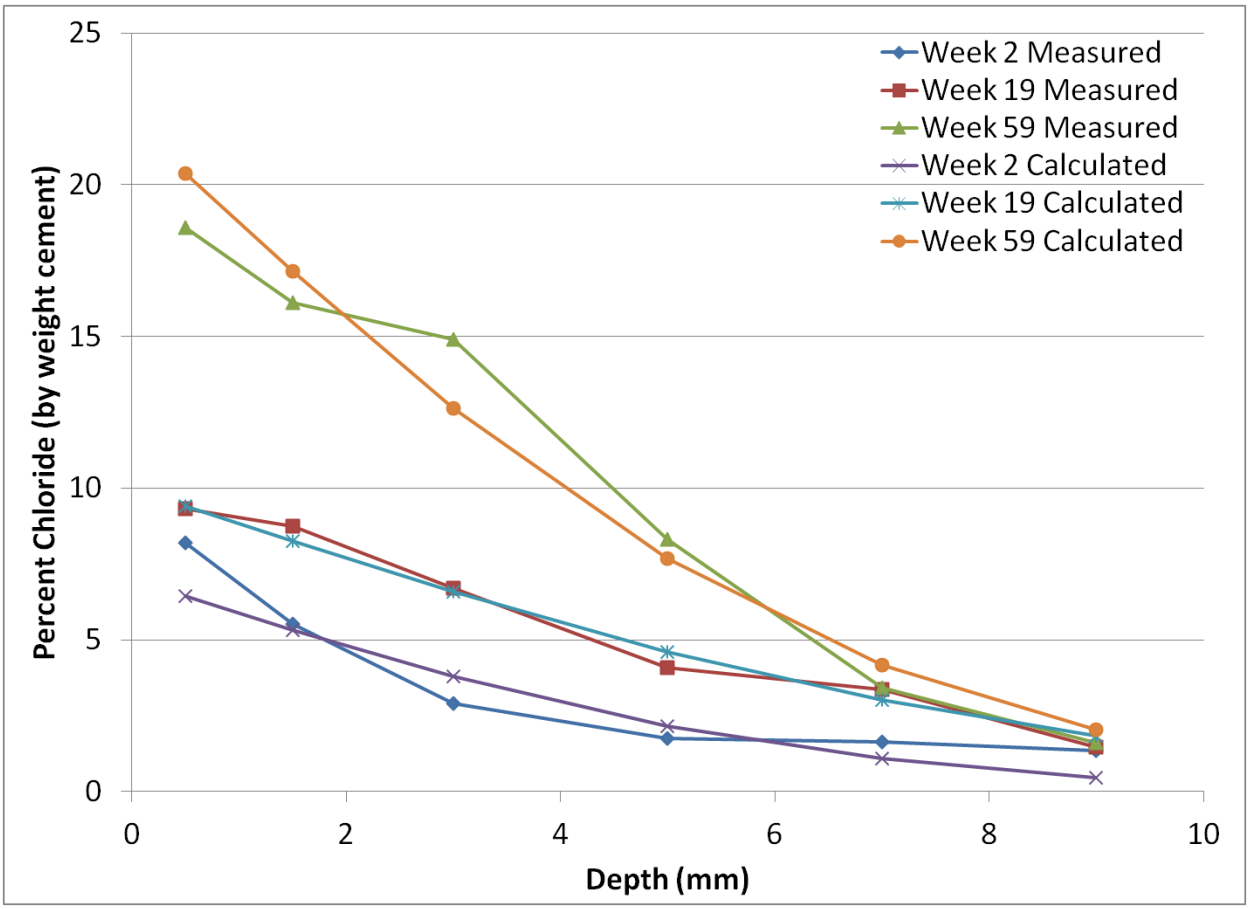

Figure B.4-11 - $CaCl_2$ penetration curves, measured and calculated, for effective diffusion coefficient determination by chloride selective electrode

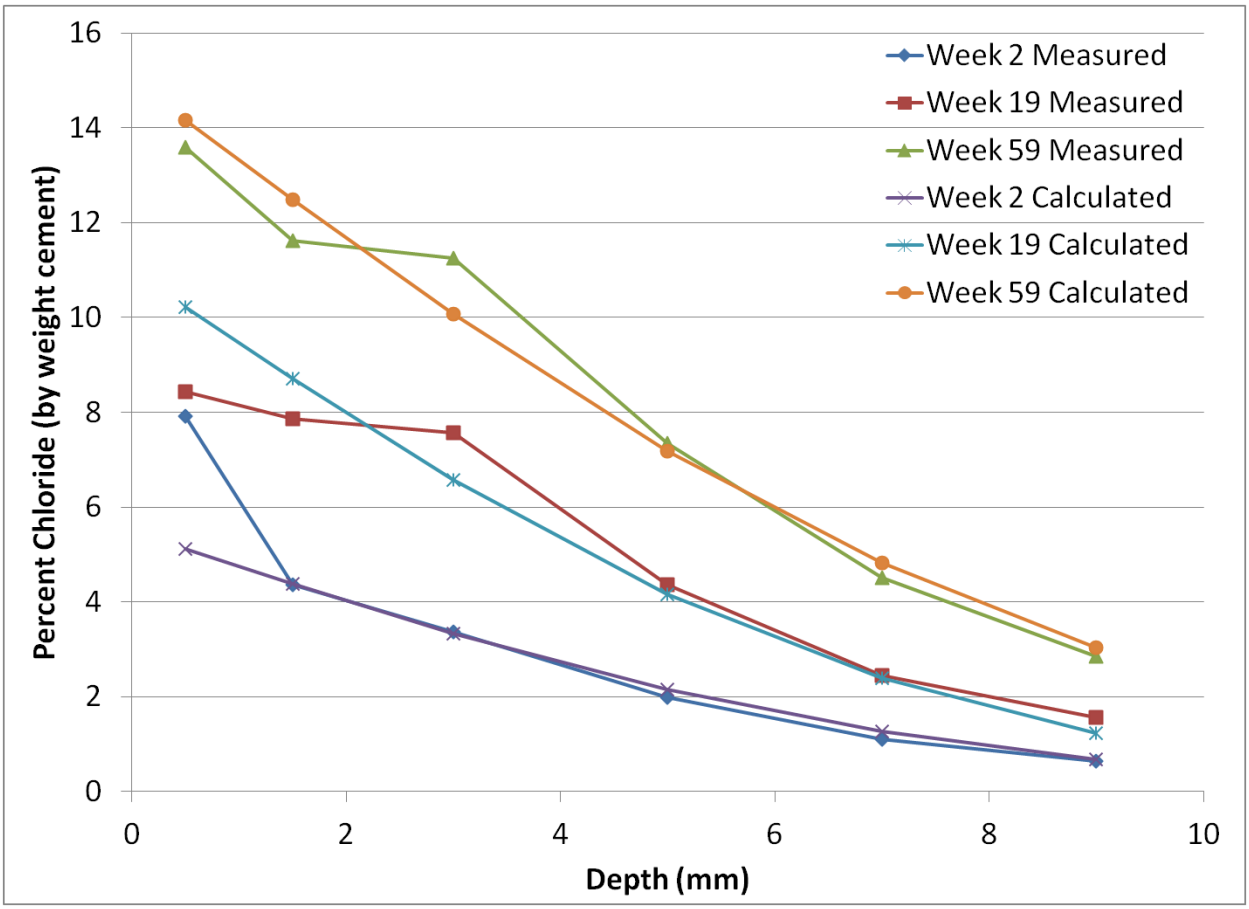

Figure B.4-12 - Multi-Cl^- penetration curves, measured and calculated, for effective diffusion coefficient determination by chloride selective electrode

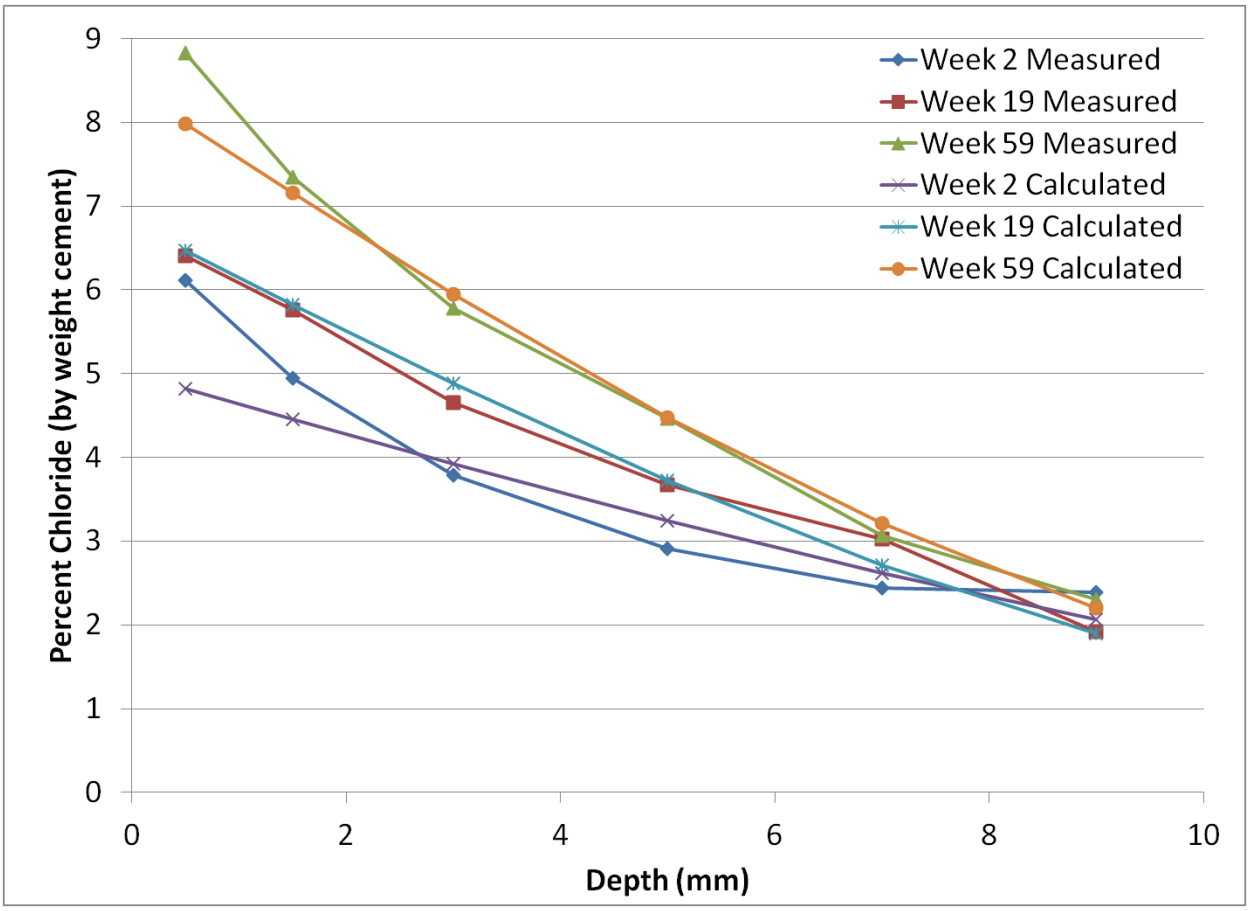

Figure B.4-13 - NaCl penetration curves, measured and calculated, for effective diffusion coefficient determination by chloride selective electrode

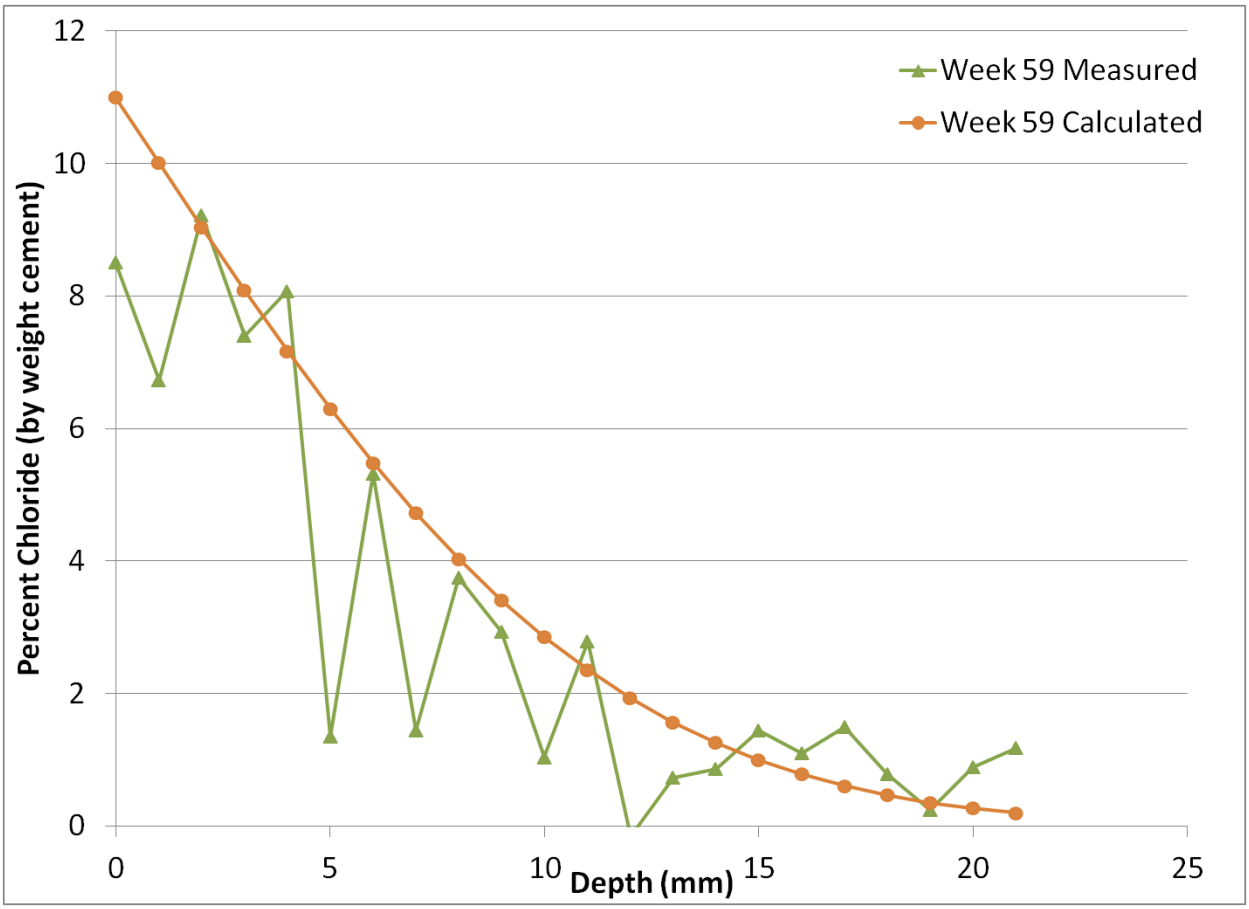

Figure B.4-14 - $MgCl_2$ penetration curves, measured and calculated, for effective diffusion coefficient determination by EDS

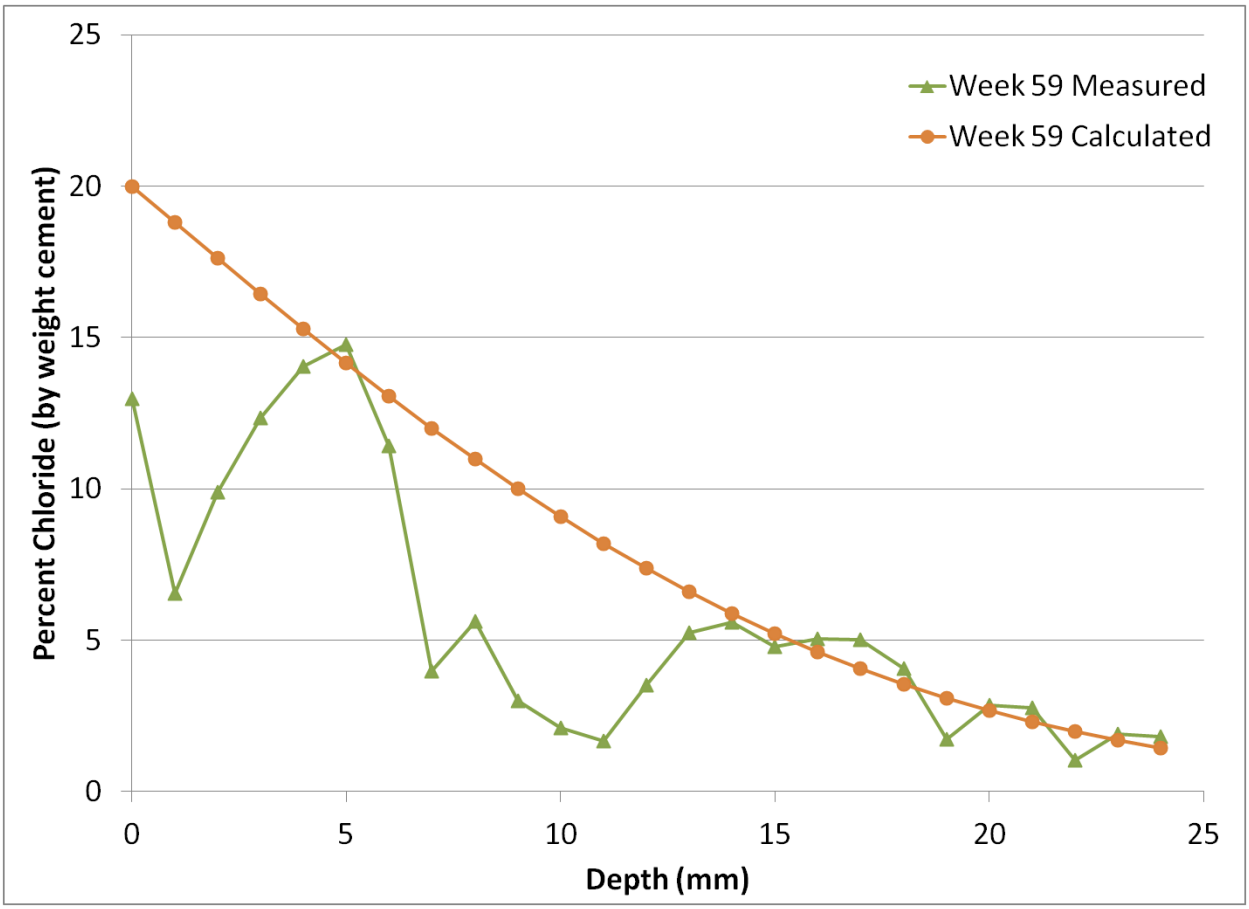

Figure B.4-15 - $CaCl_2$ penetration curves, measured and calculated, for effective diffusion coefficient determination by EDS

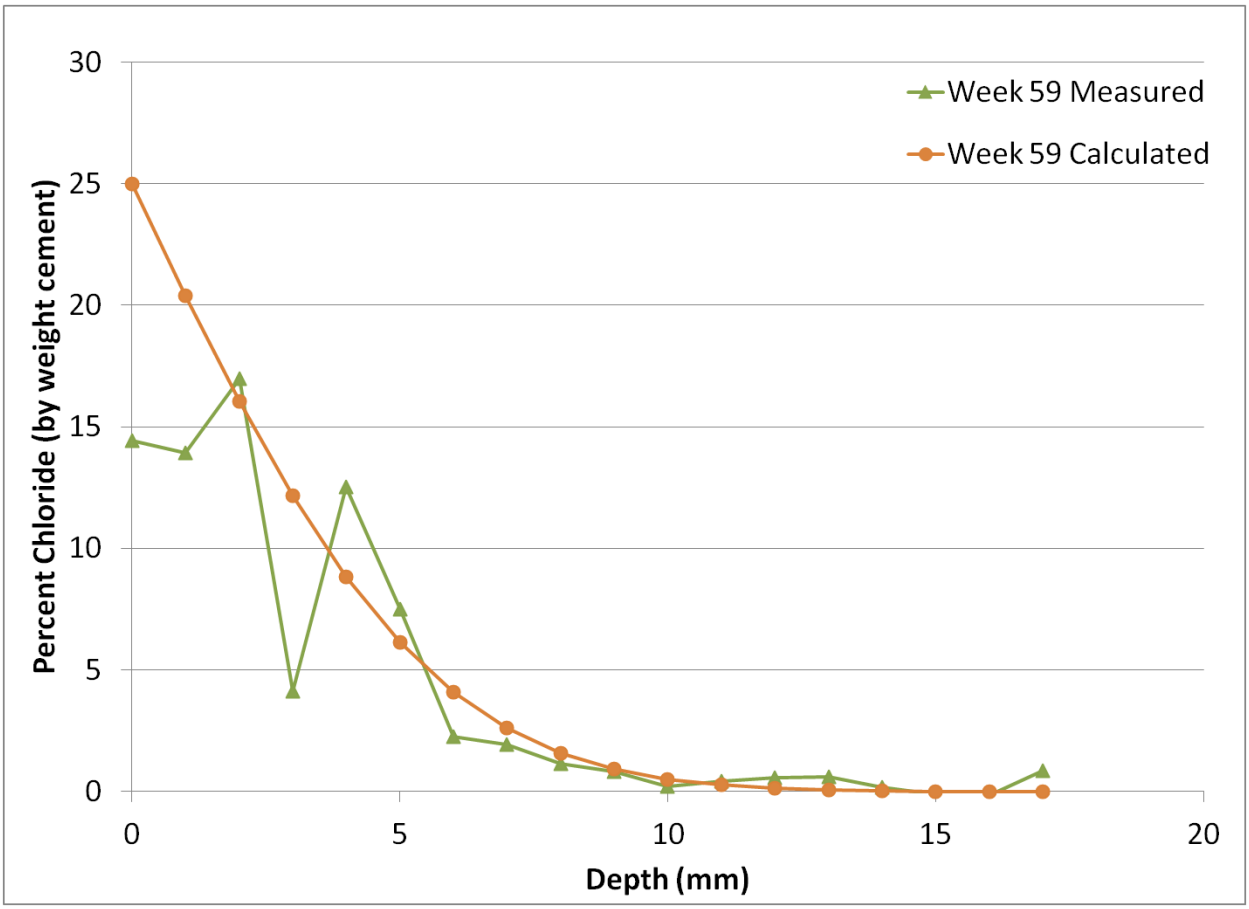

Figure B.4-16 - Multi-Cl^- penetration curves, measured and calculated, for effective diffusion coefficient determination by EDS

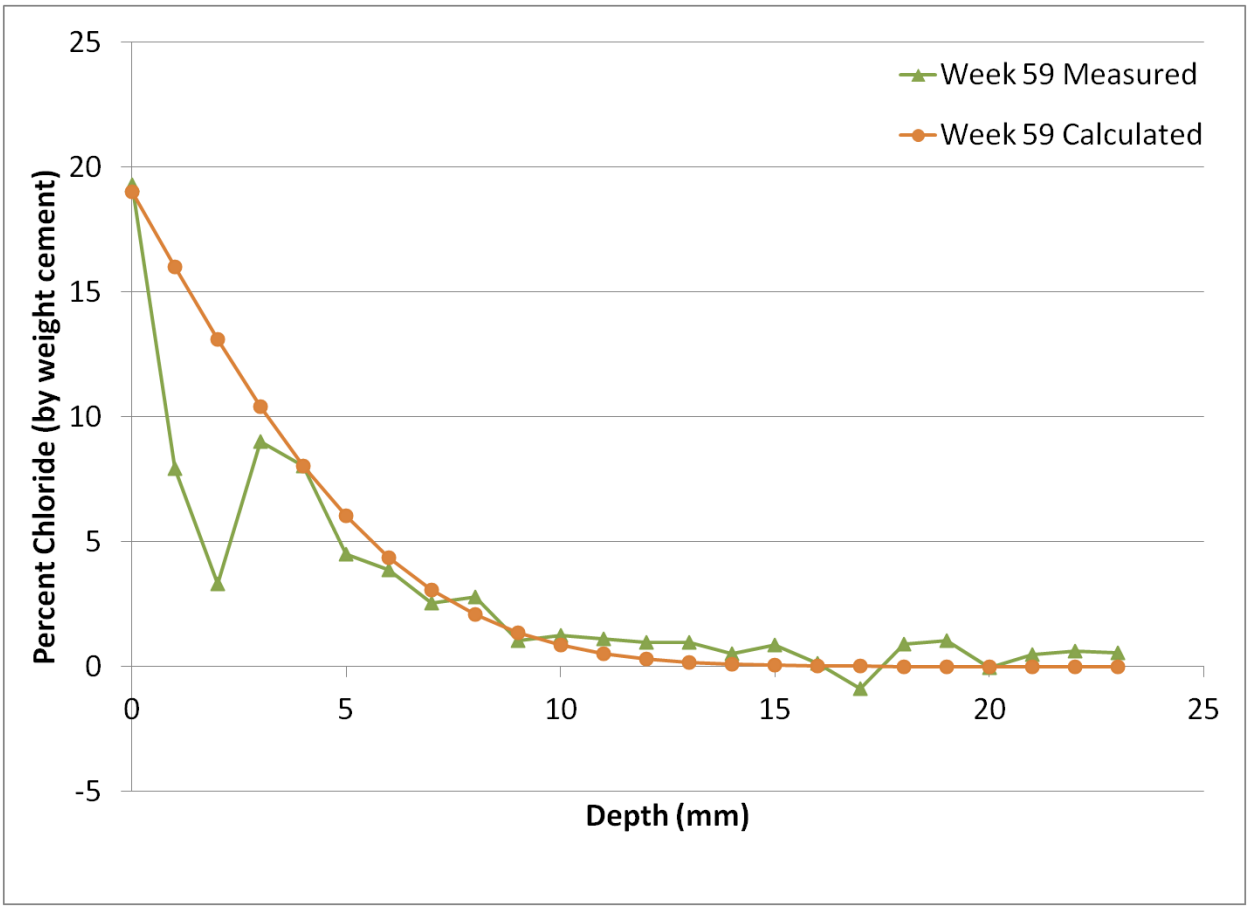

Figure B.4-17 - NaCl penetration curves, measured and calculated, for effective diffusion coefficient determination by EDS

Appendix B.5 Environmental Scanning Electron Microscopy Raw Data

The data in Table B.5-1 through Table B.5-5 show the percent of each element at each depth from the environmental scanning electron microscopy analysis.

Table B.5-1 - Environmental scanning electron microscopy results in percent for the first $MgCl_2$ sample

Depth (mm)	Na	Mg	Al	Si	Cl	K	Ca	Fe
0	1.72	3.40	4.30	45.80	1.07	2.92	38.11	2.68
1	0.73	1.81	4.13	49.40	1.13	2.30	37.34	3.15
2	1.13	2.07	4.30	54.81	1.79	1.77	31.79	2.34
3	2.21	1.34	5.00	47.25	1.37	1.55	37.62	3.66
4	1.21	1.47	3.74	53.08	2.29	1.78	34.39	2.04
5	0.94	6.46	4.66	27.48	5.90	0.87	51.31	2.37
6	2.20	1.64	6.43	47.46	0.87	3.31	34.70	3.40
7	1.67	3.98	5.24	30.24	1.71	2.28	50.70	4.18
8	1.52	4.53	3.94	38.05	1.86	1.54	46.21	2.36
9	-0.21	3.58	2.57	52.71	1.10	1.13	36.87	2.24
10	-1.76	16.18	1.63	32.46	0.34	0.73	49.77	0.64
11	1.82	16.77	1.40	26.73	0.97	0.45	50.89	0.97
12	-0.04	16.79	1.19	31.02	0.70	0.59	48.65	1.09
13	1.43	15.00	1.20	31.68	1.18	0.92	47.62	0.96
14	0.54	16.11	1.08	29.68	1.26	0.70	49.38	1.26
15	0.56	4.66	2.07	52.58	0.38	1.56	35.94	2.26
16	0.08	3.31	6.33	41.64	0.79	3.28	41.22	3.34
17	0.18	5.29	5.45	29.58	-0.25	1.52	56.61	1.62
18	0.66	5.57	4.85	31.37	-0.04	3.13	51.92	2.54
19	1.55	5.04	4.67	43.56	0.40	2.40	39.89	2.50
20	1.13	10.87	4.08	25.55	0.15	3.72	52.71	1.78
21	0.33	5.27	3.89	27.63	-0.11	1.36	58.49	3.15

Table B.5-2 - Environmental scanning electron microscopy results in percent for the second $MgCl_2$ sample

Depth (mm)	Na	Mg	Al	Si	Cl	K	Ca	Fe
0	0.42	13.30	6.56	44.54	8.51	2.90	18.06	5.72
1	1.22	6.74	6.39	57.93	6.73	2.82	12.73	5.44
2	-0.16	7.92	3.62	29.61	9.22	0.53	46.20	3.06
3	0.96	6.13	6.26	28.02	7.40	0.77	47.16	3.29
4	1.23	8.35	4.64	22.13	8.08	0.59	52.91	2.07
5	-2.67	29.05	1.79	7.15	1.35	0.61	62.60	0.11
6	-0.43	10.49	4.06	19.79	5.32	0.98	57.10	2.69
7	2.09	6.43	6.31	26.20	1.44	1.54	55.43	0.56
8	2.02	5.73	4.83	34.58	3.75	1.47	46.28	1.35
9	-0.98	8.04	5.67	29.99	2.93	3.66	48.92	1.78
10	0.16	3.44	4.66	64.28	1.04	4.47	20.92	1.03
11	1.76	7.75	6.50	30.48	2.79	3.38	45.21	2.14
12	1.46	1.05	9.23	63.84	-0.16	14.21	8.11	2.25
13	3.83	1.34	12.93	52.55	0.73	14.88	13.03	0.70
14	-0.37	9.77	4.79	23.88	0.86	1.77	58.89	0.42
15	2.09	6.43	6.31	26.20	1.44	1.54	55.43	0.56
16	1.51	22.63	1.31	13.85	1.10	1.37	57.66	0.57
17	-1.09	5.72	3.63	38.14	1.49	1.34	49.42	1.35
18	0.80	7.70	7.53	35.13	0.78	5.13	39.89	3.04
19	1.07	6.58	6.30	34.79	0.24	3.40	44.25	3.39
20	1.69	5.09	6.20	30.97	0.89	2.08	50.46	2.63
21	-0.20	6.60	4.96	22.53	1.18	1.60	61.32	2.00

Table B.5-3 - Environmental scanning electron microscopy results in percent for the $CaCl_2$ sample

Depth (mm)	Na	Mg	Al	Si	Cl	K	Ca	Fe
0	1.57	2.92	5.77	23.30	12.97	2.01	48.05	3.41
1	0.50	6.69	3.61	23.10	6.55	0.60	54.81	4.14
2	0.17	8.84	2.77	21.89	9.90	0.98	53.23	2.22
3	0.50	7.11	2.20	27.78	12.34	0.22	47.95	1.90
4	0.81	4.69	3.79	21.88	14.05	3.34	49.70	1.73
5	1.54	4.16	4.55	19.17	14.76	1.30	51.45	3.08
6	0.67	2.73	2.81	34.69	11.42	1.15	45.56	0.98
7	0.54	2.00	2.03	15.91	3.97	-0.24	74.36	1.41
8	0.03	3.09	2.65	6.83	5.62	0.53	80.58	0.67
9	1.00	2.19	1.31	7.30	3.01	-0.04	84.44	0.79
10	0.88	1.79	2.64	3.54	2.09	0.34	89.23	-0.51
11	0.09	3.44	1.24	4.38	1.68	0.20	87.84	1.14
12	1.85	3.06	2.34	9.94	3.53	0.40	78.54	0.33
13	0.77	3.79	3.74	20.70	5.24	0.62	63.94	1.20
14	0.08	3.20	3.79	39.58	5.60	2.37	43.15	2.23
15	0.74	6.67	3.49	23.96	4.78	1.12	57.05	2.19
16	-0.93	5.45	3.20	35.41	5.04	1.11	49.21	1.51
17	2.03	4.02	3.31	34.44	5.01	0.91	45.57	4.72
18	-0.48	2.76	1.52	51.64	4.06	1.84	37.27	1.38
19	0.98	3.44	5.12	38.29	1.73	1.62	45.52	3.30
20	1.43	8.70	3.04	17.28	2.86	0.84	65.35	0.51
21	0.11	17.91	2.61	12.60	2.77	1.17	61.50	1.34
22	2.03	23.53	0.26	5.92	1.04	0.80	65.69	0.73
23	-0.13	24.42	3.68	9.51	1.91	1.53	57.57	1.51
24	0.51	18.86	2.77	11.58	1.82	0.59	62.94	0.94

Table B.5-4 - Environmental scanning electron microscopy results in percent for the multi-Cl^- sample

Depth (mm)	Na	Mg	Al	Si	Cl	K	Ca	Fe
0	0.93	8.90	5.05	27.39	14.42	0.95	39.75	2.61
1	1.08	5.18	5.75	28.82	13.94	0.59	42.99	1.64
2	7.03	4.64	8.05	24.53	16.99	0.66	36.50	1.60
3	0.63	22.54	2.91	8.49	4.11	0.62	60.52	0.18
4	4.16	5.00	4.38	22.56	12.54	1.62	47.76	1.98
5	1.52	5.90	3.63	24.18	7.51	0.74	54.36	2.15
6	0.15	27.41	0.91	5.47	2.27	0.12	63.18	0.48
7	1.61	29.03	-0.10	4.70	1.95	0.13	61.85	0.84
8	-1.43	31.18	1.20	4.04	1.16	-0.05	63.11	0.79
9	-0.10	25.00	1.32	11.05	0.83	0.68	60.31	0.90
10	3.43	4.11	9.66	40.58	0.22	2.31	38.20	1.48
11	7.17	2.56	12.23	52.78	0.43	1.59	21.70	1.54
12	1.54	3.68	5.96	35.12	0.57	2.58	47.14	3.40
13	-0.57	21.11	3.92	12.56	0.60	1.33	59.11	1.93
14	-0.26	29.37	1.04	6.74	0.17	0.37	61.64	0.93
15	0.41	29.61	1.23	5.16	-0.11	0.65	62.41	0.64
16	-0.59	24.51	1.13	9.67	-0.13	0.66	63.98	0.76
17	-0.03	9.36	5.00	22.09	0.86	1.97	58.73	2.02

Table B.5-5 - Environmental scanning electron microscopy results in percent for the NaCl sample

Depth (mm)	Na	Mg	Al	Si	Cl	K	Ca	Fe
0	12.23	4.05	1.78	35.31	19.29	0.35	26.61	0.39
1	3.13	8.52	3.47	32.18	7.94	1.41	42.22	1.13
2	0.99	21.21	3.20	15.67	3.30	-0.37	54.56	1.43
3	6.04	5.09	3.80	32.96	9.00	0.95	41.28	0.89
4	3.72	3.24	5.04	29.10	8.03	3.28	45.83	1.76
5	1.90	3.59	6.91	43.09	4.51	2.59	34.44	2.97
6	3.74	4.65	11.26	42.30	3.88	4.98	22.18	7.00
7	3.64	9.49	3.45	24.89	2.56	1.03	53.45	1.48
8	2.56	2.41	3.89	42.99	2.79	1.91	42.17	1.28
9	0.95	4.92	2.74	39.61	1.05	1.24	47.78	1.71
10	1.74	3.69	1.74	39.99	1.25	1.98	48.64	0.97
11	0.50	6.27	2.71	34.59	1.12	0.23	52.83	1.75
12	0.78	6.80	5.00	35.06	0.99	1.84	48.11	1.42
13	2.16	6.08	3.14	34.16	0.96	0.91	50.13	2.46
14	-2.08	0.94	2.62	10.43	0.51	1.30	85.06	1.22
15	2.49	13.24	4.46	18.34	0.86	2.96	56.51	1.14
16	0.39	5.16	4.21	21.36	0.14	1.17	64.43	3.12
17	3.23	4.40	1.13	11.23	-0.87	1.34	76.90	2.64
18	-2.71	2.22	2.90	11.53	0.89	1.05	80.19	3.93
19	-0.62	3.64	3.23	12.01	1.05	0.96	76.79	2.95
20	1.22	3.98	0.97	10.53	-0.04	-0.13	81.13	2.35
21	1.21	2.79	2.84	15.18	0.49	0.75	72.27	4.47
22	-0.86	3.90	2.48	12.39	0.64	1.42	76.25	3.77
23	0.00	4.68	1.60	10.31	0.56	0.16	76.93	5.77

Appendix B.6 Air Void Analysis

Appendix B.6.1 Raw Data

The data in Table B.6-1 and Table B.6-2 are the summarized raw output from the air void analysis equipment.

Table B.6-1 - Air Void Analysis Raw Data Part 1

Air Void Parameter		Part 1			Part 2			Average		
		Chords < 0.5 mm	Chords < 1.0 mm	All Chords	Chords < 0.5 mm	Chords < 1.0 mm	All Chords	Chords < 0.5 mm	Chords < 1.0 mm	All Chords
Number of Voids	H2O	521	534	554	508	527	543	514.5	530.5	548.5
	$CaCl_2$	1703	1719	1742	651	676	688	1177.0	1197.5	1215.0
	$MgCl_2$	1184	1210	1230	1104	1121	1133	1144.0	1165.5	1181.5
	Multi	3318	3347	3377	2111	2139	2160	2714.5	2743.0	2768.5
	NaCl	1069	1079	1104	1133	1157	1174	1101.0	1118.0	1139.0
Percent of Total Number of Voids	H2O	94.0	96.4	100	93.6	97.1	100	93.8	96.7	100.0
	$CaCl_2$	97.8	98.7	100	94.6	98.3	100	96.2	98.5	100.0
	$MgCl_2$	96.3	98.4	100	97.4	98.9	100	96.9	98.7	100.0
	Multi	98.3	99.1	100	97.7	99.0	100	98.0	99.1	100.0
	NaCl	96.8	97.7	100	96.5	98.6	100	96.7	98.1	100.0
Length of Air Traversed (mm)	H2O	32.75	41.75	80.38	36.03	49.64	75.46	34.39	45.70	77.92
	$CaCl_2$	78.92	89.78	131.15	37.32	56.12	77.65	58.12	72.95	104.40
	$MgCl_2$	67.13	84.48	121.85	62.68	74.40	97.43	64.90	79.44	109.64
	Multi	143.68	162.85	229.52	126.12	144.41	179.94	134.90	153.63	204.73
	NaCl	50.51	57.30	95.89	59.41	76.70	105.44	54.96	67.00	100.67
Percent of Total Length of Air Traversed	H2O	40.7	51.9	100	47.8	65.8	100	44.2	58.9	100.0
	$CaCl_2$	60.2	68.5	100	48.1	72.3	100	54.1	70.4	100.0
	$MgCl_2$	55.1	69.3	100	64.3	76.4	100	59.7	72.8	100.0
	Multi	62.6	70.9	100	70.1	80.3	100	66.3	75.6	100.0
	NaCl	52.7	59.8	100	56.3	72.7	100	54.5	66.2	100.0
Air Content (%)	H2O	1.36	1.73	3.33	1.49	2.06	3.13	1.42	1.89	3.23
	$CaCl_2$	3.27	3.72	5.43	1.55	2.32	3.22	2.41	3.02	4.32
	$MgCl_2$	2.78	3.50	5.05	2.60	3.08	4.04	2.69	3.29	4.54
	Multi	5.95	6.74	9.51	5.22	5.98	7.45	5.59	6.36	8.48
	NaCl	2.09	2.37	3.97	2.46	3.18	4.37	2.28	2.77	4.17
Average Chord Length (mm)	H2O	0.063	0.078	0.145	0.071	0.094	0.139	0.067	0.086	0.142
	$CaCl_2$	0.046	0.052	0.075	0.057	0.083	0.113	0.052	0.068	0.094
	$MgCl_2$	0.057	0.070	0.099	0.057	0.066	0.086	0.057	0.068	0.093
	Multi	0.043	0.049	0.068	0.060	0.068	0.083	0.052	0.059	0.076
	NaCl	0.047	0.053	0.087	0.052	0.066	0.090	0.050	0.060	0.089

Table B.6-2 - Air Void Analysis Raw Data Part 2

Air Void Parameter		Part 1			Part 2			Average	Average	Average
		Chords < 0.5 mm	Chords < 1.0 mm	All Chords	Chords < 0.5 mm	Chords < 1.0 mm	All Chords	Chords < 0.5 mm	Chords < 1.0 mm	All Chords
Paste to Air Ratio	H2O	20.59	16.18	8.41	18.79	13.59	8.95	19.69	14.89	8.68
	$CaCl_2$	8.56	7.53	5.16	18.06	12.07	8.70	13.31	9.80	6.93
	$MgCl_2$	10.07	8.00	5.54	10.77	9.09	6.93	10.42	8.55	6.24
	Multi	4.71	4.15	2.94	5.36	4.68	3.76	5.04	4.42	3.35
	NaCl	13.40	11.81	7.05	11.38	8.81	6.41	12.39	10.31	6.73
Specific Surface (mm^{-1})	H2O	63.64	51.17	27.57	56.39	42.46	28.78	60.02	46.81	28.18
	$CaCl_2$	86.31	76.59	53.13	69.77	48.18	35.44	78.04	62.38	44.29
	$MgCl_2$	70.55	57.29	40.38	70.46	60.27	46.51	70.51	58.78	43.45
	Multi	92.37	82.21	58.85	66.95	59.25	48.02	79.66	70.73	53.44
	NaCl	84.66	75.32	46.05	76.29	60.34	44.54	80.48	67.83	45.30
Void Frequency (mm^{-1})	H2O	0.216	0.221	0.229	0.210	0.218	0.225	0.213	0.220	0.227
	$CaCl_2$	0.705	0.712	0.721	0.270	0.280	0.285	0.488	0.496	0.503
	$MgCl_2$	0.490	0.501	0.509	0.457	0.464	0.469	0.474	0.483	0.489
	Multi	1.374	1.386	1.399	0.874	0.886	0.895	1.124	1.136	1.147
	NaCl	0.443	0.447	0.457	0.469	0.479	0.486	0.456	0.463	0.472
Spacing Factor (mm)	H2O	0.137	0.153	0.213	0.148	0.171	0.210	0.142	0.162	0.211
	$CaCl_2$	0.069	0.073	0.088	0.118	0.143	0.168	0.093	0.108	0.128
	$MgCl_2$	0.090	0.100	0.120	0.093	0.101	0.116	0.092	0.100	0.118
	Multi	0.049	0.051	0.050	0.071	0.076	0.078	0.060	0.063	0.064
	NaCl	0.085	0.091	0.118	0.088	0.099	0.117	0.087	0.095	0.117

Appendix B.6.2 Microscopy Images

Figure B.6-1 through Figure B.6-5 show the microscopy images captured during air void analysis.

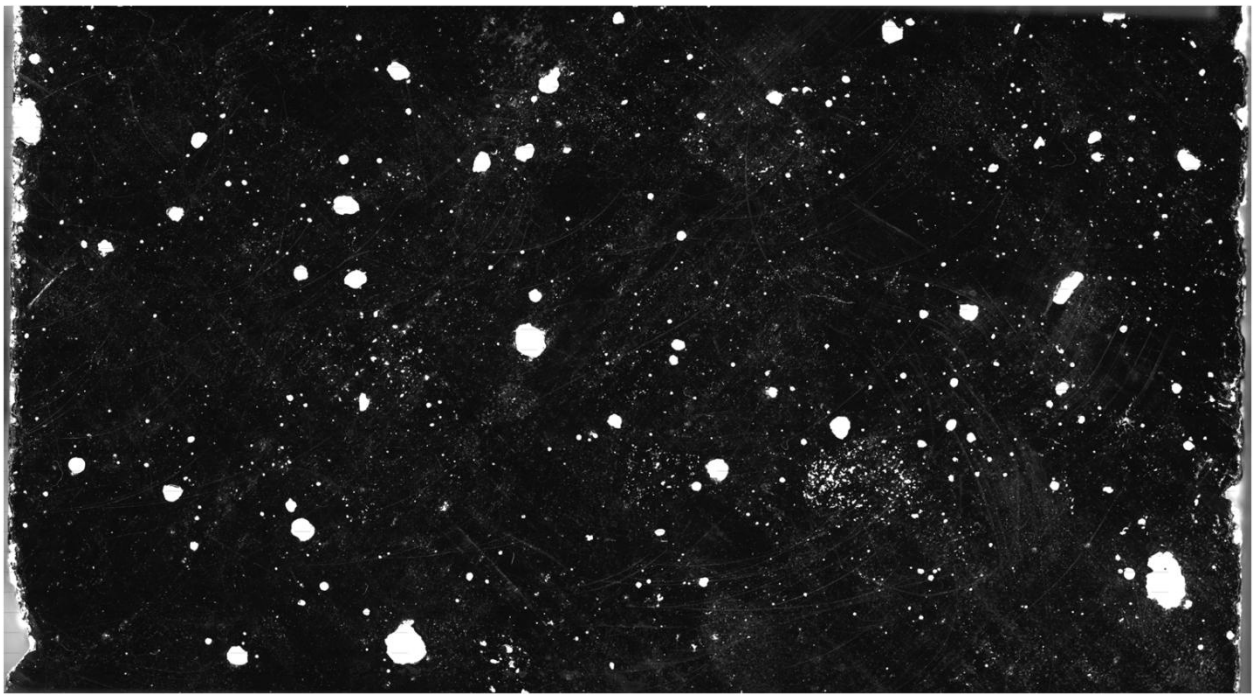

Figure B.6-1 - Microscopy image of H_2O sample from air void analysis

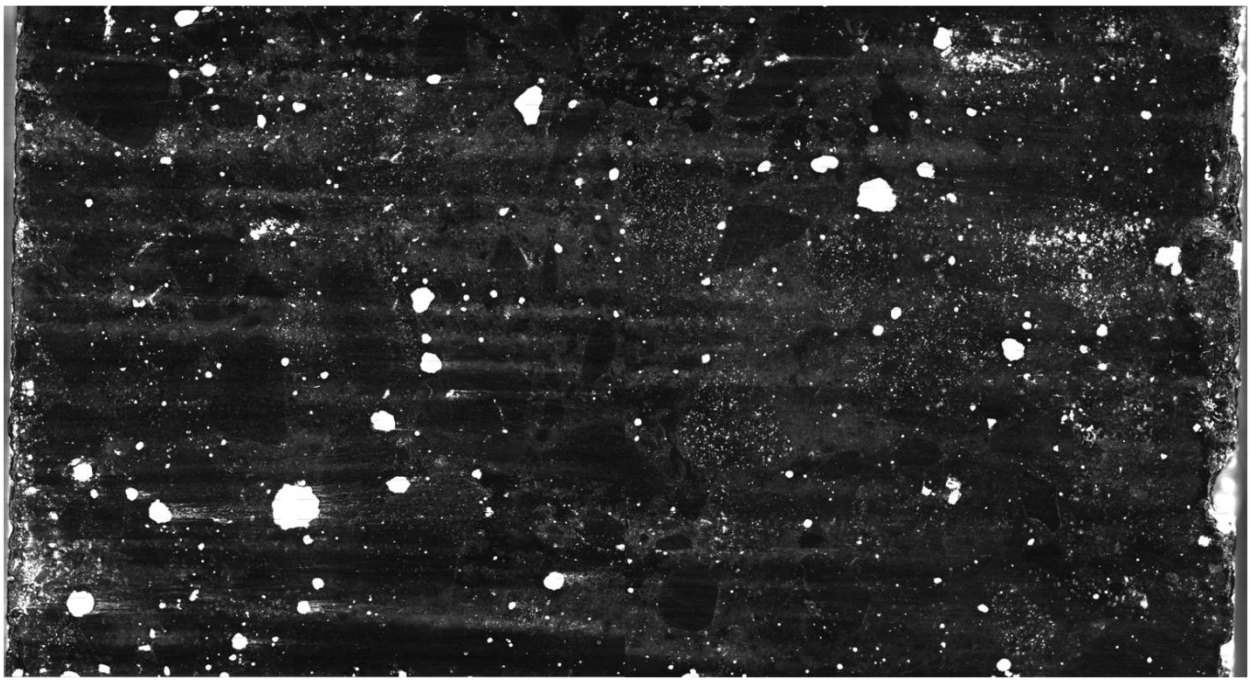

Figure B.6-2 - Microscopy image of $MgCl_2$ sample from air void analysis

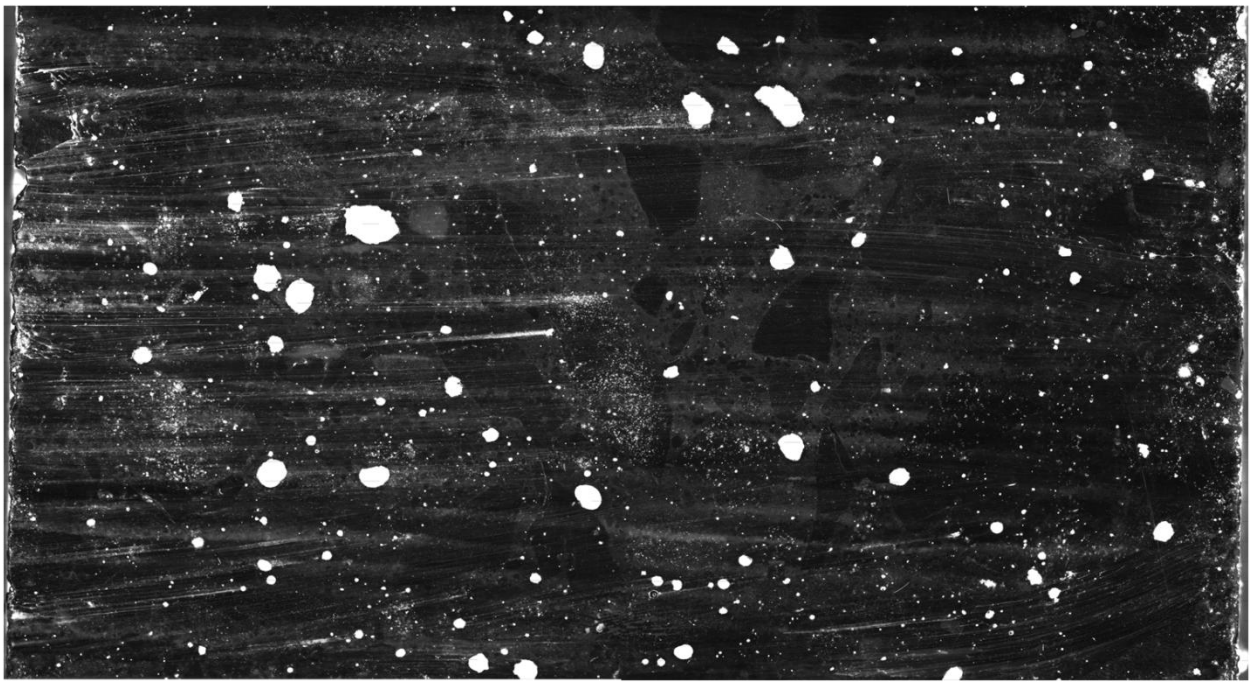

Figure B.6-3 - Microscopy image of $CaCl_2$ sample from air void analysis

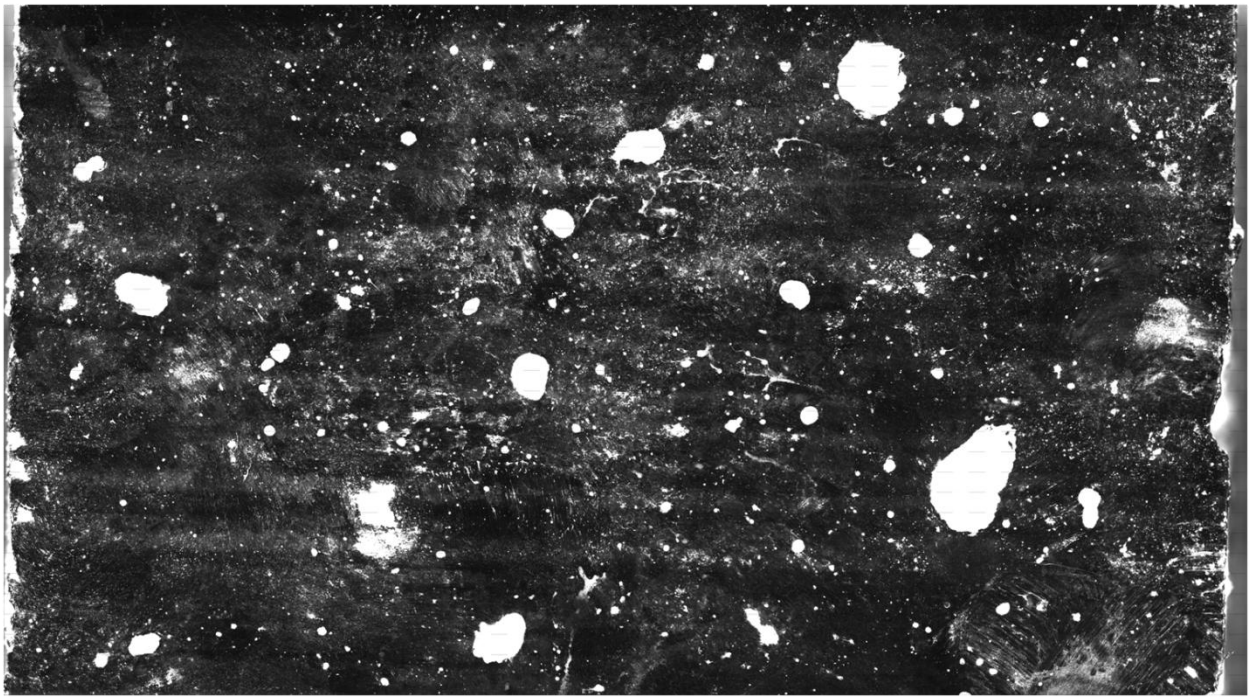

Figure B.6-4 - Microscopy image of multi-Cl^- sample from air void analysis

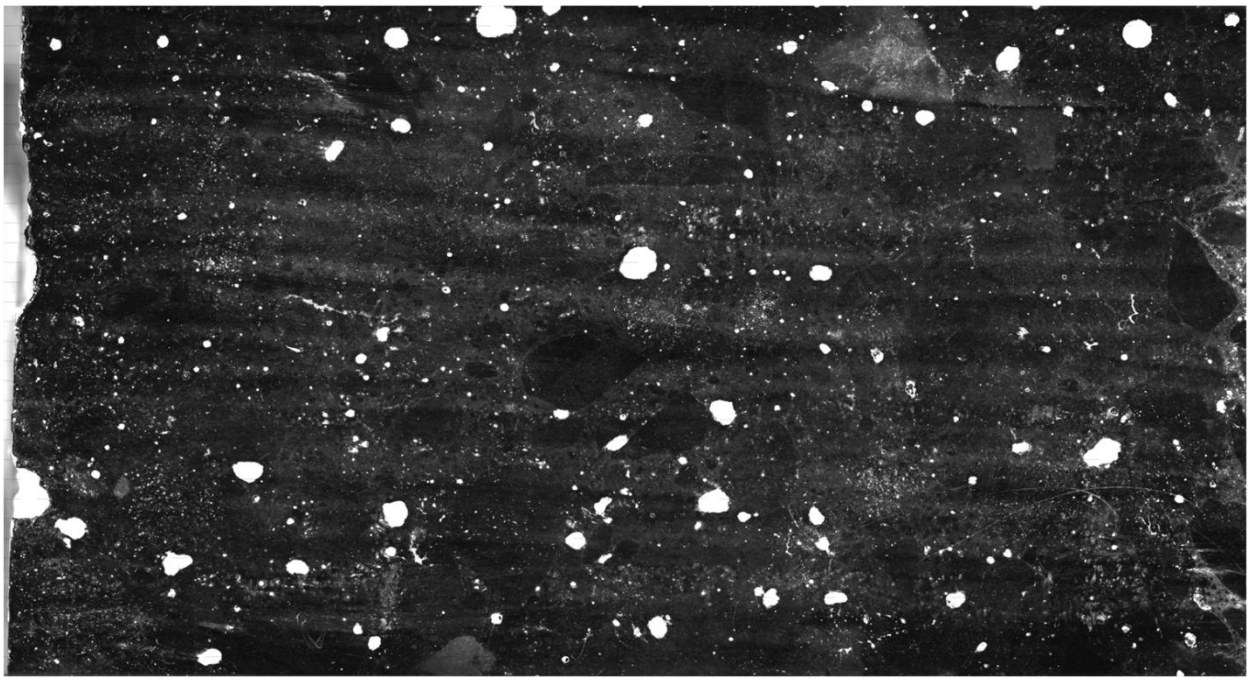

Figure B.6-5 - Microscopy image of NaCl sample from air void analysis